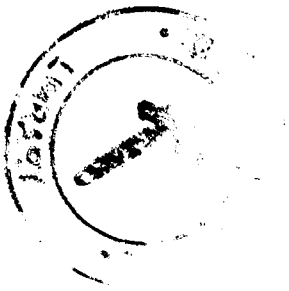

The synthesis of imidazole derivatives for the inhibition of steroid-mediated prostate tumour growth.

A THESIS SUBMITTED IN ACCORDANCE WITH THE CONDITIONS GOVERNING CANDIDATES FOR THE DEGREE OF DOCTOR OF PHILOSOPHY

BY

BALJEET KAUR JANDU

FACULTY OF SCIENCE, ENGINEERING AND COMPUTING

PENRHYN ROAD

KINGSTON-UPON-THAMES

SURREY

KT1 2EE

2013

ORIGINAL COPY TIGHTLY BOUND

TEXT BOUND CLOSE TO THE SPINE IN THE ORIGINAL THESIS

ACKNOWLEDGEMENTS

I would like to thank my supervisors Dr Adam LeGresley and Professor Sabbir Ahmed and my Director of Studies Prof. John Brown for their support and help, especially to Dr LeGresley for being so generous and for giving me constant help and advice for when I have needed it most. I would also like to thank Kingston University for providing me with such an opportunity.

I am extremely thankful to my parents and to the most significant person in my life, Rob. All of whom I love very much. Without you all, this PhD would not have been possible. Thank you for always being there to support me and to pick me back up when it was all beginning to feel too difficult to continue with.

I would also like to extend this gratitude to an important friend who has been a constant pillar throughout my PhD, Dr Jean-Marie Peron. Thank you for always being there for whenever I have needed any sort of help and most importantly for just being such a great friend. Furthermore, I would like to thank all the technicians for their help throughout my PhD, especially Julian Swinden for all his assistance and advice with spectral data.

Finally, I would like to thank all friends and family whom have all been there to give me their support throughout. I will never forget the love and support you have all given me.

ABSTRACT

The majority of prostate cancer cases areshown to be androgen-dependant for growth as the blocking of androgen production has shown to reduce the size of prostate metastasis. The biosynthesis of the androgens is catalysed by the cytochrome P450 enzyme 17α-hydroxylase/17,20-lyase ($P450_{17\alpha}$) by converting the C_{21} steroids (pregnenolone and progesterone) to the androgens (dehydroepiandrosterone and androstenedione, respectively). Inhibition of $P450_{17\alpha}$ would therefore bring about a decrease in the level of androgen production and furthermore prevent an increase in the stimulation of androgen-dependent prostate cancer cells.

The current study was concerned with designing and synthesising compounds which were able to donate a lone pair of electrons to the Fe atom of the haem group with in the active site of the enzyme $P450_{17\alpha}$. As well as this, we were also interested in being able to mimic the C(3) of the natural substrate by varying the R group. In doing so, we were able to observe the impact of the interactions which take place within the active site. The compounds synthesised are based on the benzyl imidazole and the imidazol-phenyl ethanonebackbone, where a small number of the synthesised products are phenyl alkyl imidazole based compounds, in order to consider physiochemical factors like hydrophobicity.

Overall, the results of the study showed that the benzyl imidazole-based compounds were comparable to that of the standard ketoconazole (KTZ) in their inhibitory activity against 17,20-lyase and 17α-OHase (KTZ; %inhibition = 75% against 17,20-lyase: %inhibition = 64% against 17α-OHase). The nitro substituted derivatives (**270-272**) were shown to have improved inhibitory activity when compared to KTZ against 17α-OHase. With respect to the imidazol-phenyl ethanones, all with the exception of the 3-bromo substituted derivative (**288**) were shown to possess either equipotent inhibitory activity to that of KTZ (%inhibition = 80% against 17α-OHase: %inhibiton = 82% against 17,20-lyase) or substantially lower activity. Compound **288** was found to possess greater inhibitory activity against the 17α-OHase component (**288** %inhibition = 84%).

Deliberation of structure-activity relationships determined no obvious correlation between the substitution pattern of the benzyl ring and the inhibitory activity against 17,20-lyase in the benzyl imidazole-based compounds. However, in the activity against 17α-OHase, a general trend towards the *para* substitution of the benzyl ring was shown to have an impact on the inhibition of the enzyme. In the imidazol-phenyl ethanones, consideration of the inhibitory activity of the halogen derivatives shows that there is an increase in potency with decreasing electronegativity of substituent group. In the inhibitory activity against 17α-OHase, some compounds show a correlation between decreasing electron-withdrawing ability and an increase in percentage inhibition. This would therefore appear to suggest that an interaction exists between the substituent and complementary group(s) at the active site of the enzyme – this interaction appears to be weaker within derivatives which possess substituents of high electronegativity. The substitution of the phenyl ring was too shown to influence the inhibitory activity of the compounds, which was rationalised by use of the SHC approach. This was proposed as results clearly indicate that the meta-substituted compounds were found to possess greater inhibitory activity in comparison to the para-substituted compounds.

CONTENTS

List of tables

List of figures

List of Schemes

Abbreviations

ACTH	Adrenocorticotropin
ATP	Adenosine triphosphate
Ala	Alanine residue
α	Alpha
ADT	Androgen deprivation therapy
AR	Androgen receptor
$P450_{arom}$	Aromatase
Ar	Aromatic
BPH	Benign prostate hyperplasia
β	Beta
BSA	Bovine serum albumin
Br	Bromo group
$P450_{BM-3}$	From bacillus megaterium, bacterial fatty acid monooxygenase
$P450_{cam}$	Bacterial camphor monooxygenase
δ_C	^{13}C FT-NMR
$CHCl_3$	Chloroform
Cl	Chloro group
CPM	Counts per minute
K_i	Constant of inhibition
J	Coupling constant
CN	Cyano group
DHEA	Dehydroepiandrosterone
DHEAS	Dehydroepiandrosterone sulphate
Δ	Delta

°C	Degree centigrade
DNA	Deoxyribose nucleic acid
$CDCl_3$	Deuterated chloroform
CD_3OH	Deuterated Methanol
DCM	Dichloromethane
DHT	Dihydrotestosterone
DMSO	Dimethylsulfoxide
DMEM	Dulbecco's modified essential media
DPBS	Red and phosphate buffer saline
d	doublet
dd	doublet of doublets
ER	Endoplasmic reticulum
E	*Entgegen* (*trans*-isomer)
E.coli	Escherichia coli
C_2H_5OH	Ethanol
P450	Family group of enzymes which absorb UV light at 450nm
F	Fluoro group
FT-NMR	Fourier Transform Nuclear Magnetic Resonance spectroscopy
GnRH	Gonadotropin releasing hormone
GC	Gas chromatography
GCMS	Gas chromatography mass spectrometer
g	Grams
δ_H	^1H FT-NMR
HRMS	High resolution mass spectrometry
HS	High spin
h	Hour
HCl	Hydrochloric acid
H	Hydrogen
pH	Hydrogen ion concentration
HSD	Hydroxysteroid dehydrogenase
Im	Imidazole
IR	Infra-red spectrometry
[i]	Inhibitor concentration
IC_{50}	Inhibitory concentration (causing 50% enzyme inhibitor)

cm^{-1}	Inverse if centimetre (IR radiation)
I	Iodo group
Ile	Isoleucine residue
KTZ	Ketoconazole
$LiAlH_4$	Lithium aluminium hydride
LogP	Logarithm of the partition coefficient
LRMS	Low resolution mass spectrometry
LS	Low spin
LHRH	Luteinising hormone releasing hormone
LH	Luteinising hormone
$MgSO_4$	Magnesium sulphate
m/z	Mass to charge ratio
V_{max}	Maximum frequency (IR radiation)
MHz	Mega hertz
m.p	Melting point
Met	Methionine residue
OCH_3	Methoxy group
CH_3	Methyl group
µM	Micro molar
Mg	Milligram
mL	Millilitres
mmol	Millimole
min	Minutes
M^+	Molecular ion
m	multiplet
nm	Nano meters
pKa	Negative logarithm of acid dissociation constant
NADPH	Nicotinamide adenine dinucleotide phosphate
NO_2	Nitro group
NI	No inhibition
ND	Not determined
NMR	Nuclear magnetic resonance
Pd,C	Palladium on charcoal
Ph	Phenyl

Phe	Phenylalanine residue
K_2CO_3	Potassium carbonate
Bu^tOK	Potassium tertiary butoxide
PBr_3	Potassium tribromide
Pro	Proline residue
PC	Prostate cancer
PSA	Prostate specific antigen
QSAR	Quantitative structure-activity relationship
q	quartet
R	*Rectus* (clockwise configuration of the groups in an enantiomer)
t_R	Retention time
SHBG	Sex hormone binding globulin
s	singlet
S	*Sinister* (anticlockwise configuration of the groups in an enantiomer)
$NaHCO_3$	Sodium bicarbonate
$NaOCH_3$	Sodium methoxide
SD	Sprague-dawley
SEM	Standard Error of the Mean
SHC	Substrate haem complex
H_2SO_4	Sulphuric acid catalyst
THF	Tetrahydrofuran
TLC	Thin layer chromatography
MTT	Thiozolyl blue tetrazolium bromide
Thr	Threonine residue
t	triplet
Tyr	Tyrosine residue
UV	Ultra violet light
H_2O	Water
Z	*Zusammen* (*cis*-isomer)
$P450_{17\alpha}$	17α-hydroxylase/17,20-lyase
17α-OHase	17α-hydroxylase component of $P450_{17\alpha}$
17,20-lyase	17,20-lyase component of $P450_{17\alpha}$

1.0 INTRODUCTION

Prostate cancer is the third leading cause of male cancer deaths in the United States and Europe with lung cancer being the first and colorectal cancer being the second. However, there are considerable regional differences in the occurrence and the mortality of prostate cancer[1]. It was estimated that in 2008, some 186, 320 new cases of prostate cancer were diagnosed in the United States with 28,660 deaths[2].

In Europe, the estimated incidence of prostate cancer for 2006 was 345,900 with an estimated 87,400 deaths[3]. It has been shown that prostate cancer not only varies considerably between different countries but also ethnic groups; with the highest incidence rates recorded in North America (particularly amongst African-American), Australia, New Zealand and Scandinavia. The lowest incidence rates have been recorded in Asia, in particular India, China and Japan[4,5].

Some of the most important risk factors for prostate cancer include age, ethnicity and diet, as well as genetic factors and family history[6,7]. Environmental factors such as damaging radiation and chemicals have also been linked to the initiation and promotion of prostate cancer. Studies have shown that men over the age of 45 are at greater risk of developing prostate cancer, however, the disease has been shown to occasionally occur in younger men[8,9]. Furthermore, the risk of prostate cancer is seen to increase with age, where more than 70% of the men diagnosed are over the age of 65.

1.1 The Prostate Gland

The prostate is a walnut sized exocrine secretory gland specific to the male reproductive system. It is positioned deep within the pelvis surrounding the urethra and is located just below the bladder and in front of the rectum. The size of the prostate is maintained by the balance between the process of cell proliferation and apoptosis. Approximately 80% of prostate cancer incidence is considered to be androgen-dependent for growth, as the blocking of androgen production has shown to reduce the size of prostate metastasis; however, this hormone-dependent disease has the ability to become hormone-independent[10,11].

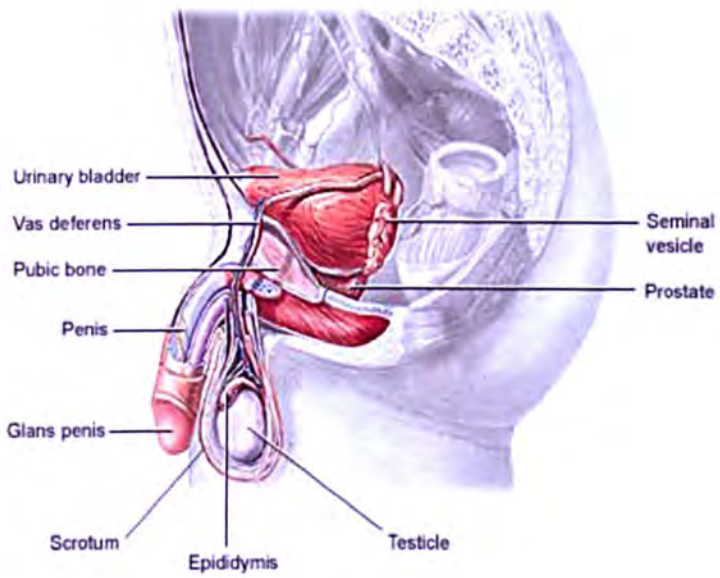

Figure 1 The male reproductive system[12].

The adult human prostate is divided into three major regions; the inner prostate consists of the transition zone, with the outer prostate consisting of the central and peripheral zones (Figure 2). Approximately 70% of adenocarcinomas have shown to arise in the peripheral zone[13,14].

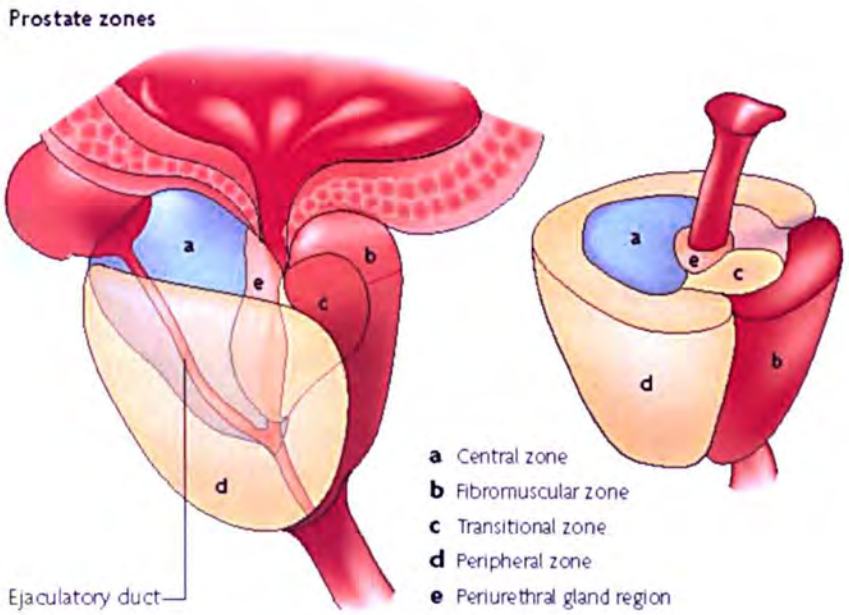

Figure 2 Showing the anatomic zones in relation to the prostate gland and surrounding tissue[15].

1.2 Androgens

Androgens are important in the growth and maintenance of prostate cells. Furthermore, they are also suggested to play an important role in the initiation, development and progression in hormone-dependent prostate cancer, as studies have revealed that long term exposure to androgens may be associated as a high risk factor in the initiation of the disease[16].

1.2.1 Androgen biosynthesis and action in the prostate

The hormonal environment of the prostate gland is largely dependent upon the hypothalamus, which initiates a series of events that result in the secretion of testosterone, the major circulating form of androgens produced by the leydig cells in the testes[10]. In addition, the adrenal androgens, androstenedione, dehydroepiandrosterone

(DHEA) and its sulfate (DHEAS) are secreted by the adrenal cortex and though they are not as potent as testosterone, they contribute to the androgenic response *in vivo*[17].

The hypothalamus releases the peptide hormone luteinising hormone-releasing hormone (LHRH) also known as gonadotropin releasing hormone (GnRH). In the pituitary gland, LHRH acts on the gonadotrope LHRH receptor inducing the release of luteinising hormone (LH) and adrenocorticotrophin (ACTH), which enter the circulation and exert their effects on the testes and adrenal glands[19,20] (Figure 3).

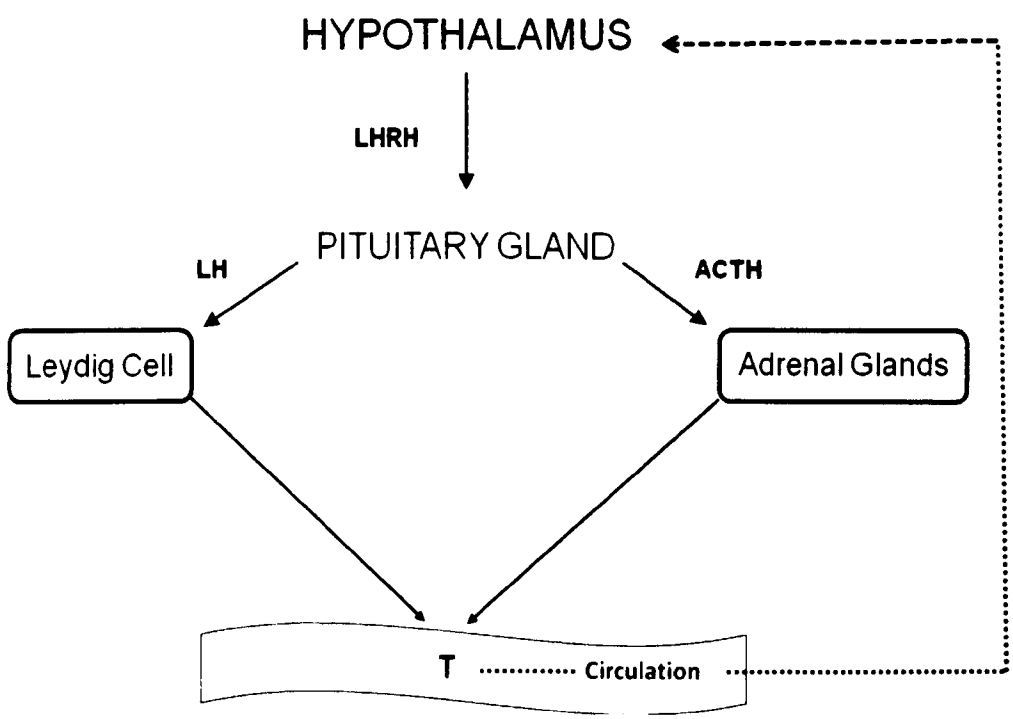

Figure 3 Showing the effects of ACTH, CRH, LH and LHRH on the leydig cells and the adrenal gland[18].

The adrenal gland produces around 10% of the circulating testosterone. The adrenal glands consist of an inner medulla and an outer cortex which is subdivided into three zones of cells; the zona glomerolusa, zona fasciculate and zona reticularis. In addition to the gonads, it is also within the zona fasciculata and the zona reticularis that the synthesis of glucocorticoids in the former and the sex steroids in the latter takes place. It is within the zona glomerulosa that the production of the mineralocorticoids take place[21,22] (Figure 4).

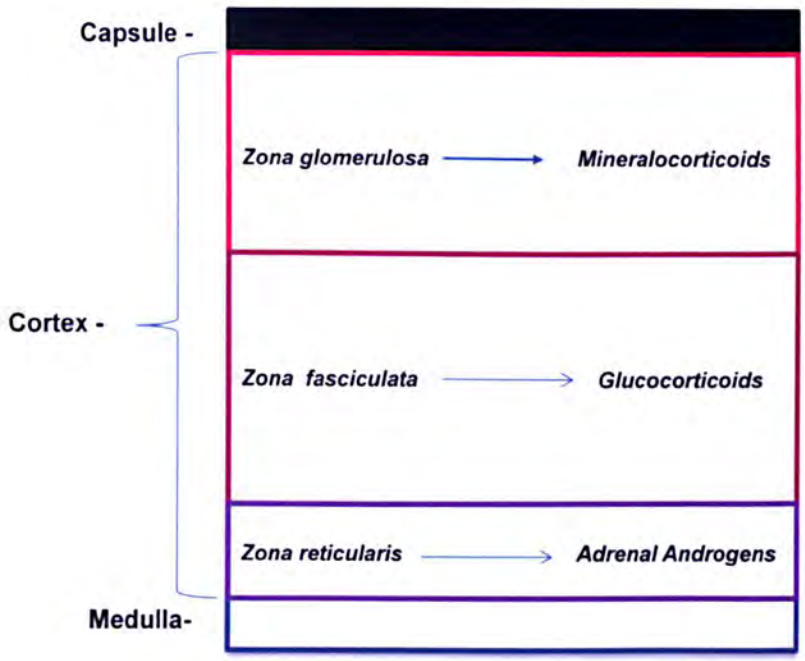

Figure 4 Showing the three zones of cells within the adrenal gland; the zona glomerolusa, zona fasciculate and zona reticularis.

DHEA and DHEAS are the principle androgens produced in the zona reticularis, but are shown to be weak in their biological activity, accounting for only 5% of the potency of testosterone[22]. When free testosterone enters prostate cells, 90% is irreversibly converted to the more potent intracellular androgen Dihydrotestosterone (DHT) by the

cytoplasmic enzyme 5α-reductase type II[23,24]. Type II has been reported to be more specific for prostatic epithelial cells, where as type I is present in most tissues in the body[25]. In both the leydig cells and the adrenal gland, the Δ-5 synthetic pathway is the more predominant, which results in testosterone and androstenedione production. The Δ-4 synthetic pathway results in the synthesis of DHEA and androstenediol (Figure 7).

In the plasma, testosterone has been shown to be bound to the serum proteins sex hormone-binding globulin (SHBG), albumin and/or corticosteroid-binding globulin[25], with less than 3% existing in an unbound bioavailable form[26]. Sex hormone-binding globulin has the highest affinity for testosterone and has been hypothesised to play a significant role in regulating the level of free testosterone available to target tissues[25].

1.2.2 Androgen receptor

The androgen receptor (AR) is a member of the steroid-thyroid-retinoid nuclear receptor superfamily, which also includes the estrogen, progesterone, mineralocorticoid and glucocorticoid receptors[25,27]. Both DHT and testosterone (to a lesser extent) can bind to the nuclear receptor, however DHT forms a more stable receptor-ligand complex than testosterone and also has a five fold higher affinity for the AR than testosterone. Unbound AR is located mainly in the cytoplasm and is bound with a complex of heat shock proteins in a conformer, which prevents DNA binding[27] (Figure 5). DHT arbitrates its actions primarily through binding to the nuclear receptor in the cytosol, inducing a series of conformational changes[24].

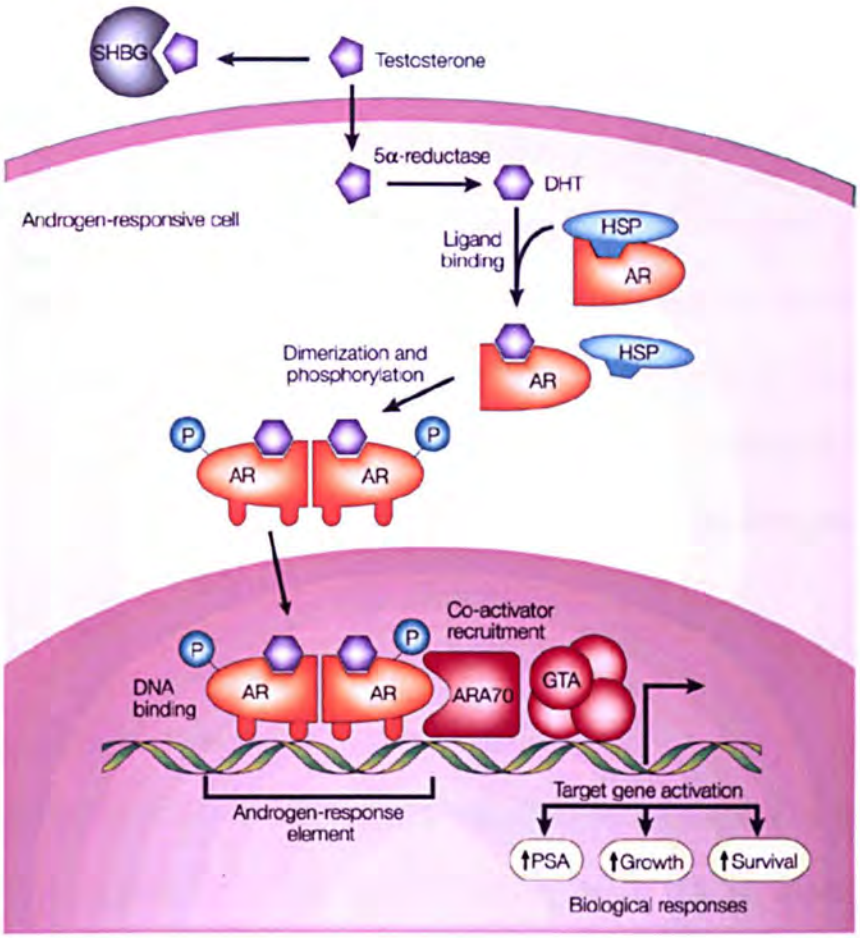

Figure 5 Showing the activity of the ligand-bound androgen receptor within the cell[24].

AR can either form homodimers or heterodimers with other proteins that regulate their biological properties[26]. The heat shock proteins dissociate from the AR facilitating the formation of AR homodimer complex[27]. Subsequent binding to the androgen response elements in the promoter regions of target genes leads to gene expression and ultimately the production of proteins necessary for survival, growth, cell proliferation and function of the prostate gland[24,27]. Studies have suggested that approximately 1.5-4.3% of genes expressed in prostate cancer cells are directly or indirectly regulated by androgens[28]. The removal of androgens is thus the rationale for the treatment in hormone-dependent prostate cancer.

1.2.3 Prostate Specific Antigen (PSA)

PSA is a serine protease secreted almost completely by prostatic epithelial cells, which is produced by both benign and malignant prostatic epithelium[29,30]. Blood levels are shown to increase when the normal glandular structure of the prostate is disrupted by benign or malignant tumour or inflammation. PSA level is directly proportional to tumour volume, with a greater enhancement per unit volume of cancer compared with benign prostate hyperplasia (BPH)[16]. PSA has been found to be a responsive indicator after most treatments for prostatic cancer, the most being in patients who have undergone radical prostatectomy[30,31].

1.2.4 Androgen independence in prostate cancer

The efficacy of hormonal treatment for advanced prostate cancer is short-lived, the median extent of response to androgen ablation being 18-24 months. Castration resistant prostate cancer is attributed to a number of complex interconnected transformations at molecular level. Five possible suggested mechanisms by Feldman and Feldman[24] were: selected outgrowth of pre-existing androgen-independent prostate cancer cells; up-regulation of anti-apoptotic survival pathways; activation of alternative growth factor pathways; increased hypersensitivity of AR to low levels of androgen; and increased mutations in AR leading to activation by other ligands (Figure 6).

Prostate cancers are heterogeneous tumours consisting of numerous subpopulations of cells. This tumour heterogeneity may reflect either a multifocal origin, an alteration to an environmental stimuli or the genetic instability of the original cancer[32]. Accumulating evidence indicates that AR continues to play an important role in prostate cancer progression, where it is found to be highly expressed in castrate tumours. The transcriptions of numerous AR-regulated genes, which are suppressed after androgen

deprivation therapy (ADT), have shown to recur[33,34].

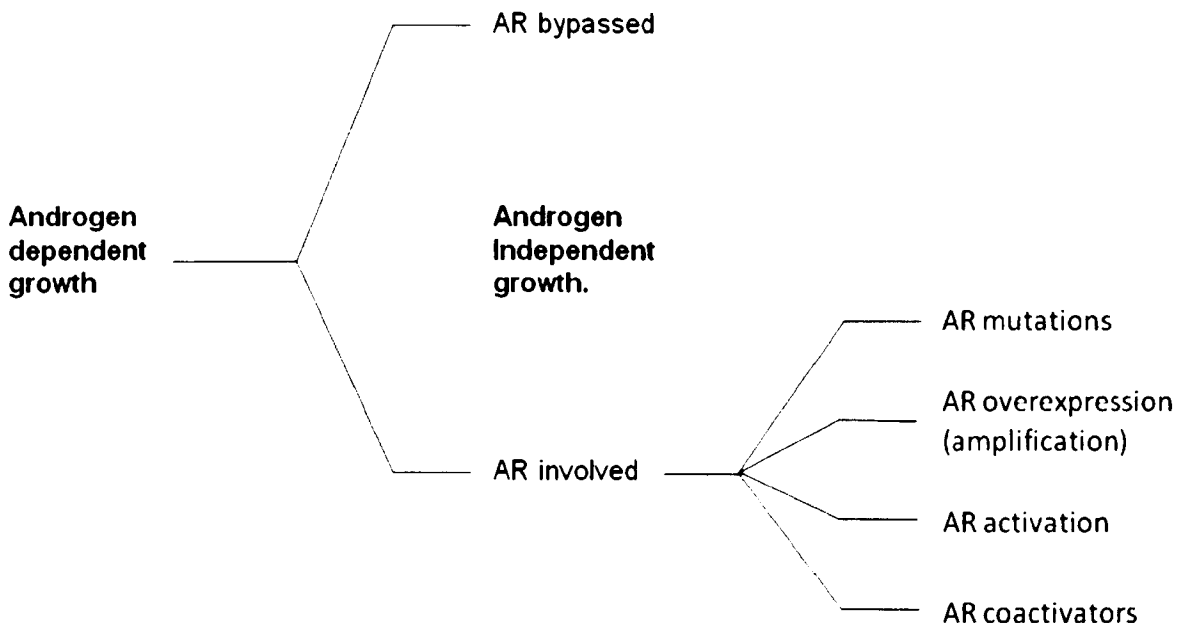

Figure 6 Showing progressive growth of prostate cancer[24].

In recent studies, levels of testosterone, DHT and enzymes responsible for their synthesis were determined from tissue samples of patients diagnosed with BPH, untreated primary prostate cancer and castrate resistant prostate cancer. In their studies, Montgomery et al[35] have shown an up-regulated expression of 17α-hydroxylase/17,20-lyase ($P450_{17\alpha}$) in castrate resistant prostate cancer tissue samples in conjunction with higher levels of testosterone. In other separate studies, the expression of $P450_{17\alpha}$ has been shown to be increased during progression to castrate resistant prostate cancer. As a result, this enzyme has become a pivotal target in drug development in the field[36].

1.3 The Cytochrome P450 Enzymes

P450 enzymes consist of a large family of enzymes which are present in all species and play a significant role in the steroidogenic pathway as they are all involved in the biosynthesis of the five main classes of steroid hormones: progestagens, mineralocorticoids, glucocorticoids, androgens and estrogens[37] (Figure 7). P450 enzymes are related yet distinct enzymes, all differing from each other by their amino acid sequence, which contain specific substrate specificities[21]. The cytochrome P450 enzymes possess a distinctive pink colour as a result of the reduced form of P450 combining with carbon monoxide[38] (absorbing light at 450nm).

Microsomal P450 enzymes play a vital role in the oxidative transformations of endogenous and exogenous molecules, such as the metabolism of drugs, xenobiotics and the natural substrates (e.g.cholesterol)[39]. These enzymes are haem containing metalloenzymes which possess a characteristic porphyrin ring system in the centre of which lies a single iron atom coordinated to a cysteine thiolate, the proximal axial ligand[40] (Figure 8). The cysteine thiolate is able to form an octahedral complex with six ligands or a penta-coordinate configuration due to the lack of the sixth ligand, which is otherwise referred to as the distal ligand. It is the sulphur ligand that is the origin of the characteristic name-giving 450-nm soret absorbance for the ferrous-CO complex[41].

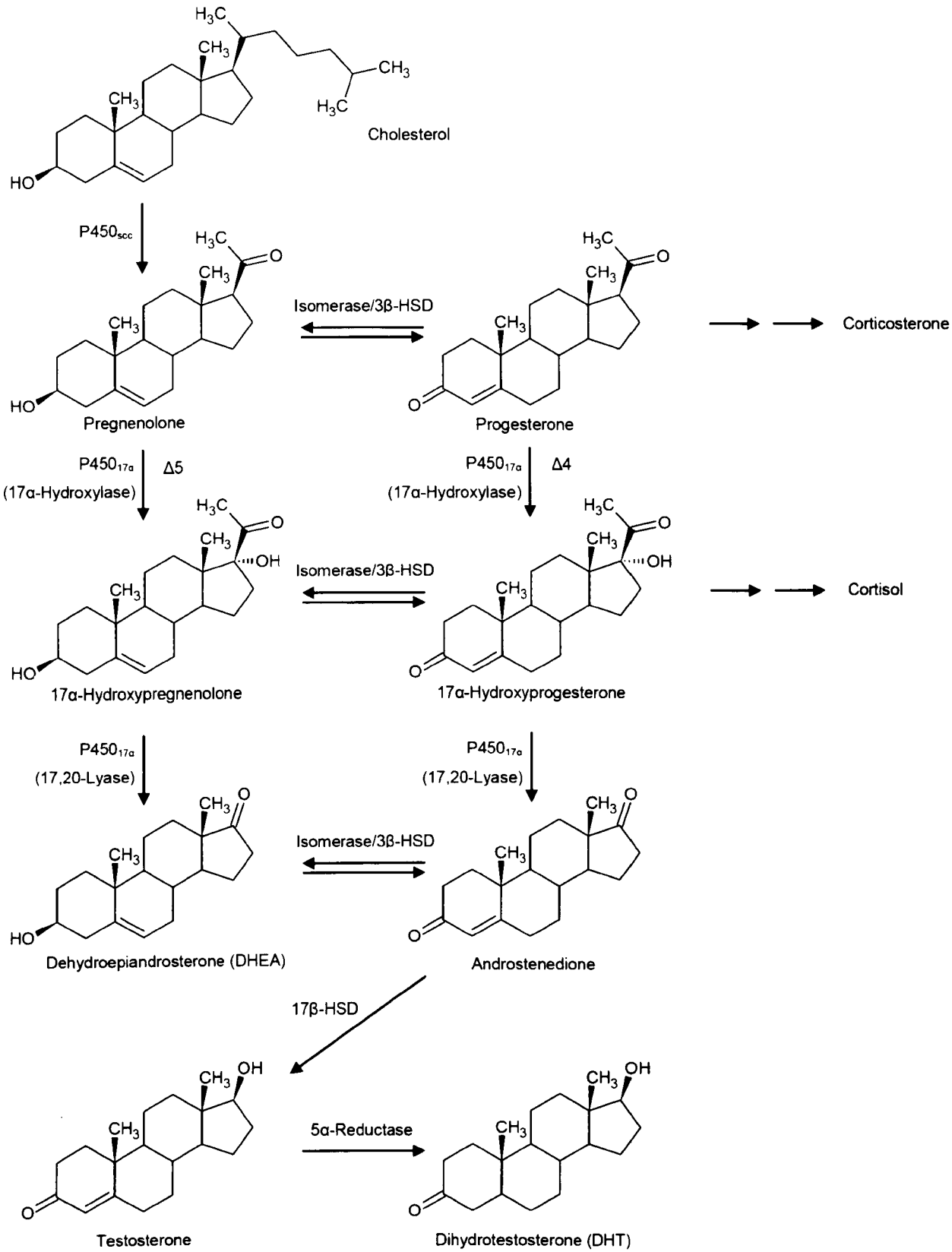

Figure 7 *Showing the steroidal cascade. (HSD = hydroxysteroid dehydrogenase).*

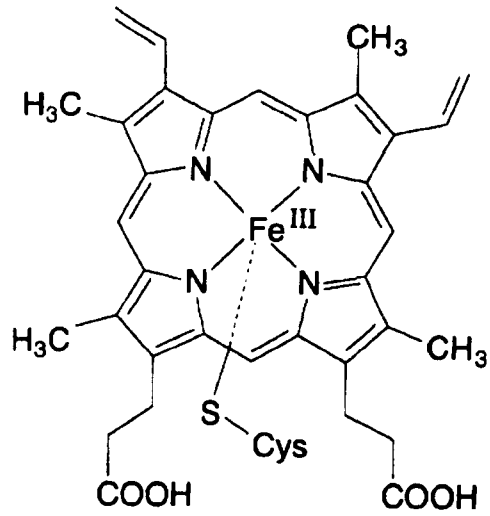

Figure 8 Showing the iron-(III) protoporphyrin with a proximal cysteine ligand of the cytochrome P450 family of enzymes (modified from Meunier[39]).

Cytochrome P450 enzymes are classified as mixed function oxidases or monooxygenases since they incorporate one atom of molecular oxygen into the substrate and one atom into water. The P450 enzymes reductively activate molecular oxygen at the iron centre to a ferrous bound species, which is incorporated into the substrate, therefore increasing its polarity. Transfer of a second electron from a flavoprotein partner, leads to the formation of a ferric peroxy anion[42].

P450 enzymes catalyse different types of reactions, the most important being hydroxylation using an iron mono-oxygen species $Fe^{V}=O$ and acyl-carbon cleavage, where the involvement of an iron peroxide intermediate Fe^{III}-OOH, has been widely suggested. A single redox partner protein, the flavoprotein NADPH-cytochrome P450 oxireductase, assists microsomal P450 enzymes. The generally accepted catalytic mechanism for the P450 catalytic cycle is outlined below and is shown in figure 9.

1. Binding of the substrate to the resting state of the low-spin (LS) ferric enzyme (**1**) takes place, changing the spin state to a high-spin (HS) substrate-bound complex (**2**), resulting from the displacement of water.
2. The HS Fe^{3+} is reduced to a ferrous state by an associated reductase (**3**).
3. Binding of molecular oxygen leads to a dioxy-P450 complex (**4**).
4. A second one-electron reduction takes place, forming a peroxo-ferric intermediate (**5**) with protonation further occurring to give a hydroperoxo-ferric intermediate (**6**).
5. The second protonation at the distal oxygen atom, followed by heterolysis of the dioxygen bond of intermediate **6** with subsequent production of a molecule of water gives rise to a reactive iron-oxo intermediate (**7**).
6. Oxygenation of the bound substrate, from intermediate **7**, results in the formation of the product complex (**1**).

Understanding the structure, active site topology and substrate activity of these enzymes has proven to be problematic as the crystal structure of mammalian P450 enzymes are not so easily achieved once removed from the endoplasmic reticulum (ER)[21]. In an attempt to elucidate structural information of P450 enzymes, the crystal structures of soluble bacterial P450 enzymes have been used by the purification of the membrane-bound enzymes, a process first discovered and facilitated by Ichikawa and Yamano[43].

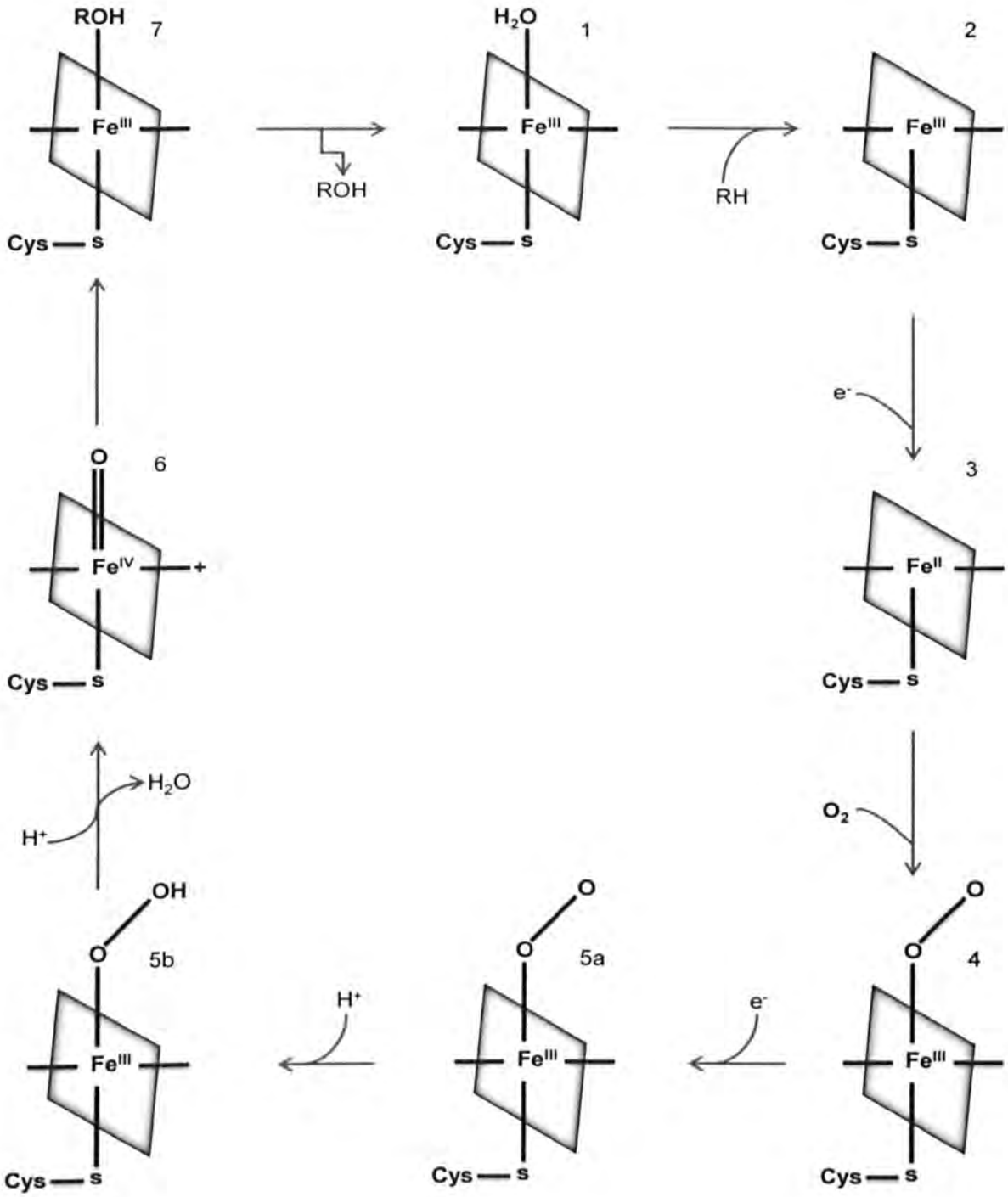

Figure 9 *Showing the P450 catalytic cycle (modified from Sliger[40]).*

1.4 $P450_{17\alpha}$

$P450_{17\alpha}$ has become the hub of research in the prevention of hormone-dependent prostate cancer. It is a bifunctional microsomal enzyme required for reproduction in all vertebrates and is a key enzyme in the synthesis of adrenal and testicular androgens from progestins and the pregnanes. The enzyme is localised within the endoplasmic reticulum in the adrenals, testes and the ovaries and is encoded for by CYP17A1, which is located on chromosome 10 in humans[44].

$P450_{17\alpha}$ was first isolated from neonatal pig testis by Nakajin[45] and was reported to be responsible for catalysing two reactions in the biosynthesis of androgens. The enzyme catalyses both reactions through the transfer of electrons from the flavoprotein NADPH-cytochrome P450 oxidoreductase, with the electron-transfer protein cytochrome b5 enhancing both the 17α-hydroxylase,17,20-lyase activity by allosteric reaction without electron donation. $P450_{17\alpha}$ is enzymatically inactive until it forms a complex with NADPH-cytochrome P450 reductase[44,46].

The 17α-hydroxylase activity of $P450_{17\alpha}$ involves the hydroxylation of pregnenolone and progesterone at the 17α-position, producing 17α-hydroxypregnenolone and 17α-hydroxyprogesterone, with hydroxylation of progesterone leading to the formation of glucocorticoids, precursors in cortisol synthesis within the adrenal cortex[47]. The 17,20-lyase activity of $P450_{17\alpha}$ catalyses the conversion of 17α-hydroxypregnenolone and 17α-hydroxyprogesterone to the corresponding 17-keto androgens dehydroepiandrosterone (DHEA) (Δ^5 pathway) and androstenedione (A) (Δ^4 pathway) respectively, via cleavage of the acetyl group. This step therefore leads to the eventual formation of the androgens[36]. Inhibition of $P450_{17\alpha}$ would therefore bring about a

decrease in the level of androgen production and furthermore prevent the production of the more potent androgens Testosterone and DHT[48] (Figure7).

1.4.1 Proposed mechanisms of action of $P450_{17\alpha}$

$P450_{17\alpha}$ is a membrane bound enzyme and so the crystal structure of the enzyme has yet to be determined. The bifunctionality of $P450_{17\alpha}$ may lead to the hypothesis that both 17-hydroxylase and 17,20-lyase activities are always simultaneous. It is unclear as to the exact nature of the iron-oxygen species involved in the catalytic activity of $P450_{17\alpha}$, however it is believed that the reaction mechanisms for both the hydroxylase and lyase activities involve the formation of distinct iron-oxygen complexes.

With regards to the hydroxylase activity of the enzyme, it has been suggested that the iron-monooxygen species ($Fe^{V}=O$) contributes to the reaction via a free radical mechanism involving hydrogen abstraction by its canonical ferroxy radical ($Fe^{IV}-O$)[49]. Whereas with reference to the lyase activity, the precise nature of the attacking species is still unresolved, however, the involvement of the iron-peroxo, ($Fe^{III}-OOH$), and the iron-oxo are suggested as possible candidates[21,50].

Homology based studies were carried out by Laughton[51] using the crystal structure of the related cytochrome P450 enzyme namely $P450_{cam}$ (bacterial camphor monooxygenase). $P450_{cam}$ was the first cytochrome P450 three-dimensional protein structure to be solved by X-ray crystallography[52]. Laughton[51] reported that the active site consised of an orthoganol bilobed structure, where one lobe was used for binding the substrate for the hydroxylase reaction and the other for the lyase reaction. The bilobed structure of the active site was further investigated using similar homology

based studies on the crystal structure of $P450_{BM-3}$ (from bacillus megaterium, bacterial fatty acid monooxygenase), predicting a similar active site to that reported of $P450_{cam}$[53]. On the contrary to that of Laughton[51], Auchus and Miller[21] had carried out modelling studies using $P450_{BMP}$ (the P450 moiety of $P450_{BM-3}$) as a template and proposed the idea that both the hydroxylase and the 17,20-lyase activities take place within a shared steroid binding site, occupying a single position in the substrate-binding pocket.

In a separate homology study[54] investigated the binding of progesterone at the active site of $P450_{17\alpha}$ by using prokaryotic $P450_{BM-3}$ crystal structure as a template. The study proposed that within the active site the substrate undergoes hydrogen bonding at the C3 carbonyl bond with a threonine residue (The77) and that the D-ring keto group undergoes hydrogen bonding interaction with a tyrosine (Tyr177) residue.

The orientation of the iron within the active site of 17α-hydroxylase with respect to the steroid backbone was postulated from the mechanism of $P450_{17\alpha}$ and on the assumption that this mechanism was similar to that of the estrogen synthetase enzyme $P450_{arom}$, a cytochrome P450 enzyme involved in the final step of the steroidal cascade[55], converting A to estrone and T to estradiol (Figure 10).

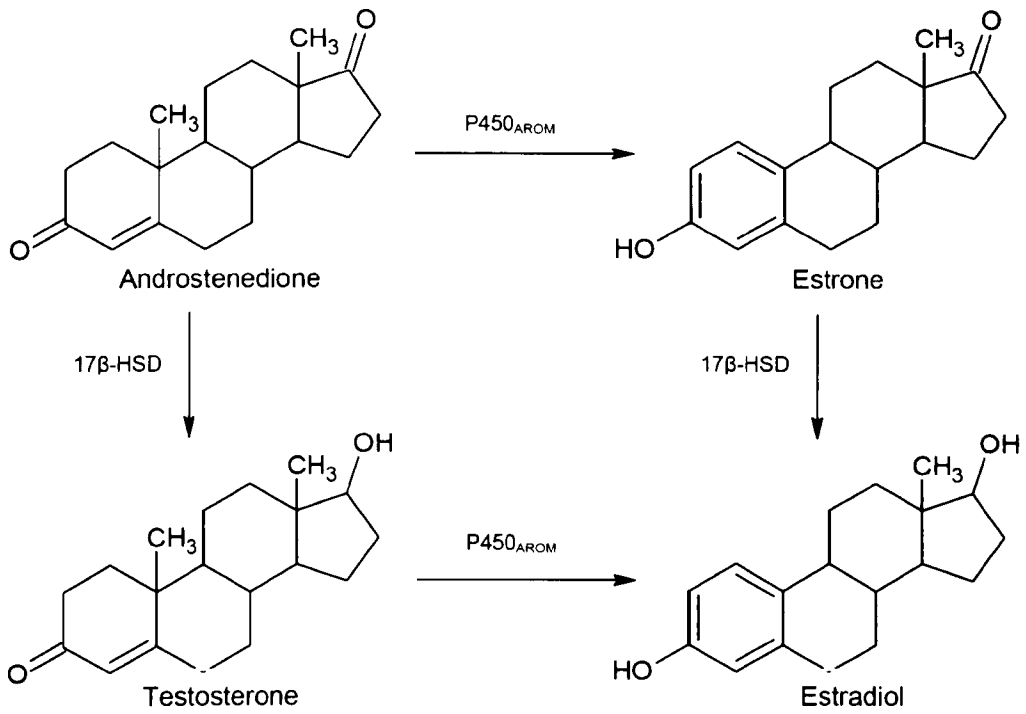

Figure 10 Showing the conversion of the androgens Androgen and Testosterone to the estrogens Estrone and Estradiol by the enzyme action of $P450_{arom}$.

For the hydroxylation step, the following mechanism was reported by Lee-Robichaud et al[54] (Figure 11). Complex **1** and **4** are shown to be the same as that of the P450 catalytic cycle (Figure 9), with the various steps carried out in order to produce a peroxy anion species. Complex **4** is further protonated, by a neighbouring amino acid residue, to produce a hydro-peroxy species **5**. Dehydration occurs as additional donation of a proton results in the formation of a feroxy radical species **6**. Hydrogen removal from the C(17) of the substrate by the feroxy radical species (**6**) results in the hydroxylation of the haem to produce an Fe^{IV}-OH species as well as radical formation at the C(17) position of the substrate.

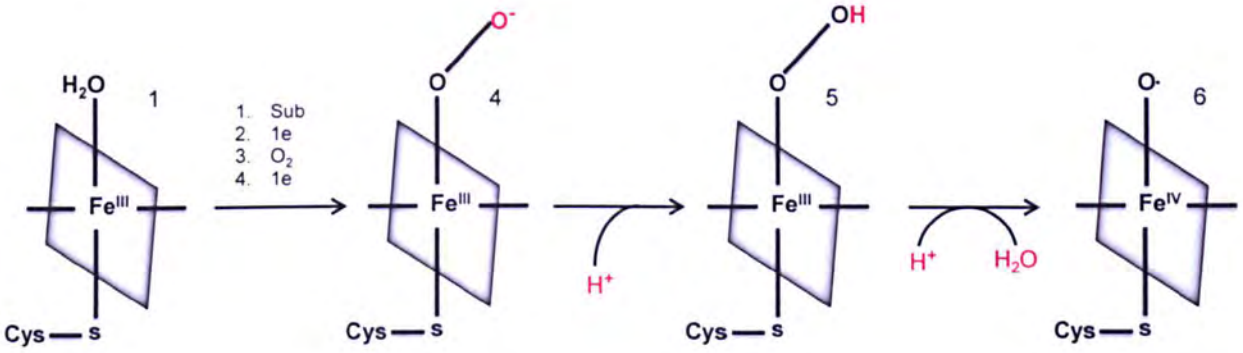

Figure 11 Showing the various steps involved in the production of peroxy anion species and the ferroxy radical (modified from Lee-Robichaud et al[54]).

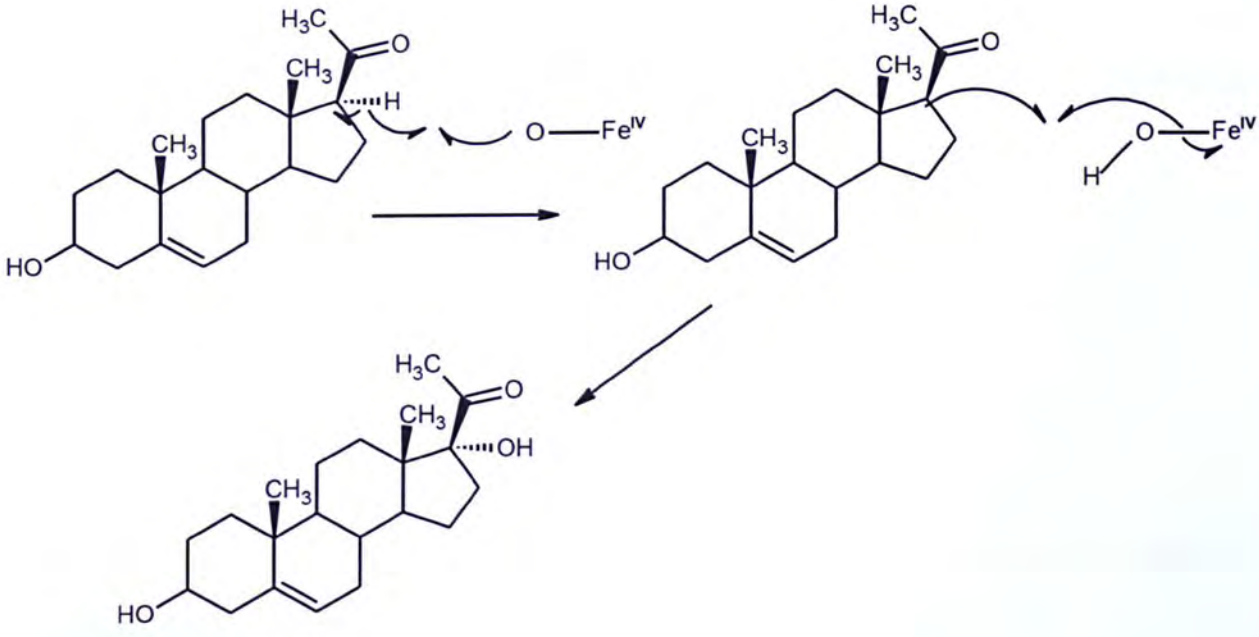

Figure 12 Showing the P450$_{17\alpha}$ catalysed 17α-hydroxylase step (modified from Lee-Robichaud et al, 1998).

The lyase step, which involves the cleavage of the (C)17-(C)20 bond to produce DHEA and androstenedione respectively, is not well understood, however, several mechanisms have been suggested. Lee-Robichaud[56] proposed that nucleophilic attack

of a ferric-peroxy anion (FeIII–O–O−) on the acyl carbon furnishes a tetrahedral intermediate which fragments, producing an alkoxy radical at the oxygen attached to the C(20) group on the substrate and a one electron oxidised feroxy radical species (Fe^{III}-O˙) (Figure 13). The alkoxy radical auto-disintergrates, expelling the side chain as acetic acid. A stable carbonyl moiety is formed at the C(17) position, producing the androgen DHEA and further resulting in the reformation of the Fe^{III} haem[54,56] (Figure 13).

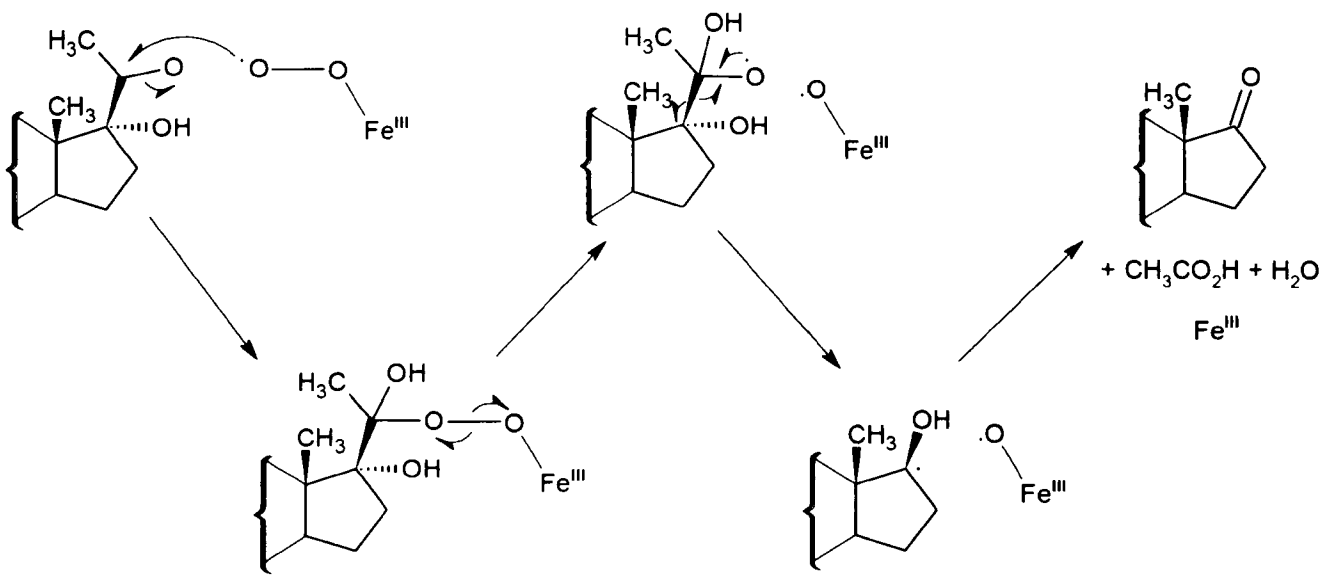

Figure 13 Showing the proposed mechanism of action of the $P450_{17\alpha}$ catalysed 17,20-lyase step, resulting in DHEA (modified from Lee-Robichaud et al[56]).

In studies carried out by Ahmed and Owen[50] and Ahmed and el[57], the proposed mode of action of $P450_{17\alpha}$ was hypothesised using innovative molecular modelling techniques. The substrate haem complex (SHC) method was specifically applied to rationalize the activity of both the 17α-hydroxylase and 17,20-lyase mechanisms of the enzyme activesite. They proposed that both the individual components of the enzyme are catalysed by the initial ferroxy radical species.

In the lyase step, which involves the conversion of 17α-hydroxypregnenolone and 17α-hydroxyprogesterone to DHEA and Androstenedione respectively, Ahmed and Owen[50] hypothesised that the oxygen radical must be positioned within the approximate bonding distance to the C(20) carbonyl of the substrate (Figure 14).

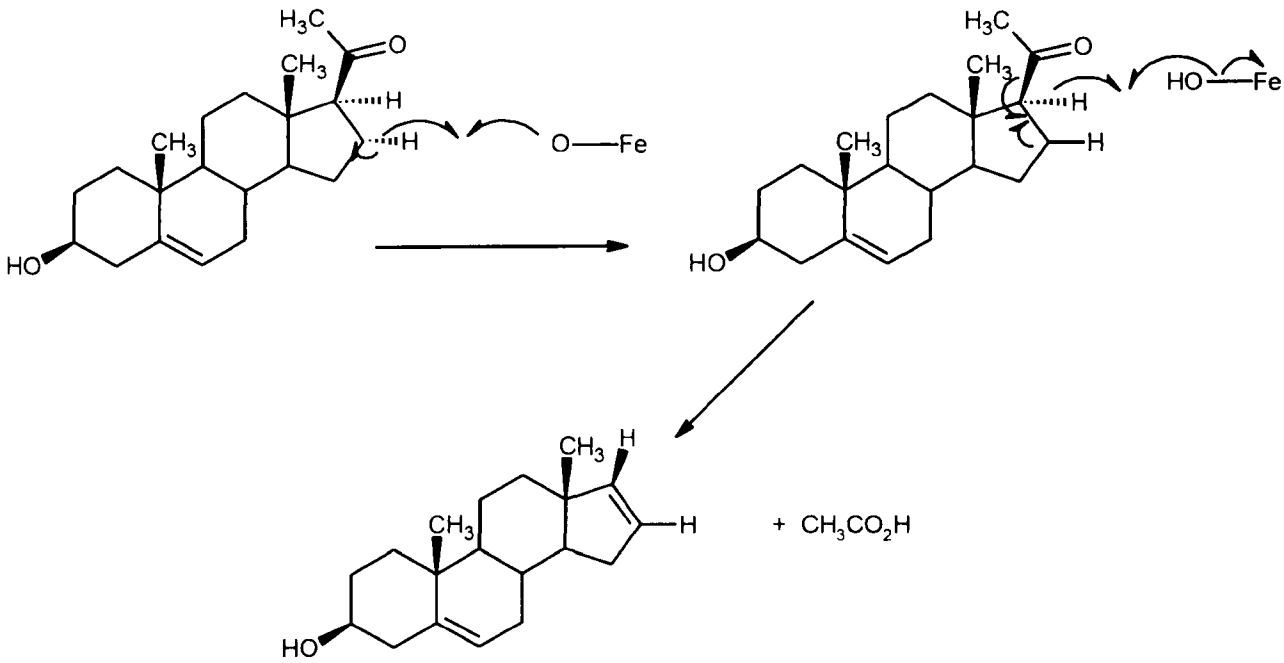

Figure 14 Showing the proposed mechanism of action in the formation of androst-5,16-diene-3β-ol using the ferroxy attacking radical (modified from Ahmed et al[57]).

This is in order to undertake hydrogen removal from the C(17) of the steroid such that when the Fe^{IV}-OH species is formed, the C(17) can be 'neutralised' by the formation of a bond with the Fe^{IV}-OH, resulting in the hydroxylation of the C(17) position ofprogesterone and the reformation of the Fe^{III} haem (Figure 14).

As previously stated, Auchus and Miller[21] conducted homology based studies which further supported this idea, where the involvement of an iron oxene species, could theoretically be utilized in the lyase step as well as the hydroxylase step (Figure 15).

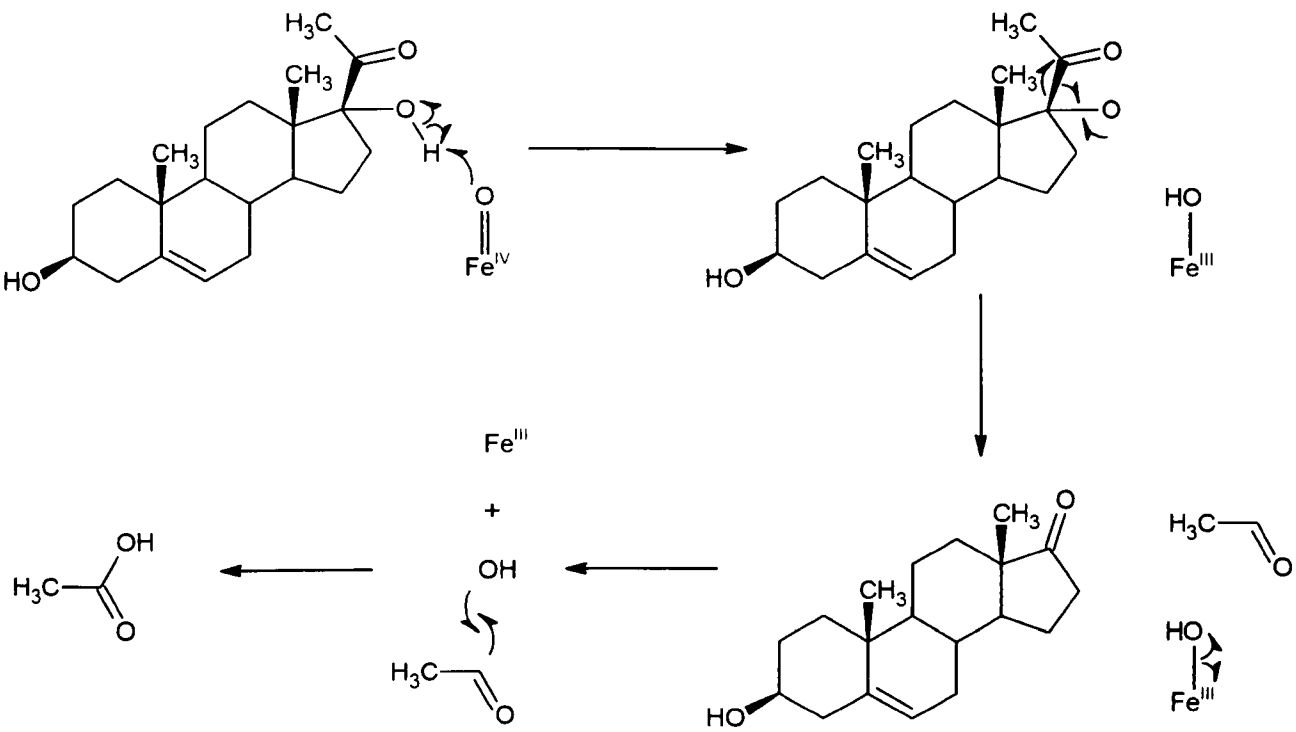

Figure 15 Showing the proposed mechanism of action for the 17,20-lyase reaction (modified from Auchus and Miller[21])

The proposal was based upon findings which showed that the hydrogen atom of the 17α-hydroxy group (17α-hydroxypregnenolone) remained in closer proximity to theoxene species than any other steroid atom. This conclusion resulted in the proposed mechanism for the lyase step by Auchus and Miller[21] (Figure 16) where the ferryl oxene abstracts the hydrogen atom at the C(17) of the substrate 17α-hydroxypregnenolone, generating a hydroxyl radical species which fragments to form DHEA and an acetyl radical. Recombination of the iron hydroxyl with the acetyl radical results in the regeneration of the resting-state haem and the formation of acetic acid.

1.5 Inhibitors of $P450_{17\alpha}$

In order to attempt the inhibition of the enzyme $P450_{17\alpha}$, a number of inhibitors have been synthesised to mimic the characteristics of the natural substrate structurally as well as mechanistically, with the aim of binding to and blocking the enzyme active site. There are a number of classes of inhibitors of $P450_{17\alpha}$ which can be categorised into steroidal and non-steroidal inhibitors and further subdivided according to their mode of action, i.e. reversible (competitive or non-competitive) or irreversible as well as the mode of binding to the active site of the enzyme, for example, type I or type II. The irreversible inhibition of the inhibitor will generally arise from its activation by $P450_{17\alpha}$ into a reactive metabolite, which binds tightly to the active site of the enzyme, resulting in long-term inactivation.

Type I inhibitors are compounds which interact with the substrate binding of $P450_{17\alpha}$ in a competitive and reversible manner, thereby generating a shift in the UV-absorption spectrum Soret band maximum from approximately 420nm to approximately 390nm, giving a so called Type 1 difference spectrum. Conversely, Type II inhibitors interact as the sixth ligand with the haem atom, most favourably by compounds that contain a heteroatom (e.g. N, S, O) possessing a lone pair of electrons in order to undergo coordination with the haem iron. Compounds which carry a nitrogen containing heteroatom produce a Type II difference spectrum on binding with $P450_{17\alpha}$ with Soret maximum at 421-430nm and minimum at 390-410nm[58].

1.6 Steroidal Inhibitors

Steroidal inhibitors are based upon the natural substrates of $P450_{17\alpha}$ i.e. pregnenolone or progesterone, where modification of the A-ring about the C(3) region and the D-ring about the C(17) region has been considered and furthermore has lead to the development of very potent steroidal inhibitors. Steroidal inhibitors interact with the active site of the enzyme by mimicking the natural substrate.

In the past decade, a number of steroidal inhibitors have been synthesised, showing potent inhibitory activity against $P450_{17\alpha}$. Steroid-related side effects are potentially a risk with steroidal agents and the lipophilic steroidal skeleton can produce low aqueous solubility and may prevent oral administration. Independent of their mode of action, steroidal compounds often show some affinity towards one or several steroid receptors, thereby acting as agonists or antagonists, where an agonist will bind to a receptor of a cell and trigger a response by that cell, an antagonist will simply block the action of the agonist[59].

1.6.1 Mechanism-based steroidal $P450_{17\alpha}$ inhibitors.

Mechanism-based inhibitors result in the irreversible inhibition of $P450_{17\alpha}$. This occurs due to the transformation of the inhibitor(s) into a species that is able to form covalent bond(s) with the active site of the enzyme, as a result in the disruption of the enzymes normal catalytic mechanism. Angelastro[60] had reported a potent time- and concentration-dependent inhibitor of cynomolgus monkey testicular $P450_{17\alpha}$, which was shown to be competitive with the substrate by kinetic studies.

The mechanism-based inhibitor cyclopropylamine 17β-(cyclopropylamino)andros-5-en-3β-ol (Figure 16) was designed to be activated via enzymatic one-electron oxidation of the cyclopropylamino nitrogen, which resulted in the rapid opening of the ring to produce a β-iminium radical, enabling it to react covalently with the enzyme whilst the drug was bound to active site of $P450_{17\alpha}$.

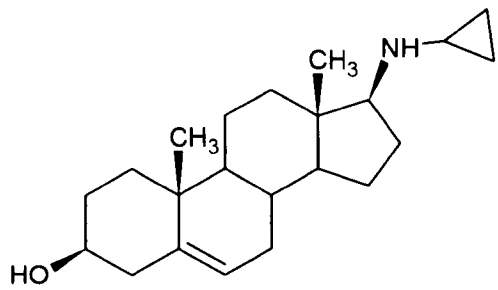

Figure 16 Structure of 17β-(cyclopropylamino)andros-5-en-3β-ol (MDL 27302).

Angelastro[46] synthesised further 17β-cyclopropyl ether-substituted steroids, which had been shown to inhibit the enzyme in a time-dependent manner of both human and cynomolgus monkey testicular enzyme by also undergoing rapid ring-opening by one-electron oxidation (Figure 17).

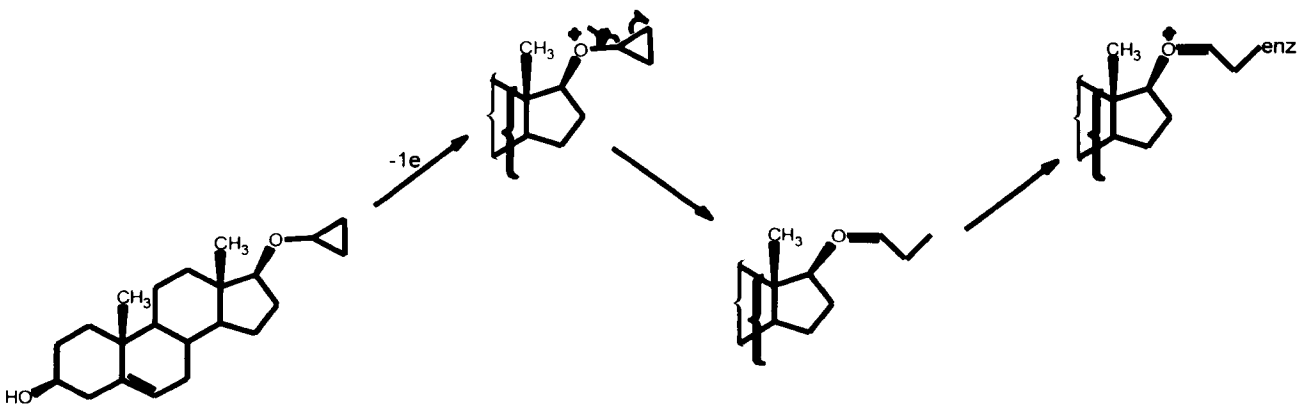

Figure 17 Showing the proposed mechanism-based inactivation of 17β-cyclopropyl ether-substituted inhibitors (modified from Angelastro[46]).

Inhibition was shown to be more potent in some cases after preincubation of the enzyme with the inhibitor. Compound (**1**) was shown to be the most potent when tested with the human enzyme (Table 1).

Compound No	Structure	Pre-incubation(time, mins)	% Inhibition (μM)
1	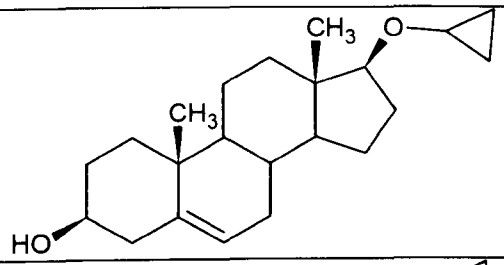	0 30	11 64
2	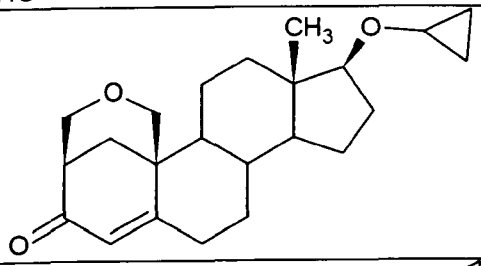	0 30	1 17
3	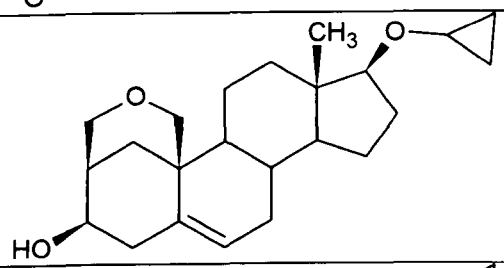	0 30	0 0
4	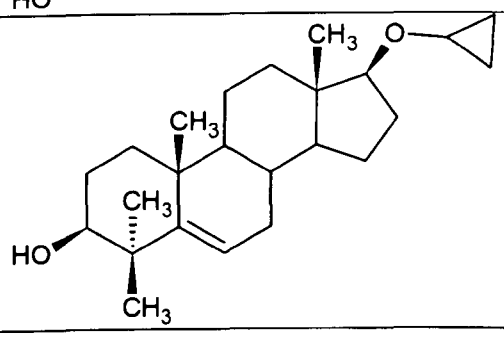	0 30	0 0

Table 1 *Showing the inhibition of human testicular $C_{17(20)}$ lyase ([I]=0.8μM)*

Compounds (**2**, **3** and **4**) had shown little affinity for human $P450_{17\alpha}$, therefore indicating that the modifications to the A ring of these compounds clearly prevented binding at the

catalytic site of the enzyme. Hence, further indication to the importance of C(3) in binding to the enzymes active site, as structure **1** closely follows the design of that of the natural substrate.

Overall, MDL 27302 had shown to be a potent, irreversible competitive inhibitor of cynomolgus monkey testicular cytochrome $P450_{17\alpha}$ by kinetic studies, with a K_i value of 90nM and furthermore showed evidence of selectivity as it had shown poor inhibition of steroid 21 hydroxylase.

Burkhart et al[61] also developed a number of 20-fluoro-17(20)-pregnenolone derivatives, which were believed to act as enol mimics and were reported to be potent time-dependent inhibitors of cynomolgous monkey $P450_{17\alpha}$ at given concentration (Figure 18). However, the results showed that only compound **7**, the Z-isomer, had clearly shown time dependency with respects to compounds **5**, **6** and **8** (Table 2).

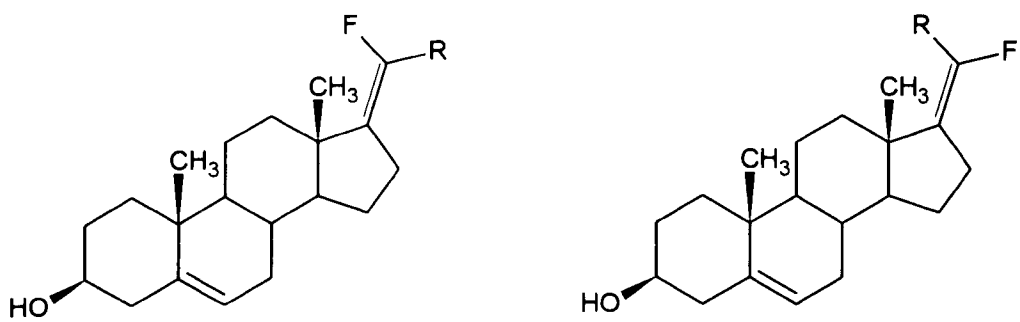

Z-isomer E-isomer

Figure 18 Showing the structures of vinyl fluoride $C_{17(20)}$ pregnenolone enol mimics (Burkhart et al[61])

Compound No.	Isomer	R group	Concn (μM)	Inhibition (%)
5	Z	CH_2OH	10 1 10 1	100 96 100 94
6	E	CH_2OH	10 1 10 1	85 63 87 61
7	Z	CH_3	10 1 10 1	78 49 94 72
8	E	CH_3	10 1 10 1	88 54 94 60

Table 2 Showing potent 20-fluoro-17(20)-ene pregnenolone inhibitors of cynomolgous monkey $P450_{17\alpha}$.

Weintraub et al[62] further synthesised a number of novel 21,21-difluorovinylsteroids, which were designed as difluorinated $C_{20(21)}$ enol mimics of pregnenolone as potential mechanism-based inhibitors of $P450_{17\alpha}$ (Figure 19).

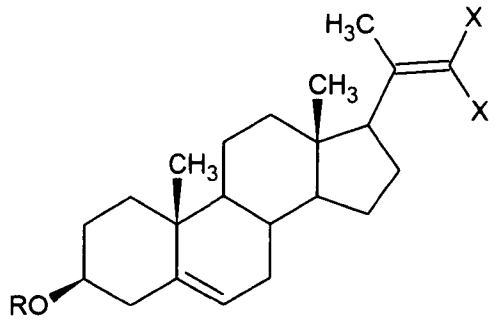

Figure 19 Showing the structure of vinyl fluoride $C_{20(21)}$ pregnenolone enol mimic (Weintraub et al[62])

Compounds **9-14** were evaluated for their capability to inhibit cynomolgous monkey $P450_{17\alpha}$ at two concentrations of inhibitor (Table 3). From his studies, weintraub[62] reported that the Z-isomer had shown time-dependent inhibitory activity, which was also previously observed by Burkhart et al[61].

Compound no	Enol mimic	Concentration (μM)	Preincubation (min)	Inhibition (%)
9	Z $C_{17(20)}$	10 10 1 1	0 40 0 40	78 94 49 72
10	E $C_{17(20)}$	10 10 1 1	0 40 0 40	88 94 54 60
11	$C_{20(21)}$	1 1 0.1 0.1	0 40 0 40	10 40 11.5 8
12	$C_{20(21)}$	1 1 0.1 0.1	0 40 0 40	7 12 5 5
13	$C_{20(21)}$	1 1	0 40	70 60
14	$C_{20(21)}$	1 1	0 40	64 62

*Table 3 Inhibition of cymologous monkey testicular $C_{17(20)}$ lyase with fluoroolefin enol mimics of pregnenolone and $C_{20(21)}$ enol mimcs (**9** R=CH_3; **10** R=CH_3; **11** R=H, X=F; **12** R=Ac, X=F; **13** R=H, X=H; **14** 16,17-unsaturated version R=H, X=F) (Weintraub et al[62]).*

The difluoro $C_{20(21)}$ enol mimic (**11**) was the only new compound synthesised to possess time-dependent behaviour at 1μM concentration of the inhibitor though results have shown it to be less potent than the Z- and E-isomers previously studied by Burkhart[61]. However, compounds**13** and **14** had still shown potent inhibition of the enzyme at both test concentrations (Table 3).

From the data shown in Table 3, the authors concluded that the monofluoro olefin were more potent than the difluoro-based compounds. Compound **12**, the *O*-acetate-based inhibitor of compound **11** had shown extremely weak inhibition, clearly stating the importance of the free hydroxyl group at the C(3) position of ring A for active site affinity. Compound **13** had shown to be a potent inhibitor; however, it did not display time dependency, suggesting that fluoro groups may be required for that area of enzyme inhibition. The 16, 17-unsaturated analogue **(14)** was again a potent inhibitor of the monkey enzyme but did not show time-dependency, further suggesting that the conjugation may entail geometry suitable for active site affinity, but not in a time-dependent manner.

Njar et al[63] reported a number of 20-amino and 20,21-aziridinyl pregnene steroids which were designed as mechanism-based inhibitors towards rat testicular $P450_{17\alpha}$ (Table 4). The Aziridine compounds **15-18** were shown to be highly active inhibitors of $P450_{17\alpha}$, their inhibitory activity being noticeably dependent upon the stereochemistry observed at the C(20) position. The 20(*S*)-aziridinyl steroids (**15** and **17**) were generally found to be more potent than the corresponding (*R*)-enantiomers (**16** and **18**). Dissimilarity was also observed in the inhibitory potency between the pregnenolone-based aziridine inhibitors (**15** and **16**) and the corresponding progesterone-based derivatives (**17** and **18**), where the former was shown to be the more potent.

Compound No.	Structure	IC_{50} (μM)
15	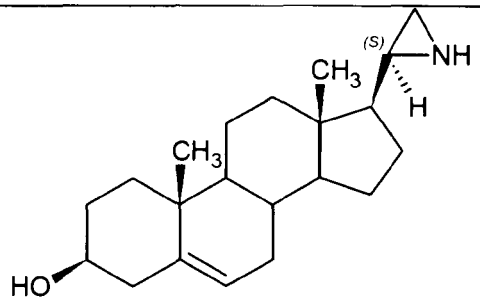 (*S*)-enantiomer	0.21
16	(*R*)-enantiomer	34
17	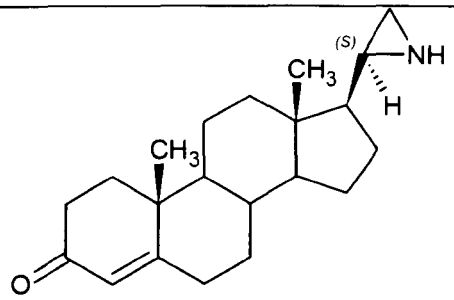 (*S*)-enantiomer	1.2
18	(*R*)-enantiomer	36
	KTZ	67

Table 4 Showing the inhibitory activity of 20-substituted pregnene inhibitors towards rat testicular $P450_{17\alpha}$ against the standard KTZ (Njar et al[63]).

In contrast, the corresponding 20 amino steroids were found to be weak inhibitors towards rat testicular $P450_{17\alpha}$, all with IC_{50} values of >125μM. The results further indicated the significance of the spacing between the amino group and the haem iron, in order for binding to occur at the enzyme active site. Compound **15** was shown to be the most active derivative in the range, with results showing it to be 319 times more potent than the inhibitor KTZ , furthermore, compound **15** was also shown to be the most potent inhibitor (IC_{50} = 0.21μM, K_i = 1.7nM) towards rat testicular $P450_{17\alpha}$.

1.6.2 Type I steroidal inhibitors.

Inhibitors of cytochrome P450 enzymes can be categorised depending on their binding to the active site of the enzyme. Once bound to the active site, Type I inhibitors displace water as the sixth ligand of the Fe haem, resulting in the Fe atom existing in a high spin (pentacoordinate) state, which produces a distinctive spectral shift with absorption atapproximately 390nm. Therefore, type I inhibitors prevent the natural substrate from binding to the active site by occupying the active site[64].

1.6.2.1 Type I Steroidal inhibitors: Hydroxy- and Oxime-based compounds

Li et al[65] synthesised a series of steroidal compounds which were based on the Δ^4progesterone and Δ^5 pregnanes and were considered to act as Type I inhibitors when tested on human testicular $P450_{17\alpha}$. Compounds based on pregnenolone were commonly found to be more potent than those based upon progesterone, as pregnenolone has been shown to be the natural and preferred substrate of human $P450_{17\alpha}$. This suggested that the A and B rings of the steroid backbone play an imperative role in the binding of the inhibitor to the enzyme active site. In more recent studies Matsunaga et al[66] proposed that the substrate 17α-hydroxypregenolone binds at the active site via hydrogen bond formation with the 3β-hydroxy group and an amino acid residue such as Thr101.

In their studies, Li et al[65] established that compounds containing 20-oxime (**19, 20**) and *20β*-ol (**21, 23**) were shown to be potent inhibitors of both 17α-hydroxylase and $C_{17,20}$-lyase (Table 5 and 6).

Compound	Structure	IC_{50} (μM) 17α-hydroxylase	$C_{17,20}$-lyase
19	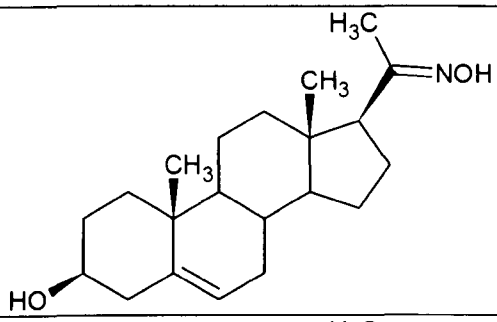	0.53	0.57
20	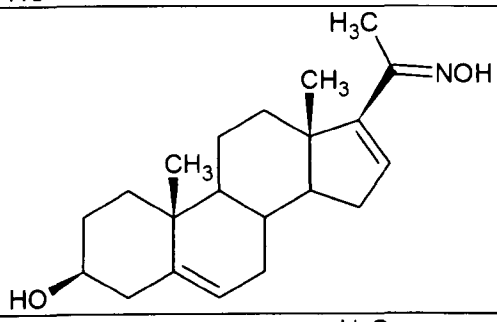	0.016	0.016
21	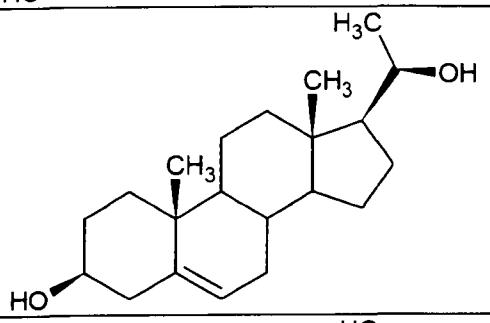	0.18	0.19
22	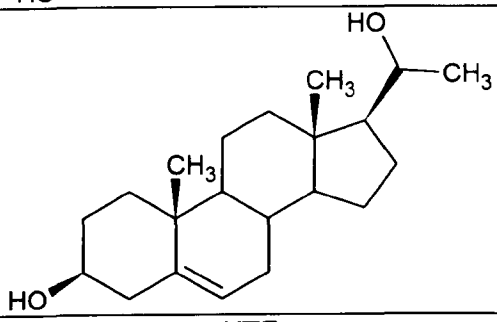	0.72	0.51
	KTZ	0.86	0.92

Table 5 Showing the inhibitory activity of Δ^5 pregnanes against human $P450_{17\alpha}$.

This increase was also reported by Ling et al[67] who had also reported 20-hydroxy and 20-oxime-based steroidal inhibitors. In particular compounds **21** and **23** also suggests that the orientation at the C20 may influence the potency of the compound as 20β-ols had shown to be 3-6 fold more potent than compounds **22** and **24**, indicating that some

steric factor may be involved in the binding of these compounds to the active site. Ling et al[67] further revealed that compounds containing a C16=C17 double bond had comparable inhibitory activity against $P450_{17\alpha}$ and that epimeric 20-hydroxy pregnane derivatives had demonstrated mild to moderate inhibition of $P450_{17\alpha}$.

Compound	Structure	IC_{50} (μM) 17α-hydroxylase	$C_{17,20}$-lyase
23	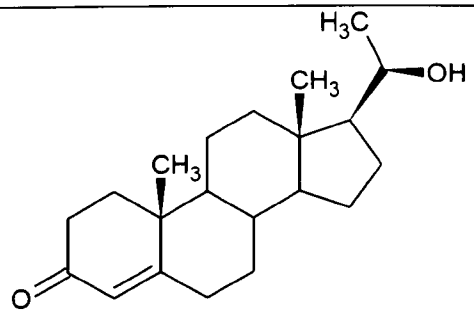	0.49	0.24
24	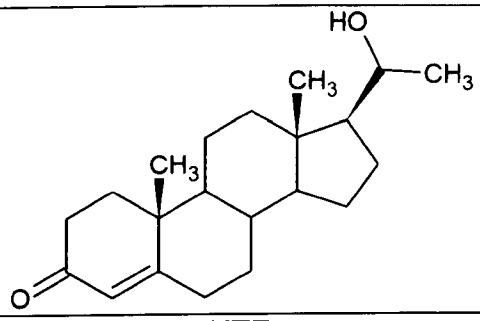	2.84	1.43
	KTZ	0.86	0.92

Table 6 Showing the inhibitory activity of Δ^4 pregnanes against human $P450_{17\alpha}$ (Li et al[65]).

Further compounds had been synthesised and evaluated, these being epimeric 20-hydroxy, 20-oxime pregnadienes and aziridine derivatives, where the introduction of a 16,17-double bond into the steroid nucleus had enhanced the activity of the compounds as inhibitors of $P450_{17\alpha}$. The inhibitory activities of the 20-hydroxy epimers are evaluated in Table 7.

Compound No	Structure	Inhibition at 150nM (%)	Human $P450_{17\alpha}$ IC_{50}(nM)
25	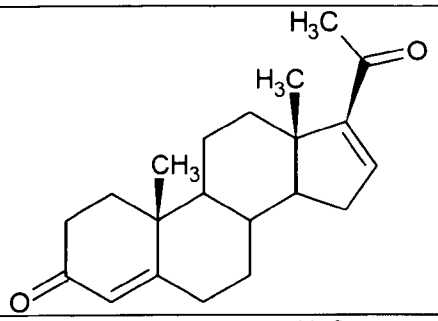	12.4	Weak
26	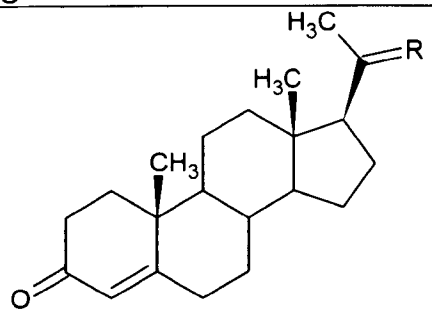 R = NOH	76.7	43
27	R = NOAc	83.8	25
28	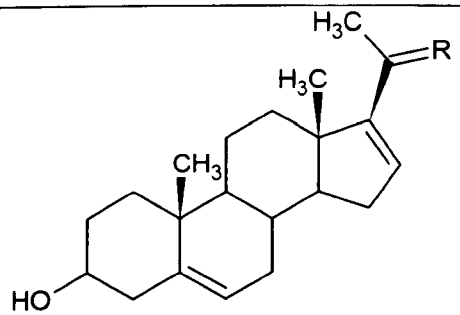 R = O	7.2	510/490
29	R = NOH	80.3	73
30	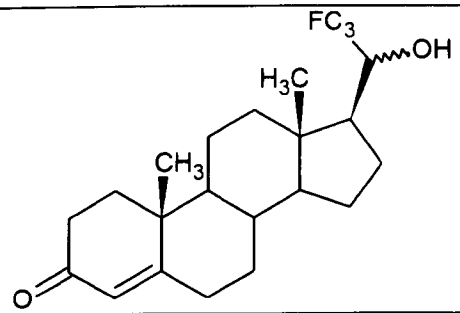	98.6 (1500nM, %)	184nM(rat $P450_{17\alpha,}$)

Table 7 Showing the inhibitory activity of Δ^4 and Δ^5 pregnanes against human $P450_{17\alpha}$. [KTZ IC_{50} = 78nM ($P450_{17\alpha}$) inhibition at 150nM = 69.5]/[KTZ IC_{50} = 900nM (rat $P450_{17\alpha,}$) inhibition At 1500nM = 65.3]. Ling et al[67].

From the data, it was proposed that these compounds were weak inhibitors of human $P450_{17\alpha}$. The pregnenolone-20-oxime compounds showed only moderate potency with the exception of compound **29** which was found to possess an IC_{50} of 73nM whilst compound **26** was found to possess an IC_{50} value of 43nM against human $P450_{17\alpha}$, which was unexpected as human $P450_{17\alpha}$ had been shown to possess greater preference towards pregnenolone in comparison to progesterone as a substrate. The evaluation of the weak activity of **25** in comparison to **26** and the activity of **28** in comparison to **29** demonstrated that the derivatisation to the 20-oxime group increased the inhibitory activity against $P450_{17\alpha}$. Acetylation of the 20-oxime (e.g. **27**) was shown to further increase the inhibitory activity against $P450_{17\alpha}$.

The aziridine derivatives were designed such that the nitrogen atom was expected to undergo coordination to the haem iron of the enzyme, whilst the aziridine ring was expected to undergo covalent bonding to the active site, thereby leading to the irreversible inhibition of the enzyme. These compounds, however, proved to be weak inhibitors of human $P450_{17\alpha}$, although compound **30** which was found to be a potent inhibitor against rat $P450_{17\alpha}$, possessing an IC_{50} value of 184nM, as such it was found to be five times more potent than KTZ (IC_{50} = 900nM).

1.6.2.2 Type I Steroidal inhibitors: *ent*-progesterone

Auchus et al[68] carried out a study to explore the active site of $P450_{17\alpha}$ by synthesising *ent*-progesterone from *ent*-Testosterone to determine as to whether the enantiomer of natural progesterone was a competitive inhibitor of $P450_{17\alpha}$ (Figure 21). *Ent*-progesterone was found to inhibit 17α-hydroxyprogesterone (17α-OHase) in an entirely competitive manner (K_i = 0.2μM of 17α-OHase) and was also shown to have high affinity when binding to the substrate of $P450_{17\alpha}$ producing a Type I difference spectrum.

However, the results also showed that the spectral change (which was observed from *ent*-progesterone) was less than that observed within the spectra of progesterone by almost 50%.

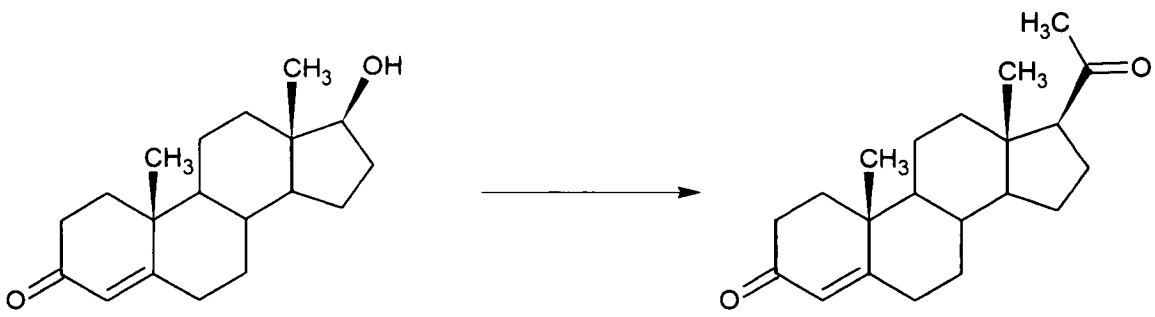

Figure 20 *Showing the synthesis of ent-progesterone from ent-testosterone.*

It was therefore concluded that the *ent*-progesterone was unable to displace the sixth ligand of the haem Fe as effectively as the substrate progesterone and that this suggested that this compound did not bind to the active site in the same way as progesterone. Molecular dynamics simulations indicated that *ent*-progesterone was situated perpendicular to the haem in the active site where as the steroid backbone of progesterone lies parallel to the haem, hence resulting in the haem centre being too far away to achieve oxygenation of *ent*-progesterone.

1.6.3 Type II steroidal inhibitors

There are a number of type II steroidal based inhibitors which have been synthesised containing groups able to form a coordinate bond with the Fe atom of the haem cofactor. Type II inhibitors bind within the active site and displace the sixth ligand of the haem Fe, allowing the inhibitor to coordinate the haem as the sixth ligand, resulting in Fe existing in a low spin (hexacoordinate) state with an absorption maximum between

421-430nm. Type II inhibitors usually contain a heteroatom which is able to donate a lone pair of electrons to the haem Fe, undergoing a coordinate bond formation, with the remainder of the inhibitor mimicking the natural substrate[69,70].

1.6.3.1 Type II steroidal inhibitors: Pyridyl and amide-based compounds

Potter et al[71] reported potent inhibitors of human $P450_{17\alpha}$ comprising of a number of pyridyl containing steroid compounds. Abiraterone (**32**), a 17-pyridyl based steroidal inhibitor with a C(16)-C(17) double bond in the D-ring, was approved for clinical trials in 1995[72] and was seen to be a potent, selective and irreversible steroidal inhibitor compared to KTZ, showing potent inhibitory activity against the human $P450_{17\alpha}$, with an IC_{50}value of 4μM against 17α-hydroxylase and 2.9μM against 17,20-lyase[73].

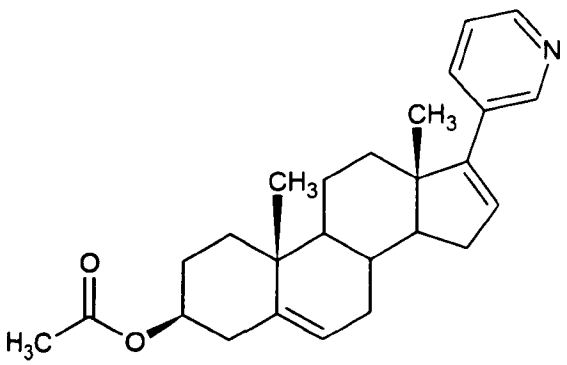

Abiraterone Acetate (**31**)

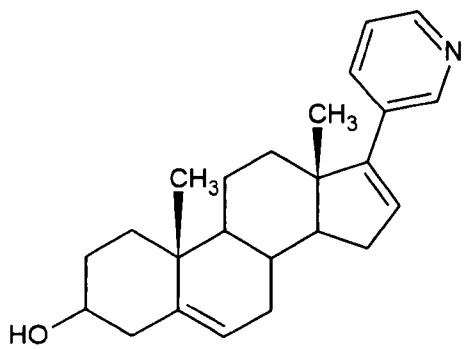

Abiraterone (**32**)

It was reported that the attachment of a 3-pyridyl substituent to the C17-position of a steroid with a $\Delta^{16,17}$-bond may lead to optimal binding to the haem Fe at the active site of the enzyme by potentially donating its lone pair of electrons and in doing so, forming a dative covalent bond with the Fe of the haem moiety[74]. Abiraterone (**32**) and its acetate prodrug, abiraterone acetate (**31**), have been shown to suppress circulating testosterone levels in mice and rats. Its 3-acetate prodrug is currently undergoing phase III clinical trials and has been shown to be well tolerated in prostate cancer patients[75].

Hartmann et al[48,59] had synthesised various steroidal inhibitors bearing a pyridine ring or an amide group connected directly to the steroidal D ring with a double bond at the C(16)-C(17) position (Tables 9 and 10). Haidar and Hartmann[59] had discovered that the position of the nitrogen within the pyridine ring along with its position in the steroidal D ring, i.e. at the C(16) or the C(17) position, contributed to the inhibitory activity of the compounds. The C(17) pyridyl-based inhibitors (**33**, **35** and **37**) showed potent inhibitory activity, with IC_{50} values of 0.11μM, 0.074μM and 0.003μM respectively in humans as opposed to the C(16) pyridyl inhibitors (**34**, **36** and **38**), which showed hardly any inhibition when tested *invitro* for human and rat $P450_{17\alpha}$ with progesterone as substrate (25μM) (Table 8).

Furthermore, Haidar and Hartmann[59] attempted to produce an active inhibitor by introducing a 2-pyridylmethyl moiety at either the C(16) or C(17) position the D ring. Compound **39** (Table 10) and its C(16) counterpart (**40**) both showed poor activity. This may possibly have been due to the position of the nitrogen within the pyridyl ring not being able to interact with the haem iron of $P450_{17\alpha}$ as a result of steric hindrance. The 4-pyridyl-based inhibitor (**41**, IC_{50}=4.0μM for human) and the C(17) amide-based compound **43** (IC_{50}=0.29μM for human) showed improved activity in comparison to compounds **39** and **40**.The C(16) analogues (**42** and **44**) produced very poor activity against human $P450_{17\alpha}$ (Table 9).It was therefore concluded that the C(17) position within the steroid backbone played a pivotal role in the inhibition of the enzyme and furthermore, any substitution at this position was likely to result in potent inhibiton[59].

Compound No	Structure	% inhibition Human (IC_{50},μM)	% i nhibition Rat (IC_{50}, μM)
33	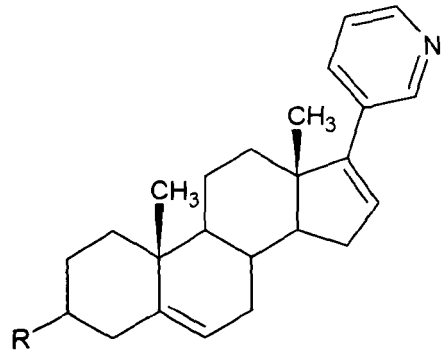 R = $OCOCH_3$	0.11	0.16
34	C(16)-substituted pyridyl inhibitor R = $OCOCH_3$	NI**	19%*
35	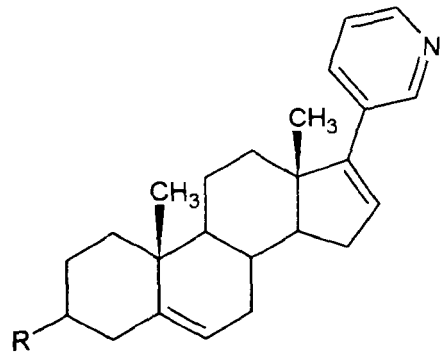 R = OH	0.074	0.20
36	C(16)-substituted pyridyl inhibitor R = OH	NI**	18%*
37	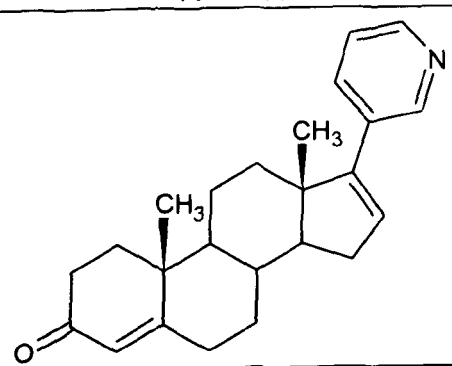	0.003	ND
38	C(16)-substituted pyridyl inhibitor	NI**	24%*
	KTZ	0.74	0.67

*Table 8 Showing pyridyl-based steroidal inhibitors. NI = no inhibition, ND = not determined, **([I] = 2.5μM), *([I] = 125μM)*[59].

Compound No	Structure	% inhibition Human (IC_{50},μM)	% inhibition Rat (IC_{50}, μM)
39	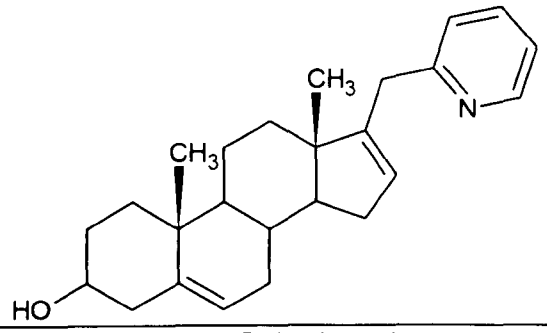	>10.0	ND
40	16 – Substituted	10%**	NI*
41	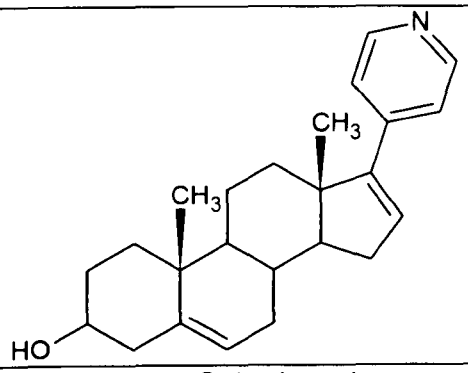	4.0	ND
42	16 – Substituted	NI**	22%*
43	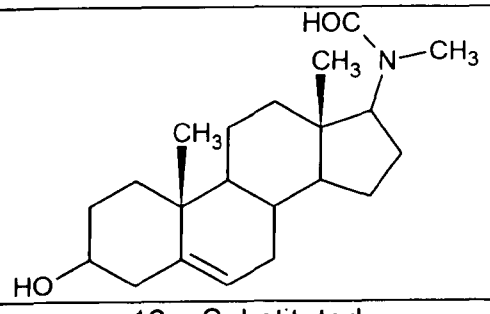	0.29	48%**
44	16 – Substituted	21%**	20%*
	KTZ	0.74	0.67

*Table 9 Showing pyridyl and amide-based steroidal inhibitors. NI = no inhibition, ND = not determined, **([I] = 2.5μM), *([I] = 125μM)*[59].

1.6.3.2 Type II steroidal inhibitors: Furan, Thiazolyl and Oxazolyl-based compounds

Burkhart et al[76] had synthesised a range of steroidal inhibitors bearing a heteroaromatic substituent at the C(17) position of the steroid to mimic the natural substrate pregnenolone. Furan and aminothiazole rings where positioned on the α-face and the β-face of the steroid and were used as substituents to test their ability to coordinate the haem iron of the $P450_{17\alpha}$ complex. The compounds were tested *in vitro* using cynomolgus monkey testicular $C_{17(20)}$ lyase.

The furan-based 16, 17-dehydro inhibitor (**45**) was found to have exceptional affinity for the enzyme (% inhibition = 91%) (Table10). It was suggested that the double bond at the C(16)-C(17) position may be the reason for enhanced inhibitory activity, as compound **46** (% inhibition = 0%), which does not contain the C(16)-C(17) double bond, showed negative results for the enzyme. This suggestion was again observed with compound **47** which showed good activity against the enzyme (%inhibition = 40%), however compound **48** (%inhibition = 0%), like compound **46** showed negative results, where again here is no double bond present at the C(16)-C(17) position.

The results obtained by Burkhart et al[76] further showed that the position of heterocycle attached at the C(17) position further influenced the interaction of the inhibitor with the haem of the enzyme. It was found that inhibitors with the heterocycle attached to the β-face of the steroid at the C(17) position, i.e. compound **49**, or compounds attached through a trigonal C(17) position, i.e. compounds **45** and **47**, were shown to be the better inhibitors. It was suggested that they were in a more ideal position to interact with active site than those where the heterocycle is attached to the α-face of the steroid or β-face of the steroid through a C(17) tetrahedral centre, i.e. compounds **46** and **48**[76].

Compound No	Structure	%inhibition*
45	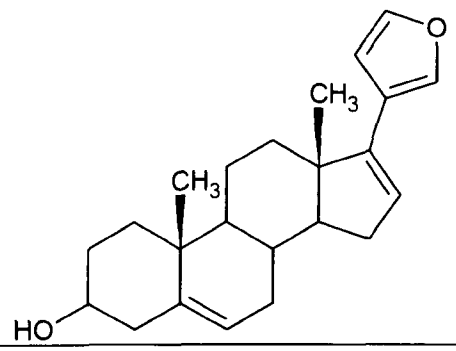	91%
46	C(17) tetrahedral analogue of **45**	0%
47	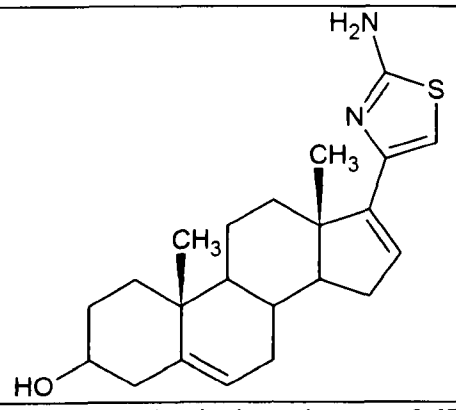	40%
48	C(17) tetrahedral analogue of **47**	0%
49	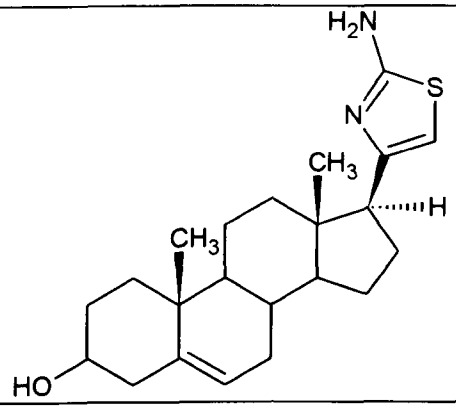	39%

*Table 10 Showing the furan and aminothiazolyl-based steroidal inhibitors of $P450_{17\alpha}$ against cynomolgus monkey testicular 17, 20-lyase. *([i]=1μM) (Burkhart et al[76]).*

A number of novel thiazolyl- and oxazolyl- based steroidal inhibitors of $P450_{17\alpha}$ were synthesised by Zhu et al[77] where either a methyl or phenyl substituent was introduced within the heterocycle ring in order to investigate their structure-activity relationship. The

compounds were generally shown to have moderate to good inhibiton of the enzyme $P450_{17\alpha}$, however, they were all shown to be less potent than the standard KTZ (%inhibiton = 100%). From the results shown, we can see that both the thiazolyl- and the oxazolyl-based inhibitors showed good inhibitory activity (i.e. compounds **52** and **50** respectively) (Table 11 and 12).

Compound No	Structure	%inhibition*
50	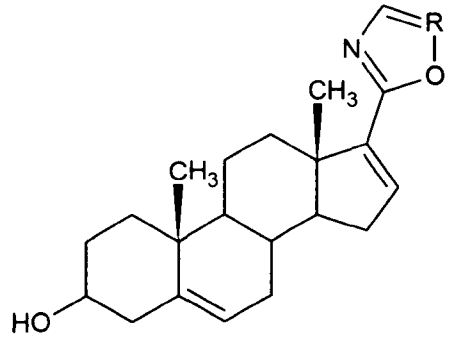 R = CH	56%
51	R = CH_3	45%

*Table 11 Showing the inhibitory activities of oxazolyl-based steroidal inhibitors *(Human $P450_{17\alpha}$)*[77].

With regards to the thiazolyl-based inhibitors, studies revealed that compound **52** (%inhibition = 72%) was found to be the most potent inhibitor against the human $P450_{17\alpha}$-expressed in *E. Coli* (Table 12). Additionally the results showed that the removal of the substituent from the C(4) position of the thiazole ring reduced the potency of the compound (**53**, %inhibition = 42%). Furthermore, the introduction of a phenyl generally decreased the inhibitory activity (**54**, %inhibition = 10%).

Compound No	Structure	%inhibition*
52	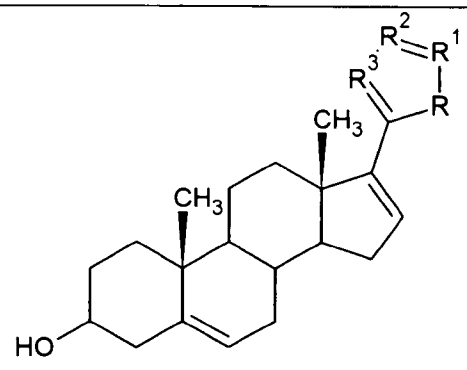 R = S, R^1 = C-CH_3, R^2 = CH, = R^3 = N	72
53	R = S, R1 = CH, R2 = CH, = R3 = N	42
54	R = S, R^1 = C-C_6H_5, R^2 = CH, = R^3 = N	10
	KTZ	100

*Table 12 Showing the inhibitory activities of thiazolyl-based steroidal inhibitors *(Human $P450_{17\alpha}$)*[77].

Compound No	Structure	%inhibition*
55	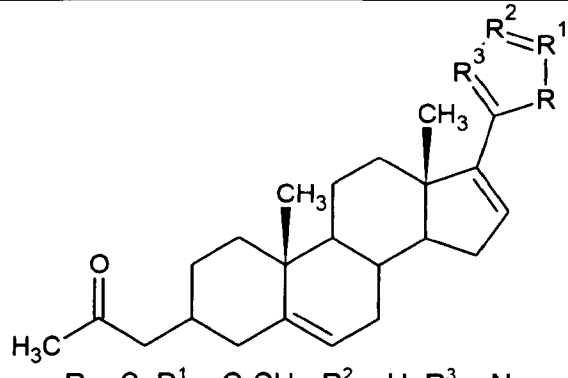 R = S, R^1 = C-CH_3, R^2 = H, R^3 = N	67
56	R = S, R^1 = CH, R^2 = C-CH_3, R^3 = N	28
57	R = O, R^1 = CH, R^2 = C_6H_5, R^3 = N	29
	KTZ	100

*Table 13 Showing inhibitory activities of acetate-based thiazolyl- and oxazolyl-based steroidal inhibitors *(Human $P450_{17\alpha}$)*[77].

A number of acetate-based steroidal inhibitors were also synthesised which showed compound **55** (which contains a methyl group at the C(4) of the thiazolyl ring) to have good inhibition against human $P450_{17\alpha}$ (%inhibition = 67%) (Table 13). Conversely, compound **56** (which contains a methyl group at the C(3) position of the thiazolyl ring) and compound **57** (which contains a phenyl ring at the C(3) position of the oxazolyl ring) decreased the inhibitory activity, showing poor inhibition (%inhibition = 28% and 29% respectively).

1.6.3.3 Type II steroidal inhibitors: Azole-based compounds

A number of azole-based steroidal inhibitors have been reported by various researchers to be potent inhibitors of the enzyme $P450_{17\alpha}$. Ling et al[78] synthesised and evaluated several progesterone and pregnenolone derivatives containing the C(16)-C(17) double bond with an azole ring present at the C17 position. The potency of these compounds was associated with the double bond present at the C(16)-C(17) position of the steroid inhibitor. Novel 17-imidazoyl, pyrazolyl, isoxazolyl and oxazole derivatives (**58-65**) were synthesised as potential inhibitors of human $C_{17,20}$-lyase and proved to be potent inhibitors of the enzyme (Tables 14 and 15). The results further showed that the presence of a double bond at the C(16)-C(17) position enhanced the activity of the inhibitor.

The 17β-(4'-imidazolyl) derivatives (**58**, **62**) were found to be very potent inhibitors against human testicular $P450_{17\alpha}$ (IC_{50} = 66nM and 58nM, respectively) (Table 14). The compounds showed greater activity than the standard KTZ (IC_{50} = 77nM), where the region between the imidazole ring and the D ring further contributes to the activity of the inhibitor. Similarly, the introduction of a C(16)-C(17)-double bond was further shown to maintain or enhance this inhibition (**59**, **63**).

Compound No	Structure	% inhibition* Human (IC_{50},nM)
58	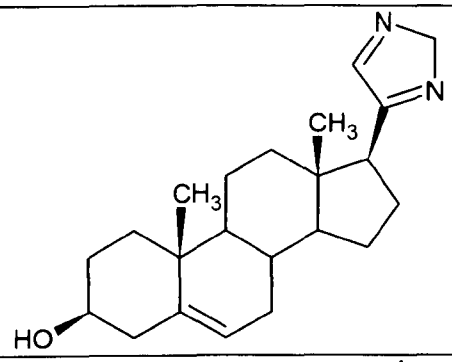	66
59	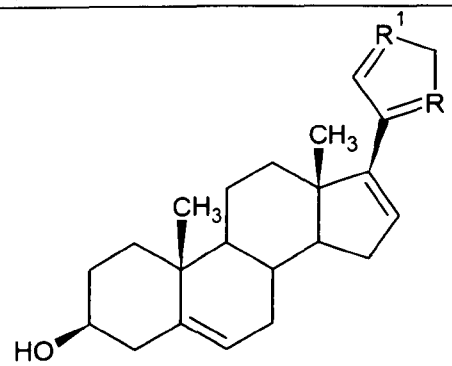 R = R^1 = N	24
60	R = N, R^1 = NH	58
61	R = NH, R^1 = N	50

Table 14 Showing potent 17-imidazoyl and pyrazolyl pregnenolone-based inhibitors(Human $C_{17,20}$-lyase)*[78].

The results also showed that the 17β-(2'-imidazolyl) derivative demonstrated poor potency (%inhibition = 24%); however the 16-unsaturated derivative (**60**) showed greater inhibitory activity. The 17β-pyrazole derivative also demonstrated poor potency (%inhibition = 20%); whereas the 16-unsaturated derivative (**61**) showed good potency towards $C_{17,20}$-lyase. Furthermore the unsaturated 3' pyrazole (**64**) and 5' isoxazolyl (**65**) derivatives were also shown to be potent inhibitors of human $C_{17,20}$-lyase, compound **65** was found to be a potent non-competitive inhibitor of $C_{17,20}$-lyase. The inhibitory data also suggested that derivatives containing substituents such as a methyl or phenyl

group on the imidazole ring decreased inhibitory activity, possibly due to steric hindrance and thus affecting the binding of the compound to the haem Fe.

Compound No	Structure	% inhibition* Human (IC_{50},nM)
62	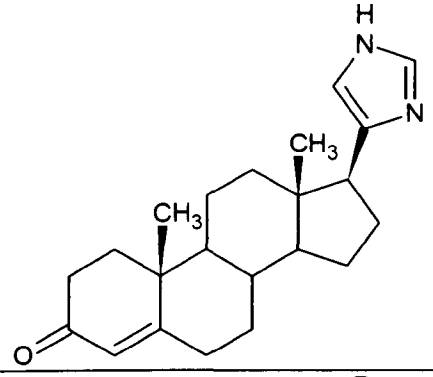	**58**
63	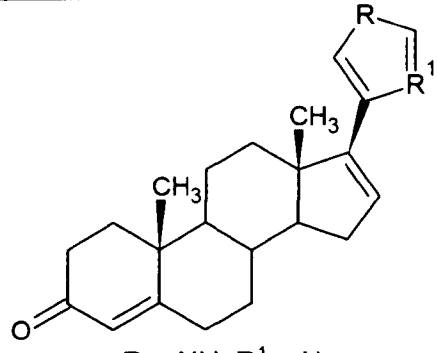 R = NH, R^1 = N	**50**
64	R = N, R^1 = NH	**59**
65	R = N, R^1 = O	**39**

*Table 15 Showing potent 17-imidazoyl, pyrazolyl, isoxazolyl progesterone-based inhibitors *(Human $C_{17,20}$-lyase)*[78].

Similar studies were also performed within the same research group on the synthesis and biochemical evaluation of a series of Δ^{16}-17-azolyl steroids, in an effort to investigate the effect of various heterocyclic rings (imidazole, triazole, tetrazole and pyrazole) at the C17 position of the pregnane backbone[80]. The study showed that compounds **66-70** were found to be the most potent inhibitors of human $P450_{17\alpha}$ with

the tetrazole derivative being the least potent and no inhibition being demonstrated by the pyrazole derivatives (Table 16).

Compound No	Structure	*IC_{50} (nM)	*K_i(nM)
66	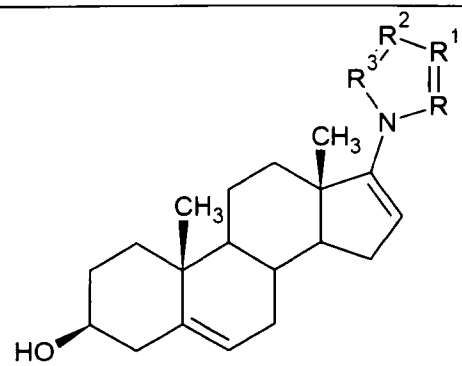 R = N, R^1 = CH, R^2 = N, R^3 = CH	90	23
67	R = N, R^1 = N, R^2 = R^3 = CH	13	1.4
68	R = R^1 = CH, R^2 = N, R^3 = CH	8	1.2
69	R = R^1 = CH, R^2 = N, R^3 = CH	7	1.9
70	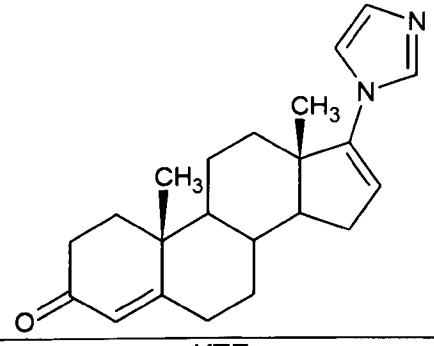	19	8
	KTZ	78	38

Table 16 *Showing the inhibitory potency of Δ^{16}-17-azolyl *(Human $C_{17,20}$-lyase)*[58,79].

The importance of the C(16)-C(17) double bond was shown to reduce the potency in compounds de-void of the double bond. The results also showed that the azole-based compounds were found to be non-competitive inhibitors of $P450_{17\alpha}$ and produced a type II difference spectrum, indicating coordination of the nitrogen lone pair of imidazole with the haem Fe.

In vivo studies in rats were also carried out where compounds **66** to **70** were also shown to be potent inhibitors of rat testicular microsomal $P450_{17\alpha}$. Results showed that compound **68** was the most effective at decreasing testosterone concentration in the serum with 100% inhibition occurring at 1μM, whereas **68** and **69** had shown to reduce testosterone levels in the testis by more than 75%. These results were also observed by Brodie et al[58].

More current studies carried out within the same research group[80] had shown that the compound VN/85-1 (**68**) and the corresponding triazole VN/87-1 (**67**) proved to be as effective, if not more, than the anti androgen finasteride. *In vivo* analysis was carried out on both inhibitors **68** and **67** regarding anti-tumour properties by use of mice with human prostate cancer (LNCap) xenografts. Both compounds were shown to successfully block the growth stimulating effects of Testosterone and DHT, reducing tumour growth by 53.4% when administered **68** at 16.6mg/kg three times daily and 58.5% when given **67** at 50mg/kg once daily over a period of four weeks.

These results proved to be as effective at reducing tumour growth as those shown by castration [castration and finasteride values were 59.7% and 27.6% respectively (50mg/kg/day)]. Studies were further carried out by Handratta et al[80] which involved the synthesis of inhibitors where the imidazole was replaced with either a benzoazole or a pyrazine group (Table 17).*In vitro* studies showed good inhibition against intact $P450_{17\alpha}$-expressing *E.coli*, this was utilised as the enzyme source.

Compound No.	Structure	*$P450_{17\alpha}$-expressing *E.coli* (nM)
71	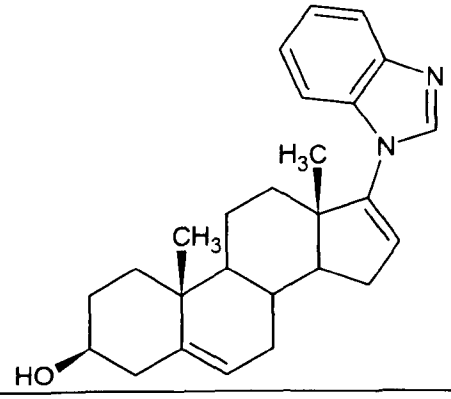	300
72	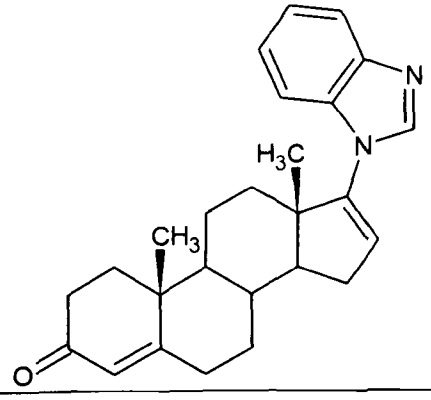	915
73	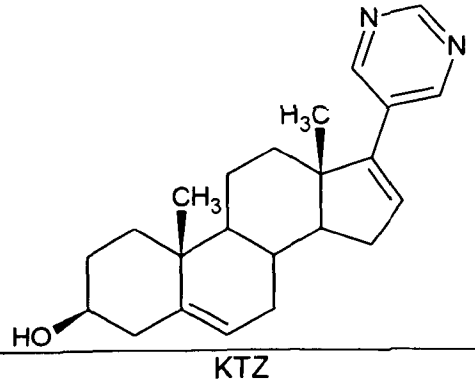	500
	KTZ	1100
	Abiraterone	800

Table 17 *$P450_{17\alpha}$ binding of 17-heteroaryl compounds *(Human $C_{17,20}$-lyase)*[80].*

Results had expressed that the pregnenolone based (Δ^5 3β-ol) benzimidazole inhibitor VN-124 (**71**, IC_{50} = 300nM) illustrated much greater inhibitory activity (by at least 3-fold more) in comparison to that achieved by the progesterone based (Δ^4 3-one) benzimidazole compound (**72**, IC_{50} = 915nM), indicating that the moiety positioned at

C3 may play an important role in the binding of these particular inhibitors within the active site of $P450_{17\alpha}$ (Table 17).

Furthermore the benzimidazoles were shown to be far more potent than the benzotriazoles synthesised by up to 4 to 6 fold more, further indicating that the nature of the 17-heterocycle may affect the inhibitory activity of the compound. Compound (**71**) was shown to reduce tumour volume by 93.8% when administered at a dose of 50mg/kg twice daily, proving to be more successful than castration in the mouse model used. The 17-pyramidine (**73**) was too found to be a potent inhibitor of $P450_{17\alpha}$ further suggesting the importance of the 17-heterocycle influence on inhibitory activity (Table 17).

1.6.3.4 Type II steroidal inhibitors: Oxime-based compounds

Hartmannet al[59,81]had synthesised a number of pregnenolone and progesterone based steroidal inhibitors bearing an oxime group connected directly to the steroidal D ring (Tables 18 and 19). The inhibitory activity of these compounds was tested using rat and human testicular microsomes where pregnenolone[81] and progesterone[59] where utilised as substrate. Evidently, the oxime group was shown to coordinate with the heme Fe of $P450_{17\alpha}$, with data further showing that potency of the inhibitors strongly depended on the position of the oxime group, with the C(21) oximes showing to be more effective at inhibiting $P450_{17\alpha}$ than the C(20) oximes.

The progesterone-based inhibitors were shown to be as equally active as their equivalent pregnenolone inhibitors. The C(21) oxime **74** showed excellent inhibitory activity toward the human enzyme $P450_{17\alpha}$ and reasonable activity toward the rat enzyme. It was shown to be the most active inhibitor of the human enzyme.

Compound No	Compound Structure	%inhibition* IC_{50} (μM)	
		Rat	Human
74	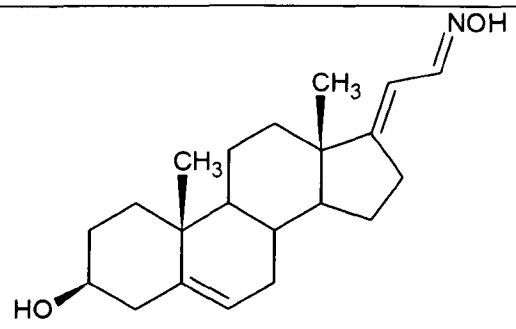	0.52	0.077
75	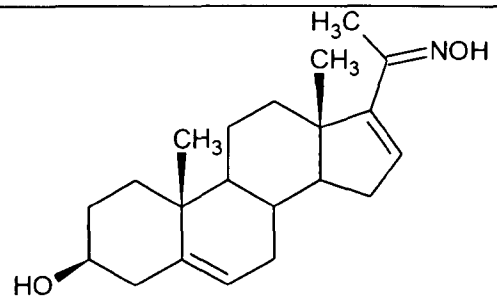	>125	0.17
76	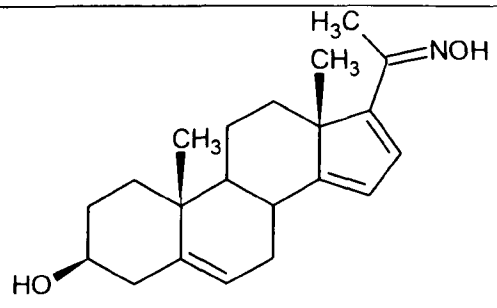	125	0.20
77	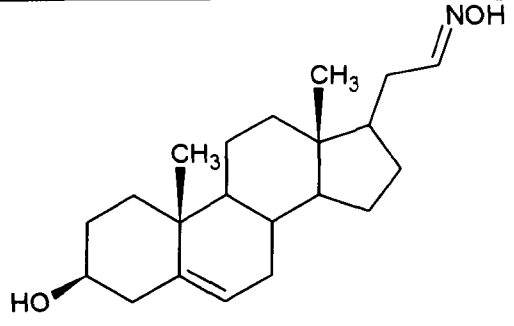	2.76	0.27

Table 18 Inhibition of $P450_{17\alpha}$ rat and human enzymes by pregnenolone-based steroidal oximes[81].

In compounds **75** and **76**, introduction of a double bond at Δ16 position (**75**) and Δ14, Δ16 position (**76**) was shown to decrease activity towards the human enzyme.

Compound **77** also a C(21) oxime was shown to have moderate inhibitory activity towards the human enzyme and reasonable activity towards the rat enzyme.

Compound No	Compound Structure	%inhibition* IC_{50} (μM)	
		Rat	Human
78	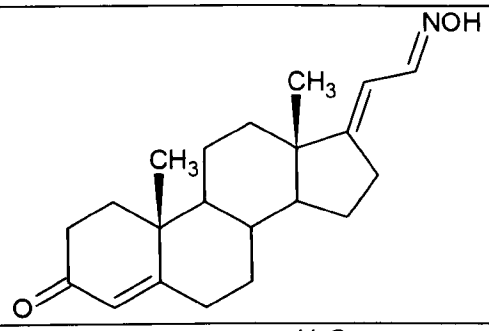	0.14	0.18
79	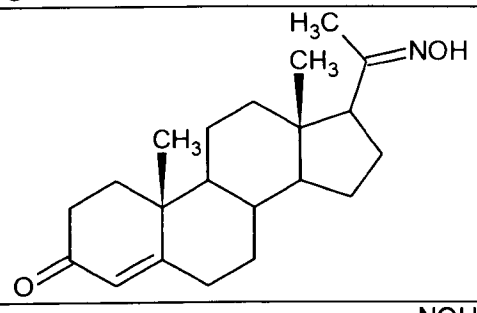	Ni	0.10
80	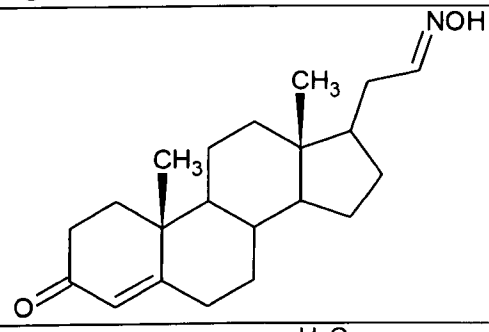	0.30	0.52
81	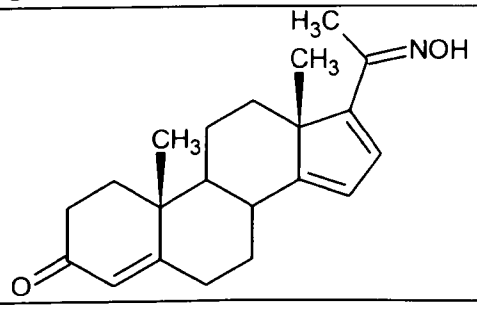	Ni	0.20

Table 19 Inhibition of $P450_{17\alpha}$ rat and human enzymes by Progesterone-based steroidal oximes[59],ni = no inhibition.

Compounds **78** and **80** were shown to be potent inhibitors of the rat enzyme exhibiting IC_{50} values of 0.14 and 0.30nM respectively (Table 20). The introduction of one or two double bonds (Δ16 and Δ14,Δ16) into the D-ring was shown to increase the activity of the compound dramatically with regards to the human enzyme (compounds **79** and **81**).

The same research group performed *in vitro* and *in vivo* studies on a number of highly potent compounds of $P450_{17\alpha}$ which have been previously described as type II steroidal inhibitors[48, 82]. The Inhibitor **73**which contained a pyrimidyl ring at the C17 moiety [**73** (IC_{50} = 24nM) and its prodrug **82** (IC_{50} = 38nM)] publicized greater potency than abiraterone (**28**) (IC_{50} = 73nM). Investigations were carried out using human testicular microsomes and progesterone as substrate.

In vitro studies of compound **73** had shown to inhibit $P450_{17\alpha}$ in a non-competitive irreversible manner and had shown type II binding via the pyrimidyl nitrogen lone pair. Compound **73** was further specified to be selective towards $P450_{17\alpha}$ as very poor inhibiton was shown towards other P450 enzymes. *In vivo* studies had too revealed compound **73** to be more potent than abiraterone with IC_{50} values of 30 and 54nM, respectively. Both compounds **73** and **82** had shown to potently inhibit the plasma testosterone concentration, almost as effectively as that achieved by castration.

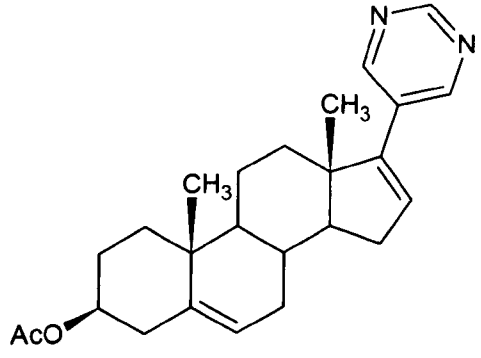

82

1.7 Non-steroidal Inhibitors

A great deal of research has been achieved in the pursuit of identifying potent non-steroidal inhibitors of $P450_{17\alpha}$.The majority of non-steroidal inhibitors have a functionality which is able to coordinate with the haem of $P450_{17\alpha}$ and a hydrophobic backbone to facilitate binding to the hydrophobic pocket within the active site and hence mimic the natural substrate. In most cases, the moiety which binds to the haem contains a nitrogen atom which is able to utilise its lone pair of electrons. A substituent has also been used generally to mimic the hydrophilic C(3) group of the substrate. Unlike steroidal inhibitors, however, non-steroidal inhibitors do not (in general) possess steroid related side effects.

KTZ (Figure 21) is a synthetic azole-based antifungal agent, was first discovered in 1976 and has been used to treat skin and fungal infections. KTZ is the only non-steroidal $P450_{17\alpha}$ inhibitor to have been evaluated clinically in the treatment of prostate cancer as it was found to result in gynaecomastia in a proportion of men[83] and was later found to be due to the inhibition of testosterone production as KTZ suppressed both testicular and adrenal androgen production[84, 85].

KTZ achieves the inhibiton of testosterone via the inhibition of cytochrome P450 14α-demethylase, the enzyme required for the conversion of lanosterol to ergosterol. KTZ was discontinued as treatment for prostate cancer and was removed from the market due to the side-effects which included; poor selectivity (as it too inhibits $P450_{11\beta}$), gastrointestinal symptoms, gynaecomastia and hepatotoxicity when given at a daily dose of 800-1200mg (400mg three times a day). Its use was also found to require the additional treatment of corticosteroids as a result of the inhibiton of cortisol production[86]; however, a great deal of interest has been shown in using KTZ in patients with

advanced prostate cancer, with clinical trials to research its efficacy at lower doses (i.e. 200mg three times a day) alone and in combination with other agents[87].

The inhibitory activity of KTZ, with regards to its structure, was found to be in the presence of the imidazole ring, where the lone pair of electrons could undergo type II binding with the Fe haem, resulting in the formation of a dative covalent bond.

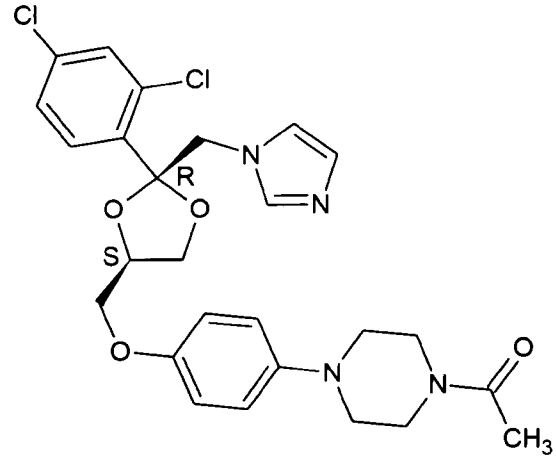

Figure 21 Showing the structure of KTZ.

As a result of the observations with KTZ, a number of non-steroidal $P450_{17\alpha}$ inhibitors were synthesised. The imidazole based antimycotics bifonazole and clotrimazole (Figure 23) were found to possess greater inhibitory activity than KTZ, but were not found to be selective. The potency of these antimycotics was rationalised by Ahmed[88]by superimposing their structures onto the steroid skeleton, where the biphenyl structure of bifonazole formed a good overlay with the rings A and C of the steroid backbone. Econazole (Figure 23) showed less inhibition towards $P450_{17\alpha}$ than KTZ, however, has been found to be a very potent inhibitor of aromatase. Due to the lack of selectivity for $P450_{17\alpha}$ by the antimycotic drugs (Figure 23) and KTZ, it is vital for future inhibitors of

the enzyme to mimic the natural substrates pregnenolone or progesterone, in order to achieve improved selectivity for $P450_{17\alpha}$.

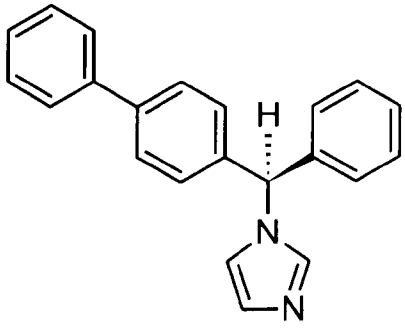

Bifonazole

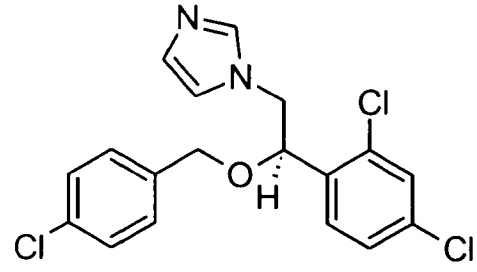

Econazole

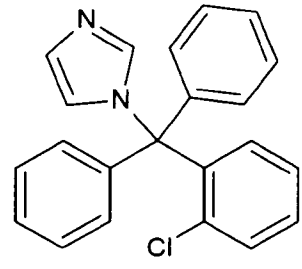

Clotrimazole

Figure 22 Showing the structures of three antimycotics compounds; Bifonazole, econazole and clotrimazole.

1.7.1 Non-steroidal inhibitors: Pyridyl-based tetralones, tetralines and indanones.

Sergejew and Hartmann89 reported a sequence of pyridyl-based benzocycloalkenes as non-steroidal inhibitors of $P450_{17\alpha}$, which were designed to be AB and BC ring mimics of the steroidal backbone. The unsaturated tetralones (**83-90**) were shown to inhibit rat testicular $P450_{17\alpha}$ ranging from around 4-70% (Table 20).The results revealed that the

3-pyridyl derivative (**89**) was a better inhibitor of rat testicular $P450_{17\alpha}$ than the 4-pyridyl derivative (**83**) (%inhibition = 48% and 37%, respectively).

Compound No	Structure	%inhibition*
83	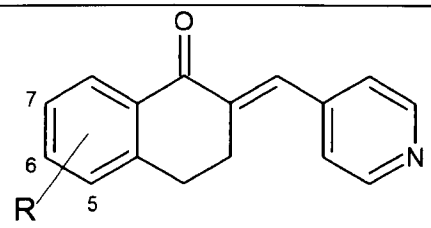 R = H (*E*)	37%
84	R = H (*Z*)	70%
85	R = 5-OCH_3 (*E*)	53%
86	R = 5-OH (*E*)	23%
87	R = 6-OH (*E*)	8%
88	R = 7-OH (E)	10%
89	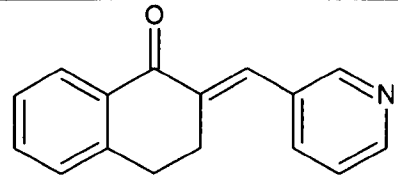	48%
90	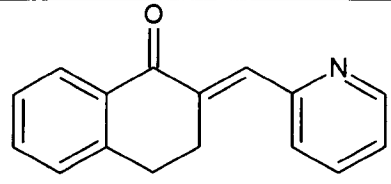	4%
91	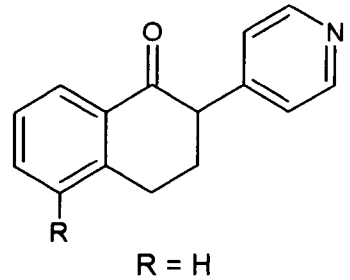 R = H	71%
92	R = OCH_3	86%
	KTZ	62%

*Table 20 Showing a range of pyridyl-based tetralones *([I] = 125μM, rat testicular $P450_{17\alpha}$) (Sergejew and Hartmann[89]).*

The methoxy derivative (**85**) showed an increase in activity (%inhibition = 53%), however, the introduction of a hydroxyl group (**86**, **87** and **88**) resulted in an overall

decrease in activity (producing %inhibition of 23%, 8% and 10%, respectively). Compound **84** (the *Z*-isomer of compound **83**) was found to be almost twice as potent (%inhibition = 70%) and comparable to results shown by KTZ (%inhibition = 62%). Compounds **91** and **92** were further shown to be very good inhibitors of the rat $P450_{17\alpha}$, proving to be more potent than KTZ, with the 5-methoxy compound (**92**) showing the greatest potency (%inhibition = 71% and 86%, respectively).

Sergejew and Hartmann[89] also synthesised a number of 4-pyridyl-based hydrogenated tetralones (compounds **93-95**) which demonstrated very good inhibition, ranging from 67-84% against rat testicular $P450_{17\alpha}$. From the 4-pyridyl-based tetraline inhibitors synthesised, the unsubstituted analogue (**99**) was shown to be the most potent inhibitor of rat testicular $P450_{17\alpha}$ (%inhibition = 85%; IC_{50} = 22μM) showing greater inhibition than the standard KTZ (%inhibition = 62%; IC_{50} = 67μM). The addition of a hydroxyl group at either the C(5), C(6) or C(7) position (**100-102**) was shown to decrease the activity of the inhibitor as compared to the unsaturated compound **99**. From the study carried out by Sergejew and Hartmann[89], both the saturated tetralones **92** (Table 20) and **94** (Table 21) were shown to be the most active (both with an IC_{50} value of 13μM). Comparison of results to the unsaturated compounds revealed that compound **93** (%inhibition = 67%, IC_{50} = 13μM) was almost twice as potent as its equivalent unsaturated analogue **83** (%inhibition = 37%).

Results further showed that the addition of a methoxy group at the C(5) or C(6) position gave an increase in activity. In addition, Sergejew and Hartmann[89] had synthesised compounds where the 3-pyridyl moiety had been utilised instead of the 4-pyridyl moiety, where a hydroxyl group present at either the C(5) or C(7) position [compounds **96** and **98** (%inhibition = 83 and 79%, respectively) gave an increase in activity. Conversely,

when the hydroxyl group was present at the C(6) position (**97**), a considerable decrease in activity was observed (%inhibition = 34%) (Table 21).

Compound No	Structure	%inhibition*
93	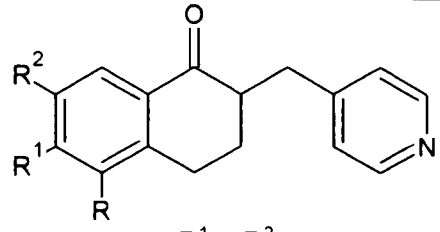 $R = R^1 = R^2 = H$	67
94	$R = OCH_3$, $R1 = R^2 = H$	84
95	$R = H$, $R^1 = OCH_3$, $R^2 = H$	83
96	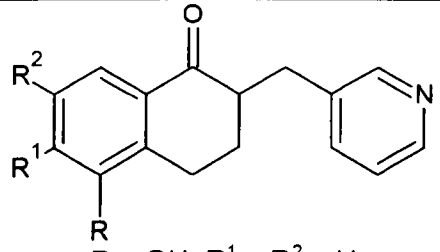 $R = OH$, $R^1 = R^2 = H$	83
97	$R = H$, $R^1 = OH$, $R^2 = H$	34
98	$R = R^1 = H$, $R^2 = H$	79
	KTZ	62

*Table 21 Showing a range of 3- and 4-pyridyl-based non-steroidal hydrogenated tetralones. *([I] = 125μM, Rat testicular $P450_{17\alpha}$) (Sergejew and Hartmann[89]).*

The tetralines synthesised (compounds **99** to **102,** Table 22) were shown have greater inhibition (with %inhibition ranging from 55-85%) than the unsaturated tetralones **83** and **85-90**, however, similar activity to the saturated tetralones was revealed.

Compound No	Structure	%inhibition*
99	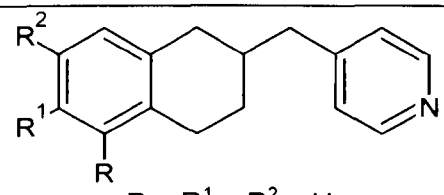 $R = R^1 = R^2 = H$	85
100	$R = OH, R^1 = R^2 = H$	55
101	$R = H, R^1 = OH, R^2 = H$	70
102	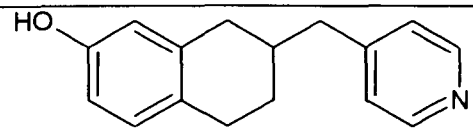 $R = R^1 = H, R^2 = OH$	67
	KTZ	62

*Table 22 Showing a range of 4-pyridyl-based tetralines. *([I] = 125μM, Rat testicular $P450_{17\alpha}$) (Sergejew and Hartmann[89]).*

Compounds **103-110** were, in general shown to be weaker inhibitors than the standard KTZ, with the unsaturated indanones (**103-107**) proving to be the weakest. Compound **103** demonstrated very weak activity against rat testicular $P450_{17\alpha}$ (%inhibition = 24%) with the 5-methoxy (**105**) and the 4-hydroxy (**106**) compounds showing improved activity in comparison to **103** (%inhibition=40% and 51% respectively) (Table 23).

Unlike the unsaturated indanones, the saturated compounds **108-110** were shown to have improved activity for rat testicular $P450_{17\alpha}$. Compound **108** (%inhibition=66%) was shown to be almost three times more potent than its corresponding unsaturated indanone (**103**) and furthermore, was shown to be more potent than the standard KTZ The addition of a Methoxy group at C(5) position (**109**, %inhibition=67%) gave similar activity to that of compound **108**, whereas the addition of a hydroxyl group at the C(5) position (**110**, %inhibition=75%) further increased the activity for rat testicular $P450_{17\alpha}$ (Table 24).

Compound No	Structure	%inhibition*
103	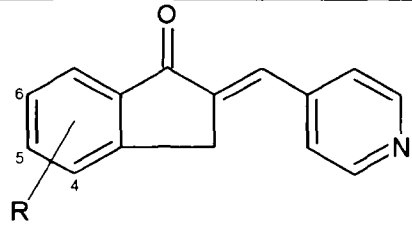 R=H	24
104	R=4-OCH_3	27
105	R=5-OCH_3	40
106	R=4-OH	51
107	R=5-OH	7
	KTZ	62

*Table 23 Showing a range of unsaturated pyridyl-based indanones. *([I] = 125μM, Rat testicular $P450_{17\alpha}$) (Sergejew and Hartmann[89]).*

Compound No	Structure	%inhibition*
108	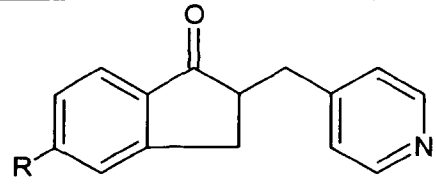 R = H	66
109	R = CH_3O	67
110	R = OH	75
	KTZ	62

*Table 24 Showing a range of saturated pyridyl-based indanones. *([I] = 125μM, Rat testicular $P450_{17\alpha}$) (Sergejew and Hartmann[89]).*

1.7.2 **Non-steroidal inhibitors**: **Pyridyl-based esters**

Rowland et al[90] had synthesised a number of esters of 2-, 3- and 4-pyridyl acetic acid, which were designed to mimic the steroidal backbone of pregnenolone via the B ring. A number of alcohols were utilised in the synthesis of the pyridyl-based esters,

thesespecifically being isopinocampheol, 1-adamantanol, 2-methyl-2-adamantanol and cedrol (Tables 25 and 26).

Compound No	Structure	IC_{50}* 17-hydroxylase	IC_{50}* 17,20-lyase
111	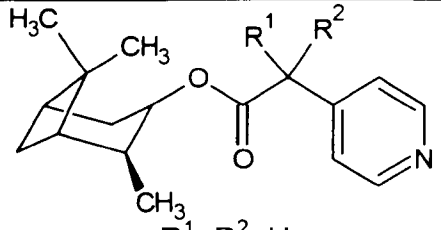 $R^1=R^2=H$	14nM	5nM
112	$R^1=CH_3, R^2=H$	19nM	6nM
113	$R^1=R^2=CH_3$	26nM	10nM
114	$R^1=C_2H_5$, $R^2=H$	34nM	9nM
115	$R^1=R^2=C_2H_5$	140nM	35nM
116	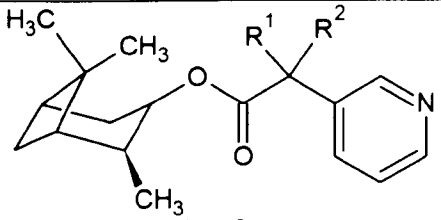 $R^1=R^2=H$	260nM	88nM
117	$R^1=CH_3, R^2=H$	82nM	14nM
118	$R^1=R^2=CH_3$	29nM	15nM
119	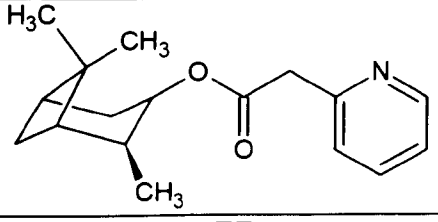	>1000nM	>1000nM
	KTZ	65Nm	28nM

*Table 25 Showing pyridyl-based non-steroidal esters as inhibitors of $P450_{17\alpha}$. (Rowlands et al[90]) (*Human testicular $P450_{17\alpha}$).*

The inhibitors synthesised using isopinocampheol (compounds **111-119**) were in general shown to be good inhibitors with IC_{50} ranging from 4nM – 1000nM with regards to the 17α-hydroxylase component and 5nM – 1000nM for the 17,20-lyase component of the enzyme. From the results present in table 26, it is evident to see that the 4-pyridyl

based compounds were more potent inhibitors than the 2- and 3-pyridyl based compounds. Compound **83** revealed very good inhibitory activity against human testicular $P450_{17\alpha}$ (IC_{50} = 14nM for 17α-hydroxylase; 5nM for 17,20-lyase) and was found to be the most potent compound amongst the 4-pyridyl based series (**111-115**).

With respect to the 3-pyridyl based compounds (**116-118**) introduction of a methyl group at the R^1 position (**117**) resulted in an increase in potency against human testicular $P450_{17\alpha}$ (IC_{50} = 82nM for 17α-hydroxylase; 14nM for 17,20-lyase). Potency was further increased with the addition of another methyl group at the R^2 position (**118**), however this was only observed for the 17α-hydroxylase competent of the enzyme (IC_{50} = 29nM; 15nM for 17,20-lyase component). The 2-pyridyl based inhibitor (**119**) proved to be a weaker inhibitor for the enzyme than the standard KTZ (Table 25).

The esters synthesised where 1-adamantanol was used as the alcohol (compounds **120-122**) generally proved to be weaker inhibitors than the inhibitors synthesised using isopinocampheol, with the exception of the 2-pyridyl based inhibitor (**119**). The introduction of a methyl group at the R^1 and R^2 position was shown to increase the potency of the compound (**122**, IC_{50} = 90nM for 17α-hydroxylase; 13nM for 17,20-lyase component) (Table 26). Similar results were observed in the esters synthesised using 2-methyl-2-adamantanol as alcohol (**123** and **124**) where a noticeable increase in potency was shown with the introduction of methyl groups at the R^1 and R^2 position (**124**, IC_{50} = 75nM for 17α-hydroxylase; 13nM for 17,20-lyase component) (Table 26). Compounds **125** and **126** were synthesised using cedrol as alcohol, which were shown to be weaker inhibitors than the standard KTZ.

Compound No.	Structure	IC_{50}* 17α-hydroxylase	IC_{50}* 17,20-lyase
120	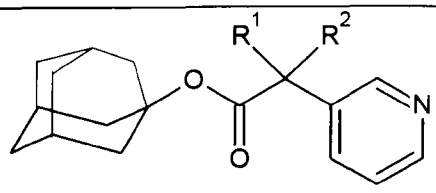 $R^1=R^2=H$	930nM	130nM
121	$R^1=CH_3$, $R^2=H$	220Nm	35nM
122	$R^1=R^2=CH_3$	90Nm	13nM
123	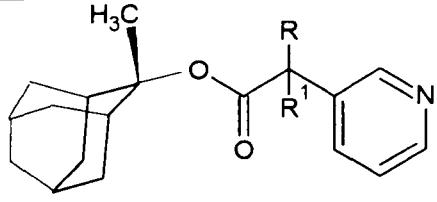	1900nM	320nM
124	$R = R^1 = CH_3$	75nM	13nM
125	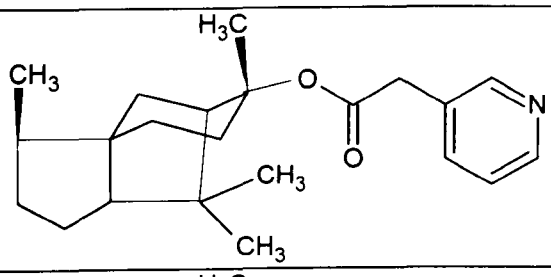	230nM	38nM
126	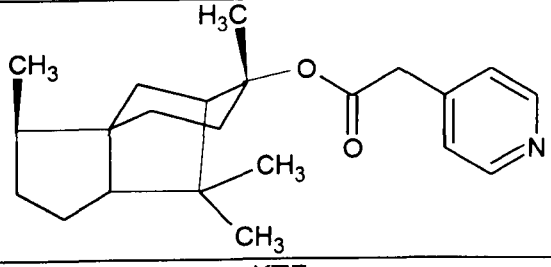	270nM	52nM
	KTZ	65Nm	26Nm

*Table 26 Showing pyridyl-based non-steroidal esters as inhibitors of $P450_{17\alpha}$. (Rowlands et al[90]) (*Human testicular $P450_{17\alpha}$).*

1.7.3 **Non-steroidal inhibitors**: **Pyrrolidine-2,5-dione-based inhibitors**

A range of pyrrolidine-2,5-based inhibitors were synthesised and reported by Ahmed et al[91] as A ring mimics of the steroid progesterone (Compounds **127-133**) (Table 27).

Compound No	Structure	%inhibition*	IC_{50}
127	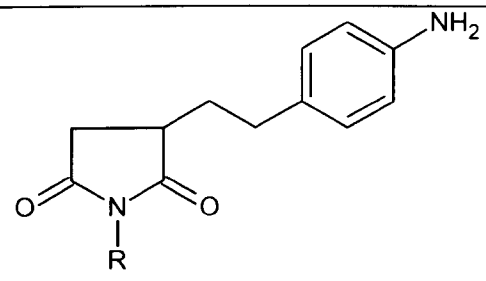 R = H	58%	112μM
128	R = *n*-butyl	61%	59μM
129	R = *n*-octyl	88%	26μM
130	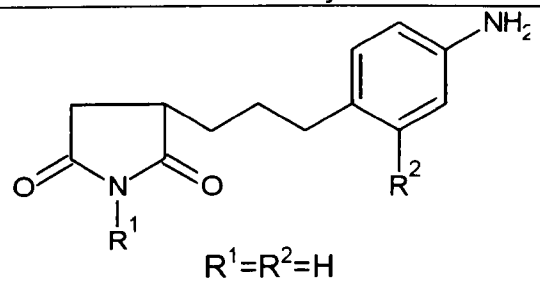 R^1=R^2=H	62%	28μM
131	R^1=H, R^2=NH_2	95%	ND
132	R^1=methyl, R^2=NH_2	81%	ND
133	R^1= *n*-butyl, R^2=NH_2	75%	ND
	KTZ	91%	12μM

Table 27 Showing pyrrolidine-2,5-dione based non-steroidal inhibitors (Ahmed et al[91]([I] = 33μM, rat testicular $P450_{17\alpha}$). ND = not determined.*

The compounds were designed with the introduction of an amino group at the para-position of the phenyl ring in order for binding to take place with the haem Fe via a dative covalent bond. Additionally, the pyrrolidine-2,5-dione ring was drawn upon to mimic the A ring of progesterone, with the carbonyl moiety at the C(3) position, which is suggested to interact with a possible hydrogen binding site at the active site of the enzyme $P450_{17\alpha}$. Increasing the alkyl chain length between the pyrrolidine-2,5-dione ring and the phenyl ring, as well as *N*-alkylation of the pyrrolidinone nitrogen by an alkyl group were other factors which were contemplated in the design concept of the compounds.

The pyrrolidine-2,5-based inhibitors were shown to be good inhibitors with inhibition ranging from 58-95%. The addition of a second amino group to the phenyl ring (compound **131-133**) was shown to increase the inhibitory activity of the compounds (% = 75-95%). Compounds **129** and **131** were shown to have the strongest activity from the range of compounds (%inhibition = 88%; IC_{50} = 26μM and 95%, respectively).Amongst the mono-amino compounds researched, compounds with a two spacer group (**127-129**) (Table 27) revealed an increase in activity in the *N*-substituted alkyl chain from butyl (**128**, %inhibition = 61%; IC_{50} = 59μM) to octyl (**129**, %inhibition = 88%; IC_{50} = 26μM) (Table 27).

The diamino-based compounds amongst the three carbon spacer group were shown to be the very good inhibitors (compounds **130-133**). However, a decrease in activity was seen with an increase in the *N*-substituted alkyl chain from methyl (**132,** %inhibition = 81%) to butyl (**133,** %inhibition = 75%). Compound **131** was found to be the most potent inhibitor of the range (%inhibition = 95%) (Table 27)

1.7.4 Non-steroidal inhibitors: Imidazole-based inhibitors

The discovery of KTZ was a break through in the treatment of PC and has led to the synthesis of many potent imidazole-based non-steroidal inhibitors of $P450_{17\alpha}$.The synthesis and evaluation of Compound **134**, 2-(1*H*-imidazol-4-ylmethyl)-9*H*-carbazole (YM116) (Table 28) was carried out to see the inhibitory effects of this compound against human testicular $P450_{17\alpha}$ and adrenocortical carcinoma cells. Compound **134**was reported to be a potent inhibitor of human 17,20-lyase (IC_{50} = 4.2nM) as compared to the standard KTZ (IC_{50} = 17nM). The study also showed that YM116 was a selective inhibitor of 17,20-lyase action in human adrenocortical carcinoma cells than

17α-hydroxylase step and was also revealed to be more selective against cortisol biosynthesis, with YM116 showing to be 50 times more potent that KTZ[92].

Compound No	Structure	IC_{50}	K_i
134	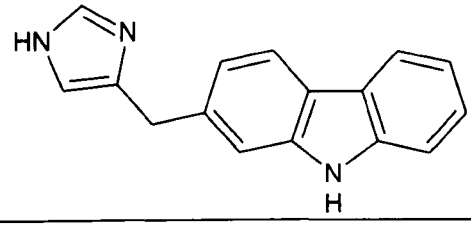	4.2nM (Human 17,20-lyase)	7nM (Rat 17,20-lyase)

Table 28 Showing the structure of YM116 [2-(1H-imidazol-4-ylmethyl)-9H-carbazole] a potent inhibitor of 17,20-lyase component of $P450_{17\alpha}$[92,93].

Ideyama et al[93] carried out a study to determine the inhibitory effects of the non-steroidal $P450_{17\alpha}$ inhibitor YM116 (Compound **134**) on rat testicular $P450_{17\alpha}$ plus serum concentrations of testosterone and DHEA sulfate, with the results being further compared with those of KTZ. The inhibitor YM116 was shown to be more than 100 times more potent than KTZ (IC_{50} = 584nM) and agonist 17,20-lyase activity in rat testicular microsomes [possessing an IC_{50} value of 5.4nM for YM116 (Ideyama et al[93])] proving to be a competitive inhibitor of rat 17,20-lyase based on kinetic studies (*Ki* = 7nM) (Table 28).

In addition, YM116 was furthermore shown to dose-dependently reduce the serum testosterone concentration in GnRH-treated rats, with results revealing YM116 to be 21 to 24 times more potent that KTZ. YM116 was also shown to decrease testosterone concentrations in untreated normal rats in a dose-dependent manner. Consistent to these findings, YM116 decreased serum concentrations of DHEA sulfate in castrated

rats more than KTZ as well as reducing rat prostatic weights close to or within that of castration levels in a dose-dependent manner.

1.7.5 Non-steroidal inhibitors: Imidazole-based biphenyl inhibitors

Hartmann et al had discovered a class of imidazolyl and triazolyl substituted biphenyls, which were shown to be potent inhibitors of $P450_{17\alpha}$. The biphenyl backbone was proposed to mimic the A and C rings of the natural substrate. A number of 3- and 4-imidazol-1-yl-methyl substituted biphenyl compounds were also synthesised, which were either unsubstituted, meta- and/or para-substituted on the phenyl ring so as to mimic the steroid A ring[94].

The inhibitory activity against rat and human $P450_{17\alpha}$ testicular enzyme was evaluated using microsomal fractions and progesterone as the substrate and were shown to be moderate to excellent in activity against both enzymes (Table 29). Results of the study revealed that the 4-imidazol-1-yl methyl biphenyls, in particular, those containing a meta- and/or para-OH group on the phenyl ring (compounds **137**, **144** and **152**, IC_{50} = 0.31μM, 0.13μM and 0.087μM, respectively) had shown the greatest potency towards human testicular enzyme than KTZ (IC_{50}=0.74μM) (Table 29) with the most active compound from the study being compound **152**.

Similar activity was also observed in the meta- and/or para-substituted 1-(biphenyl-3-ylmethyl)-1*H*-imidazole compounds (Table 30), with compound **155**, containing para-OH group on the phenyl ring, showing the greatest potency towards the human testicular enzyme.In the evaluation of the 4-imidazol-1-yl methyl biphenyl compounds, QSAR studies performed for the inhibition of the human enzyme showed the meta-substituted

biphenyls to generally be more potent than the corresponding para-substituted biphenyls.

Compound No	Structure	IC_{50} (Rat)	IC_{50} (Human)
135	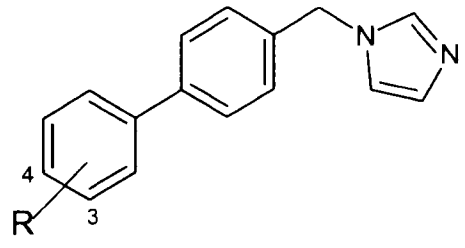 R = H	2.0μM	0.98μM
136	R = 4-OMe	7.9μM	3.7μM
137	R = 4-OH	2.6μM	0.31μM
138	R = 4-F	0.98μM	0.96μM
139	R = 4-Cl	1.4μM	5.8μM
140	R = 4-CH_3	1.3μM	4.2μM
141	R = 4-CN	1.2μM	2.5μM
142	R = 4-SMe	8.5μM	7.7μM
143	R = 3-OMe	6.5μM	0.59μM
144	R = 3-OH	0.63μM	0.13μM
145	R = 3-F	4.9μM	0.66μM
146	R = 3-Cl	11μM	1.3μM
147	R = 3-Me	7.6μM	1.3μM
148	R = 3-NO_2	4.6μM	1.8μM
149	R = 3-$NHCOCH_3$	3.0μM	0.23μM
150	R = 3-NH_2	6.0μM	0.21μM
151	R = 3,4-OCH_2O-	20μM	3.1μM
152	R = 3,4-diOH	3.1μM	0.087μM
	KTZ	67μM	0.74μM

Table 29 Showing the inhibitory activity of meta- and/or para-substituted 1-(biphenyl-4-ylmethyl)-1H-imidazole compounds against rat and human $P450_{17\alpha}$.

Results against rat $P450_{17\alpha}$ had shown moderate to excellent activity with the most potent compounds being those which possessed a lipophilic para-substituent (**138**) or a meta-hydroxyl group (**144**) which in respect to the standard KTZ (IC_{50}=67μM) were correspondingly observed to be around 68 and 106 times more potent. These promising

compounds were further tested *in vivo* on Sprague-Dawley (SD) rats for reduction of plasma testosterone concentrations (Table 29).

Compound No	Structure	IC_{50} (Rat)	IC_{50} (Human)
153	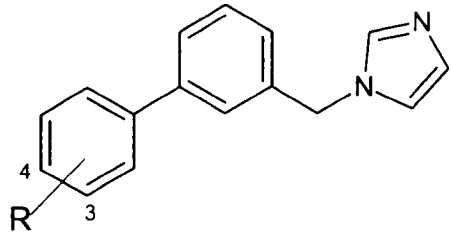 R = H	5.3μM	2.2μM
154	R = 4-OMe	32μM	4.5μM
155	R = 4-OH	2.9μM	0.86μM
156	R = 4-F	6.1μM	2.9μM
157	R = 4-Cl	5.0μM	13μM
158	R = 3-OMe	16μM	3.7μM
159	R = 3-OH	5.1μM	1.2μM
160	R = 3-$NHCOCH_3$	13μM	2.1μM
161	R = 3-NH_2	27μM	4.2μM

Table 30 Showing the inhibitory activity of meta- and/or para-substituted 1-(biphenyl-3-ylmethyl)-1H-imidazole compounds against rat and human $P450_{17\alpha}$. (Wachall et al[94]).

Both compounds **138** and **144** had shown to be more successful at decreasing testosterone levels than KTZ, with compound **138** showing to completely inhibit testosterone biosynthesis 2h post administration, reducing testosterone plasma concentration to castration levels. Compound **144** had shown poor *in vivo* activity within SD rats, suggesting a possibility of fast phase II metabolism, such as, glucuronidation or possibly sulfation of the phenolic O[94].

Zhuang et al[95] synthesised and evaluated a series of biphenyl imidazole based compounds which comprised of an open-ring formation. They were shown to be very good inhibitors towards rat and human $P450_{17\alpha}$. The imidazol-1-yl compounds were generally found to show much greater potency than the 1, 2, 4-triazol-1-yl compounds in both the human and rat *in vitro* testing, the most active compounds being **162** and **163** with IC_{50} values of 0.17 and 0.24μM respectively (KTZ IC_{50}=0.74μM) (Table 31) against the human enzyme, with similar results being observed against the rat enzyme with IC_{50} values of 1.2 and 0.54μM respectively (KTZ IC_{50}=67μM).

Compound No	Structure	IC_{50} (Rat)	IC_{50} (Human)
162	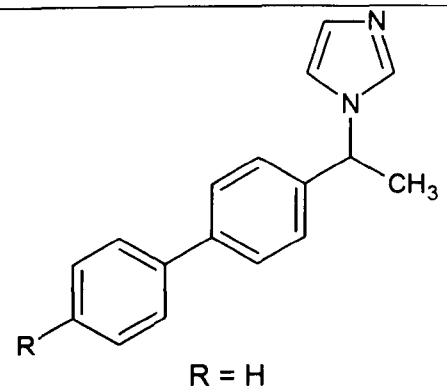 R = H	1.2μM	0.17μM
163	R = F	0.54μM	0.24μM
164	R = OCH_3	2.51μM	1.8μM
	KTZ	67μM	0.74μM

Table 31 Showing the Inhibitory activities of imidazolyl-based non-steroidal inhibitors of $P450_{17\alpha}$ (Zhuang et al[95]).

A study was further carried out by Leroux et al[96] on the effects of synthesised fluorinated 1-[([1,1'-biphenyl]-4-yl)methyl]-1*H*-imidazoles where the fluoro substituent was either situated 3,3',5,5' *meta* or2,2',6,6' *ortho* (Table 32). From previous studies it was presumed that the fluoro was more impervious to metabolism thus further improving lipophilicity, resulting in the assistance in membrane permeability. Results

had revealed that *ortho*-fluoro substituents (**173-176**) generally resulted in a reduction in potency as opposed to the non-fluorinated parent compounds which proved to have greater potency (**165-168**).

Compound No	Structure	(Rat) IC_{50}
165	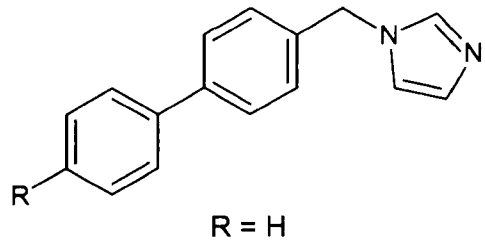 R = H	0.96μM
166	R = CH_3	36μM
167	R = CH_3O	43μM
168	R = OH	0.31μM
169	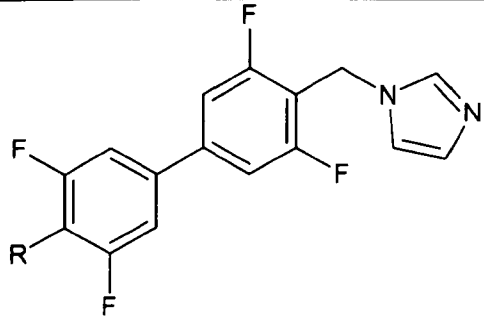 R = H	0.37μM
170	R = CH_3	39μM
171	R = CH_3O	46μM
172	R = OH	0.38μM
173	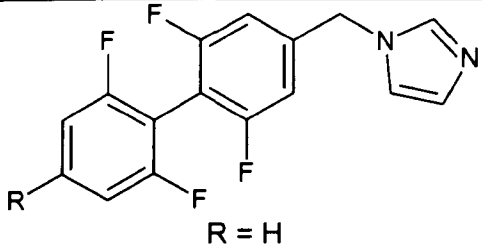 R = H	73μM
174	R = CH_3	38μM
175	R = CH_3O	4μM
176	R = OH	75μM

Table 32 Inhibition of Rat $P450_{17\alpha}$ by fluorinated 1-[([1,1'-biphenyl]-4-yl)methyl]-1H-imidazoles (Leroux et al[96]).

Meta-substituted fluoro substituents had shown to either exceed in potency (**169-172**) or maintain the potency against human $P450_{17\alpha}$ with respect to the inhibitory activity shown by the unsubstituted non-fluorinated parent compounds. Compound **169** was approximately threefold more potent against $P450_{17\alpha}$ (IC_{50} = 0.37μM) than its corresponding non-fluorinated analogue **165** (IC_{50} = 0.96μM).Introduction of a non-hydrophilic *p*-substituent was shown to decrease the inhibition potency of both the non-fluorinated parent compounds and the fluorinated products, whereas the introduction the hydroxyl group at the *para*-position was shown to increase the inhibiton of $P450_{17\alpha}$ considerably, indicating that the potency of the compounds may be affected by the nature of the *p*-substituent.

In vitro analysis was further carried out to investigate the effect of fluoro-substitution on the metabolic stability of both compounds **172** and **176**, where the unsubstituted analogue (**168**) was used as a reference. Results had revealed that the metabolic stability of **172** was considerably less than that of **168**, whereas compound **176** was shown to be metabolised quicker than **168**, further indicating that phase I metabolism may be affected by the introduction of fluoro-substituents in the *meta* position.

1.7.6 Non-steroidal inhibitors: Imidazole-based phenylindane inhibitors

Zhuang et al[95] synthesised and evaluated a series of biphenyl imidazole and triazole based compounds, comprising of an indane group (Table 33). The compounds were shown to have good inhibitory action towards rat and human $P450_{17\alpha}$. The imidazol-1-yl compounds were generally found to show much greater potency than the 1, 2, 4-triazol-1-yl compounds in both the human and rat *in vitro* testing, the most active compound being **177**with an IC_{50} value of 0.25μM (KTZ IC_{50}=0.74μM) (Table 33) against the human enzyme, with a similar result being observed against the rat enzyme with an IC_{50}

value of 2.1μM (KTZ IC_{50}=67μM). The majority of the 1, 2, 4-triazol-1-yl compounds resulted in no inhibition taking place. The 1,2,4-triazol-1-yl compounds were shown to be less active, whilst the 1,2,4-triazol-4-yl compounds were shown to be inactive.

Compound No	Structure	IC_{50} (Rat)	IC_{50} (Human)
177	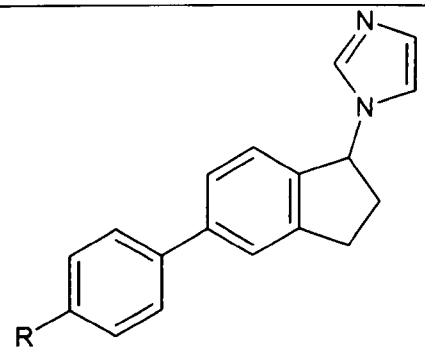 R = H	2.1μM	0.25μM
178	R =F	1.7μM	1.11μM
179	R = OCH_3	10μM	2.1μM
	KTZ	67μM	0.74μM

Table 33 Showing the Inhibitory activities of imidazolyl-based non-steroidal inhibitors of $P450_{17\alpha}$ (Zhuang et al[95]).

Methoxy substitution of the phenyl ring was shown to decrease the activity of the imidazole-based compound **164** and **179**, with fluorine substitution leading to an increase against the rat enzyme and inactivation against the human enzyme. These results went on to show that the open ring compounds (Table 32) were more potent than the equivalent indane structure, with the *para*-fluoro compound **163** showing to be almost 4 times more potent than **178** against the rat enzyme and almost 5 times more potent against the human enzyme (Table 32 & 33).

In order to rationalize such results, molecular modelling research was carried out using energy-minimised conformations of the compounds. The results had shown that the

imidazole based indane compounds had a dissimilar orientation to the more active open ring inhibitors which possibly signifies that the indane structure of the inhibitor isunsuccessful in its ability to interact with the enzyme active site, therefore resulting in a decrease in potency[95]. Molecular modelling studies further illustrated that the *para*-fluoro inhibitors **163** and **178** were more potent than the unsubstituted inhibitors **162** and **177** against the rat enzyme, where surprisingly the opposite was observed against the human enzyme. The introduction of the *para*-methoxy group consequently showed a decrease in inhibition against both enzymes in respect to the unsubstituted and the *para*-fluoro inhibitors.

Compounds **163** and **164** (Table 31) were tested *in vivo* for reduction of the plasma testosterone concentration using SD rats, where compound **163** was found to strongly inhibit testosterone concentration two hours following application. On the contrary, compound **164** decreased testosterone concentration to within castration levels after two hours of application and went on to further demonstrate strong activity after six hours of application. Both studies carried out on the substituted imidazolyl-methyl substituted biphenyls had revealed that the introduction of a methyl group into the methylene spacer amidst the imidazole and biphenyl moiety displayed greater inhibitory activity against both the rat and human enzyme compared to (**138** and **144**), however ring closure resulting in the corresponding phenylindanes had shown to reduce inhibiton of the target enzyme.

1.7.7. **Non-steroidal inhibitors**: **Imidazole-based naphthalene inhibitors**

Hartmann et al[97] had synthesised several fluorinated imidazoles as potential inhibitors of human $P450_{17\alpha}$ enzyme using fluorinated 2-naphthaldehydes and methyl 2-naphthoates as building blocks. The compounds, especially with regards to **182** and **186** where a

methoxy group was present at the *para*-position (Table 34). The mono-fluorinated compounds were shown to be more active than the non- (**188**) and the difluorinated derivatives (**183** and **185**) (Table 35). An increase in the inhibitory activity was further observed when a methyl group was present on the naphthyl ring (R^4).

Compound No	Structure	IC_{50} (Human)
180	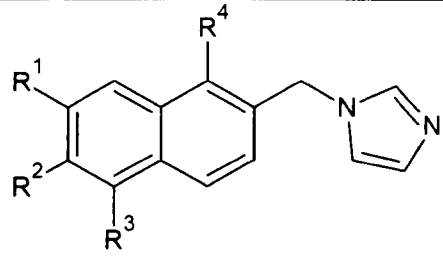 R^1=F, R^2=R^3=H, R^4=CH_3	1.0μM
181	R^1=F, R^2=H, R^3=F, R^4=CH_3	ND
182	R^1=F, R^2=OCH_3, R^3=H, R^4=CH_3	0.27μM
183	R^1=F, R^2=OCH_3, R^3=F, R^4=CH_3	0.50μM
184	R^1=F, R^2=R^3=R^4=H	ND
185	R^1=F, R^2=H, R^3=F, R^4=H	ND
186	R^1=F, R^2= OCH_3, R^3=R^4=H	0.41μM
187	R^1=F, R^2= OCH_3, R^3=F, R^4=H	1.0μM
188	R^1=H, R^2= OCH_3, R^3=R^4=H	3.1μM
189	R^1=R^2=R^3=R^4=H	ND

Table 34 Showing the results of Inhibition of $P450_{17\alpha}$ by fluorinated 1-[(naphth-2-yl)methyl]-1H Imidazoles (Hartmann et al[97]). ND = not determine.

In his study, Hartmann had established that human $P450_{17\alpha}$ was strongly inhibited by Matsunaga et al[98] had more recently discovered novel and potent $P450_{17\alpha}$ inhibitors through structure-based *de novo* design based on 17α-hydroxypregnenolone. The imidazole ring is combined with a steroid mimicking ring system such as naphthalene. In his study, Matsunaga carried out *in vitro* testing using rat and human $P450_{17\alpha}$ enzyme on various reported naphthalene-based 1- and 4-imidazolyl derivatives, mimicking the B and C ring of the steroid substrate, which was shown to exhibit potent inhibition.

Matsunaga based the inhibitors upon compound **190**, as it had shown to be potent inhibitor (Table 35).

Compound No	Structure	IC_{50}* (Rat)	IC_{50}* (Human)
190	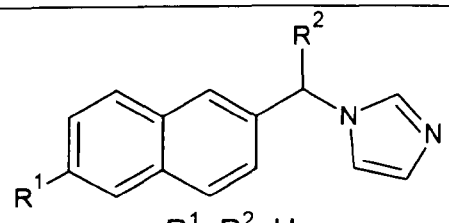 $R^1=R^2=H$	53nM	43nM
191	$R^1=OCH_3$, $R^2=H$	27nM	27nM
192	$R^1=C_2H_5O$, $R^2=H$	26nM	23nM
193	$R^1=i\text{-}OC_3H_7$, $R^2=H$	24nM	46nM
194	$R^1=PhCH_2O$, $R^2=H$	670nM	230nM
195	$R^1=SCH_3$, $R^2=H$	18nM	20nM
196	$R^1=CH_3SO$, $R^2=H$	270nM	240nM
197	$R^1=CH_3SO_2$, $R^2=H$	230nM	200nM
198	$R^1=CH_3O$, $R^2=CH_3$	22nM	21nM
199	$R^1=CH_3O$, $R^2= i\text{-}OC_3H_7$	26nM	24nM

*Table 35 Showing the Inhibitory activities of 1-imidazoyl derivatives *(17,20-Lyase) (Matsunaga et al[98]).*

The study was based on the substrate mimic strategy and a number of analogues exhibited potent inhibition for the rat enzyme. Matsunaga was attracted to these compounds for their simplicity with regards to their structure, where a wide range of modification could take place relatively easy. Docking studies using a homology model of the human enzyme insinuated that the C6 position of the naphthalene ring of **190** may possibly interact with the same area (Thr101) as the 3β-hydroxy group of 17α-hydroxypregnenolone. Therefore compound **190** was modified, giving rise to a series of analogues which had exhibited potent inhibition against $P450_{17\alpha}$ (Table 35).

In the imidazoyl derivatives, small alkoxy substituents for R^1, **191** and **192**, slightly increased the inhibitory activity towards rat and human enzymes compared to the unsubstituted compound **190**. The addition of an isopropoxy group **193** was shown to have an increase in the activity against the rat enzyme only. The addition of a benzyloxy group **194**, resulted in significantly less inhibition with regards to both the rat and human enzyme, compared to the other alkoxy compounds. The methylsulfide substituent **195** exhibited potent activity, whereas the methylsulfoxide and methylsulfone, **196** and **197**, resulted in a decrease in the inhibition. The addition of alkyl groups for R^2, **198** and **199**, was shown to have a similar level of activity as that for compound **192** (Table 35).

Both compounds **191** and **195** were further shown to reduce testosterone levels in rats significantly, producing 1% of testosterone concentration after 5 hours in contrast to controls. Referring back to molecular modelling studies regarding the above compounds, it was further implied that the introduction of a lipophilic group on the methylene bridge between the naphthalene and the imidazole of the compound could possibly interact with a small lipophilic pocket consisting of Ala367, Met369, Ile371, Pro372 and Phe484, near to the heme at the active site.

In his study, Matsunaga[98] further investigated 4-imidazoyl compounds (Table 36) and discovered that the orientation of the 4-imidazoyl group corresponded to the potency of the 1-imidazoyl compounds (comparison of **202** and **193**, **202** and **198**,**203** and **200**). The addition of alkyl substituents at the R^1 position had insignificant effect on the enzyme inhibiton, which was also the case regarding the 1-imidazoyl compounds. Incorporation of a hydroxyl group and an isopropyl group at R^1 and R^2 resulted in serum testosterone reduction[100]. From observation of the two enantiomers (**214** and **215**),

compound **215** was shown to be the more potent of the two, with IC_{50} values of 21nM for the rat enzyme and 28nM against the human enzyme.

Compound No	Structure	IC_{50}* (Rat)	IC_{50}* (Human)
200	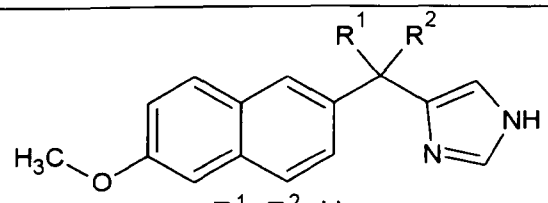 R^1=R^2=H	13nM	18nM
201	R^1=CH_3, R^2=H	28nM	23nM
202	R^1= *i*-OC_3H_7, R^2=H	22nM	30nM
203	R^1=H, R^2=OH	170nM	63nM
204	R^1= CH_3, R^2=OH	130nM	35nM
205	R^1=C_2H_5, R^2=OH	41nM	27nM
206	R^1=*n*-C_3H_7, R^2=OH	43nM	36nM
207	R^1=*i*-OC_3H_7, R^2=OH	33nM	32nM
208	R^1=*c*-C_3H_7, R^2=OH	64nM	35nM
209	R^1= *i*-OC_4H_9, R^2=OH	85nM	41nM
210	R^1= *t*-C_4H_9, R^2=OH	160nM	83nM
211	R^1=*c*-C_5H_{11}, R^2=OH	48nM	42nM
212	R^1=Ph, R^2=OH	230nM	110nM
213	R^1=3-pyridyl, R^2=OH	420nM	270nM
214	R^1=4-pyridyl, R^2=OH	240nM	54nM
215	R^1=(S)-*i*-C_3H_7, R^2=OH	21nM	28nM
216	R^1=(R)-*i*-C_3H_7, R^2=OH	52nM	54nM

*Table 36 Showing the Inhibitory activities of 4-imidazoyl derivatives *(17,20-Lyase) (Matsunaga et al[98]).*

Both smaller and larger alkyl groups decreased the activity, **204** to **211**, for the rat enzyme. For the human enzyme, methyl to propyl groups in the R^1 position, such as in **204**, **205** and **207 - 209**, were shown to reduce activity (Table 36). In further studies carried out by Matsunaga et al[98] AB ring mimics were designed where the naphthalene ring was modified by the addition of a heteroatom within the naphthalene ring (compounds **218** and **219**) (Table 37). The inhibitors showed potent inhibition for rat

17,20-lyase. Compound **217** (IC_{50} = 26nM) was shown to be the most potent of the whole range of compounds, as compared to the standard KTZ (IC_{50} = 240nM). Compound **219**, which is a *2H*-chromene-based derivative, also proved to be a potent inhibitor (IC_{50} = 29nM) with similar inhibition to that of compound **217**. The quinoline inhibitor **218** (IC_{50} = 95nM) was shown to be a weaker inhibitor as compared to compounds **217** and **218**; however, it was shown to be a potent inhibitor in comparison to the standard KTZ (Table 37).

Compound No	Structure	IC_{50}*
217	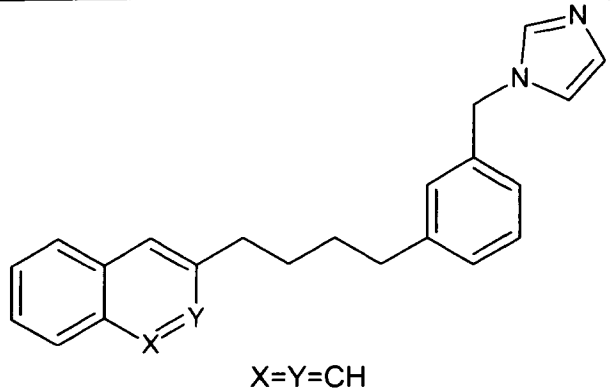 X=Y=CH	26Nm
218	X=N, Y=CH	95nM
219	X = O, Y = CH_2	29nM
	KTZ	240nM

*Table 37 Showing the inhibitory activities of imidazole-based non-steroidal inhibitors *(rat 17,20-lyase) (Matsunaga et al[98]).*

1.7.8 **Non-steroidal inhibitors**: **Imidazole-based benzothiophene inhibitors.**

In addition to his studies, Matsunaga et al[98] synthesised a range of benzothiophene compounds which proved to be very potent inhibitors of $P450_{17\alpha}$ (Table 38 and 39). With regards to the 1-imidazolyl-based inhibitors (**220-228**) compound **220** was shown to be a potent inhibitor as compared to the standard KTZ (IC_{50} = 16nM and 240nM, respectively.

Compound No	Structure	IC_{50}*
220	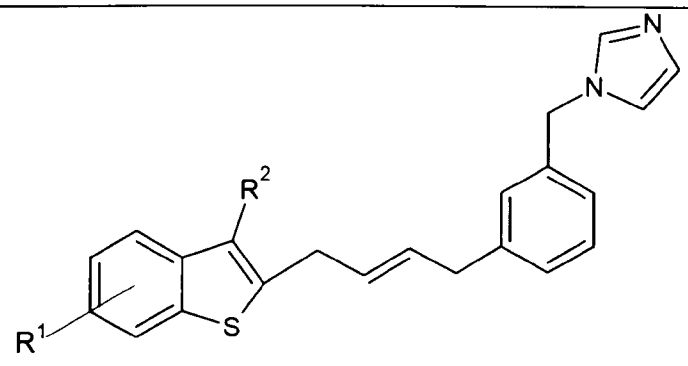 R^1=R^2=H	16nM
221	R^1=4-F, R^2=H	20nM
222	R^1=5-F, R^2=H	25nM
223	R^1=6-F, R^2=H	26nM
224	R^1=7-F, R^2=H	10nM
225	R^1=5-Cl, R^2=H	29nM
226	R^1=5-F, R^2=CH_3	25nM
227	R^1=5-Cl, R^2=CH_3	26nM
228	R^1=5-OCH_3, R^2=CH_3	33nM
	KTZ	240nM

*Table 38 Showing the Inhibitory activities of 1-imidazoyl naphthalene-based derivatives *(Rat 17,20-Lyase) (Matsunaga et al[98]).*

The potency of compound **220** was shown to be influenced with the addition of a fluoro group at the C(7) position of the benzothiophene ring, further increasing the duration of action *in vivo* (compound **224**, IC_{50} = 10nM). Addition of a methyl group at the C(2) position of the benzothiophene ring was shown to produce a decrease in activity with IC_{50} values ranging from 25-33nM (compounds **226-228**) (Table 38).

The 4-imidazolyl moiety within the benzothiophene ring was revealed to enhance *in vivo* potency than the corresponding 1-imidazolyl compounds. The 4-imidazolyl-based inhibitors, compounds **229**, **230** and **232**, were shown to display potent inhibition against $P450_{17\alpha}$, with compound **229** proving to be the most potent (IC_{50} = 4nM, 9nM and 6nM, respectively) (Table 39).

Compound No	Structure	IC_{50}*
229	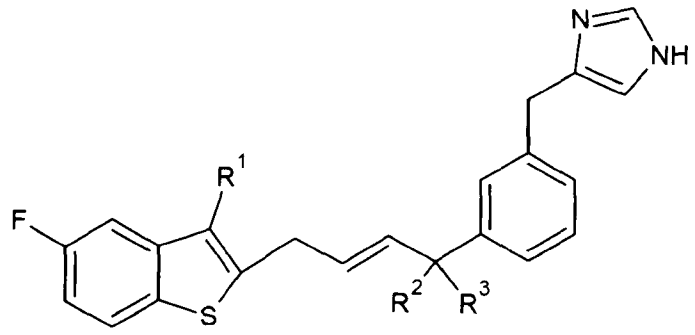 $R^1=R^2=H$, $R^3=CH_3$	4nM
230	$R^1= CH_3$, $R^2=H$, $R^3=CH_3$ (S)	9nM
231	$R^1= CH_3$, $R^2=H$, $R^3=CH_3$ (R)	8nM
232	$R^1=R^2=R^3=CH_3$	6nM
233	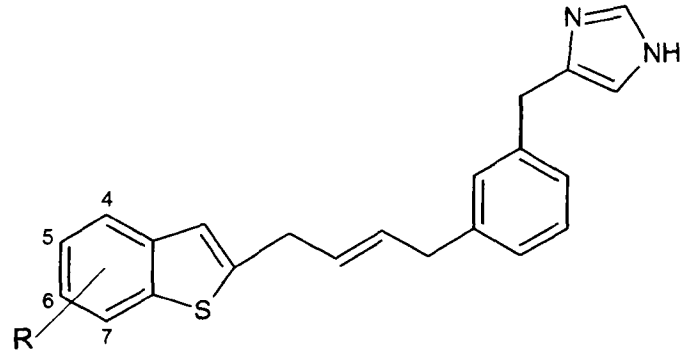 R = 4-F	19nM
234	R = 5-F	23nM
235	R = 6-F	27nM
236	R = 7-F	25nM
	KTZ	240nM

*Table 39 Showing the Inhibitory activities of 4-imidazoyl naphthalene-based derivatives *(Rat 17,20-Lyase) (Matsunaga et al[98]).*

The potency of these compounds was established in the function of the 4-imidazolyl ring and the 5-fluoro group on the benzothiophene ring (compounds **229-232**). Additional 4-imidazolyl-based inhibitors were also designed with the fluoro-group being placed in different positions of the benzothiophene ring (compounds **233-236**). These compounds furthermore proved to be potent inhibitors of human $P450_{17\alpha}$ with IC_{50} values of 19-27nM, with compound **233** proving to be the most potent of the range[100] (Table 39).

Both the 1- and 4-imidazolyl-based benzothiophene inhibitors were shown to be far more potent than the standard KTZ (IC_{50} = 240nM).

1.7.9 Non-steroidal inhibitors: Imidazole-based phenylthiophene inhibitors

A range of substituted phenylthiophenes were reported by Jagusch et al[99] as inhibitors of $P450_{17\alpha}$ (Compounds **237-242**) (Table 40).

Compound No	Structure	%inhibition*
237	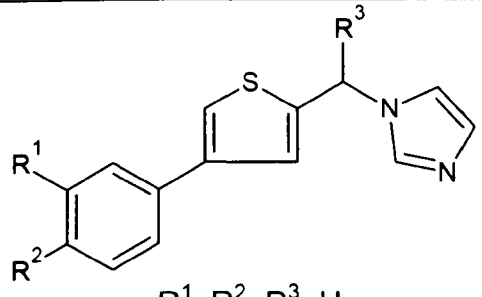 $R^1=R^2=R^3=H$	21%
238	$R^1=OCH_3$, $R^2=R^3=H$	24%
239	$R^1=R^2=F$, $R^3=H$	25%
240	$R^1=R^2=F$, $R^3=C_2H_5$	68%
241	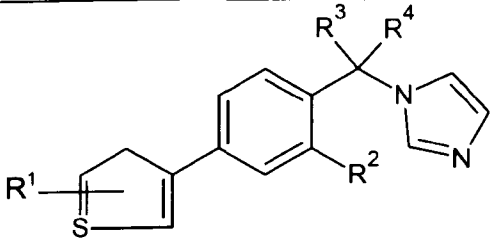 $R^1=H$, $R^2=H$, $R^3=$ *i*-C_3H_7, $R^4=OH$	49%
242	$R^1=2$-CH_3, $R^2=F$, $R^3=C_2H_5$, $R^4=H$	92%, IC_{50}=236nM
243	$R^1=5$-Cl, $R^2=F$, $R^3=C_2H_5$, $R^4=H$	85%, IC_{50}=263nM
	KTZ	92%, IC_{50}=280nM

*Table 40 Showing the inhibitory activity of a range of non-steroidal imidazole-based phenylthiophenes. *([i]=2.0μM) (Jagusch et al[99]).*

Compounds **237**-**239** were shown to have relatively weak inhibition for $P450_{17\alpha}$, ranging from 21% to 25%. However, the addition of an ethyl group at the methylene bridge to compound **239**, producing compound **240**, resulted in a noticeable increase in activity from 25% (**239**) to 68% (**240**). Compounds **242** and **243** were shown to be potent inhibitors of $P450_{17\alpha}$ (IC_{50} = 236 and 263, respectively) with similar results to that of the standard KTZ (IC_{50} = 280nM).

The addition of the fluorine atom on the phenyl ring (**242**) and the 5-chloro substituent on the thiophene ring (**243**) were major contributors to the potency of these compounds. Structure-activity relationship studies revealed that an alkyl group at the methylene bridge may possibly contribute to the inhibitor being able to position itself closer to the haem within the proposed hydrophobic pocket of the enzyme, thus influencing the inhibitory activity of these compounds[99].

1.7.10 Non-steroidal inhibitors: Imidazole-based phenylnaphthalene inhibitors

Mendieta et al[99] had too designed and synthesised a number of ABD- and ACD ring mimics in the form of substituted phenylnaphthalene-based inhibitors (Tables 41). The reported ABD-ring mimics, compounds **244** and **245**, were shown to have poor to moderate activity (%inhibition = 28% and 61%, respectively) as compared to the potent inhibition demonstrated by the standard KTZ (%inhibition = 92%) (Table 41). With regards to the ACD-ring mimics, compounds **246** to **248**, were too shown to be weak to moderate inhibitors in respects to activity, with compound **198** proving to be the most potent from the range (%inhibition = 50%) (Table 35).

Compound No	Structure	%inhibition*
244	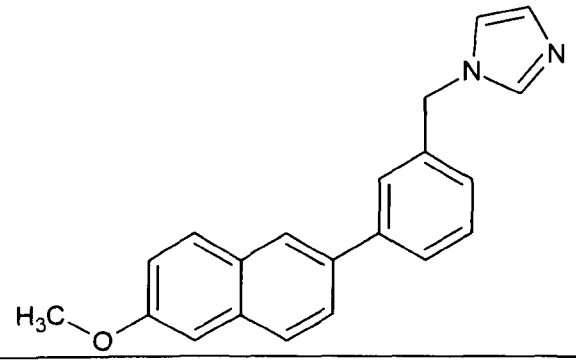	28%
245	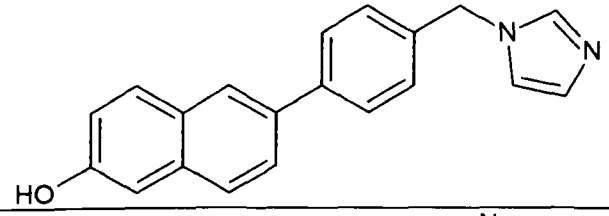	61%
246	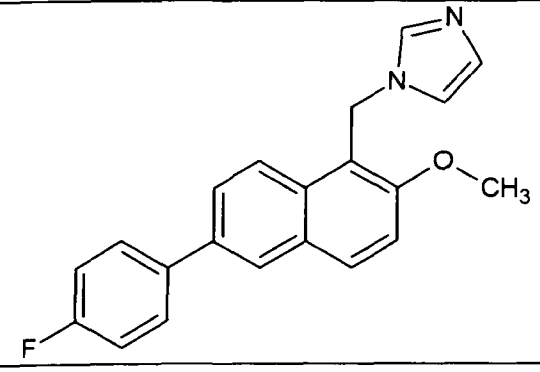	45%
247	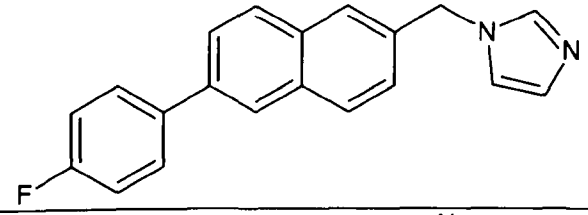	14%
248	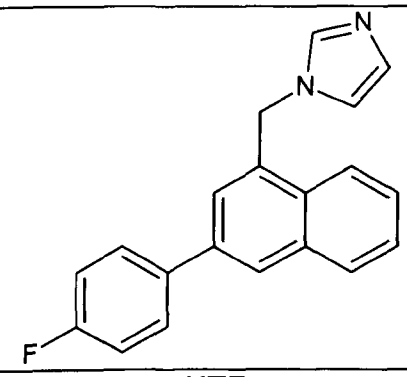	50%
	KTZ	92%

Table 41 *Showing the inhibitory activity of non-steroidal phenylnaphthalene-based ABD- and ACD-ring mimics *([i] = 2.0μM) (Mendieta et al[102]).*

2.0 Aims

The design and synthesis of $P450_{17\alpha}$ inhibitors are noted to be beneficial in the treatment of hormone-dependent prostate cancer as development of the disease is associated with the ongoing exposure of prostate tissue to androgens, increasing the risk of tumour growth. Location of the enzyme within the endoplasmic reticulum of the prostate cell is problematic, owing to the absence of information regarding its crystal structure. Research has been carried out regarding the utilisation of molecular modelling[51, 100] in order to acquire additional information about the enzyme $P450_{17\alpha}$.

The alternative method to molecular modelling proposed by Ahmed and Davis[101, 102] involved the approximate representation of the active site of the enzyme complex. The substrate haem complex (SHC) approach requires the viewpoint of the imperative components which are expected to be at the active site; primarily the haem, substrate and possible hydrogen bonding groups which will be capable of binding to specific binding regions of the substrate.

Since the discovery of this innovative approach, the SHC was completed for both the 17α-hydroxylase[57] and the 17, 20-lyase component[103] of the enzyme, where a number of synthesised compounds had been assessed for activity. It was hypothesised that the principle interaction was that of the lone pair of electrons on the nitrogen of the heteroatom (imidazole or triazole) of the inhibitor and the heme Iron within the enzyme. The remainder of the molecule binds to the steroid binding region within the active site via polar-polar/hydrogen bonding.

In the past decade, there have been a number of azole-based inhibitors which have been reported to be potent in the inhibition of the enzyme $P450_{17\alpha}$, but only a few have entered clinical trials. This has mainly been due to the lack of information regarding the crystal structure of the enzyme.Azole based compounds have been shown to be of great interest in the treatment of prostate cancer with the discovery of ketoconazole.

The aims of this investigation is the synthesis of non-steroidal substituted benzyl imidazole based compounds such as those shown in figure 23.Molecular modelling based studies suggest derivatives of the benzyl imidazole core could be good inhibitors of $P450_{17\alpha}$. Varying the electronic and steric nature of the R groups will impacton the interactions which take place within the active site[108]; where n will be an alkyl chain of varying length, allowing consideration of physicochemical factors such as hydrophobicity with respects to active site inhibition.

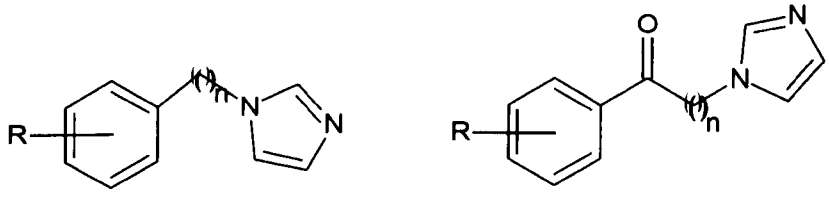

Figure 23 Showing the non-steroidal substituted benzyl imidazole based target compounds synthesised.

3.0 Results and discussion

3.1 Synthesis of benzylimidazole derivatives

In the synthesis of the *N*-alkylated benzyl imidazole-based compounds, an alkyl halide in the presence of a base, such as potassium carbonate was used[104]. Another method involves the synthesis of the imidazole moiety from the appropriate amine[105], however this was not used as the prior method has shown to be more favourable[104, 109]. The synthesis of the benzyl imidazole derivatives were carried out using the conditions outlined in scheme 1 below.

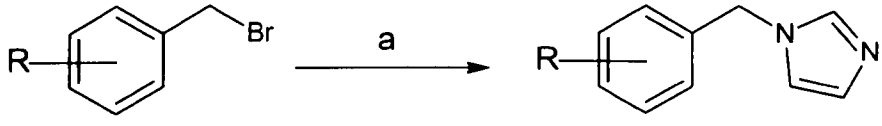

Scheme 1 Synthesis of derivatives of benzyl imidazole-based compounds (a=K_2CO_3/THF/imidazole/Δ; R=H, 2-, 3-, 4-F, Cl, Br, I, NO_2, CN, OCH_3, CH_3, 3-, 4-difloro and dichloro).

The proposed mechanism of reaction outlined in scheme 1 primarily involves attack of the imidazolium anion on the relevant benzyl bromide. The reactions were carried out on a 1:1.5:3 ratio (benzylbromide:K_2CO_3:imidazole), which was found to give the highest yields. These reactions generally proceeded well and in fairly good yield (ranging from 34.0% to 89.97%) without any major problems being encountered. All derivatives required purification by column on silica gel, using the solvent system 90:10 diethyl

ether/methanol which gave very good separation for the product and the substituted benzyl bromide starting material.

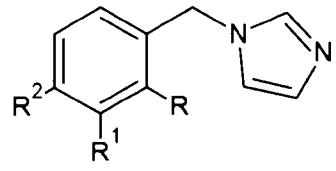

Compound	Structure	% yield	Compound	Structure	% yield
250	R=F, R^1=R^2=H	78.17	**263**	R=R^1=H, R^2=I	64.85
251	R=H, R^1=F, R^2=H	65.16	**264**	R=CN,R^1=R^2=H	34.13
252	R=R^1=H, R^2=F	84.94	**265**	R=H, R^1=CN,R^2=H	69.11
253	R=H, R^1=R^2=F	84.43	**266**	R=R^1=H, R^2=CN	79.01
254	R=Cl, R^1=R^2=H	76.57	**267**	R=CH_3, R^1=R^2=H	34.0
255	R=H, R^1=Cl,R^2=H	66.47	**268**	R=H,R^1=CH_3,R^2=H	80.3
256	R=R^1=H, R^2=Cl	77.96	**269**	R=R^1=H, R^2=CH_3	76.66
257	R=H, R^1=R^2=Cl	66.0	**270**	R=NO_2, R^1=R^2=H	89.97
258	R=Br, R^1=R^2=H	71.51	**271**	R=H,R^1=NO_2,R^2=H	89.65
259	R=H, R^1=Br,R^2=H	66.45	**272**	R=R^1=H, R^2=NO_2	83.51
260	R=R^1=H, R^2=Br	53.06	**276**	R=OCH_3, R^1=R^2=H	84.72
261	R=I, R^1=R^2=H	35.46	**277**	R=R^2=H, R^1=OCH_3	83.15
262	R=H, R^1=I, R^2=H	74.05	**278**	R=R^1=H, R^2=OCH_3	65.26

Table 42 Showing the percentage yields achieved of the substituted benzyl imidazoles synthesised.

Table **42**shows some of the yields achieved from the products synthesised. The percentage yields achieved for the range of compounds varied from a low yield of 34.0 to 89.97. The halogen substituted products were achieved in relatively good percentage yields (**250-263**). The 2- and 4-substituted halogens were generally shown to give the

highest yields. Within the nitro group of compounds, the 3-nitro substituted product was synthesised in very good yield (**271**, 89.65%).

In the synthesis of the methoxy range of compounds, the 4-methoxy product was shown to give satisfactory yield (**278**, 65.26%) whilst the 3- and 4-methoxy compounds show high yields of 84.72% and 83.15%, respectively. Both the 3- and 4-methyl products gave very good yields from this range of products (**268**, 80.3% and **269**, 76.66%, respectively). The cyano group of compounds were synthesised from satisfactory to very good yield, with the 4-cyano substituted compound achieving the best yield (**266**, 79.01%). In the synthesis of the halogen substituted compounds only, the ortho and para-substituted compounds were generally shown to give the better yield. However, in the remaining compounds synthesised, the meta- and para-substituted compounds were shown to give the highest yields with the exception of the nitro and methoxy range which were shown to give higher yields in the ortho and meta-positions.

An alternative method was required for the synthesis of the 2-, 3-, and 4-methoxybenzyl imidazoles (**276-278**) as the relevant benzyl bromide starting material was not commercially available (scheme 3). The reaction used the relevant substituted benzyl alcohol as the starting material undergoing bromination of the hydroxy moiety to give the required *N*-alkylated benzyl bromide (scheme 2).

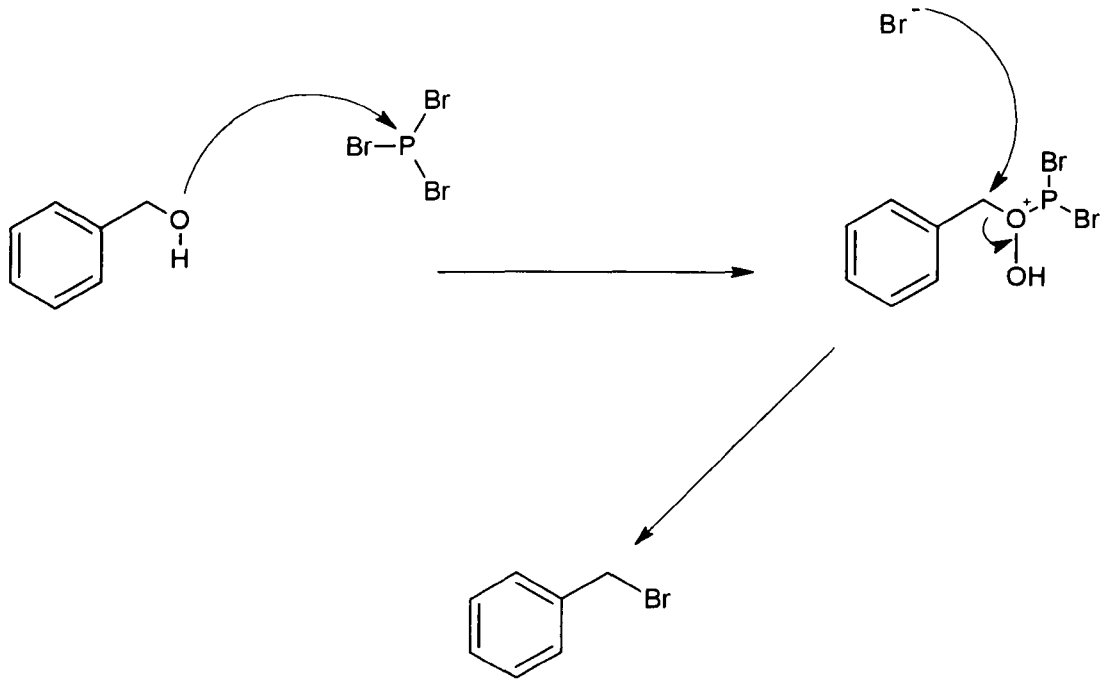

Scheme 2 Showing the mechanism for the bromination of the hydroxyl moiety.

The reaction involving the bromination of the hydroxyl moiety (Scheme 3) generally proceeded in very good yield with 85% achieved for the 4-methoxybenzyl bromide and 86% for both the 2- and 3-methoxybenzyl bromides. Their synthesis was confirmed by NMR. The desired substituted methoxybenzyl imidazoleswere subsequently synthesised following the conditions outlined in scheme 1. These compounds were purified from starting material*via* column on silica gel, using the same solvent system of 90:10 diethyl ether/methanol to give a pure product, achieving yields of 84.72% (**276**), 83.15% (**277**) and 65.26% (**278**) (2-, 3- and 4-methoxy consecutively).

In the NMR analysis, several of the fluorinated compounds presented fluorine coupling, leading to problematic ^{1}Hspectra in particular. The J values regarding the H-F splitting could not be resolved due to the overlapping of H-H signals, resulting in the formation of complex multiplets.

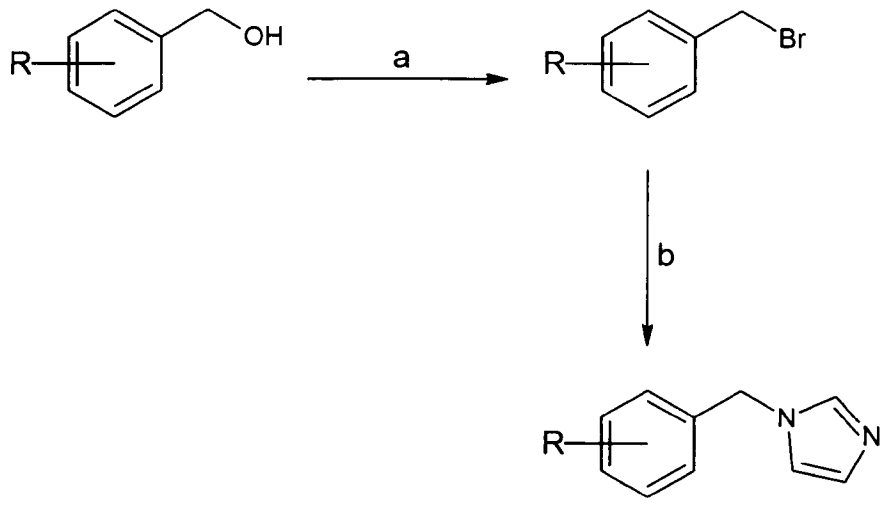

Scheme 3 Reactions carried out in the synthesis of the o,m,p-methoxy substituted benzyl imidazoles (a=PBr_3/diethyl ether; b=K_2CO_3/THF/imidazole/Δ; R=2-, 3- and 4-OCH_3).

Figure 24 shows the ^1H NMR for para-cyanobenzyl imidazole. The spectrum gives a clear splitting pattern of the para-disubstituted benzene, with the distinctive pattern of doublets. The remaining three singlets are characteristic of the imidazole protons.The ^{13}C NMR was also shown to be characteristic of the N-substituted imidazole (figure 25). The spectrum showing the $^{13}CNMR$ for para-cyanobenzyl imidazole, gives the correct number of peaks expected.

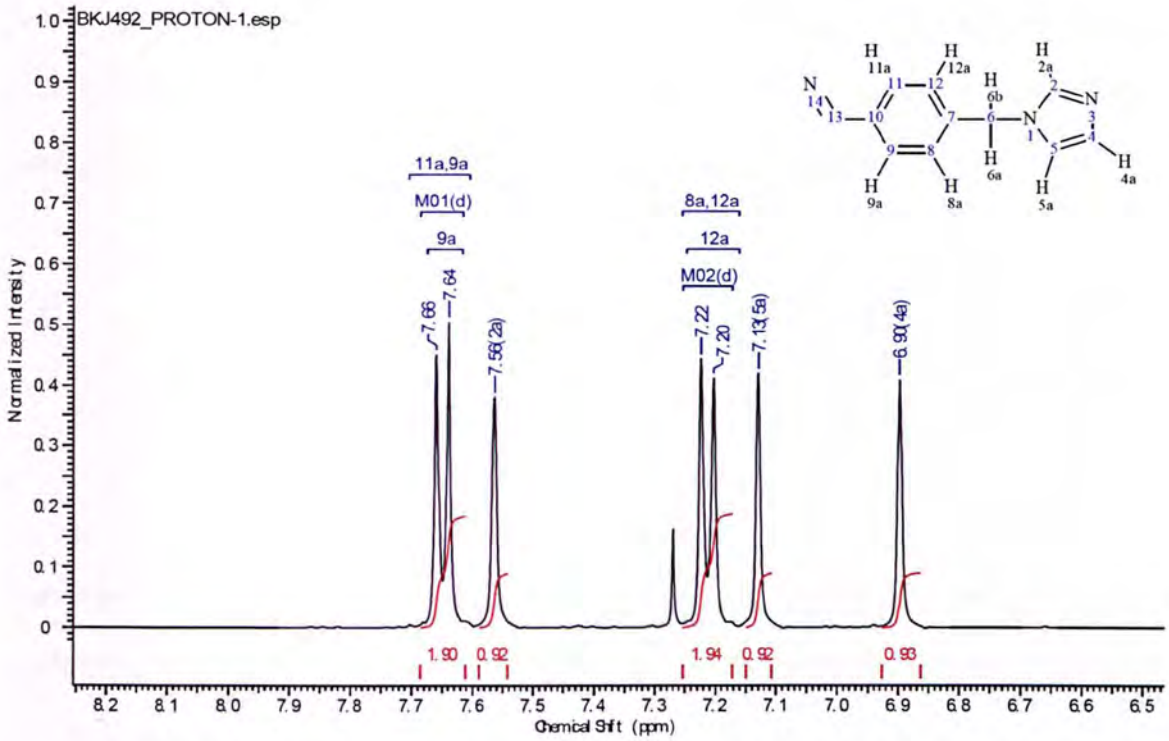

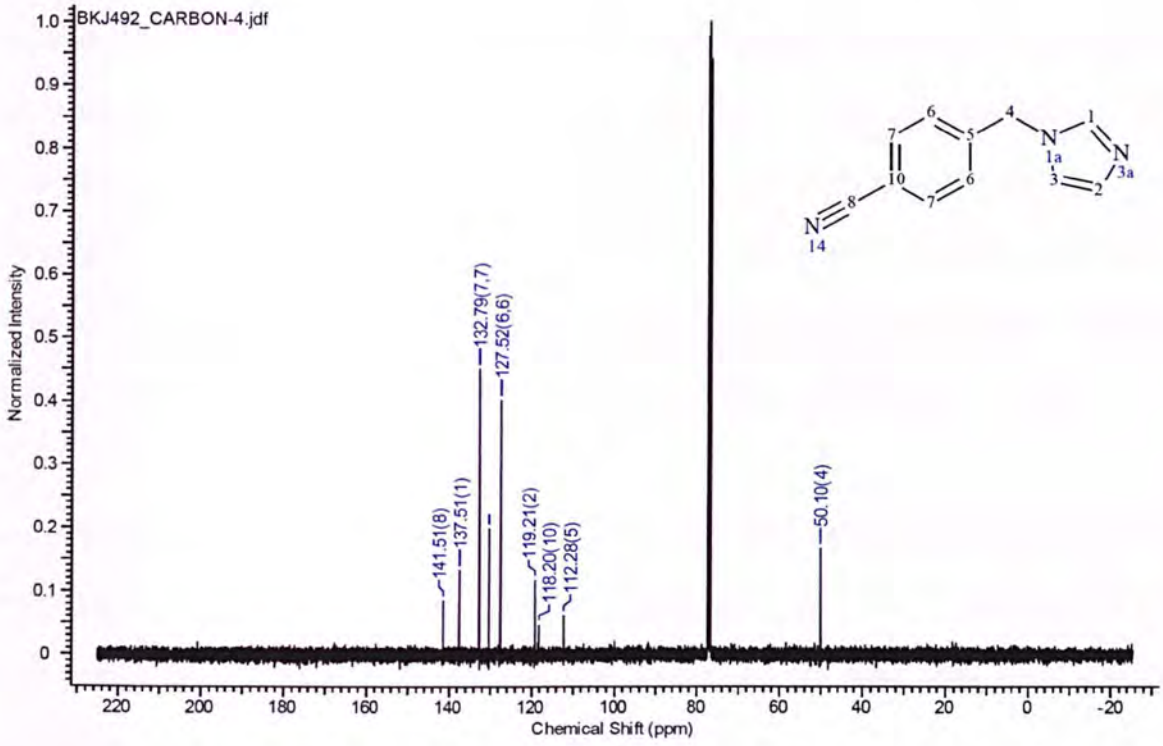

Figure 24 & 25 *^{1}H and ^{13}C NMR spectra for para-cyanobenzyl imidazole*

3.2 *Synthesis of substituted imidazol-phenyl ethanones*

In the synthesis of the substituted imidazol-phenyl ethanones, the reaction outlined in scheme 4 was used. The relevant phenylbromoethanone, which was commercially available, was used as starting material as outlined in scheme 4.

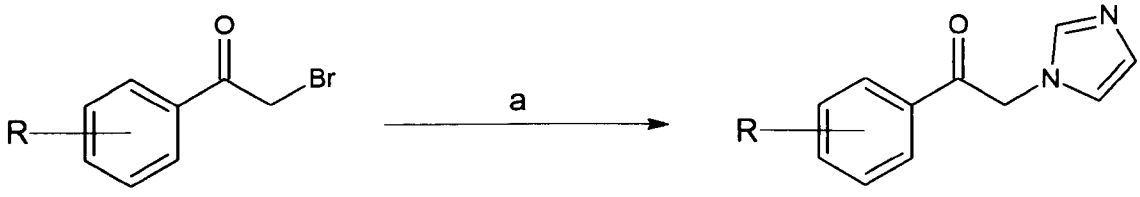

Scheme 4 Synthesis of derivatives of imidazol-phenylethanone based compounds (a=K_2CO_3/THF/imidazole/Δ; R=H, 2-, 3-, 4-F, Cl, Br, NO_2, OCH_3,3-, 4-CN, 4-CH_3, 4-I, 4-Ph, 3-, 4-dichloro & 3-, 4-dichloro).

The reactions proceeded in moderate to good yield (ranging from 41% to 91%) (Table 43), and without any major problems with the exception of the synthesis of the 1-(2-chlorophenyl)-2-(1*H*-imidazol-1-yl)ethanone (**283**). The GC-MS analysis indicated that the product was synthesised giving a single peak with the correct m/z ion peak of 220. However 1H NMR showed a number of impurities, one of which was shown to be the starting material and some were hard to work out as there were so many of these.

Purification was carried out via column on silica gel, using a solvent system of 20:80 methanol/diethyl ether.However, further analysis by ^{1}H NMRrevealed a numberimpurities. The starting material was shown to be pure, indicating possible contamination during the reaction procedure.

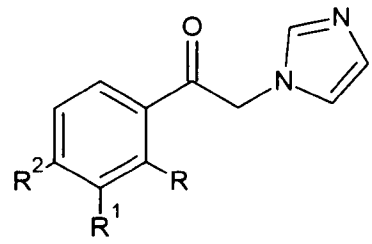

Compound	R group	% yield	Compound	R-group	% yield
279	R=R^1=R^2=H	69.35	**289**	R=R^1=H, R^2=Br	63.15
280	R=F, R^1=R^2=H	61.83	**290**	R=R^1=H, R^2=I	46.31
281	R=H, R^1=F, R^2=H	85.02	**291**	R=NO_2, R^1=R^2=H	48.15
282	R=R^1=H, R^2=F	87.16	**292**	R=H,R^1=NO_2,R^2=H	75.0
283	R=Cl, R^1=R^2=H	N/A	**293**	R=R^1=H, R^2=NO_2	47.08
284	R=H, R^1=Cl,R^2=H	43.0	**294**	R=OCH_3,R1=R^2=H	75.53
285	R=R^1=H, R^2=Cl	65.95	**295**	R=H,R^1=OCH_3,R^2=H	84.04
286	R=H, R^1=R^2=Cl	68.42	**296**	R=R^1=H, R^2=OCH_3	72.87
287	R=Br, R^1=R^2=H	85.26	**297**	R=R^1=H, R^2=CH_3	60.96
288	R=H, R^1=Br,R^2=H	65.78	**298**	R=H, R^1=CN, R^2=H	76.62

Table 43 Percentage yields achieved in the synthesis of the substituted imidazol-phenylethanones.

The reaction was repeated, using the same reaction conditions outlined in scheme 4, however, repetition of this reaction resulted in a similar mixture being produced and again it proved difficult to work out the impurities as there were so many. As the starting material was difficult to obtain with the added inconvenience of also being quite expensive, it was decided to no longer pursue the synthesis of the compound 1-(2-chlorophenyl)-2-(1*H*-imidazol-1-yl)ethanone *via* this route and to try and look into an alternative method. Unfortunately this target was not reached.

The percentage yields achieved were relatively good ranging from a satisfactory 43.0 to 87.16%. The substituted halogens (**280-290**) were shown to give very good percentage yields, especially the 3 and 4-fluoro substituted products (**281**, 85.02% and **282**, 87.16%, respectively) and the 2-bromo (**287**, 85.26%). In the range of the nitro substituted products, the best yield was achieved by the 3-nitro (**292**, 75.0%). However, in the range of the methoxys, this was achieved by the 2-, 3- and the 4-methoxy product (**294**, 75.5%, **295**, 84.04 % and **296**, 72.87%, respectively). For the cyano-substituted products, the 3-cyano showed very good yield of 76.62% (**298**).

Figure 26 shows the ^{1}H NMR for 1-(4-Fluoro-phenyl)-2-imidazol-1-yl-ethanone (**282**). The spectrum gives a clear splitting pattern characteristic of the para-disubstituted benzene, giving the distinctive pattern of doublets. The remaining three singlets are characteristic of the imidazole protons. The ^{13}C NMR was also shown to be characteristic of the N-substituted imidazole. Figure 27 shows the ^{13}C NMR for 1-(4-Fluoro-phenyl)-2-imidazol-1-yl-ethanone. The correct number of peaks can be observed, where the carbonyl is very distinctive and fluorine coupling is also present.

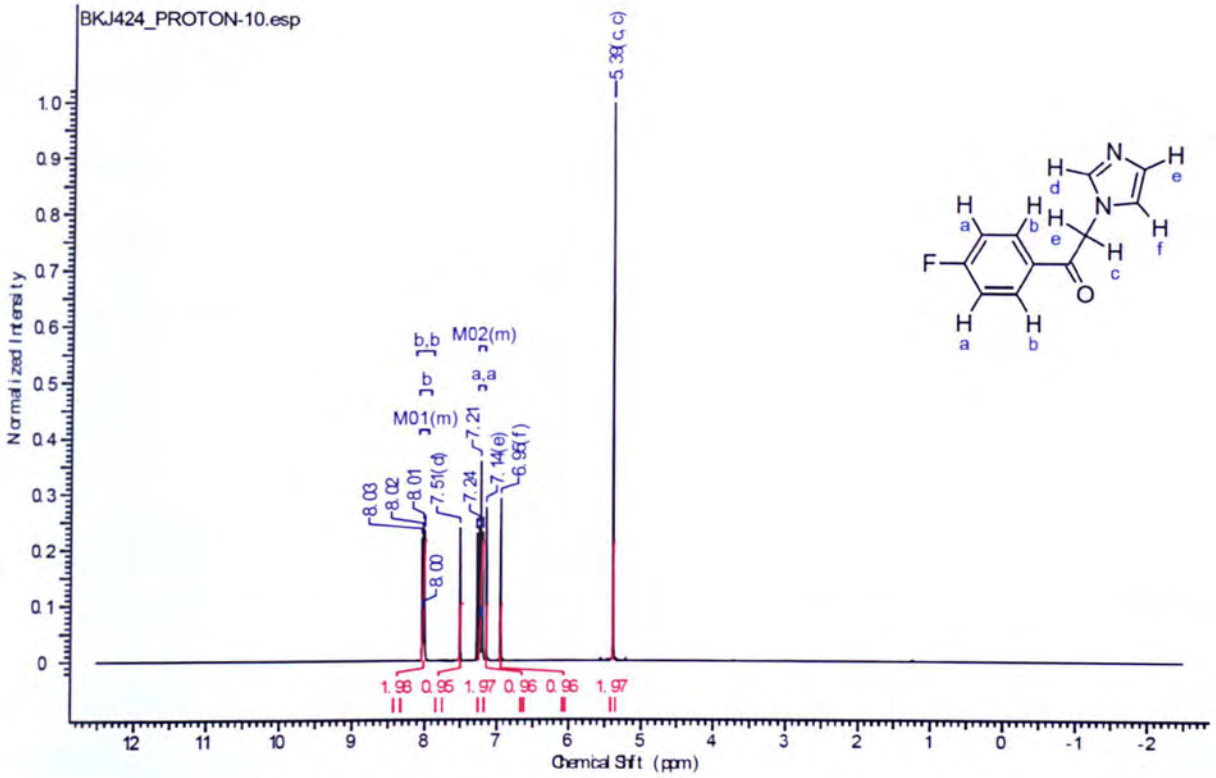

Figure 26 *^{1}H NMR of1-(4-Fluoro-phenyl)-2-imidazol-1-yl-ethanone.*

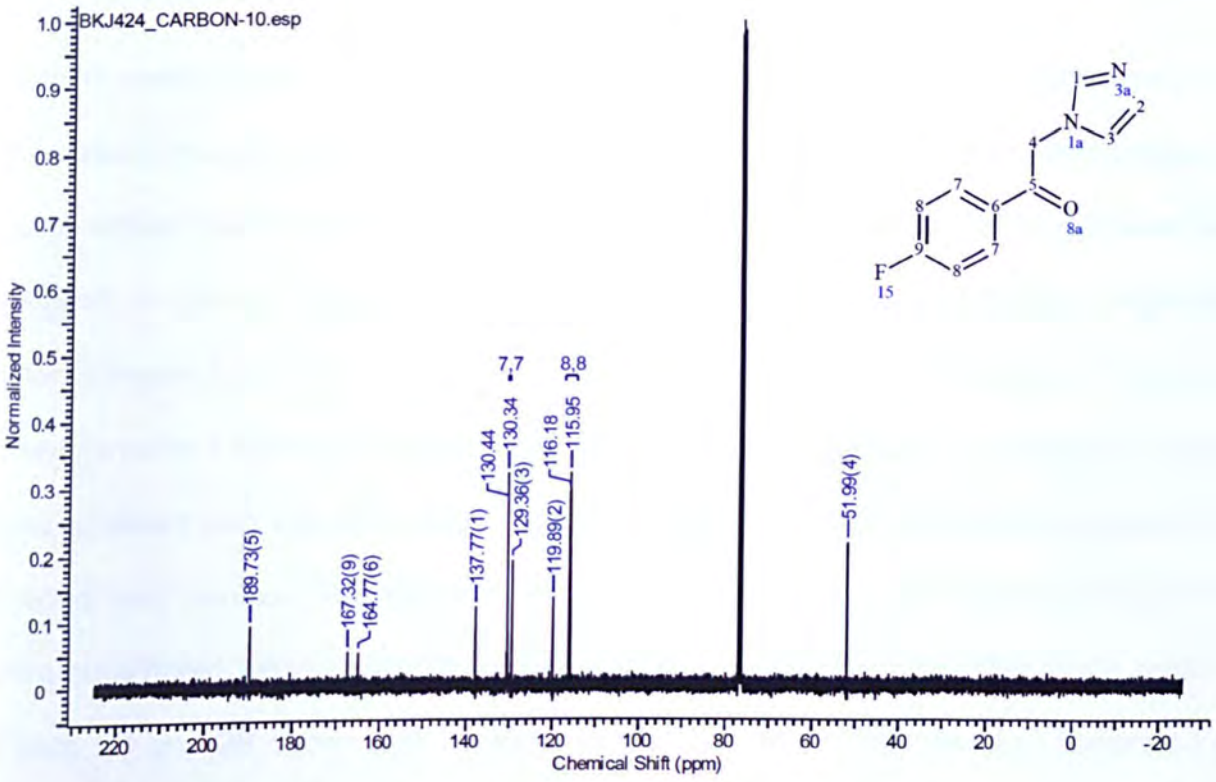

Figure 27 *^{13}C NMR of1-(4-Fluoro-phenyl)-2-imidazol-1-yl-ethanone.*

As per the original aims of the project, attention was turned to the synthesis ofcompounds where the alkyl chain was extended in order to observe the effect of enhanced Van-der walls interations as well as the interaction of the benzylimidazole derivative with the active site of the enzyme(Scheme 5). The reactions outlined in scheme 5 generally proceeded in good yields (ranging from 41% to 91%).

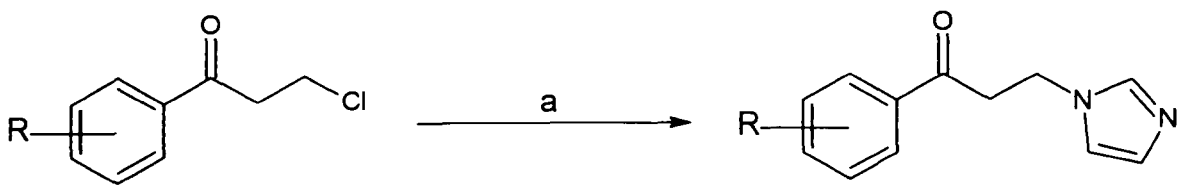

Scheme 5 Synthesis of derivatives of imidazol-phenylpropan-1-one based compounds (a=$NaOCH_3$/THF/imidazole/Δ; R=H, 4-F, Cl, Br).

Sodium methoxide was required as a base in place of potassium carbonate, as it was too weak a base for the reaction to proceed. A number of test reactions were carried out using sodium carbonate but the reactions would not proceed forward. This problem was rectified by using Sodium methoxide instead. The relevant substituted 3-chloro-1-phenylpropan-1-one was used as starting material as the substituted 3-bromo-1-phenylpropan-1-one compounds were not commercially available. The desired product was achieved with a small amount of the substituted starting material being present.The product was purified. The spectrum gives a clear splitting pattern characteristic of the para-substituted benzene and the same can be observed for the alkyl chain protons. Figure 28 and 29 shows the ^{1}H and ^{13}C NMR for 1-(4-fluoro-phenyl)-3-imidazol-1-yl-propan-1-one. The correct number of peaks can be observed, where the carbonyl is very distinctive and so too is the alkyl chain carbons.

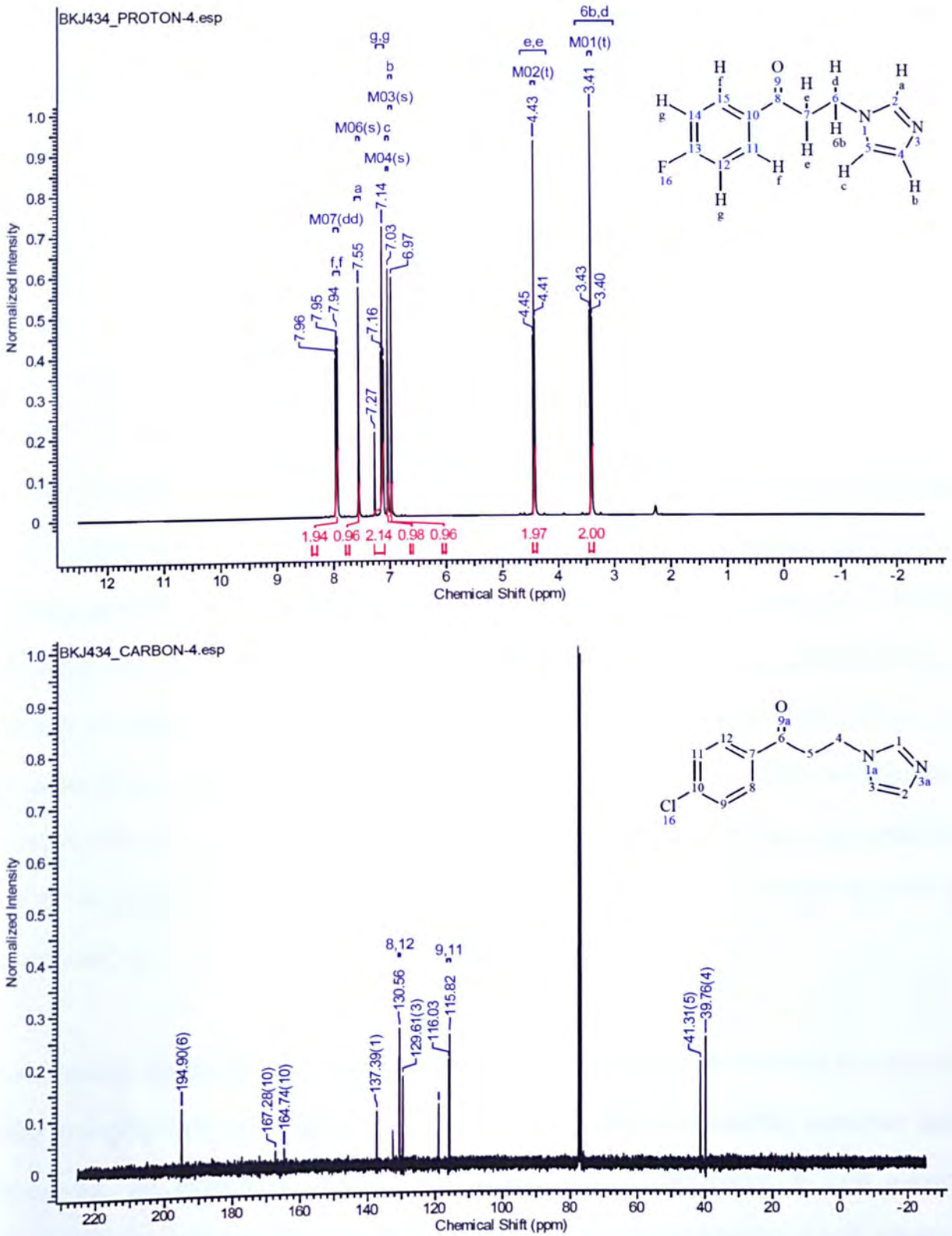

Figure 28 & 29 *^{1}H NMR and ^{13}C NMR for 1-(4-fluoro-phenyl)-3-imidazol-1-yl-propan-1-one.*

3.3 Synthesis of phenyl alkyl imidazole-based compounds

To further observe the effects of chain length and benzyl substituents, it was decided that a range of 3- and 4-substituted phenyl alkyl azoles should be synthesised.

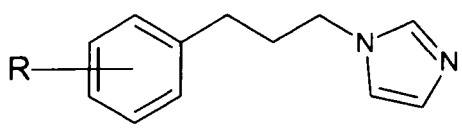

Figure 30 3- and 4-substituted phenylpropyl imidazoles (R=H, F, Cl, Br, I).

In the synthesis of these azoles, none of the 3- or 4-substituted phenyl propyl bromides were commercially available. The reactions outlined in Scheme 6 (where X=F, Cl and Br) were used to produce the substituted phenyl propyl bromide, which is then further converted into the imidazole-containing target compound. The Fischer esterification reaction of the 3- and 4-substituted fluoro, chloro and bromo cinnamic acids was achieved using sulphuric acid catalyst (H_2SO_4). The use of excess alcohol as a solvent limitsthis method of synthesis to the lower alkyl chain alcohols only (i.e. upto pentanol) due to the high boiling point of the higher alkyl alcohols which are difficult to remove during work up.

The reactions proceeded without problems to give the desired ethyl esters in excellent yields (ranging from 61% to 81%) for both the 3- and 4-substituted cinnamic acid derivatives. An alternative method was carried out to synthesise 3- and 4-iodo-substituted phenylpropyl imidazoles as the 3- and 4-iodocinnamic acids werenot commercially available. This method is discussed later in the chapter.

The second step in Scheme 6 involved the catalytic hydrogenation of the C=C moiety by use of palladium on charcoal under an atmosphere of hydrogen gas. Alkenes react quantitatively with molecular hydrogen, regardless of the nature of the substituents on the double bond[106]. The reaction may be carried out using a range of transition metal catalysts, such as palladium, platinum, ruthenium or nickel[107]. When palladium was used as catalyst, the reaction proceeded in very good yield (ranging from 77% to 89%) for the fluoro derivatives.

Problems were observed in the reduction of the substituted chloro- and bromo-derivatives. GC-MS analysis of the products showed that catalytic hydrogenation of these compounds resulted in the formation of two compounds, namely the desired phenyl propionate and the dehalogenated form. It was postulated that dehalogenation may have occurred as a consequence of sunlight, resulting in the cleavage of the carbon-halogen bond. The reaction was repeated under dark condition however; this still resulted in the synthesis of the dehalogenated product, although in greatly reduced quantities. An alternative reason may be due to cleavage of the carbon-halide onto the palladium metal surface[110].

The reaction time for the coupling was varied, using 12h, 8h and 6h instead of the original 24h. The reaction proved to be successful in synthesising the chlorophenylderivatives when carried out for 6h, but not for the bromophenyl compounds. The GC-MS analysis for the bromophenyl derivatives revealed several peaks: starting material, product and debrominated product. The effect on the reaction by the catalyst used was then investigated and reactions were carried out using various amounts of palladium on charcoal, ranging from 15% to 5% by weight of the starting

material. However, no difference was noticed as this too resulted in obtaining starting material, product and a small quantity of the ethyl 3-phenylpropanoate product.

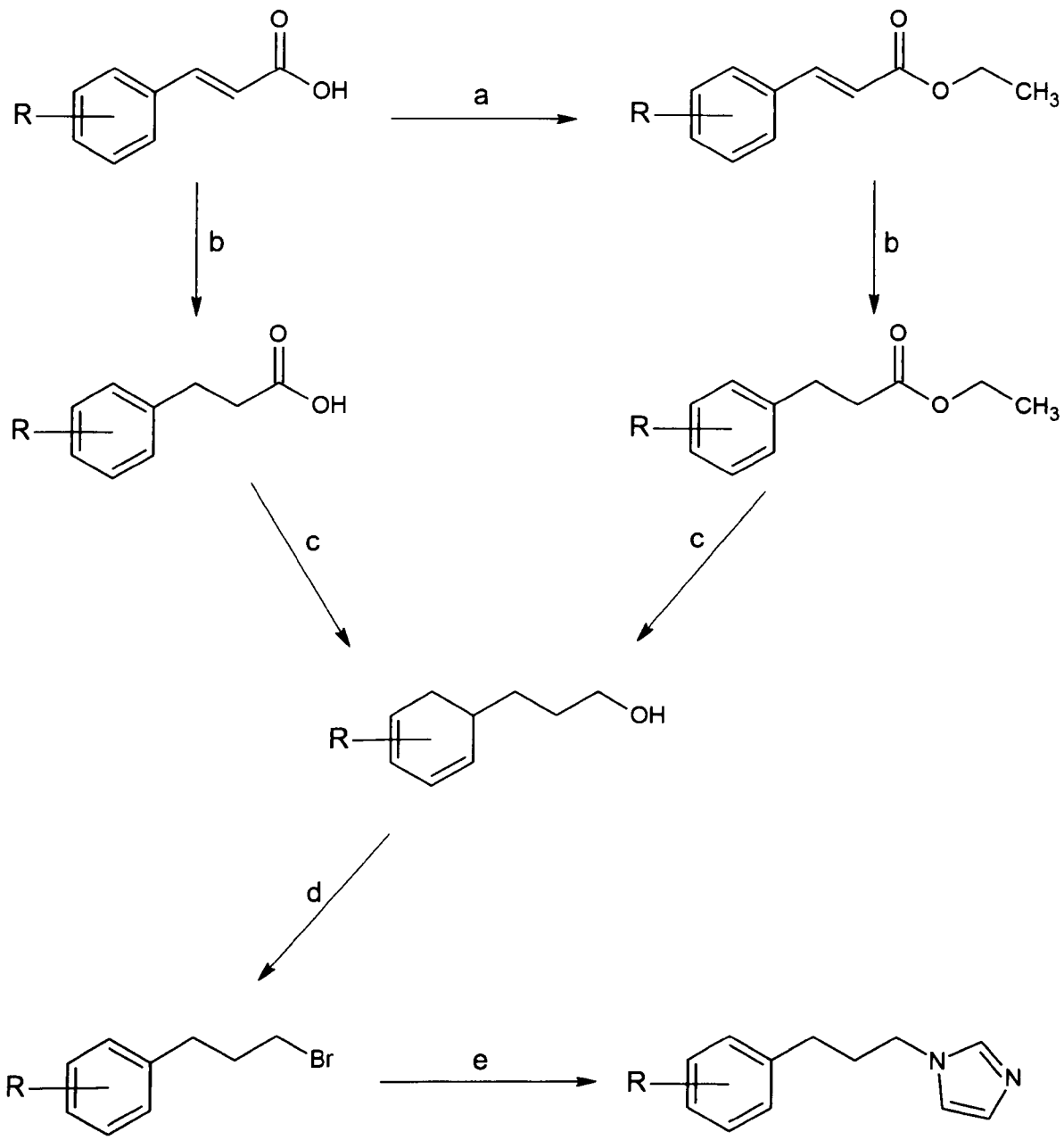

Scheme 6 Synthesis of 3- and 4-substituted phenyl propyl imidazole-based compounds (a=$H_2SO_4/C_2H_5OH/\Delta$; b=H_2, Pd,C/$CHCl_3$; c=$LiAlH_4$/THF; d=PBr_3/ether/Δ; e=Imidazole/K_2CO_3/THF; R=H, F, Cl, Br).

Owing to the difficulties encountered when attempting to purify the bromophenyl derivatives (Scheme 6) an alternative route was considered, which involves the direct reduction of the cinnamic acid using catalytic hydrogenation ofthe propionic acid. This method results in the alcohol being synthesised directly from the propionic acid using lithium aluminium hydride ($LiAlH_4$). This route was attempted using the fluoro, chloro and bromo derivatives and the reactions were found to proceed in satisfactory yield with respect to the 3- and 4-substituted fluoro compounds (ranging from 52-55%).

The chlorophenyl and bromophenyl compounds again resulted in dehalogenation, which may have been as a result of reductive dehalogenation occurring with the use of $LiAlH_4$, resulting from the excess of hydride. It was decided therefore to revert back to the original scheme used, as this gave better results for the fluorophenyl and chlorophenyl series. The synthesis of the bromo substituted phenylpropyl imidazoles was produced by deciding to follow the same reaction route intended for the iodo-substituted phenylpropyl imidazoles discussed later.

The third step in Scheme 6involvedthe reduction of the ester functionality using $LiAlH_4$to form the appropriate alcohol in an anhydrous aprotic solvent, e.g tetrahydrofuran (THF). The reactions were found to proceed in satisfactory yield (ranging from 37-62%) though problems were initially encountered with the dehalogenation of the chloro derivatives in the 3- and 4-substituted products, which was observed by GC-MS and NMR. This problem was resolved by reducing the reaction time.

Initially the reactions were refluxed for 6h and then left to stir at room temperature overnight. Due to the dehalogenation, the reaction time was reduced to stir for 4h.

However, analysis showed that dehalogenation had again occurred. A standard reaction time of 45mins resulted in the synthesis of the target compound in good yield for both the 3- and 4-chloro substituted compounds.

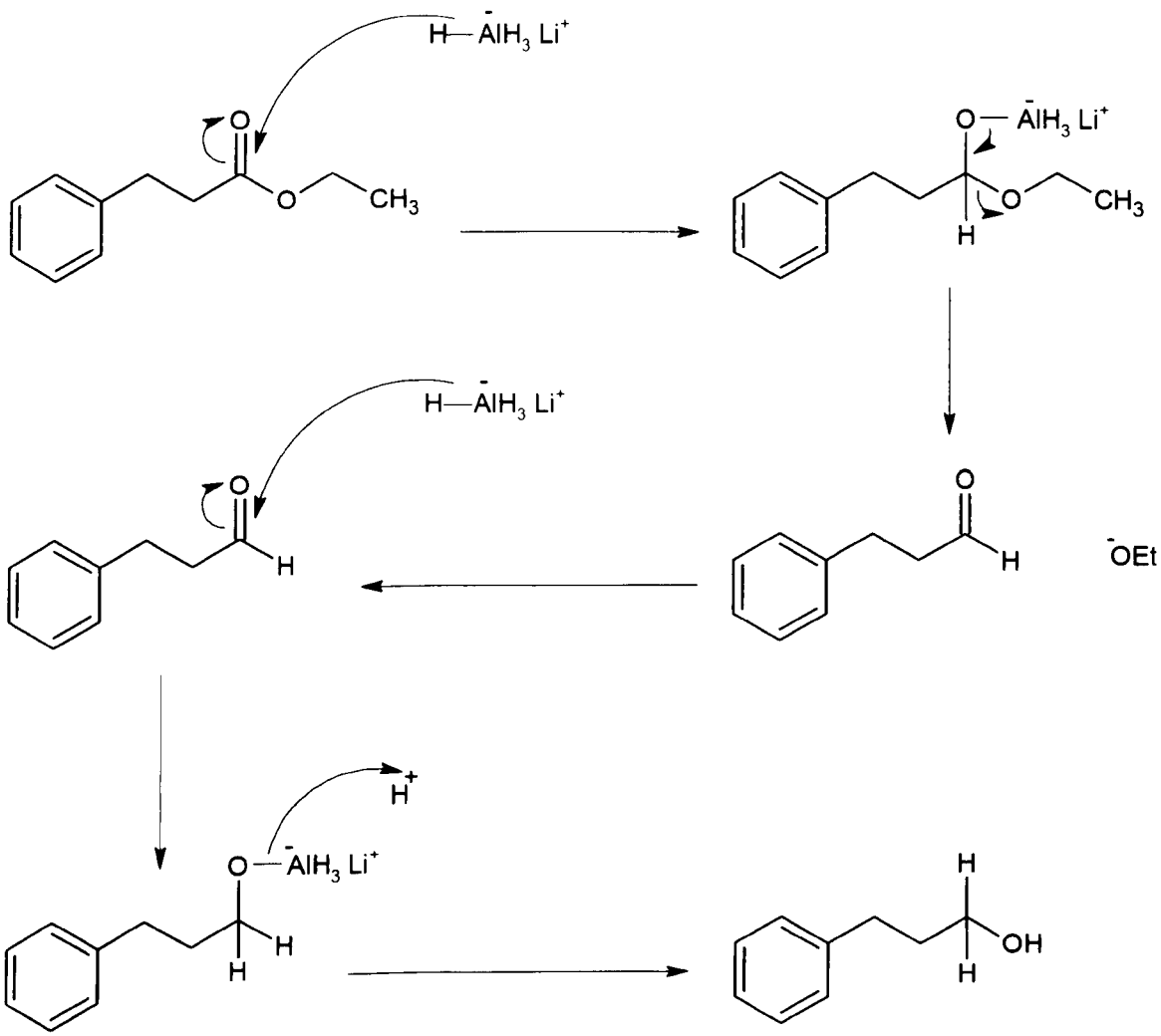

Scheme 7 Mechanism for the acid hydrolysis of the ester moiety.

The fourth step in Scheme 6 involves the bromination of the alcohol synthesised in step 3 using phosphorous tribromide (PBr_3). Reaction of PBr_3 with an alcohol occurs *via* initial activation of the alcohol oxygen by the electrophilic phosphorus, resulting in the

formation of an intermediate inorganic ester. The resulting inorganic ester group is readily displaced by the halide ion (Scheme 2).

This reaction was carried out as a model reaction using 1-phenyl-1-propanol as the starting material. GC-MS results suggested that the correct product was formed with slight impurity. However, this may have been due to the ether not being dry enough for the reaction. Chlorination was also used as a possible alternative to bromination. The chlorination of 1-phenyl-1-propanol was carried out successfully using sulphonyl chloride in place of phosphorus tribromide, where a percentage yield of 75% was achieved.

The fifth step in Scheme 6 involves the *N*-alkylation of the imidazole ring. The *N*-alkylation of the azole using an alkyl halide in the presence of a base is the most common method[89]. 3-Fluorobenzyl bromide was used as starting material in this reaction. The reaction model proceeded without problems in good yield of 58%. With regards to extending the alkyl chain to achieve the propyl imidazoles, this final step was not achieved for any of the alkyl propyl intermediates synthesised as it was decided that an alternative route, discussed below, may be more appropriate due to the complications with steps b and c in scheme 6.

3.4 Synthesis of substituted-benzyl Malonic acid diethyl ester

In the synthesis of the longer chain alkyl azoles for the bromo and iodo substituted products, extension of the carbon chain was achieved using the reactions outlined in Scheme 8. The first step in Scheme 8 involved the reaction between diethyl malonate and the 4-substituted benzylbromide using potassium tertiary butoxide as the base.

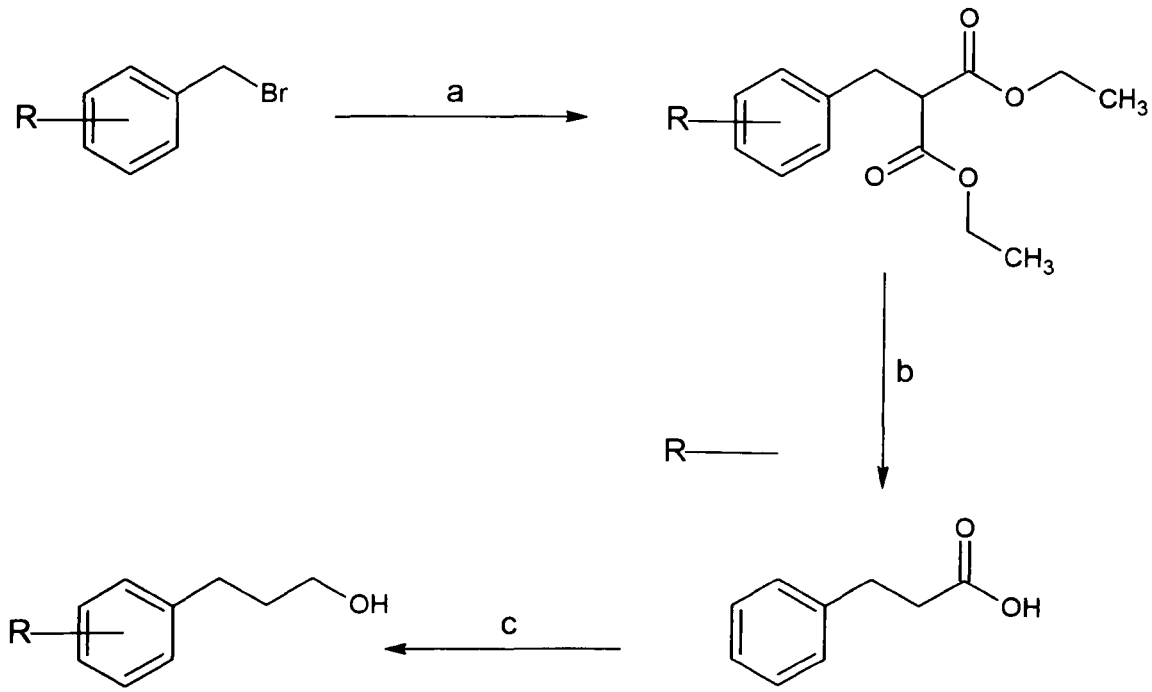

Scheme 8 Reactions undertaken for the extension of the alkyl chain (a=diethyl malonate/ Bu^tOK/THF; b=HCl/H_2O/Δ;$LiAlH_4$/THF; R=3-, 4-Br, I).

The reaction was carried out using 4-bromo and iodobenzyl bromide, however although GC-MS analysis revealed the desired product, the starting material and a bisphenyl impurity, were also present as a result of the disubstitution of the α-carbon (Scheme 9). The product was purified by column chromatography, which proved to be problematic as the desired product and impurities were so similar. A number of different solvent systems were used to try and find one that would work well enough to isolate the desired product.

Purification using a solvent system of 30:70 diethyl ether/petroleum ether did not work well enough to separate the three compounds sufficiently, even though by TLC this seemed to be the case. From the TLC plate it was difficult to know which one was my

product, so a number of collections were made and tested to reveal that the product was the final spot to elute using the solvent system 30:70 diethyl ether/petroleum ether.

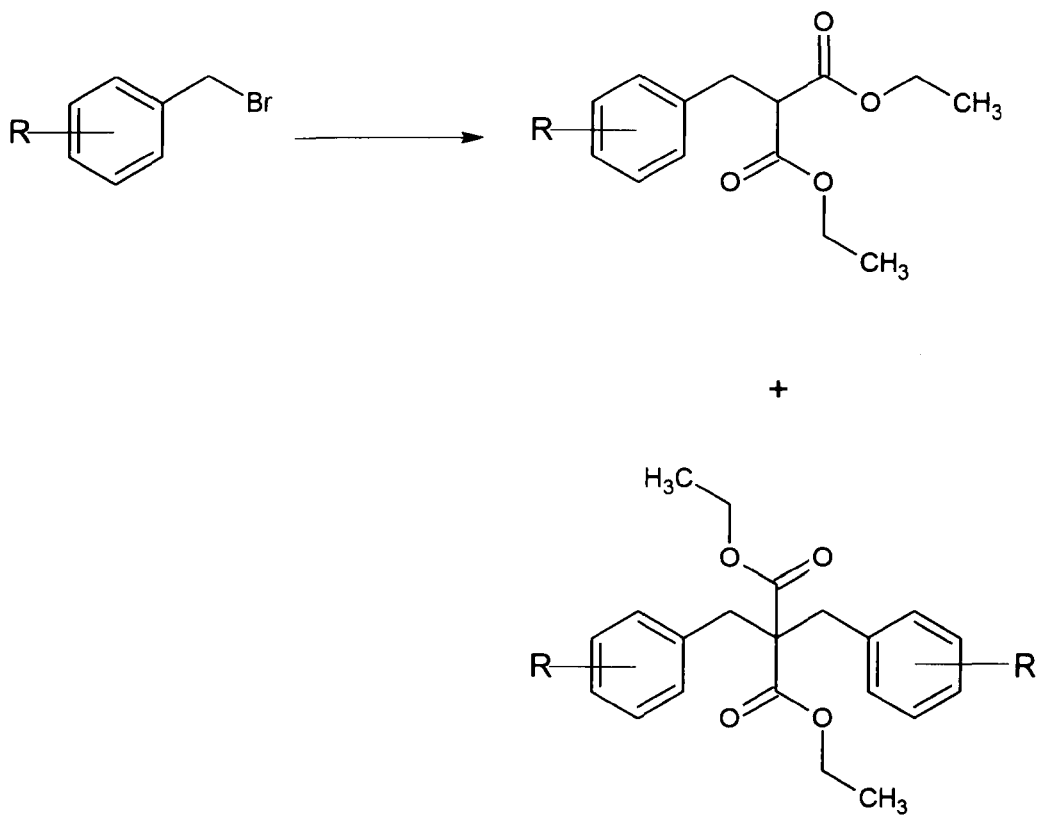

Scheme 9 Synthesis of bisphenyl derivative (a=diethyl malonate/Bu^{t}OK/THF; R=H, 3, 4-F).

This solvent system was then changed to 15:85 diethyl ether/hexane in the hope of being able to separate the three spots further along the column by using an even more non-polar solvent than petroleum ether. The results showed that the three spots were still eluting together, even under gravity. After many attempts of using different column lengths and widths, using different amounts of compound to column and sampling a number of different solvent systems, the solvent gradient system worked the best at

separating the three compounds. This also involved the use of a long column length with smaller width, to get the best purification.

The solvent gradient system consisted of starting with 100ml 15:85, then 100ml 10:80 and finishing with 5:95 diethyl ether/hexane, all under gravity. Using just 5:95 diethyl ether/hexane under pressure again resulted in all three compounds eluting together and under gravity became even more time consuming. Therefore by using the gradient system, the slowest rate took part right at the end where it was required for a better separation of the product. Around 70% of the crude compound consisted of the right product and the majority of this was collected through this process (Figure 31).

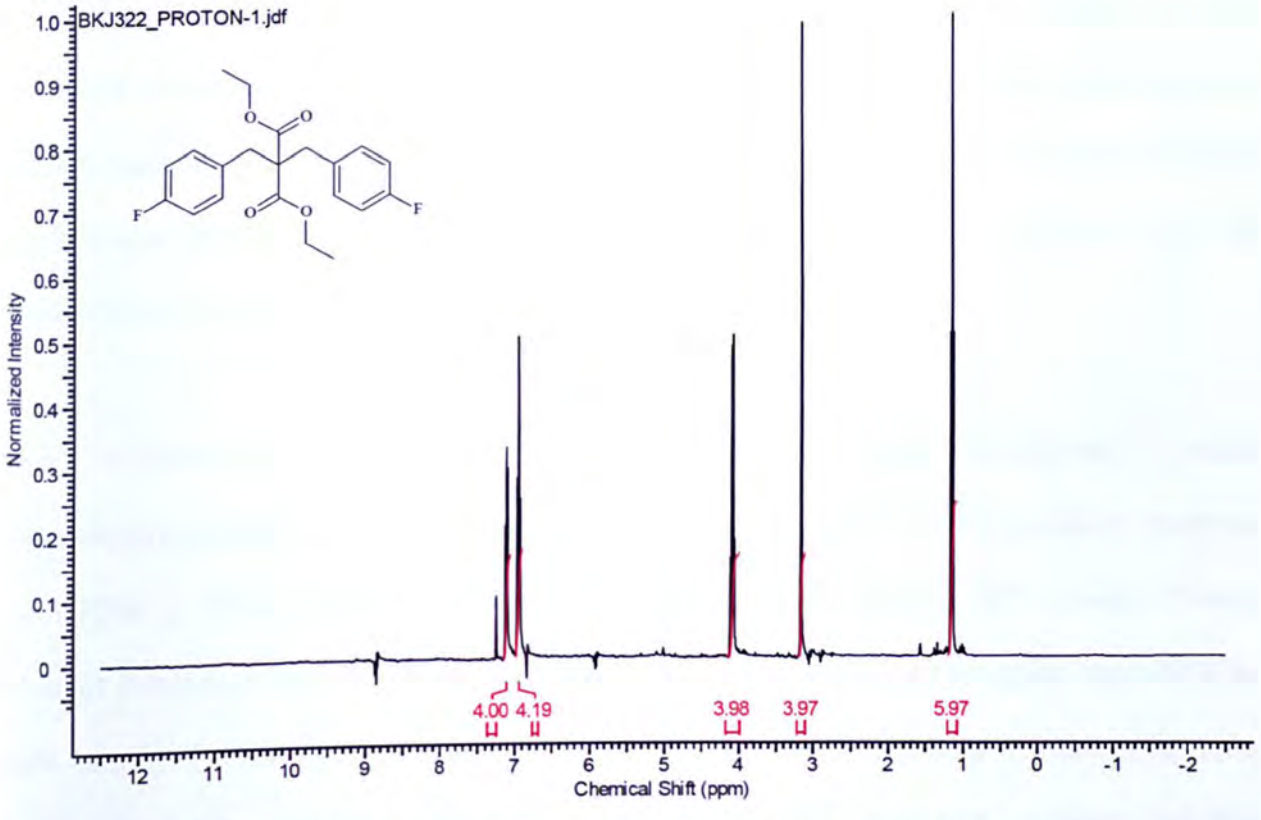

Figure 31 *^{1}H NMR for 2,2-bis-(4-fluorophenyl)-malonic acid diethyl ester.*

GC-MS analysis showed the desired compound, but the purification process was, for this reason, even more time consuming. The products were however collected in poor to satisfactory yields (ranging from 25% to 52%). The compounds synthesised in this range was the diethyl dibenzylpropanedioate (25.86% first attempt and 44.22% second attempt) and the 3 and 4-fluorosubstituted bisphenyl products, achieving yields of 52.41% and 41.17%, respectively (Table 48). These intermediates were further used in scheme 12 which is discussed later in the chapter (page 141).

The second step in Scheme 8 involves the conversion of the malonic acid diethyl ester to acid via acid hydrolysis under reflux. The reaction proceeded in good yield to achieve 51% in the synthesis of 3-phenylpropanoic acid (**320**). However the prior step had demonstrated some drawbacks with the purification of the compound being a time consuming process and only small quantities can be columned each time. It was therefore considered that triethylmethane tricarboxylate would be a better alternative to diethyl malonate in order to extend the alkyl chain because only one product could be synthesised and any residual starting material remaining in the product would be removed via the acid hydrolysis step (Scheme 10).

The synthesis of the bromo or iodophenylpropyl imidazoles using triethylmethanetricarboxylate afforded good yields for the 3-bromo product (ranging from 72% to 91% crude), 4-bromo product (ranging from 88% to 92% crude), 3-iodo product (ranging from 57% to 92% crude) and the 4-iodo product (ranging from 44% to 89% crude). As the intermediates in the pathway shown in scheme 10 lack a labile α proton, they are unlikely to dimerise or polymerise. We therefore decided that the methods outlined in scheme 10 would be utilised rather than the reactions outlined in scheme 8.

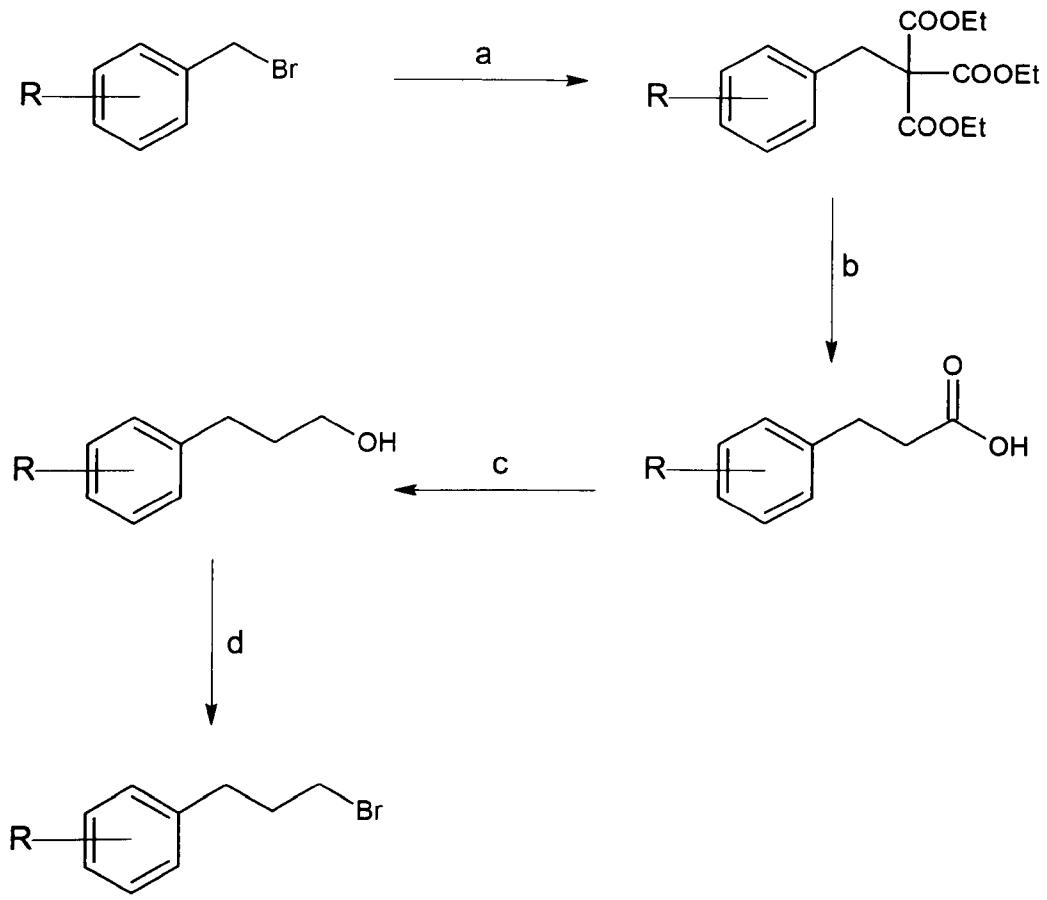

Scheme 10 Synthesis of the substituted phenylpropyl imidazoles (a=triethylmethanetricarboxylate/Bu^{t}OK/THF; b=HCl/H_2O/Δ;c=$LiAlH_4$/THF; d=PBr_3/ether/Δ; e=Imidazole/K_2CO_3/THF; R=H, 2-, 3-, 4-F, Cl, Br, I, 3-, 4-diF, diCl).

Not only did this eliminate two steps, therefore being less time consuming, but it further proved to be more cost effective for all the target compounds. Step **a** in scheme 10 generally proceeded in good yield (crude) regarding the unsubstituted product (85%), 2-iodo product (ranging from 55% to 73%), the 2-bromo product (ranging from 42% to

89%), the 2-fluoro product (87%), the 3-fluoro product (ranging from 31% to 91%), the 4-fluoro product (89%), the 2-chloro product (ranging from 38% to 84%), the 3-chloro

product (ranging from 73% to 89%), the 4-chloro product (86%), the difluoro product (50%) and the dichloro product (60%) (**319**).

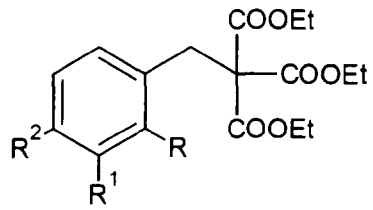

Compound	Structure	% Yield	Compound	Structure	% Yield
305	R=R^1=R^2=H	85	**312**	R=Br, R^1=R^2=H	89
306	R=F, R^1=R^2=H	87	**313**	R=H, R^1=Br, R^2=H	91
307	R=H, R^1=F, R^2=H	91	**314**	R=R^1=H, R^2=Br	92
308	R=R^1=H, R^2=F	89	**315**	R=I, R^1=R^2=H	73
309	R=Cl, R^1=R^2=H	84	**316**	R=H, R^1=I, R^2=H	92
310	R=H, R^1=Cl,R^2=H	89	**317**	R=R^1=H, R^2=I	89
311	R=R^1=H, R^2=Cl	86	**318**	R=H, R^1=R^2=F	50

Table 44 Percentage yields achieved in the synthesis of the substituted triethyl 2-phenylethane-1,1,1-tricarboxylate

Step b in scheme 10 involved the acid hydrolysis of the compounds synthesised in step one (Scheme 11). All the reactions for this step proceeded forward, achieving poor to good yields (ranging from 22% to 73%), with the removal of the triethylmethanetricarboxylate which was found as an impurity in all the synthesis that were carried out in step a. The products were all recrystallised from 50:50 methylated spirits/water as other slight impurities were observed.

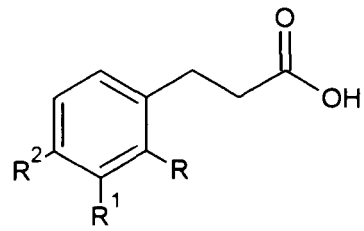

Compound	Structure	% Yield	Compound	Structure	% Yield
320	R=R^1=R^2=H	41	**327**	R=Br, R^1=R^2=H	52
321	R=F, R^1=R^2=H	52	**328**	R=H,R^1=Br,R^2=H	64
322	R=H, R^1=F, R^2=H	59	**329**	R=R^1=H, R^2=Br	59
323	R=R^1=H, R^2=F	73	**330**	R=I, R^1=R^2=H	45
324	R=Cl, R^1=R^2=H	65	**331**	R=H, R^1=I, R^2=H	64
325	R=H, R^1=Cl, R^2=H	54	**332**	R=R^1=H, R^2=I	56
326	R=R^1=H, R^2=Cl	63	**333**	R=H, R^1=R^2=F	58

Table 45 Percentage yields achieved in the synthesis of the substituted phenylpropanoic acids

The reaction gave the following yields; the unsubstituted product (41%), 2-fluoro product (52%), 3-fluoro product (59%), 4-fluoro product (ranging from 22% to 73%), 2-chloro product (65%), 3-chloro product (ranging from 40% to 54%), 4-chloro product (ranging from 57% to 63%), 2-bromo product (52%), 3-bromo product (64%), 4-bromo product (59%), 2-iodo product (45%), 3-iodo product (64%), 4-iodo product (56%), 3,4-difluoro product (58%) and the 3,4-dichloro (61%) (**334**).

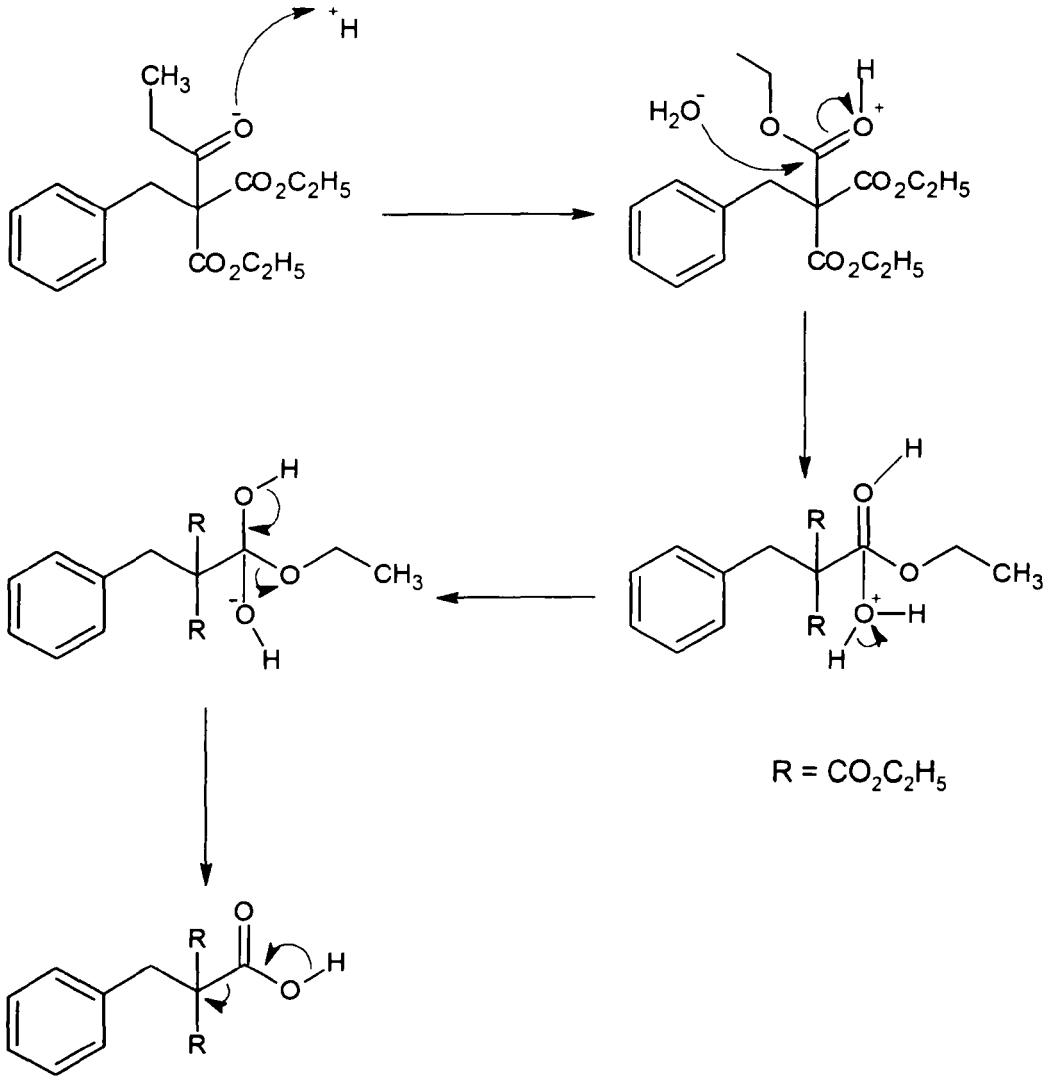

Scheme 11 Showing the mechanism for the decarboxylation of the tri-ester functionality.

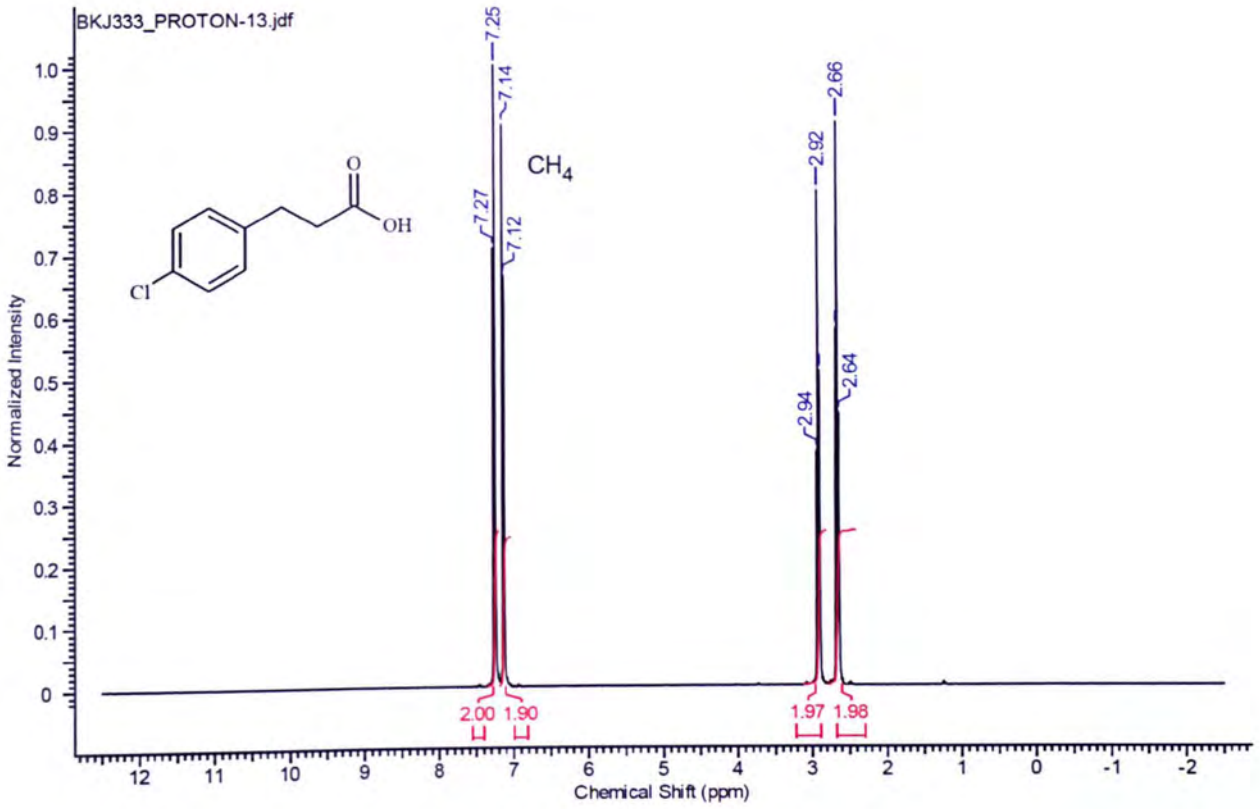

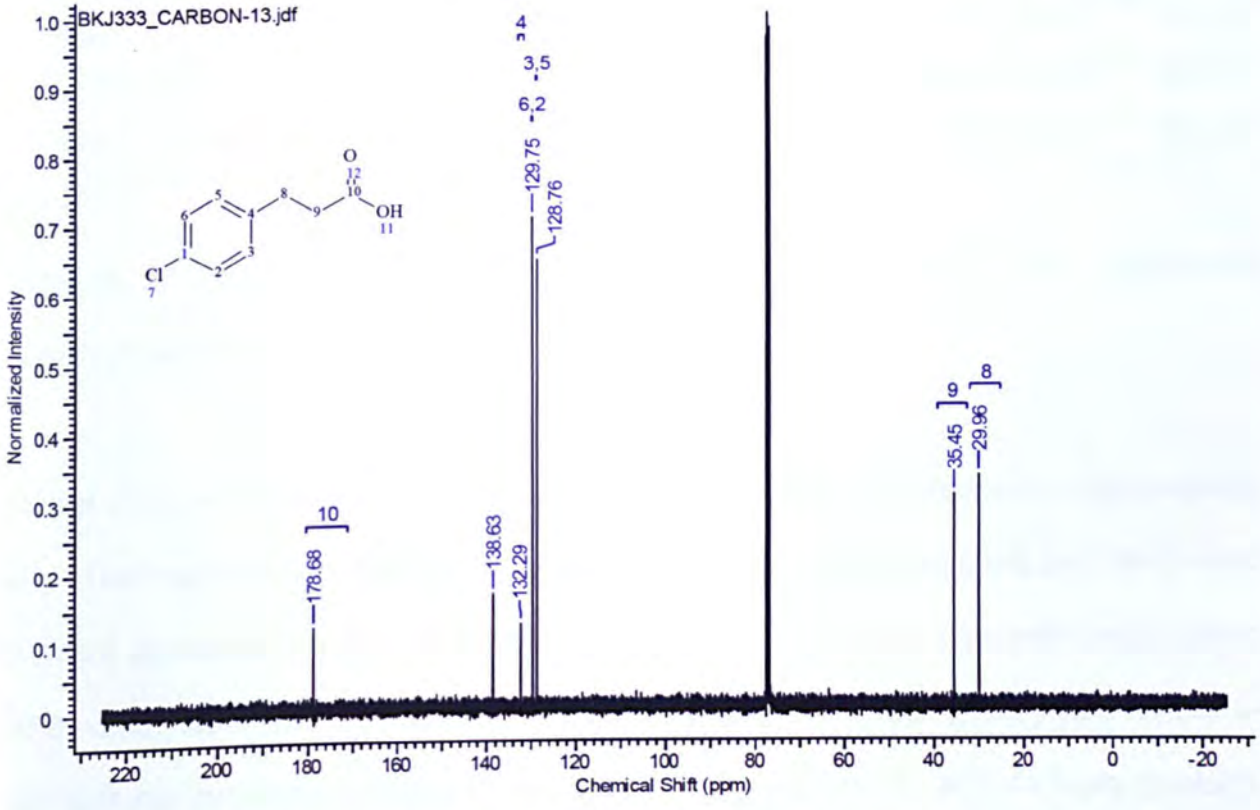

Figure 32 & 33 *^{1}H NMR and ^{13}C NMR for 3-(4-chlorophenyl)propanoic acid.*

Step c in scheme 10 involved the reduction of the acid functionality to produce the corresponding alcohol. This reaction was carried forward for only the unsubstituted, the fluoro and the chloro-substituted acids. The alcohols were purified by column chromatography using a solvent system of 40:60 diethylether/petroleum ether. The reactions proceeded well and in good yields for the unsubstituted (58%) (**335**), the 2-, 3 and 4-fluoro alcohols (ranging from 60% to 88%) and the 2-, 3- and 4-chloro alcohols (ranging from 42% to 89%)(Table 46).

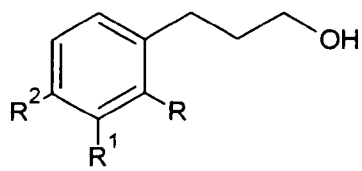

Compound	Structure	% Yield	Compound	Structure	% Yield
336	R=F, R^1=R^2=H	88.76	**339**	R=Cl, R^1=R^2=H	42.38
337	R=H, R^1=F, R^2=H	60.82	**340**	R=H, R^1=Cl, R^2=H	89.47
338	R=R^1=H, R^2=F	70.71	**341**	R=R^1=H, R^2=Cl	61.23

Table 46 Percentage yields achieved in the synthesis of the substituted phenylpropanols.

Step **d** of scheme 10 involved the bromination of the alcohol synthesised in the previous step. This reaction was carried out for only the 3- and 4-fluoro alcohols and the 3- and 4-chloro alcohols. The reactions were again purified by column chromatography using 40:60 diethylether/petroleum ether as solvent system to produce good yields for the 3- and 4-fluoro products (ranging from 25% to 88%) and the 3- and 4-chloro products (ranging from 28% to 72%)(Table 47).

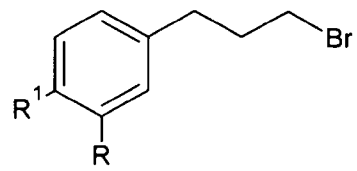

Compound	Structure	% Yield	Compound	Structure	% Yield
342	R=F, R^1=H	25.36	**344**	R=Cl, R^1=H	72.23
343	R=H, R^1=F	88.12	**345**	R=H, R^1=Cl	28.76

Table 47 Percentage yields achieved in the synthesis of the substituted phenylbromides.

The final step would involve the *N*-alkylation of the imidazole ring to achieve the desired product, of which the reaction conditions are outlined in scheme 1.

3.5 Synthesis of the substituted-bisphenyl imidazoles

We decided to attempt to synthesise the following range of compounds (scheme 12) to investigate how well two imidazole rings will interact with P450 haem moiety. Homology-based modelling studies have suggested that $P450_{17\alpha}$ may possess an active site made up of a bilobed structure with two substrate binding sites[51, 52]. However more recent molecular modelling studies would suggest that the enzyme consists of a single substrate-binding pocket[21]. There is potential for two azole groups to bind within the active site, which could possibly be achieved from one inhibitor.

The first step in scheme 12 involved the same reaction as that outlined in scheme 8 in order to achieve the substituted bisphenyl ester. This reaction afforded mostly the substituted benzyl malonate acid ester. In order to overcome this problem, the reaction

was carried out using excess benzyl bromide to achieve more of the bisubstituted product, which worked successfully.

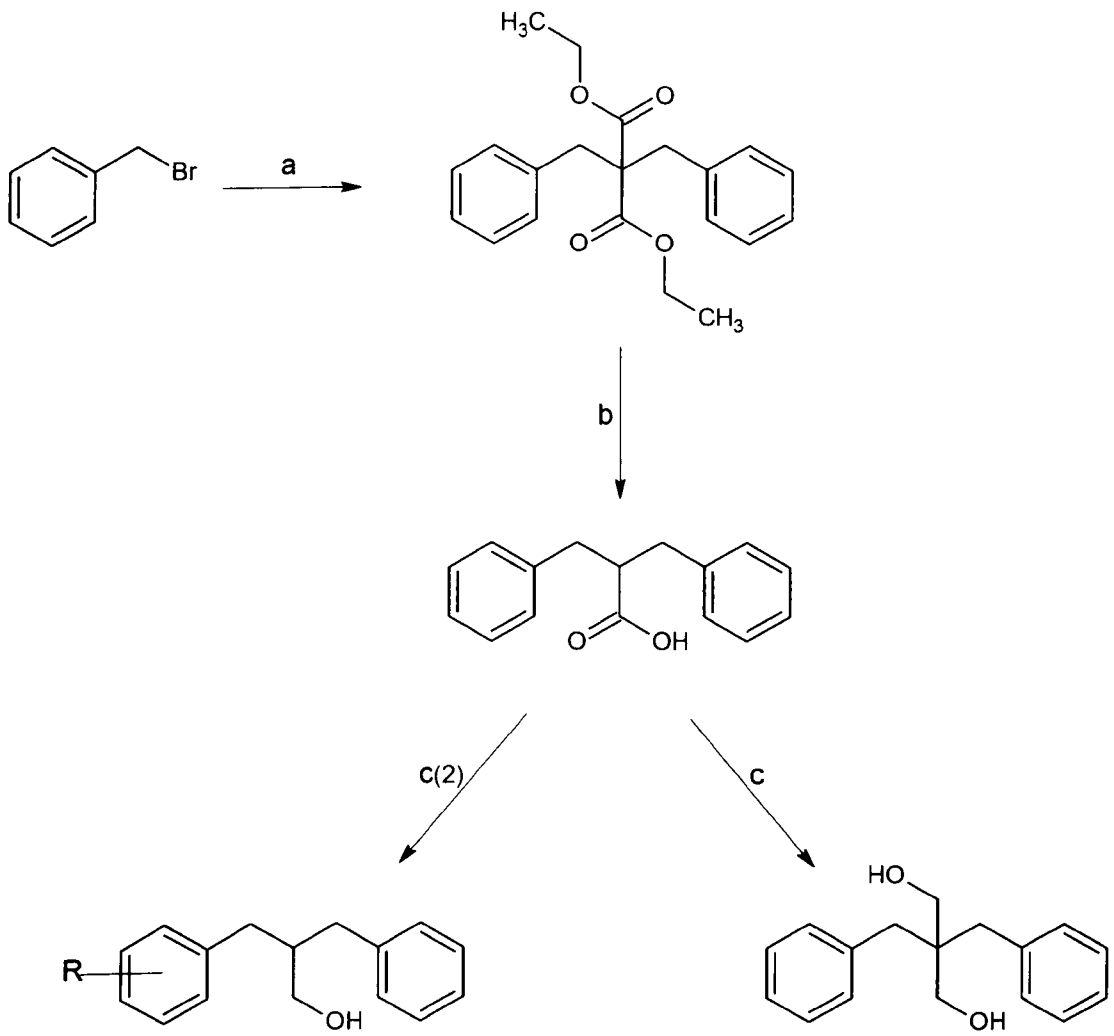

Scheme 12 Synthesis of the substituted-bis phenyl imidazoles (a=diethyl malonate/ Bu^tOK/THF; b=HCl/H_2O/Δ;c=$LiAlH_4$/THF; b(2)=$LiAlH_4$/THF; R=H, 3- & 4-F).

Column chromatography was carried out with the use of the tried and tested solvent gradient system method, which was used previously to isolate the substituted-diethyl dibenzylpropanedioate. As discussed, this proved to be effective but time-consuming. Precision in collecting purified sample were important to maintain. Though the gradual

system worked well, some of the collection vials did contain both the substituted-benzyl malonate acid ester and the bisubstituted product. These vials had to be very carefully tested, carrying out TLC, GC-MS and in some cases NMR. The total amount collected of the mixture containing the two products were so minute that it would have been even more time consuming to consider purifying it again in order to collect more of the product. The products were however collected in satisfactory yields (ranging from 25% to 56%).

The first product of the range synthesised was of the diethyl dibenzylpropanedioate. The theoretical yield was calculated to be 2.59g with the starting material weight of 1.90g. The actual amount of crude synthesised was 1.73g (66.79%). The amount ofpurified product collected was a poor 0.67g (25.86%). Repetition of this reaction showed an improvement in the yield collected (44.22%). An increase of the starting material was added to the reaction and the use of a longer column tube for purification also proved, through trial and error, to result in some satisfactory yields to carry forward. Other compounds synthesised in this range were the 3 and 4-fluorosubstituted bis-phenyl products, achieving yields of 52.41% and 41.17%, respectively (Table 48).

The reactions were, to begin with, left to stir for 7 days with results showing no trace of the product having been produced. The reaction was put back on again for a further 11 days to reveal that the product had been synthesised. ^{1}H NMR had shown a smallimpurity, which was the starting material, removed by column chromatography using a solvent system of 50:50 diethyl ether/petroleum ether.

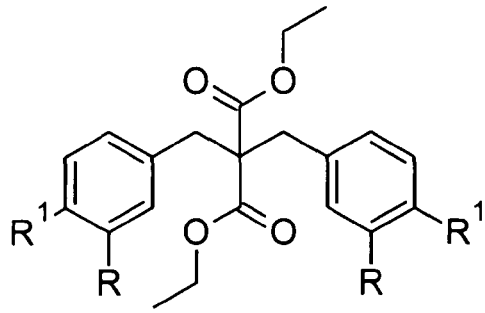

Compound	Structure	%Yield
346	R=R^1=H	44.22
347	R=F, R^1=H	52.41
348	R=H, R^1=F	41.17

Table 48 Percentage yields achieved in the synthesis of the substituted diethyl dibenzylpropanedioate.

Step **b** in scheme 12 achieved satisfactory yields ranging from 41–63% (Table 49). The first product synthesised was 2-benzyl-3-phenylpropanoic acidand the TLC analysis of the product showed two spots, which proved to be the starting material and the product from GC-MS analysis. I decided to put the reaction on again to see if more of the product could be achieved as only a small amount was synthesised.

The first reaction was left to stir for 8 days and this was then further reacted for another 2 days to still give the same two compounds on analysis, achieving 71.55% crude. The crude product was purified by column chromatography using 40:60 diethyl ether/petroleum ether as the solvent system to achieve 41.28% yield. After purification,2-(3-fluorobenzyl)-3-(3-fluorophenyl)propanoic acidwas also synthesised (57.64%), as well as 2-(4-fluorobenzyl)-3-(4-fluorophenyl)propanoic acid(63.33%).

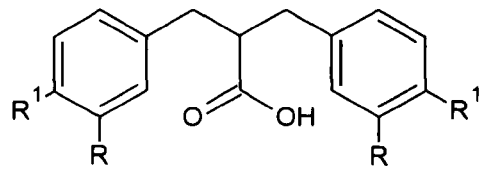

Compound	Structure	%Yield
349	R=R^1=H	41.28
350	R=F, R^1=H	57.64
351	R=H, R^1=F	63.33

Table 49 Percentage yields achieved in the synthesis of the substituted 2-benzyl-3-phenylpropionic acid

Since the acid hydrolysis step was proving to be time consuming, base hydrolysis was considered and attempted as an alternative method to synthesising the acid. The reaction was left to reflux for 7 days initially and then 14 days, but neither showed any signs of the product being synthesised. This reaction was carried out using the 4-fluoro bis-phenyl propionic acid ester (1.023g, 0.0031mmol) as the starting material and potassium hydroxide (0.341g, 0.00604mmol) in ethanol.

The product was taken forward to synthesise the alcohol (step c) where the acid is reduced to the alcohol using the reaction conditions outlined in scheme 12. The reaction proceeded without any major problems and in satisfactory yield (43%) in the synthesis of 2-(4-fluorobenzyl)-3-(4-fluorophenyl)propan-1-ol (**352**). GC-MS revealed that the product had been synthesised without any indication to impurities. Unfortunately I was unable to complete the synthesis of all the desired final products regarding this synthetic

route. I would have liked to carry out the bromination of the alcohol followed by the *N*-alkylation of the imidazole ring to achieve the final product.

Step C(2) outlined in scheme 12 proved to be very problematic and was unachievable. A number of reactions were carried out to achieve the target compound but the reactionfailed to move forward. The reaction was initially carried out for thirty minutes on a 1:1molar ratio of the starting material and lithium aluminium hydride ($LiAlH_4$) as the reducing agent. $LiAlH_4$ contains four hydride ions, which is sufficient enough to attack and reduce two ester groups. However the reaction did not work and was re-run again increasing this molar ratio to 1:2. This reaction proved to be of similar results with not a hint of the product being synthesised from analysis. The conclusion leads us to believe that the problem may be due to steric hindrance.

I decided to try an alternative method in producing the diol, where I would first try to synthesise the di-acid and then attempt the diol if all goes well. The di-ester was reacted with glacial acetic acid (CH_3CO_2H) and hydrochloric acid (HCl) in water and was left to stir for 24h. From NMR analysis we can see that the product has been synthesised (crude yield 62.65%), giving the correct number of protons, however this reaction was not carried forward

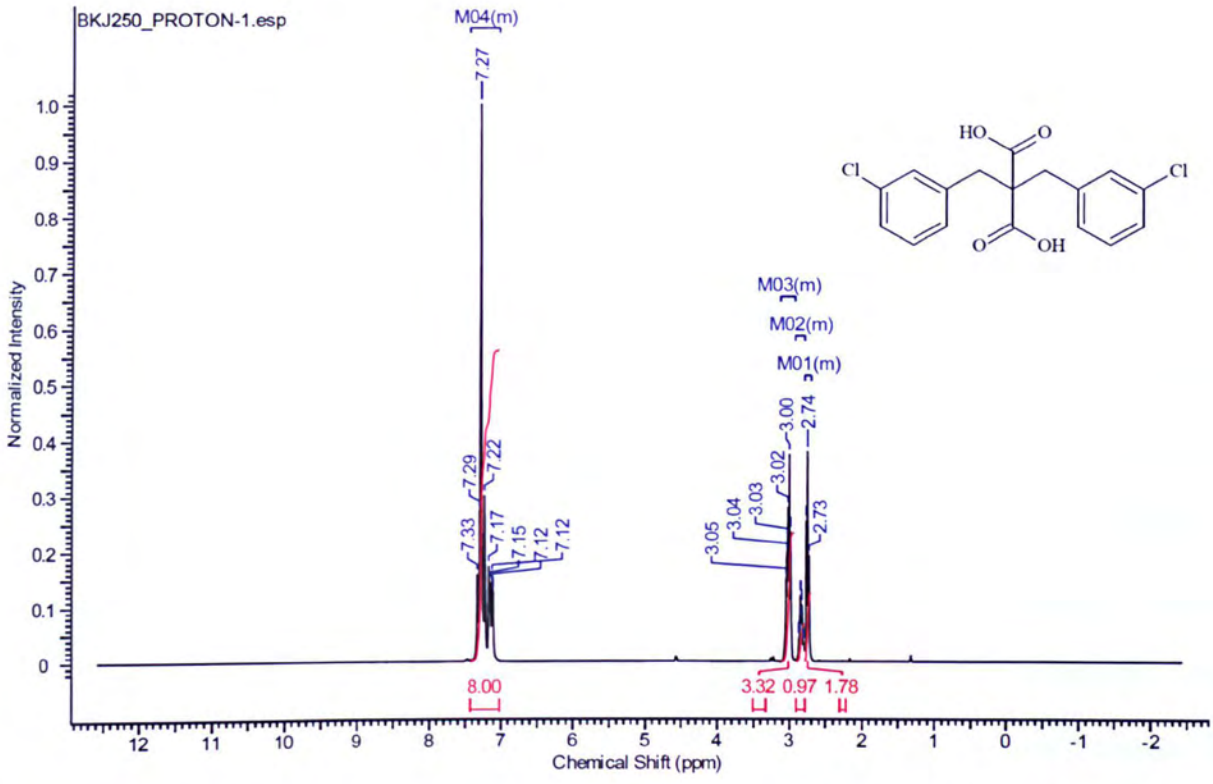

Figure 34 Showing the proton for the bis(3-chlorobenzyl)propanedioic acid.

4.0 Biochemical estimation of the inhibitory activity of compounds synthesised against CYP17.

The biochemical estimation process was carried out by my colleague Amara Abdullah. This section explains the work and the processes used in order to obtain the results in section 4.2.3. The aim of the biochemical estimation of inhibitory activity is to investigate potential compounds which have been designed and synthesised within laboratories at Kingston University to inhibit the progression of prostate cancer (Ahmed et al, 2011[108]). The study involves the initial screening of a range of compounds synthesised to inhibit the activity of both components of CYP17. The enzyme CYP17 is predominantly found in the testes of rats[112] and so for this reason was used as a source for the enzyme. The enzymatic assay for the enzyme CYP17 was based on that of Owen et al[50].

The concentration of total protein in the testicular homogenate was hypothesised by the Folin-Lowry method (section 4.1.4). The radiolabelled substrates were combined with non-radiolabelled substrates in order to gain the required concentrations (section 4.1.2). NADPH was used as a co-factor for the cytochrome P450 enzymes, so that the substrate was mixed with an NADPH generating system[113]. The reaction was carried out at a physiological pH of 7.6 and at a temperature of 37°C.

The kinetic parameters of the enzyme CYP17 was determined prior to the evaluation of the inhibitory activity of the compounds synthesised as potential inhibitors. The enzymatic reaction was performed using different protein concentrations (protein-dependency assay) ay varying time intervals (time-dependency assay) and different substrate concentrations (K_m determination) to find the optimum protein concentration, time and K_m values. The evaluation of the inhibitory activity of synthesised compounds was carried out, along with the evaluation of the controlled drugs KTZ, 7-hydroxyflavone

and biacalein. With use of a statistics package (Graphpad Prism 5.0 Software, Inc. USA), the IC_{50} and IC_{80} for the compounds were determined.

4.1 Radiometric enzyme assay

The assay required the use of tritium (^3H) labelled substrates, which upon addition of enzyme, was converted into ^3H labelled products.The source of enzyme was provided by rat testicular microsomes. Both the radiolabelled substrate and product were separated on a thin layer silica chromatogram, where the samples were futher added into a scintillation counter and the counts per minute (CPM) were recorded. The inhibitory activity of the compounds synthesised was too determined.

4.1.1 Materials and instrumentation

All non-radioactive steroids and laboratory reagents were Analar grade; β-NADP (mono sodium salt), D-glucose-6-phosphate (mono sodium salt) and D-glucose-6-phosphate dehydrogenase (5mg/mL). Grade II from yeast (specific activity 140U/mg with glucose-6-phosphate) were obtained from Roche Diagnostics (Lewes, UK). Ketoconazole was purchased from Sigma-Aldrich (Dorset, UK). Rdaiolabelled [1, 2, 6, 7^3H] progesterone, [1, 2, 6, 7^3H] 17α-hydroxyprogesterone and [1, 2, 6, 7^3H] androstenedione were purchased from GE Healthcare (Amersham, UK). A Perkin-Elmer Tri-Carb 2900TR scintillation counter was used to measure radioactivity. The scintillation fluid was Optiscint Hisafe and was obtained from Perkin-Elmer Life and Analytical Sciences (Beaconsfield, UK).

Testes of Sprague-Dawley rats were obtained from Charles Rivers (Margate, Kent). Homogenisation of rat testicular tissue was carried out bu use of an Ultra-Turrax

homogeniser (Janke and Kunkel, Germany). Further homogenisation of the excess tissue and the microsomal fraction was performed by the use of a Potter-Elvehjem homogeniser (Fischer Scientific UK). Centrifugation was performed by using a Beckmann Coulter Ultracentrifugation machine. The optical density of the solutions was measured by the use of a UNICAM 8700 series UV/VIS spectrophotometer from Thermo Scientific (Loughborough, UK).

All assays for the 17α-Hydroxylase and 17,20-lyase were based on the work of Owen et al[50], which were carried out in triplicate and as such each value is the mean ± SEM of nine determinations.

4.1.2 Substrate, buffer and solution preparation

4.1.2.1 Substrate preparation of [1, 2, 6, 7-^{3}H] Progesterone

A stock solution was prepared by transferring 40μL of radiolabelled [1, 2, 6, 7-^{3}H] progesterone (0.74μM) in toluene to a glass vial, where the toluene was then removed under a stream of nitrogen. To the radiolabelled residue, a mixture of unlabelled progesterone in propane-1-2-diol (199.26μM, 1mL) was added and mixed thoroughly to give an end concentration of 200μM.

4.1.2.2 Substrate preparation of [1, 2, 6, 7-^{3}H] 17α-hydroxyprogesterone

A stock solution was prepared by transferring 40μL of radiolabelled [1, 2, 6, 7-^{3}H] 17α-hydroxyprogesterone (0.57μM) in toluene to a glass vial, where the toluene was then removed under a stream of nitrogen. To the radiolabelled residue, a mixture of

unlabelled progesterone in propane-1-2-diol (199.43μM, 1mL) was added and mixed thoroughly to give an end concentration of 200μM.

4.1.2.3 Substrate preparation of [1, 2, 6, 7-^{3}H] androstenedione

A stock solution was prepared by transferring 20μL of radiolabelled [1, 2, 6, 7-^{3}H] androstenedione (0.22μM) in toluene to a glass vial, where the toluene was then removed under a stream of nitrogen. To the radiolabelled residue, a mixture of unlabelled progesterone in propane-1-2-diol (99.78μM, 1mL) was added and mixed thoroughly to give an end concentration of 100μM.

4.1.2.4 Sodium phosphate buffer pH 7.4

(A) 1.95g of sodium dihydrogen orthophosphate ($NaH_2PO_4.2H_2O$) was dissolved in 250mL of distilled water.

(B) 2.23g of disodium dihydrogen orthophosphate ($Na_2HPO4.2H_2O$) was dissolved in 250mL of distilled water.

Solution A was added to Solution B until a pH of 7.4 was achieved.

4.1.2.5 Potassium phosphate buffer pH 7.4

(A) 13.84g of potassium dihydrogen orthophosphate ($KH_2PO_4.2H_2O$) was dissolved in 500mL of distilled water.

(B) 34.84g of dipotassium dihydrogen orthophosphate ($K_2HPO4.2H_2O$) was dissolved in 1L of distilled water.

Solution A was added to Solution B until a pH of 7.4 was achieved. The resultant buffer solution (250mL) was further diluted with water (750mL) to achieve a solution of 50mM. The pH of the solution was checked and adjusted to pH 7.4 if required.

4.1.2.6 Sucrose phosphate buffer pH 7.4

21.39g of sucrose was dissolved in 250mL of 50mM potassium phosphate buffer (pH 7.4).

4.1.2.7 NADPH – generating system

15µL D-glucose-6-phosphate dehydrogenase (140 U/mg), 8.6mg of NADP – sodium salt and 28.2mg of D-glucose-6-phosphate were added to 1mL of sodium phosphate buffer (pH 7.4).

4.1.3 Preparation of testicular microsomes

The preparation of testicular microsomes was carried out with rat testes being de-capsulated and placed in the sucrose phosphate buffer (pH 7.4). Using the Ultra-Turrax homogeniser, the rat tissue was homogenised with short bursts. The tissues were kept on ice in order to keep the temperature below 4°C. Further homogenisation was carried out by use of a Potter homogeniser, followed by the tissue being centrifuged for 20 minutes at 4°C at 10,000*g*. The supernatant was retained and the pellet was disposed. The supernatant was further centrifuged for 1h at 4°C at 100,000*g* and the resulting pellet (microsomal fraction) was retained and re-suspended in sodium phosphate buffer (pH 7.4) using a Potter homogeniser. Aliquots of 500µL of suspension were pipette and stored at -80°C.

4.1.4 Estimation of protein content of rat testicular microsomes

The Folin-Lowry assay was used to determine the protein content of the microsomal fraction. The Folin-Lowry assay is dependent upon the presence of aromatic amino

acids within the protein[114]. A cupric/peptide bond complex is formed (between the alkaline copper-phenol reagent used and the tyrosine and tryptophan residues of the protein) and is enhanced by a phosphomolybdate complex with the aromatic amino acids. The content of protein was measured colorimetrically with reference standard curve of bovine serum albumin[115]. The optimum absorbance was measured at λmax 750nm.

A stock protein solution (200µg/mL) was prepared using bovine serum albumin (5mg in 25mL of distilled water). Standard solutions (0, 40, 80, 160 and 200 µg/mL, 1mL) were prepared containing different amounts of bovine serum albumin protein stock. The microsomes were diluted by a factor of 100 (250µL of microsomes in 25mL of distilled water) and were tested in triplicate using 1mL of the dilution against the standards.

Anhydrous sodium carbonate was dissolved in 0.1M sodium hydroxide to make 2% of solution A. A mixture of 2mL of 1% copper sulphate and 2mL of 2% sodium potassium tartrate was mixed with 200mL of solution A to make up solution B. To each test tube, 5mL of solution B was added at 30 second intervals.After resting for 10 minutes, a 50% diluted solution of Folin-Ciocalteu's phenol reagent (0.5mL) was added to each tude, which were then vortexed and left to stand for 30 minutes at room temperature. The optical density at λ_{max} 750nm of each solution was measured against the blank.

4.1.5 Radiometric assays for 17α-OHase activity

The kinetic parameters of 17α-OHase have been determined as follows.

4.1.5.1 Validation of 17α-OHase activity

In order to validate the assay, it was essential to determine the dependency of the assay on a number of factors. The progesterone (2μM) was incubated at 37°C for 30 minutes in the following solutions.

- Sodium phosphate buffer (50mM, pH7.4)
- Testicular microsomes (0.13mg/mL, 10μL) and sodium phosphate buffer, lacking the NADPH-generating system.
- Testicular microsomes, denatured with addition of diethyl ether (2mL), sodium phosphate buffer and an NADPH-generating system.
- Testicular microsomes (0.13mg/mL, 10μL), sodium phosphate buffer and the NADPH-generating system.

After incubation, diethyl ether (DEE) (2mL) was used to quench the assay and the solutions were vortexed and left to stand on ice for 15 minutes. The organic layer was extracted into a separate clean tube. The assay mixture was further extracted into DEE (2 x 2mL) and the organic layers are separated by use of liquid nitrogen, in which the bottom aqueous layer is freezed.

The assay tubes where left in a fume cupboard overnight in order to evaporate of the DEE. To each tube, Ethanol (30ml) was added and the solution was then spotted onto silica-based TLC plates. Carrier steroids progesterone, 17α-hydroxyprogesterone, testosterone and androstenedione (5mg/ml) were also onto the TLC plate and a solvent system of 70/30 DCM/EA was used as the mobile phase.

Identification of the separated spots was carried out by use of a UV lamp, where the spots were cut from the TLC plates and were placed into a scintillation vial. To this, scintillation fluid (3ml) and acetone (1ml) were added and the samples were vortexed and put in the scintillation counter to count ^{3}H for 3 minutes. A detectable quantity of products was not observed in any of the samples, which indicated that both testicular microsomes and NADPH were required for the conversion of progesterone to its subsequent products. This was proven to be the case, as detectable quantity of product was found to be present when both testicular microsome and NADPH system were added to the reaction tube.

4.1.5.2 Protein determination for assay for 17α-OHase activity

This assay was carried out to ensure that the rate of appearance of product during the enzymatic reaction was proportional to the protein concentration. The assay mixture contained protein at concentrations of 0.625, 1.25, 2.5, 3.75, 5.0 and 6.25mg/ml (final concentration). Radiolabelled progesterone (2μM, 10μl), an NADPH generating system (50μl) and sodium phosphate buffer (pH 7.4, made up to 1ml) was also contained in the assay mixture. By adding protein (enzyme), the assay was initiated and the mixture was incubated at 37°C for 30 minutes. DEE (2ml) was added to quench the reaction and complete the reaction as previously mentioned (Section 4.1.5.1). The percentage conversion of each sample was calculated as follows:

$$\% \text{ conversion} = \frac{\text{CPM (17α-hydroxyprogesterone + androstenedione + testosterone)}}{\text{CPM (progesterone + 17α-hydroxyprogesterone + androstenedione + testosterone)}} \times 100$$

4.1.5.3 *Time dependent assay for 17α-OHase activity*

In order to determine the optimum time for the enzymatic reaction and to ensure that the assay was within the linear phase of the enzyme reaction, a time dependent assay was carried out. The radiolabelled progesterone (2μM, 10μl), NADPH generating system and sodium phosphate buffer (pH 7.4, 930μl) were incubated at 37°C in triplicate, in a shaking bath for 5 minutes. The assay was initiated by the addition of testicular microsomes (final assay concentration 1.25mg/ml, 10μl). The assay tubes were quenched by the addition of 2ml of DEE and placed on ice after 5, 10, 20, 30, 45, 60 and 90 minutes of incubation respectively. The assay was completed, as previously mentioned (Section 4.1.5.1) and the percentage conversion was determined.

4.1.5.4 *Determination of the Michaelis constant (K_m) for 17α-OHase activity*

The assay was carried out in triplicate. Propane-1,2-diol was used to serially dilute the radiolabelled progesterone in order to give a range of final incubation concentrations of 0.25, 0.5, 1, 2, 3, 4 and 5μM. Assay mixtures (1ml) contained the NADPH-generating system (50μl), progesterone (10μl) and phosphate buffer (930μl, pH7.4). The assay was initiated by the addition of the microsomes (10μl, 1.25mg/ml) and the mixture was incubated for 25 minutes. The addition of DEE (2ml) quenched the reaction and the mixture was placed on ice. The assay was completed as previously described (Section 4.1.5.1).

The velocity of the reaction (V: μM/min/mg) was calculated using the following equation:

$$V = \frac{\text{CPM (AD + T + 17αOHP) x substrate concentration. [S] (μM)}}{\text{CPM (AD + T + 17αOHP + P) x Protein Conc. (mg/ml) x time (min)}}$$

4.1.5.5 Preliminary screening of synthesised compounds for 17α-OHase inhibitory activity.

The reference drug KTZ and the synthesised inhibitors were dissolved in dimethylsulfoxide (DMSO) and diluted to give the required final incubation concentration of 5μM and 100μM. The total assay volume was 1ml. Substrate (10μl, 2μM) was added to each tube, as well as inhibitor (20μl), an NADPH generating system (50μl) and sodium phosphate buffer (pH 7.6, 910μl). The assay was initiated by the addition of microsomes (10μl, 1.25mg/ml). Incubation of the tubes was carried out for 25 minutes at 37°C, followed by quenching with the addition of DEE (2ml) and finally placing the tubes on ice. Control samples minus inhibitor were also incubated. To finish, the assay was completed as previously described (Section 4.1.5.1). The percentage inhibition for each sample was calculated as follows:

$$\% \text{ Inhibition} = \frac{\text{Avg \% coversion of blank} - \text{Avg \% conversion of compound}}{\text{Avg \% conversion of blank}} \times 100$$

4.1.5.6 Determination of IC_{50} of compounds synthesised against 17α-OHase activity

IC_{50} is defined as the inhibitor concentration required for 50% inhibition of the enzyme activity. To compare the inhibition presented by the synthesised compounds against 17α-OHase activity, KTZ was used as a reference. With regards to the IC_{50} assay, different concentrations of a single inhibitor (20μl) were testing depending on their initial screening results. The assay was carried out in the same process as previously stated (Section 4.1.5.1). The % inhibition was calculated using the equation previously stated

(Section 4.1.5.5). The IC_{50} of the inhibitors were calculated by use of a statistic package (Graphpad Software Inc, USA).

4.1.6 Radiometric assays for lyase activity

The inhibitors synthesised were tested for 17,20-lyase inhibitory activity using the rat testicular microsome preparation. This allowed the measurements of the the effect of the novel compounds on the rate of converstion of radiolabelled 17α-hydroxyprogesterone to androstenedione by the enzyme lyase, to be recorded. The assay was performed in the same manner as previously stated (Section 4.1.5.1 - 4.1.5.6). The percentage converstion of 17α-hydroxyprogesterone to androstenedione and testosterone was determined by use of the following equation;

$$\% \text{ converstion} = \frac{\text{CPM (androstenedione and testosterone)}}{\text{CPM (androstenedione + testosterone + 17α-hydroxyprogesterone)}} \times 100$$

4.1.6.1 Validation of the 17,20-lyase activity of the conversion of 17α-hydroxyprogesterone to androstenedione.

Radiolabelled 17α-hydroxyprogesterone (final concentration 2μM) was incubated in the presence and absence of an NADPH system and enzyme in order to validate the lyase assay. The assay was completed as previously explained (Section 4.1.5.1). Detectable quantities of product were not shown to be present in any of the samples. However, as soon as both the testicular microsome and NADPH system was added into the reaction tube, detectable amount of products were found to be present. This indicated that both the testicular microsomes and NADPH were essential for the conversion of 17α-hydroxyprogesterone.

4.1.6.2 Protein determination for 17,20-lyase activity

The assay was carried out in the same manner as previously described (Section 4.1.5.2), however 17α-hydroxyprogesterone was used as a substrate.

4.1.6.3 Time-dependent assay for 17,20-lyase activity

The time-dependent assay was carried out in the same manner as previously described in (Section 4.1.5.3), however with the exception that the initiation of the assay was carried out by the addition of 40μL (2.5mg/mL) of testicular microsomes and 17α-hydroxyprogesterone was used as a substrate.

4.1.6.4 Determination of the Michaelis constant (K_m) for 17,20-lyase activity

The testicular microsome (40μL, 2.5mg/mL) was defrosted and combined with the reaction mixture which contained radiolabelled substrate, an NADPH system and phosphate buffer. The tubes were incubated for 15 minutes and the assay was completed in the same process as previously mentioned (Section 4.1.5.4).

4.1.6.5 Preliminary screening of compounds synthesised against 17,20-lyase inhibitory activity

To each tube, the prepared substrate (10μL, 2μM), synthesised inhibitors (20μL), an NADPH generating system (50μL) and sodium phosphate buffer (pH7.4) were added. The initiation of the assay was carried out by the addition of microsomes (40μL, 2.5mg/mL) and the tubes were incubated at 37°C for 15 minutes. The assay was completed in the same manner as previously mentioned (Section 4.1.5.5).

4.1.6.6 Determination of IC_{50} of compounds synthesised against 17,20-lyase activity

Depending on their initial screening results, different concentrations of a single inhibitor (20µL) were tested for the IC_{50} assay. The assay was carried out in the same manner as previously mentioned (Section 4.1.5.6).

4.2 Materials and Instrumentation

Dulbecco's modified essential media (DMEM) without phenol red and phosphate buffer saline (DPBS) was purchased from Gibco Invitrogen, UK. Trypsin:EDTA (0.25:0.1%) was purchased from Thermo Scientific. Non-enzymatic cell dissociation solution (EDTA diluted to 0.1% in Phosphate Buffered Saline), bovine serum albumin (BSA), Thiazolyl Blue Tetrazolium Bromide (MTT) dye and DMSO were obtained from Sigma Aldrich (Poole, UK). Microvascular endothelial cell attachment factor was purchased from TCS cell works (Buckingham, UK). Phorbol-12-myristate-13-acetate (PMA) was purchased from Merck Chemicals Ltd, UK. TNF-alpha was obtained from R & D systems (Abingdon, UK). Cell tracker green^{TM} was obtained from Invitrogen (Paisley, UK).

Hawksley improved Neubauer (BS.748) chambers were used to count the cells (Lancing, UK). A labtech LT-4000 microplate reader was used to read the absorbance at 570nm (East Sussex, UK). A Fluostar Optima plate reader (BMG Labtech) was used to measure the intensity at an excitation wavelength set at 485nm and emission at 520nm (Bucks, UK). A fluorescent microscope (Leica DFC420C) was used for phase-contrast and fluorescent microscopy (Bucks, UK).

4.2.1 MTT assay

This particular assay was used to determine the cytotoxicity of the compounds synthesised as potential CYP17 inhibitors. Based upon the IC_{50} and IC_{80} values (Table 50), the more potent compounds were were short-listed.

MTT was first developed by Mosmann[116]. In living cells, yellow tetrazsolium MTT (Thiazolyl Blue Tetrazolium Bromide) is reduced by mitochondrial dehydrogenases to a blue-magenta coloured formazan precipitate. In DMSO, the resulting intracellular purple formazan can be solubilised and further quantified by spectrophotometric means. The intensity of the purple formazan crystals, which are formed during the assay, is directly proportional to the viability of cells. This is measured at a wavelength of 570nm[117,118].

4.2.2 Results of biological screening

As discussed in the introduction, the fact that prostate cancer is androgen dependent in its early stages allows the $P450_{17\alpha}$ class of enzymes to be considered valid targets as they facilitate the conversion of progesterone to androstenedione. The $P450_{17\alpha}$ facilitates two specific reactions. One is the 17α-hydoxylase step and the second, the 17,20 lyase step. Ketoconazole has previously been reported as an azole-based $P450_{17\alpha}$ inhibitor and it is for this reason it has been used in the treatment of prostate cancer.

The withdrawal of ketoconazole as a treatment was due to the adverse side effects and these have arguably been attributed to the role of the 17α-OHase component being responsible for corticosteroid biosynthesis and the inhibition of this by Ketoconazole can interrupt this pathway[86]. This point is contentious as it has also been proposed that

since the same haem moiety in $P450_{17\alpha}$ is responsible for both the hydroxylation and the cleavage of the C17-C20 bond that inhibition of either component of the reaction could interfere with corticosteroid biosynthesis[108]. Nevertheless, Ketoconazole is a useful experimental tool when considering the screening of potential 17,20 lyase inhibitor, such as those synthesised during the course of the project.

Based on their similiarity, in terms of electron density, with the established 17α-OHase and 17,20 lyase inhibitor Ketoconazole, the synthesised compounds **264-266** and **270-272** were selected for screening and the results of this was recently reported by Abdullah *et al*[111]. From the imidazol-phenyl ethanones family of compounds, **279**,**281-282**, **285**, **289**, **293** & **295-298** were also tested for activity against 17α-OHase and 17,20 lyase[108].

The screening assays for both enzymes are based on a radio-labelled substrate in testicular microsomal homogenates and details of the procedure are reported elsewhere[111&108]. The positive control used for the inhibition in both cases was ketoconazole and the percentage enzyme inhibition (n=3) was reported with variance given as *Standard Error of the Mean* (SEM).

4.2.3 Screening of benzylimidazole derivatives for inhibitory activity against 17,20-lyase

The novel benzylimidazole derivatives showed comparable inhibitory activity of 17,20 lyase to ketoconazole with an unpaired, two-tailed t-test showing $P>0.05$ for all cases when compared to the ketoconazole. In terms of structure-activity relationships there is

no obvious correlation between the substitution pattern of the benzyl ring and the inhibitory activity.

Compound	% Inhibition of 17,20 lyase + SEM
Ketoconazole	75.58± 6.84
270	87.17 ± 3.52
271	86.28 ± 4.52
272	87.40 ± 4.25
264	85.76 ± 4.15
265	85.76 ± 4.49
266	86.80 ± 4.25

Table 50 Summary of the screening of benzylimidazole derivatives compared with reference drug ketoconazole against the enzyme 17,20 lyase[111]

4.2.4 Screening of benzylimidazole derivatives for inhibitory activity against 17α-OHase

Inhibition of 17α-OHase by the benzylimidazole derivatives **264-266** was shown to be similar to ketoconazole and the nitro substituted derivatives **270-272** appeared to show improved activity when compared to ketoconazole. There would appear to be a general trend towards the *para* substitution of the benzyl ring having an impact on the inhibition of the enzyme, however the level of error lends reduced statistical significance to thistrend when compared with ketoconazole (P=0.07 on a two-tailed unpaired t-test) and it should be treated with caution.

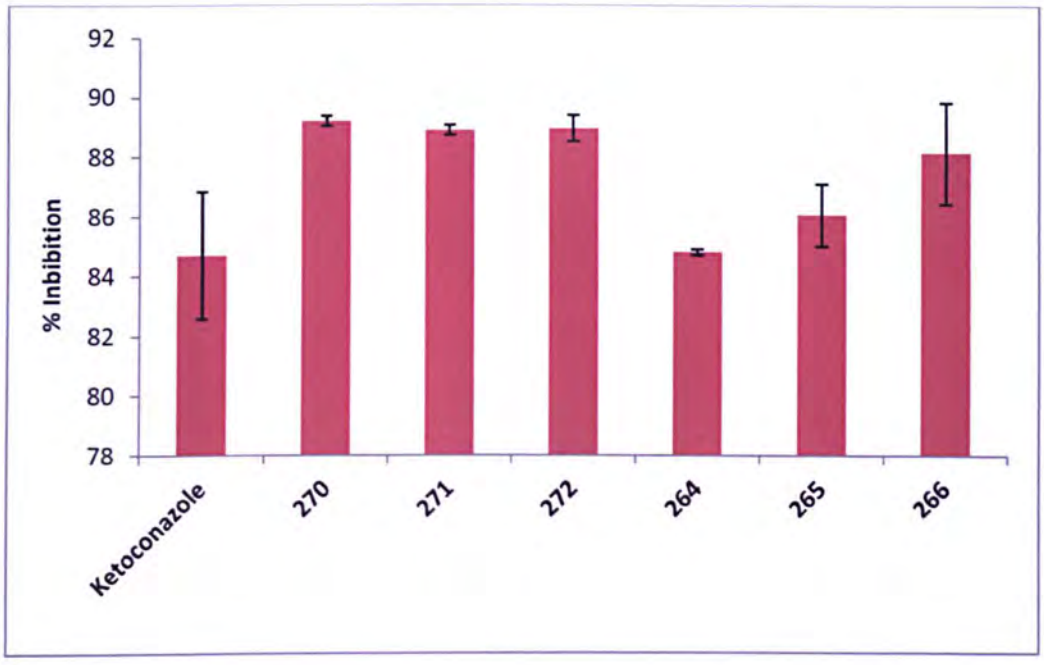

Figure 35 Comparison of percentage inhibition of 17α-OHase by derivatives ***264-266*** *&* ***270-272*** *when compared to Ketoconazole*[111]

4.2.5 Screening of imidazol-phenyl ethanonederivatives for inhibitory activity against 17α-OHase and 17,20lyase

When compared to the assayed benzyl imidazole derivatives, the phenyl vinyl ketone compounds showed considerable variation in terms of their inhibitory activity of both the OHase and lyase activities. With the exception of **288** all of the other phenyl vinyl ketones gave either equipotent inhibitory activity with respect to ketoconazole or substantially lower activity (Figure 33). The same is when the 17,20 lyase activity is considered. With the exception of **288** it could be argued that none of the other phenyl vinyl ketones possess as potent inhibitory potential as ketoconazole.

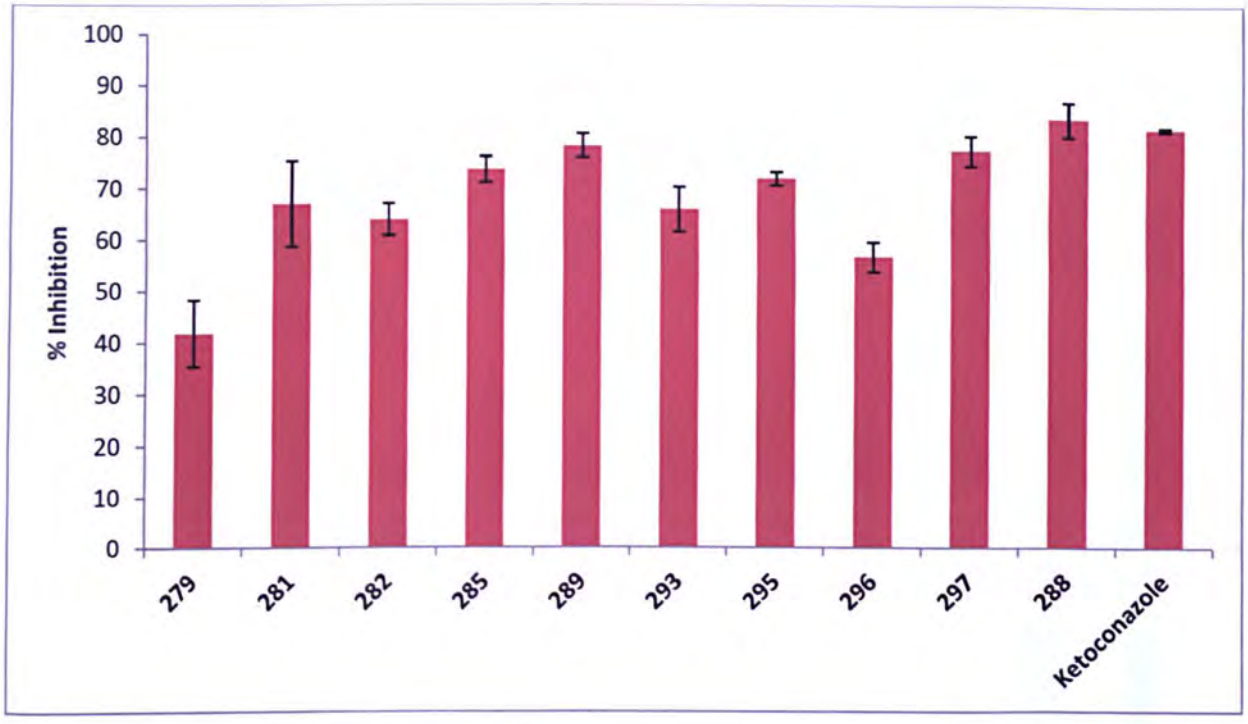

Figure 36 Comparison of percentage inhibition of 17α-OHase by **279**, **281-282**, **285**, **289**, **293** & **295-298** *when compared to Ketoconazole.*

Evaluation of the inhibitory activity of **279**, **281-282**, **285**, **289**, **293** & **295-298** indicates that there are a number of structure activity relationships which exist within the small range of imidazol-phenyl ethanones. Consideration of the inhibitory activity of the halogen derivatives shows that there is an increase in potency with decreasing electronegativity of substituent group.

The 17α-OHase inhibitory activity for compounds **282**, **285** and **289**, shows that as the electron-withdrawing ability of the substituent on the phenyl ring decreases, the percentage inhibition increases. This would therefore appear to suggest that an interaction exists between the substituent (for example, Br in the case of compound **289**) and complementary group(s) at the active site of the enzyme – this interaction

appears to be a weaker when the derivatives of **279** possess substituent of high electronegativity.

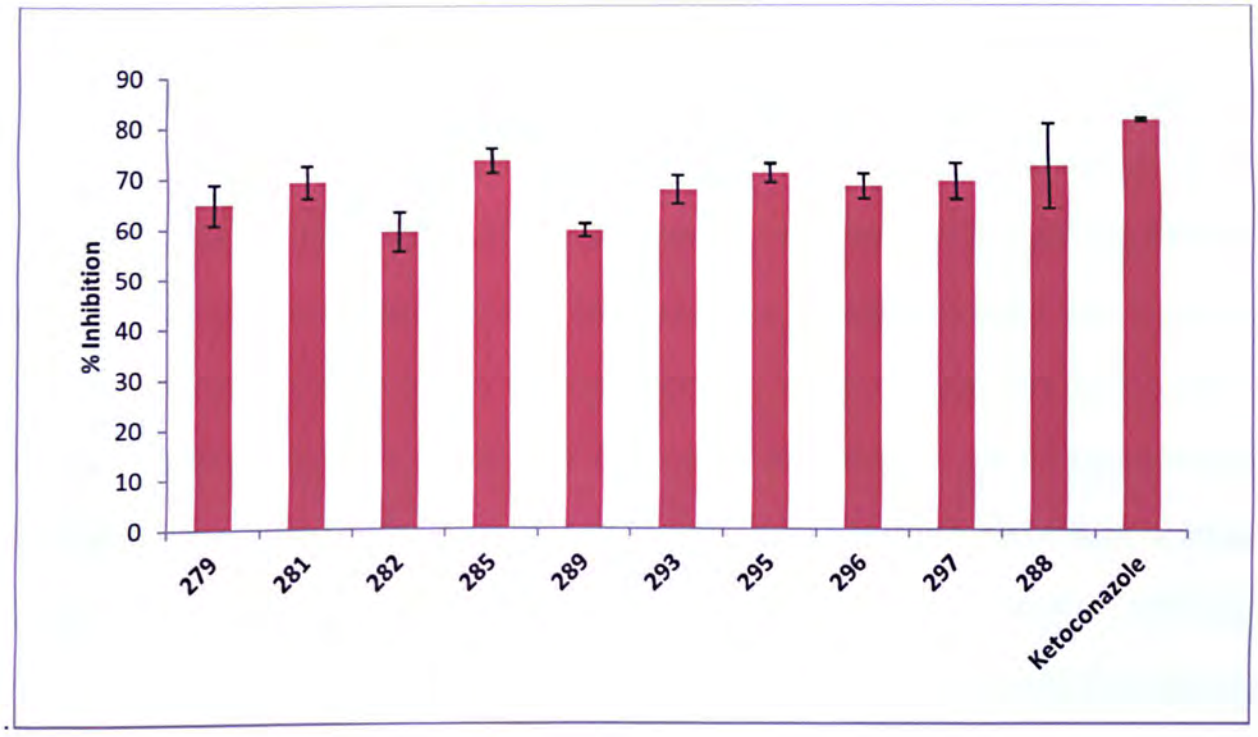

Figure 37 Comparison of inhibition of 17,20 Lyase ***279, 281-282, 285, 289, 293 & 295-298*** *when compared to Ketoconazole*

It is also noteworthy that compounds, which contain strong electron withdrawing groups, such as compound **293,** were found to possess similar weak inhibitory activity for both enzymes as compound **282**. The suggestion of reduced OHase and lyase inhibitory activity with increasing electronegativity is further supported by the stronger inhibitory activity observed for compound **279**. It has been reported elsewhere that greater inhibitory activity was observed with an increase in the hydrophobicity of a potential OHase/lyase inhibitor. As such this adds further support to our previous studies where

we have suggested that hydrophobicity is a major physicochemical factor in the inhibition of $P450_{17\alpha}$.

Another relationship which can be observed within the range of derivatives of 2-imidazol-1-yl-1-phenyl-ethanone considered within the current study is that the positioning of the substituent on the phenyl ring appears to significantly affect the inhibitory activity of the compounds. For example, consideration of compounds **296** and **295** shows that the metasubstituted compound (i.e. compound **295**) was found to possess greater inhibitory activity than compound 5 which contains the substituent at the para position within the phenyl ring. In an effort to rationalise the inhibitory activity observed, we undertook the molecular modelling of two halogen derivatives, namely compound **289** and **288** since the two compounds were found to possess strongest inhibitory activity against the 17α-OHase component (as well as **288** being more potent than KTZ).

5.0 Conclusion

To conclude, we have synthesised a range of benzyl imidazoles and 2-imidazol-1-yl-1-phenyl-ethanone compounds as $P450_{17\alpha}$ inhibitors. Imidazole based compounds were synthesised as it has been through the investigation of some antimycotics compounds that has led to the discovery of KTZ as a potent azole based $P450_{17\alpha}$ inhibitor. Azole based compounds have since been of great interest in the treatment of prostate cancer, where only a few have entered clinical trials, the most successful to date being Abiraterone acetate.

These specific compounds were synthesised in the hope that they would possess potent inhibitory activity against the enzyme $P450_{17\alpha}$. The 2-imidazol-1-yl-1-phenyl-ethanone range of compounds were designed with the purpose of the C=O moiety interacting with one of the two hydrogen bonding sites within the active site of the enzyme. Furthermore, the substituted group on the phenyl ring system may result in additional interactions within the active site for not only this particular range of compounds but also for the range of benzyl imidazoles.

The use of the SHC approach has led to the hypothesis that the lone pair of electrons on the nitrogen of the azole moiety interact with the heme iron within the enzyme. By extending the alkyl chain length of the inhibitor, interactions may also take place within the steroid binding region via polar-polar/hydrogen bonding. Biochemical evaluation was carried out on a number of the 2-imidazol-1-yl-1-phenyl-ethanone compounds using KTZ as the standard compound. These compounds were shown to have moderate inhibitory activity against the enzyme. One compound in particular was shown to have

greater inhibitory activity than the standard KTZ. Furthermore, a number of compounds were found to possess inhibitory activity similar to that of KTZ.

Overall, a number of compounds were also shown to be more potent against the 17α-OHase component in contrast to the lyase component of the enzyme. This proved to be a drawback as inhibition of 17α-OHase would result in the disruption of corticosteroid synthesis, the outcome of which would result in adverse side effects as these steroids are necessary for carbohydrate regulation and mineral balance within the body. The substitution of the phenyl ring was shown to determine the overall inhibitory activity of the compounds, which was rationalised by use of the SHC approach. This was proposed as results clearly indicate that the meta-substituted compounds were found to possess greater inhibitory activity in comparison to the para-substituted compounds. At the same time, the results also revealed that the stronger electron withdrawing groups resulted in a decrease in inhibitory activity. Finally, though it was proposed that the C=O moiety of the inhibitor may possibly be able to interact with one of two hydrogen bonding sites, it was determined that C=O moiety of this particular range of compounds was not utilised as results indicated a highly strained conformer being formed.

The screening of some of the benzylimidazoles synthesised (**264-266** and **270-272**) were reported by Abdullah et al[ref]. The compounds synthesised were shown to be equivalent in inhibitory activity of 17,20-lyase to KTZ, where the substitution on the benzyl ring showed no connection to the results observed. In addition to this, the inhibitory activity of 17α-OHase to KTZ was also shown to be comparable with compounds **270–272** showing even greater inhibitory activity in comparison to KTZ. Though these compounds were shown to have no connection with regards to the

substitutionon the benzyl ring in the screening against 17,20-lyase, the results against 17α-OHase showed a general trend towards the para-substitution of the benzyl ring in the compounds **264-266**.

6.0 Experimental

6.1 Methods and materials

All NMR spectra were recorded on a JEOL ECP 400MHz. Chemical shifts are reported as δ values in ppm relative to TMS (δ 0.00). All coupling constants are quoted in Hz. Infrared spectra were determined on a ThermoNicolet 380 FT-IR. The mass spectra (*m/z*) were recorded on a Varian CP-3800 Gas Chromatograph with Varian 1200L Quadrupole Mass Spectrometer. TLC was carried out using (normal phase) silica gel polyester plates. Melting points were determined by using a Stuart Scientific SMP3 melting point apparatus or a Gallenkamp melting point instrument. High Resolution Mass Spectrometry was carried out at The Analytical Department, Kingston University. Elemental analysis was carried out by the CHN microanalysis service (London School of Pharmacy) bu use of a Bruker Apex III system. All chemicals were purchased from the Sigma-Aldrich Chemical Company LTD, Lancaster Synthesis Ltd and Avacado Research Chemicals.

249 1-benzyl-1H-imidazole

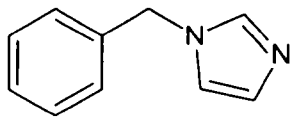

Benzyl Bromide (1.0g, 5.84mmol) was added to a solution of Potassium Carbonate (K_2CO_3) (1.23g, 8.89mmol) and Imidazole (1.23g, 17.5mmol) in Tetrahydrofuran (THF, 150ml) and left to stir for 48hr. After stirring, the reaction mixture was poured in Dichloromethane (DCM, 50ml) and washed with water (50ml). The solution was then acidified using hydrochloric acid solution (1M, 4 x 50ml) and neutralised using saturated sodium bicarbonate solution ($NaHCO_3$, 300ml). The resulting solution was then extracted into DCM (4 x 50ml) and dried over magnesium sulphate ($MgSO_4$). It was then filtered under suction and the DCM was removed under vacuum. The crude product was re-crystallised using a 50:50 solution of water and methylated spirit to give **249** (0.67g, yield 73%) as a white solid; [m.p.=68.1-68.8°C]; R_f=0.48 [90/10 diethyl ether/methanol].

$\nu_{(max)}$(Film)cm^{-1}: 3111 (Ar, C-H), 3031 (C-H), 1605 (Ar, C=C); δ_H (400MHz, $CDCl_3$): 7.51 (1H, s, NC<u>H</u>N Imidazole),7.31 (3H, m, Ph-<u>H</u>),7.13 (2H, m, Ph-<u>H</u>),7.06 (1H, s, CH_2-NC<u>H</u> imidazole),6.87 (1H, s, NC<u>H</u> Imidazole), 5.08 (2H, s, C<u>H</u>$_2$);δ_c($CDCl_3$): 137.53 (Im, N**C**N), 136.26, 129.89, 129.07 (Ar, **C**), 128.35 (Im, N**C**H), 127.36 (Ar, **C**), 119.38 (Im, N**C**H), 50.87 (**C**H_2): GC tR=13.19 min; LRMS (m/z) 158 (M^+, 38%), 91 (M^+-$C_3H_3N_2$, 100%), 77 (M^+-$C_4H_5N_2$, 6%).

250 1-(2-Fluoro-benzyl)-1H-imidazole

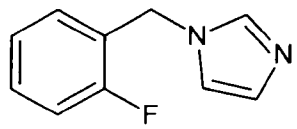

Compound **250** was synthesised in a similar manner to **1** with the exception that imidazole (1.1g, 16.1mmol), anhydrous K_2CO_3 (1.1g, 7.95mmol) 2-fluorobenzyl bromide (1.0g, 5.28mmol) were used. The crude product was re-crystallised using a 50:50 solution of water and methylated spirit to give **250** (0.72g, yield 78%) as a light yellow oil; R_f=0.57 [90/10 diethyl ether/methanol].

$\nu_{(max)}$(Film)cm^{-1}: 3113 (Ar, C-H), 1618, 1588 (Ar, C=C); δ_H(400MHz, $CDCl_3$): 7.53 (1H, s, NC<u>H</u>N Imidazole), 7.28 (1H, m, Ph-<u>H</u>), 7.09 (1H, s, CH_2-NC<u>H</u> imidazole), 7.06 (3H, m, Ph-<u>H</u>), 6.91 (1H, s, NC<u>H</u> Imidazole), 5.13 (2H, s, C<u>H</u>$_2$);δ_c(100MHz, $CDCl_3$): 161.73, 159.26 (**C**-F, Ar), 137.50 (Im, N**C**N), 130.47 (Ar, **C**), 129.92 (Im, N**C**H), 129.54, 124.77, 123.35 (Ar, **C**), 119.30 (Im, N**C**H), 115.93 (Ar, **C**), 44.65 (**C**H_2): GC tR=12.99 min; LRMS (m/z) 176 (M^+, 41%), 109 (M^+-$C_3H_3N_2$, 100%), 95 (M^+-$C_4H_5N_2$, 2%), 75 (M^+-$C_4H_5N_2F$, 4%).HRMS (EI): *m/z* calcd for $C_{10}H_9N_2F$: 176.0749; found: 176.0742.

251 1-(3-Fluoro-benzyl)-1H-imidazole

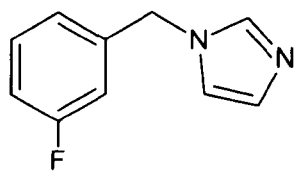

Compound **251** was synthesised in a similar manner to **249** with the exception that imidazole (1.1g, 16.1mmol), anhydrous K_2CO_3 (1.1g, 7.93mmol) 3-fluorobenzyl bromide (1.0g, 5.28mmol) were used. The crude product was re-crystallised using a 50:50 solution of water and methylated spirit to give **251** (0.61g, yield 65%) as a yellow oil; R_f=0.44 [90/10 diethyl ether/methanol].

$\nu_{(max)}$(Film)cm^{-1}: 3111 (Ar, C-H), 2360 (C=N), 1617, 1592 (Ar, C=C); δ_H (400MHz, $CDCl_3$): 7.56 (1H, s, NC<u>H</u>N Imidazole), 7.29 (1H, m, Ph-<u>H</u>),7.08 (1H, s, CH_2-NC<u>H</u> imidazole), 6.98 (1H, m, Ph-<u>H</u>), 6.89 (2H, m, 1H, Ph-<u>H</u>, 1H, NC<u>H</u> Imidazole), 6.80 (1H, m, Ph-<u>H</u>), 5.10 (2H, s, C<u>H</u>$_2$);δ_C(100MHz, $CDCl_3$): 162.14 ,161.93 (F, Ar), 138.82 (Ar, **C**), 137.53 (Im, N**C**N), 130.75 (Ar, **C**), 130.12 (Im, N**C**H), 122.80 (Ar, **C**), 119.35 (Im, N**C**H), 115.45, 114.39 (Ar, **C**), 50.26 (**C**H_2): GC tR=13.25 min; LRMS (m/z) 176 (M^+, 43%), 109 (M^+-$C_3H_3N_2$, 100%), 95 (M^+-$C_4H_5N_2$, 7%) 75 (M^+-$C_4H_5N_2F$, 7%). HRMS (EI): *m/z* calcd for $C_{10}H_9N_2F$: 176.0749; found: 176.0031.

252 1-(4-Fluoro-benzyl)-1H-imidazole

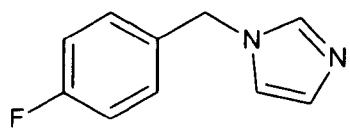

Compound **252** was synthesised in a similar manner to **249** with the exception that imidazole (1.1g, 16.1mmol), anhydrous K_2CO_3 (1.1g, 7.93mmol) 4-fluorobenzyl bromide (1.0g, 5.28mmol) were used. The crude product was re-crystallised using a 50:50 solution of water and methylated spirit to give **252** (0.79g, yield 84%) as a yellow oil; R_f=0.46 [90/10 diethyl ether/methanol].

$\nu_{(max)}$(Film)cm^{-1}: 3113 (Ar, C-H), 1606, 1512 (Ar, C=C); δ_H (400MHz, $CDCl_3$): 7.51 (1H, s, NC<u>H</u>N Imidazole),7.11 (2H, ,Ph-<u>H</u>),7.06 (1H, s, CH_2-NC<u>H</u> imidazole), 7.01 (2H, m, Ph-<u>H</u>),6.85 (1H, s, NC<u>H</u> Imidazole), 5.06 (2H, s, C<u>H</u>$_2$);δ_C (100MHz, $CDCl_3$): 163.92, 161.97 (F, Ar), 137.40 (Im, N**C**N), 132.15 (Ar, **C**), 130.05 (Im, N**C**H), 129.20 (Ar, **C**), 119.21 (Im, N**C**H), 116.16 (Ar, **C**), 50.18 (**C**H_2): GC tR=13.27 min; LRMS (m/z) 176 (M^+, 27%), 109 (M^+-$C_3H_3N_2$, 100%), 95 (M^+-$C_4H_5N_2$, 2%) 75 (M^+-$C_4H_5N_2F$, 4%). HRMS (EI): *m/z* calcd for $C_{10}H_9N_2F$: 176.0749; found: 176.0731.

253 1-(3, 4-Difluoro-benzyl)-1H-imidazole

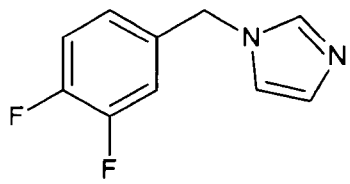

Compound **253** was synthesised in a similar manner to **249** with the exception that imidazole (1.0g, 14.5mmol), anhydrous K_2CO_3 (1.0g, 7.24mmol) 3, 4-difluorobenzyl bromide (1.0g, 4.83mmol) were used. The crude product was re-crystallised using a 50:50 solution of water and methylated spirit to give **253** (0.79g, yield 84%) as a yellow oil; R_f=0.49 [90/10 diethyl ether/methanol].

$\nu_{(max)}$(Film)cm^{-1}: 3114 (Ar, C-H), 1611 (Ar, C=C); δ_H(400MHz, DMSO):7.45 (1H, s, NC<u>H</u>N Imidazole), 7.02 (1H, m, Ph-<u>H</u>),6.97 (1H, s, CH_2-NC<u>H</u> imidazole),6.82 (1H, m, Ph-<u>H</u>),6.78 (1H, s, Ph-<u>H</u>),6.74 (1H, s, NC<u>H</u> Imidazole), 4.95 (2H, s, C<u>H</u>$_2$);δ_C(100MHz, $CDCl_3$): 151.16, 150.76, 148.68, 148.28 (Ar, F), 136.60 (N**C**N), 132.42 (Ar, **C**), 129.27 (N**C**H), 122.53 (Ar, **C**), 118.42 (N**C**H), 117.27, 115.70 (Ar, **C**), 49.02(**C**H_2):GC tR=12.75 min; LRMS (m/z) 194 (M^+, 36%), 127 (M^+-$C_3H_3N_2$, 100%), 113 (M^+-$C_4H_5N_2$, 2%), 107 (M^+-$C_3H_3N_2F$, 6%), 87 (M^+-$C_3H_3N_2F_2$, 2%), 77 (M^+-$C_4H_5N_2F_2$, 4%).

254 1-(2-Chloro-benzyl)-1H-imidazole

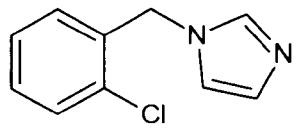

Compound **254** was synthesised in a similar manner to **249** with the exception that imidazole (1.0g, 14.6mmol), anhydrous K_2CO_3 (1.1g, 7.95mmol) 2-chlorobenzyl bromide (1.0g, 4.86mmol) were used. The crude product was re-crystallised using a 50:50 solution of water and methylated spirit to give **254** (0.70g, yield 75%) as a yellow oil; R_f=0.51 [90/10 diethyl ether/methanol].

$\nu_{(max)}$(Film)cm^{-1}: 3112 (Ar, C-H), 1642, 1594 (Ar, C=C); δ_H (400MHz, $CDCl_3$): 7.55 (1H, s, NC<u>H</u>N Imidazole), 7.38 (1H, dd, *J*=1.46Hz, *J*=7.87Hz,Ph-<u>H</u>),7.24 (2H, m, Ph-<u>H</u>),7.08 (1H, s, CH_2-NC<u>H</u> imidazole), 7.06 (2H, m, 1H, Ph-<u>H</u>, 1H, NC<u>H</u> Imidazole), 5.21 (2H, s, C<u>H</u>$_2$);δ_C (100MHz, $CDCl_3$): 137.75 (N**C**N), 134.16 (Cl, Ar), 133.14, 129.95 (Ar, **C**), 129.90 (N**C**H), 129.75, 129.0, 127.54 (Ar, **C**), 119.45 (N**C**H), 48.40 (**C**H_2): GC tR=15.14 min; LRMS (m/z) 192 (M^+, 20%), 157 (M^+-Cl, 29%), 125 (M^+-$C_3H_3N_2$, 100%), 111 (M^+-$C_4H_5N_2$, 1%), 89 (M^+-$C_3H_3N_2Cl$, 23%), 75 (M^+-$C_4H_5N_2Cl$, 7%): HRMS (EI): *m/z* calcd for $C_{10}H_9N_2Cl$:192.6445; found: 192.0453.

255 1-(3-Chloro-benzyl)-1H-imidazole

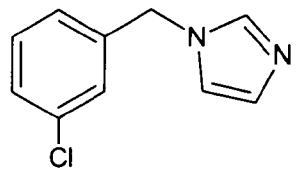

Compound **255** was synthesised in a similar manner to **249** with the exception that imidazole (1.0g, 14.6mmol), anhydrous K_2CO_3 (1.1g, 7.95mmol) 3-chlorobenzyl bromide (1.0g, 4.86mmol) were used. The crude product was re-crystallised using a 50:50 solution of water and methylated spirit to give **255** (0.62g, yield 66%) as a yellow oil; R_f=0.52 [90/10 diethyl ether/methanol].

$\nu_{(max)}$(Film)cm^{-1}: 3112 (Ar, C-H), 1638, 1599 (Ar, C=C); δ_H (400MHz, $CDCl_3$): 7.52 (1H, s, NC<u>H</u>N Imidazole), 7.25 (2H, m, Ph-<u>H</u>),7.10 (1H, m, Ph-<u>H</u>),7.08 (1H, s, CH_2-NC<u>H</u> imidazole),6.99 (1H, m, Ph-<u>H</u>),6.87 (1H, s, NC<u>H</u> Imidazole), 5.07 (2H, s, C<u>H</u>$_2$);δ_C(100MHz, $CDCl_3$): 138.28 (Cl, Ar), 137.52 (N**C**N), 135.06, 130.38 (Ar, **C**), 130.20 (N**C**H), 128.59, 127.40, 125.34 (Ar, **C**), 119.33 (N**C**H), 50.21 (**C**H_2): GC tR=15.14 min; LRMS (m/z) 192 (M^+, 20%), 157 (M^+-Cl, 34%), 125 (M^+-$C_3H_3N_2$, 100%), 111 (M^+-$C_4H_5N_2$, 1%), 89 (M^+-$C_3H_3N_2Cl$, 24%), 75 (M^+-$C_4H_5N_2Cl$, 6%):HRMS (EI): *m/z* calcd for $C_{10}H_9N_2Cl$:192.6445; found: 192.0453.

256 1-(4-Chloro-benzyl)-1H-imidazole

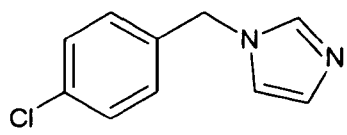

Compound **256** was synthesised in a similar manner to **249** with the exception that imidazole (1.0g, 14.6mmol), anhydrous K_2CO_3 (1.1g, 7.95mmol) 4-chlorobenzyl bromide (1.0g, 4.86mmol) were used. The crude product was recrystallised using a 50:50 solution of water and methylated spirit to give **256** (0.66g, yield 70%) as a yellow oil; R_f=0.50 [90/10 diethyl ether/methanol].

$\nu_{(max)}$(Film)cm^{-1}: 3111 (Ar, C-H), 1644, 1597 (Ar, C=C); δ_H (400MHz, $CDCl_3$): 7.54 (1H, s, NC<u>H</u>N Imidazole),7.43 (2H, d, J=8.79Hz Ph-<u>H</u>), 7.22 (2H, d, J=8.79Hz Ph-<u>H</u>), 7.10 (1H, s, CH_2-NC<u>H</u> imidazole), 6.89 (1H, s, NC<u>H</u> Imidazole), 5.08 (2H, s, C<u>H</u>$_2$);δ_C(100 MHz, $CDCl_3$): 138.54 (Cl, Ar), 137.53 (N**C**N), 131.52, 130.65 (Ar, **C**), 125.82 (N**C**H), 123.16 (Ar, **C**), 119.32 (N**C**H), 50.15 (**C**H_2): GC tR=15.72 min; LRMS (m/z) 192 (M^+, 28%), 125 (M^+-$C_3H_3N_2$, 100%), 111 (M^+-$C_4H_5N_2$, 1%), 89 (M^+-$C_3H_3N_2Cl$, 21%), 75 (M^+-$C_4H_5N_2Cl$, 6%).

257 1-(3, 4-Dichloro-benzyl)-1H-imidazole

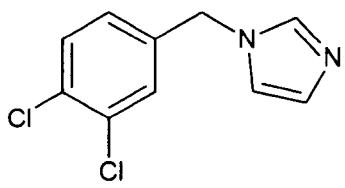

Compound **257** was synthesised in a similar manner to **249** with the exception that imidazole (0.86g, 12.6mmol), anhydrous K_2CO_3 (0.87g, 6.29mmol) 3, 4-dichlorobenzyl bromide (1.0g, 4.16mmol) were used. The crude product was recrystallised using a 50:50 solution of water and methylated spirit to give **257** (0.62g, yield 66%) as a yellow solid; [m.p.=51.4-52.2°C]; R_f=0.54 [90/10 diethyl ether/methanol].

$\nu_{(max)}$(Film)cm^{-1}: 3112 (Ar, C-H), 1594 (Ar, C=C); δ_H(400MHz, $CDCl_3$):7.62 (1H, s, NC<u>H</u>N Imidazole), 7.42 (1H, d, *J*=8.24Hz, Ph-<u>H</u>),7.23 (1H, s, Ph-<u>H</u>),7.12 (1H, s, CH_2-NC<u>H</u> imidazole), 6.98 (1H, m, Ph-<u>H</u>),6.89 (1H, m, NC<u>H</u> Imidazole), 5.09 (2H, s, C<u>H</u>$_2$);δ_C(100MHz, $CDCl_3$): 139.05 (Ar, C), 137.95 (N**C**N), 134.95, 134.27 (Ar, Cl) 132.70 (Ar, **C**), 131.65 (N**C**H), 130.81, 128.09 (Ar, **C**), 120.84 (N**C**H), 51.32 (**C**H_2):GC tR=17.12 min; LRMS (m/z) 226 (M^+, 36%), 159 (M^+-$C_3H_3N_2$, 100%), 123 (M^+-$C_3H_3N_2Cl$, 16%), 89 (M^+-$C_3H_3N_2Cl_2$, 16%), 76 (M^+-$C_4H_5N_2Cl_2$, 5%).

258 1-(2-Bromo-benzyl)-1H-imidazole

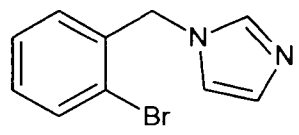

Compound **258** was synthesised in a similar manner to **249** with the exception that imidazole (0.83g, 12.2mmol), anhydrous K_2CO_3 (0.83g, 6.0mmol) 2-bromobenzyl bromide (1.0g, 4.0mmol) were used. The crude product was recrystallised using a 50:50 solution of water and methylated spirit to give **258** (0.67g, yield 71%) as a yellow oil: R_f=0.56 [90/10 diethyl ether/methanol].

$\nu_{(max)}$(Film)cm^{-1}: 3111 (Ar, C-H), 1636, 1590 (Ar, C=C); δ_H (400MHz, $CDCl_3$): 7.58 (2H, m,1H, Ph-H, 1H, NCHN Imidazole), 7.25 (1H, m, Ph-H),7.17 (1H, m, Ph-H); 7.09 (1H, s, CH_2-NCH imidazole); 6.92 (1H, s, NCH Imidazole); 6,87 (1H, m, Ph-H); 5.19 (2H, s, CH_2). δ_C(100MHz, $CDCl_3$): 137.80 (**N**CN), 135.78 (Ar, Br), 133.19 (Ar, **C**), 129.97 (N**C**H), 129.94, 129.01 128.17, 123.04 (Ar, **C**), 119.46 (N**C**H), 50.83 (**C**H_2): GC tR=16.23 min; LRMS (m/z) 236 (M^+, 22%), 169 (M^+-$C_3H_3N_2$, 100%), 157 (M^+-Br^{79}, 96%), 90 (M^+-$C_3H_3N_2Br^{79}$, 45%), 77 (M^+-$C_4H_5N_2Br$, 10%). HRMS (EI): *m/z* calcd for $C_{10}H_9N_2Br$: 235.9948; found: 235.9959 $^{(79)}$ and 237.9935$^{(81)}$.

259 1-(3-Bromo-benzyl)-1H-imidazole

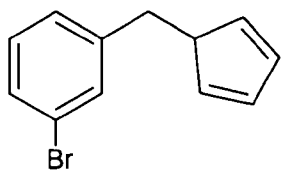

Compound **259** was synthesised in a similar manner to **249** with the exception that imidazole (0.83g, 12.2mmol), anhydrous K_2CO_3 (0.83g, 6.0mmol) 3-bromobenzyl bromide (1.0g, 4.0mmol) were used. The crude product was re-crystallised using a 50:50 solution of water and methylated spirit to give **259** (0.63g, yield 66%) as a yellow oil; R_f=0.58 [90/10 diethyl ether/methanol].

$\nu_{(max)}$(Film)cm^{-1}: 3112(Ar, C-H), 1646, 1596 (Ar, C=C); δ_H(400MHz, $CDCl_3$): 7.51 (1H, s, NC<u>H</u>N Imidazole), 7.30 (2H, m, Ph-<u>H</u>), 7.07 (1H, s, CH_2-NC<u>H</u> imidazole), 7.04 (3H, m, 2H, Ph-<u>H</u>, 1H, NC<u>H</u> Imidazole), 6.82 (1H, s, NC<u>H</u> Imidazole), 5.06 (2H, s, C<u>H</u>$_2$). δ_C(100MHz, $CDCl_3$):137.48 (N**C**N), 134.77 (Ar, Br), 134.31, (Ar, **C**), 130.15 (N**C**H), 129.27, 128.66 (Ar, **C**), 119.25 (N**C**H),50.17 (**C**H_2): GC tR=16.64 min; LRMS (m/z) 236 (M^+, 59%), 169 (M^+-$C_3H_3N_2$, 100%), 90 (M^+-$C_3H_3N_2Br^{79}$, 33%), 78 (M^+-$C_4H_5N_2Br$, 8%). HRMS (EI): *m/z* calcd for $C_{10}H_9N_2Br$: 235.9948; found: 235.9959 $^{(79)}$ and 237.9935$^{(81)}$.

260 1-(4-Bromo-benzyl)-1H-imidazole

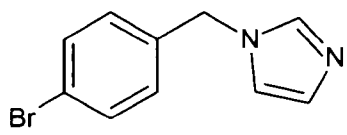

Compound **260** was synthesised in a similar manner to **249** with the exception that imidazole (0.83g, 12.2mmol), anhydrous K_2CO_3 (0.83g, 6.0mmol) 4-bromobenzyl bromide (1.0g, 4.0mmol) were used. The crude product was recrystallised using a 50:50 solution of water and methylated spirit to give **260** (0.5g, yield 53%) as a white solid; [m.p.=81.4-81.8°C]; R_f=0.38 [90/10 diethyl ether/methanol].

$\nu\nu_{(max)}$(Film)cm^{-1}: 3112 (Ar, C-H), 1592, 1506 (Ar, C=C); δ_H (400MHz, $CDCl_3$): 7.51 (1H, s, NC<u>H</u>N Imidazole), 7.45 (2H, d, *J*=8.42Hz, Ph-<u>H</u>),7.07 (1H, s, CH_2-NC<u>H</u> imidazole),6.99 (2H, d, *J*=8.42Hz, Ph-<u>H</u>),6.85 (1H, m, NC<u>H</u> Imidazole); 5.05 (2H, s, C<u>H</u>$_2$). δ_C(100MHz, $CDCl_3$): 137.50 (N**C**N), 135.33 (Ar, Br), 132.23 (Ar, **C**), 130.22 (N**C**H), 128.95, 122.33 (Ar, **C**), 119.25 (N**C**H), 50.21 (**C**H_2): GC tR=16.86 min; LRMS (m/z) 236 (M^+, 38%), 171 (M^+-$C_3H_3N_2$, 100%), 155 (M^+-$C_4H_5N_2$, 2%), 90 (M^+-$C_3H_3N_2Br^{79}$, 37%), 75 (M^+-$C_4H_5N_2Br$, 5%). HRMS (EI): *m/z* calcd for $C_{10}H_9N_2Br$: 235.9948; found: 235.9959 $^{(79)}$ and 237.9935$^{(81)}$.

261 1-(2-Iodo-benzyl)-1H-imidazole

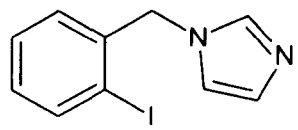

Compound **261** was synthesised in a similar manner to **249** with the exception that imidazole (0.7g, 10.2mmol), anhydrous K_2CO_3 (0.7g, 5.0mmol) 4-iodobenzyl bromide (1.0g, 3.36mmol) were used. The crude product was recrystallised using a 50:50 solution of water and methylated spirit to give **261** (0.33g, yield 35%) as a white solid; [m.p.=61.3-62.7°C]; R_f=0.59 [90/10 diethyl ether/methanol].

$\nu_{(max)}$(Film)cm^{-1}: 3109 (Ar, C-H), 2926 (C-H), 1584, 1504 (Ar, C=C); δ_H(400MHz, $CDCl_3$): 7.86 (1H, m, Ph-H),7.55 (1H, s, NCHN Imidazole), 7.28 (1H, m, Ph-H),7.09 (1H, s, CH_2-NCH imidazole), 7.02 (1H, m, Ph-H);6.91 (1H, m, NCH Imidazole); 6.83 (1H, m, Ph-H);5.19 (2H, s, CH_2).δ_C(100MHz, $CDCl_3$): 139.87 (**N**CN),138.70 (Ar, I), 137.85 (**N**CH), 130.04, 130.00, 129.01, 128.53 (Ar, **C**), 119.46 (**N**CH), 98.10 (Ar, **C**), 55.51 (**C**H_2): GC tR=17.97 min; LRMS (m/z) 284 (M^+, 32%), 217 (M^+-$C_3H_3N_2$, 100%), 157 (M^+- I, 94%), 90 (M^+-$C_3H_3N_2I$, 36%), 77 (M^+-$C_4H_5N_2I$, 9%).

262 1-(3-Iodo-benzyl)-1H-imidazole

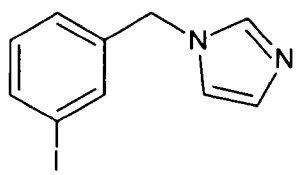

Compound **262** was synthesised in a similar manner to **249** with the exception that imidazole (0.7g, 10.2mmol), anhydrous K_2CO_3 (0.7g, 5.0mmol) 3-iodobenzyl bromide (1.0g, 3.36mmol) were used. The crude product was recrystallised using a 50:50 solution of water and methylated spirit to give **262** (0.70g, yield 74%) as a white solid; [m.p.=81.9-82.5°C];R_f=0.60 [90/10 diethyl ether/methanol].

$\nu_{(max)}$(Film)cm^{-1}: 3109 (Ar, C-H), 1591, 1566 (Ar, C=C); δ_H (400MHz, $CDCl_3$):7.63 (1H, m, Ph-H),7.52 (1H, s, NCHN Imidazole), 7.48 (1H, s, CH_2-NCH imidazole),7.07 (3H, m, Ph-H),6.87 (1H, m, NCH Imidazole), 5.04 (2H, s, CH_2). δ_C(100MHz, $CDCl_3$): 138.56 (Ar, I), 137.53 (**N**CN), 137.49, 136.20, 130.77 (Ar, **C**), 130.25 (**N**CH), 126.48 (Ar, **C**), 119.30 (**N**CH), 94.84 (Ar, **C**),50.21 (**C**H_2):GC tR=17.57 min; LRMS (m/z) 284 (M^+, 100%), 217 (M^+-$C_3H_3N_2$, 98%), 203 (M^+-$C_4H_5N_2$, 0.8%), 157 (M^+- I, 2%), 90 (M^+-$C_3H_3N_2I$, 37%), 76 (M^+-$C_4H_5N_2I$, 4%).

263 1-(4-Iodo-benzyl)-1H-imidazole

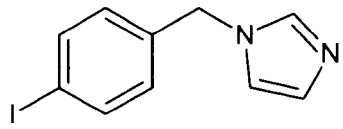

Compound **263** was synthesised in a similar manner to **249** with the exception that imidazole (0.7g, 10.2mmol), anhydrous K_2CO_3 (0.7g, 5.0mmol) 4-iodobenzyl bromide (1.0g, 3.36mmol) were used. The crude product was recrystallised using a 50:50 solution of water and methylated spirit to give **263** (0.62g, yield 64%) as a white solid; [m.p.=105.2-106.0°C];R_f=0.61 [90/10 diethyl ether/methanol].

$\nu_{(max)}$(Film)cm^{-1}: 3083.1 (Ar, C-H), 1590.3 (Ar, C=C); (400MHz, $CDCl_3$):7.68 (2H, d, *J*=8.42Hz, Ph-H),7.64 (1H, s, NCHN Imidazole), 7.08 (1H, s, CH_2-NCH Imidazole), 6.88 (2H, d, *J*=8.42Hz, Ph-H),6.85 (1H, s, NCH imidazole), 5.06 (2H, s, CH_2).δ_C(100MHz, $CDCl_3$): 138.23 (Ar, **C**), 137.40 (N**C**N), 135.74 (Ar, I), 129.53 (N**C**H), 129.22 (Ar, **C**), 119.33 (N**C**H), 94.04 (Ar, **C**), 50.47 (**C**H_2):GC tR=17.57 min; LRMS (m/z) 284 (M^+, 47%), 217 (M^+-$C_3H_3N_2$, 100%), 203 (M^+-$C_4H_5N_2$, 0.9%), 157 (M^+- I, 2%), 90 (M^+-$C_3H_3N_2I$, 34%), 76 (M^+-$C_4H_5N_2I$, 4%).

264 1-(2-Cyano-benzyl)-1H-imidazole

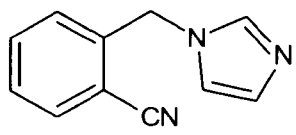

Compound **264** was synthesised in a similar manner to **249** with the exception that imidazole (1.9g, 28.0mmol), anhydrous K_2CO_3 (1.9g, 13.8mmol) 2-cyanobenzyl bromide (2.0g, 9.28mmol) were used. The crude product was recrystallised using a 50:50 solution of water and methylated spirit to give **264** (0.63g, yield 34%) as a yellow oil; R_f=0.45 [90/10 diethyl ether/methanol].

$\nu_{(max)}$(Film)cm^{-1}: 3116 (Ar, C-H), 2227 (C≡N), 1647, 1600 (Ar, C=C); δ_H (400MHz, $CDCl_3$): 7.70 (1H, m, Ph-H), 7.59 (1H, s, NCHN Imidazole),7.57 (1H, m, Ph-H),7.43 (1H, m, Ph-H),7.09 (2H, m, 1H, CH_2-NCH imidazole, 1H, Ph-H),7.08 (1H, m, Ph-H),6.95 (1H, s, NCH Imidazole),5.33 (2H, s, CH_2). δ_C (100MHz, $CDCl_3$): 139.88 (**C**N), 137.62 (N**C**N), 133.73, 133.27 (Ar, **C**), 130.32 (N**C**H), 129.05, 128.29 (Ar, **C**), 119.39 (N**C**H), 116.96, 111.50 (Ar, **C**), 48.77 (**C**H_2):GC tR=15.75 min; LRMS (m/z) 183 (M^+, 40%), 157 (M^+-CN, 2%), 116 (M^+-$C_3H_3N_2$, 100%), 102 (M^+-$C_4H_5N_2$, 2%), 89 (M^+-$C_4H_5N_3$, 26%), 76 (M^+-$C_5H_5N_3$, 4%).

265 1-(3-Cyano-benzyl)-1H-imidazole

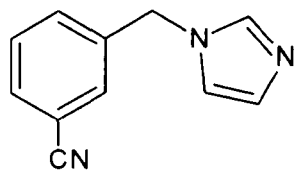

Compound **265** was synthesised in a similar manner to **249** with the exception that imidazole (1.9g, 28.0mmol), anhydrous K_2CO_3 (1.9g, 13.8mmol) 3-cyanobenzyl bromide (2.0g, 9.27mmol) were used. The crude product was recrystallised using a 50:50 solution of water and methylated spirit to give **265** (1.29g, yield 69%) as a white solid; [m.p.=64.3-65.2°C];R_f=0.42 [90/10 diethyl ether/methanol].

$\nu_{(max)}$(Film)cm^{-1}: 3114 (Ar, C-H), 2231 (C≡N), 1585 (Ar, C=C); δ_H (400MHz, $CDCl_3$): 7.62 (1H, m, Ph-H), 7.56 (1H, s, NCHN Imidazole), 7.47 (1H, t, J=7.79Hz Ph-H), 7.42 (1H, s, Ph-H), 7.33 (1H, m, Ph-H), 7.12 (1H, s, CH_2-NCH Imidazole), 6.89 (1H, s, NCH Imidazole),5.17 (2H, s, CH_2). δ_C (100MHz, $CDCl_3$): 138.02 (**C**N), 137.53 (**NC**HN), 132.07, 131.39, 130, 78, 130.56 (Ar, **C**), 130.04, 119.25 (**NC**H), 118.23, 113.37 (Ar, **C**), 49.92 (**C**H_2):GC tR=16.72 min; LRMS (m/z) 183 (M^+, 38%),116 (M^+-$C_3H_3N_2$, 100%), 102 (M^+-$C_4H_5N_2$, 1%), 89 (M^+-$C_4H_5N_3$, 29%), 75 (M^+-$C_5H_5N_3$, 4%).

266 1-(4-Cyano-benzyl)-1H-imidazole

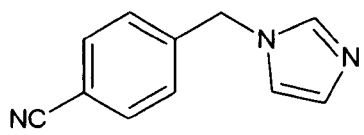

Compound **266** was synthesised in a similar manner to **249** with the exception that imidazole (2.1g, 30.9mmol), anhydrous K_2CO_3 (2.1g, 15.5mmol) 4-cyanobenzyl bromide (2.0g, 10.2mmol) were used. The crude product was recrystallised using a 50:50 solution of water and methylated spirit to give **266** (1.47g, yield 79%) as a white solid; [m.p.=106.8-107.6°C];R_f=0.45 [90/10 diethyl ether/methanol].

$\nu_{(max)}$(Film)cm^{-1}: 3111 (Ar, C-H), 2230 (C≡N), 1610 (Ar, C=C); δ_H(400MHz, $CDCl_3$): 7.64 (2H, d, J=8.42Hz, Ph-H), 7.56 (1H, s, NCHN Imidazole), 7.21 (2H, d, J=8.42Hz, Ph-H),7.13 (1H, s, NCH Imidazole), 6.89 (1H, s, NCH Imidazole), 5.20 (2H, s, CH_2). δ_C (100MHz, $CDCl_3$): 141.63 (**C**N), 137.63 (N**C**HN), 132.91 (Ar, **C**), 130.55 (N**C**H), 127.64 (Ar, **C**), 119.33 (N**C**H), 118.32, 112.40 (Ar, **C**), 50.22 (**C**H_2):GC tR=16.88 min; LRMS (m/z) 183 (M^+, 41%), 116 (M^+-$C_3H_3N_2$, 100%), 102 (M^+-$C_4H_5N_2$, 3%), 89 (M^+-$C_4H_5N_3$, 27%), 75 (M^+-$C_5H_5N_3$, 3%).

267 1-(2-Methyl-benzyl)-1H-imidazole

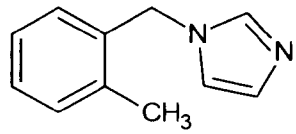

Compound **267** was synthesised in a similar manner to **249** with the exception that imidazole (2.20g, 32.4mmol), anhydrous K_2CO_3 (2.25g, 16.3mmol) 2-methylbenzyl bromide (2.0g, 10.8mmol) were used. The crude product was recrystallised using a 50:50 solution of water and methylated spirit to give **267** (0.63g, yield 34%) as a yellow oil; R_f=0.43 [90/10 diethyl ether/methanol].

$\nu_{(max)}$(Film)cm^{-1}: 3111.6 (Ar, C-H), 1606.3 (Ar, C=C), 1462.4 (CH_2); δ_H(400MHz, $CDCl_3$): 7.47 (1H, s, NC<u>H</u>N Imidazole); 7.23 (1H, m, Ph-<u>H</u>); 7.18 (2H, m, Ph-<u>H</u>); 7.07 (1H, s, NC<u>H</u> Imidazole); 6.96 (1H, m, Ph-<u>H</u>); 6.85 (1H, s, NC<u>H</u> Imidazole); 5.10 (2H, s, C<u>H</u>$_2$) 2.22 (3H, s, C<u>H</u>$_3$). δ_C (100MHz, $CDCl_3$): 137.50 (N**C**HN), 136.19 (**C**-CH_3, Ar), 134.02,130.83, 129.67 (Ar, **C**), 128.62, 128.33 (N**C**H), 126.66, 119.35 (Ar, **C**), 49.06 (**C**H_2), 18.98 (**C**H_3):GC tR=13.14 min; LRMS (m/z) 172 (M^+, 22%), 157 (M^+-CH_3, 1%), 105 (M^+-$C_3H_3N_2$, 100%), 91 (M^+-$C_4H_5N_2$, 4%), 77 (M^+-$C_5H_8N_2$, 15%).

268 1-(3-Methyl-benzyl)-1H-imidazole

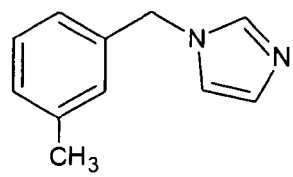

Compound **268** was synthesised in a similar manner to **249** with the exception that imidazole (2.2g, 32.4mmol), anhydrous K_2CO_3 (2.25g, 16.2mmol) 3-methylbenzyl bromide (2.0g, 10.8mmol) were used. The crude product was recrystallised using a 50:50 solution of water and methylated spirit to give **268** (1.49g, yield 80%) as a yellow oil; R_f=0.39 [90/10 diethyl ether/methanol].

$\nu_{(max)}$(Film)cm^{-1}: 3111.5 (Ar, C-H), 2923.3 (C-H), 1609.3 (Ar, C=C), 1506.7 (CH_2);δ_H(400MHz, $CDCl_3$): 7.53 (1H, s, NC<u>H</u>N Imidazole); 7.23 (1H, t, J=7.87Hz, Ph-<u>H</u>); 7.13 (1H, m, Ph-<u>H</u>); 7.07 (1H, s, NC<u>H</u> Imidazole); 6.94 (2H, m, Ph-<u>H</u>); 6.89 (1H, s, NC<u>H</u> Imidazole); 5.06 (2H, s, C<u>H</u>$_2$) 2.32 (3H, s, C<u>H</u>$_3$). δ_C (100MHz, $CDCl_3$): 138.89 (**C**-CH_3, Ar), 137.50 (N**C**HN), 136.16,129.78 (Ar, **C**), 129.08, 128.06 (N**C**H), 128.06, 124.46, 119.40 (Ar, **C**), 50.87 (**C**H_2), 21.44 (**C**H_3):GC tR=13.59 min; LRMS (m/z) 172 (M^+, 34%), 157 (M^+-CH_3, 1%), 105 (M^+-$C_3H_3N_2$, 100%), 91 (M^+-$C_4H_5N_2$, 3%), 77 (M^+-$C_5H_8N_2$, 20%).

269 1-(4-Methyl-benzyl)-1H-imidazole

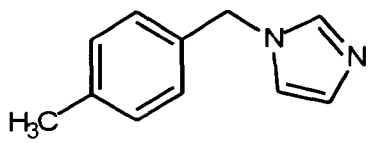

Compound **269** was synthesised in a similar manner to **249** with the exception that imidazole (2.2g, 32.3mmol), anhydrous K_2CO_3 (2.25g, 16.3mmol) 4-methylbenzyl bromide (2.0g, 10.8mmol) were used. The crude product was recrystallised using a 50:50 solution of water and methylated spirit to give **269** (1.42g, yield 76%) as a yellow solid; [m.p.=52.3-53.4°C];R_f=0.38 [90/10 diethyl ether/methanol].

$\nu_{(max)}$(Film)cm^{-1}: 3111.7 (Ar, C-H), 2923.4 (C-H), 1615.1 (Ar, C=C), 1507.9 (CH_2);δ_H(400MHz, $CDCl_3$): 7.64 (1H, s, NC<u>H</u>N Imidazole); 7.14 (2H, d, *J*=7.87Hz, Ph-<u>H</u>); 7.09 (1H, s, NC<u>H</u> Imidazole); 7.02 (2H, d, *J*=7.87Hz, Ph-<u>H</u>); 6.85 (1H, s, NC<u>H</u> Imidazole); 5.09 (2H, s, C<u>H</u>$_2$) 2.32 (3H, s, C<u>H</u>$_3$). δ_C (100MHz, $CDCl_3$): 138.33 (**C**-CH_3, Ar), 137.41 (N**C**HN), 133.54, 129.72 (Ar, **C**), 129.67 (N**C**H), 127.23 (Ar, **C**), 119.35 (N**C**H), 50.54 (**C**H_2), 21.07 (**C**H_3):GC tR=13.80 min; LRMS (m/z) 157 (M^+-CH_3, 1%), 105 (M^+-$C_3H_3N_2$, 100%), 91 (M^+-$C_4H_5N_2$, 4%), 77 (M^+-$C_5H_8N_2$, 18%).

270 1-(2-Nitro-benzyl)-1H-imidazole

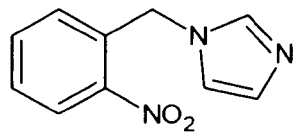

Compound **270** was synthesised in a similar manner to **249** with the exception that imidazole (1.9g, 28.0mmol), anhydrous K_2CO_3 (1.9g, 13.8mmol) 2-nitrobenzyl bromide (2.0g, 9.28mmol) were used. The crude product was recrystallised using a 50:50 solution of water and methylated spirit to give **270** (1.69g, yield 89%) as a white solid; [m.p.=82.3-83.4°C];R_f=0.51 [90/10 diethyl ether/methanol].

$\nu_{(max)}$(Film)cm^{-1}: 3112.4 (Ar, C-H), 1610.3 (Ar, C=C), 1525.3 (N=O); δ_H(400MHz, $CDCl_3$): 8.14 (1H, m, Ph-H); 7.58 (1H, s, NCHN Imidazole); 7.50 (2H, m, Ph-H); 7.15 (1H, s, NCH Imidazole); 6.94 (1H, s, NCH Imidazole); 6.80 (1H, m, Ph-H); 5.57 (2H, s, CH_2). δ_C (100MHz, $CDCl_3$): 147.18 (**C**-NO_2, Ar), 138.13 (N**C**HN), 134.52, 132.19, 130.42 (Ar, **C**), 129.24, 128.70 (N**C**H), 125.51, 119.83 (Ar, **C**), 48.06 (**C**H_2):GC tR=16.67 min; LRMS (m/z) 203 (M^+, 9%), 186 (M^+-O, 3%), 156 (M^+-NO_2, 8%), 135 (M^+-$C_3H_3N_2$, 6%), 119 (M^+-$C_3H_3N_2O$, 64%), 103 (M^+-$C_3H_3N_2O_2$, 19%), 89 (M^+-$C_3H_3N_3O_2$, 43%), 78 (M^+-$C_4H_5N_3O_2$, 100%).

271 1-(3-Nitro-benzyl)-1H-imidazole

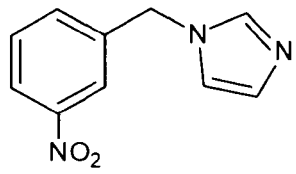

Compound **271** was synthesised in a similar manner to **249** with the exception that imidazole (1.9g, 28.0mmol), anhydrous K_2CO_3 (1.9g, 13.8mmol) 3-nitrobenzyl bromide (2.0g, 9.28mmol) were used. The crude product was recrystallised using a 50:50 solution of water and methylated spirit to give **271** (1.69g, yield 89%) as a white solid; [m.p.=88.3-89.5°C];R_f=0.53 [90/10 diethyl ether/methanol].

$\nu_{(max)}$(Film)cm^{-1}: 3113.4 (Ar, C-H), 1619.8 (Ar, C=C), 1529.2 (N=O); δ_H(400MHz, $CDCl_3$): 8.19 (1H, m, Ph-H); 8.04 (1H, s, NCHN Imidazole); 7.58 (1H, s, Ph-H); 7.55 (1H, s, Ph-H); 7.43 (1H, s, Ph-H); 7.13 (1H, s, NCH Imidazole); 6.92 (1H, s, NCH Imidazole); 5.22 (2H, s, CH_2). δ_C (100MHz, $CDCl_3$): 148.68 (**C**-NO_2, Ar), 138.49 (Ar, **C**), 137.54 (**N**CHN), 133.04 (Ar, **C**), 130.66, 130.29 (**N**CH), 123.44, 122.18, 119.22 (Ar, **C**), 49.97 (**C**H_2):GC tR=17.83 min; LRMS (m/z) 203 (M^+, 72%), 156 (M^+-NO_2, 5%), 136 (M^+-$C_3H_3N_2$, 100%), 103 (M^+-$C_3H_3N_2O_2$, 4%), 90 (M^+-$C_3H_3N_3O_2$, 70%), 78 (M^+-$C_4H_5N_3O_2$, 13%).

272 1-(4-Nitro-benzyl)-1H-imidazole

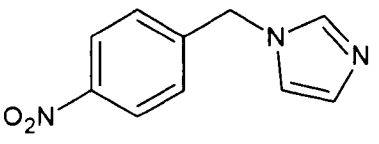

Compound **272** was synthesised in a similar manner to **249** with the exception that imidazole (1.9g, 28.0mmol), anhydrous K_2CO_3 (1.9g, 13.8mmol) 4-nitrobenzyl bromide (2.0g, 9.28mmol) were used. The crude product was recrystallised using a 50:50 solution of water and methylated spirit to give **272** (1.57g, yield 83%) as a yellow solid; [m.p.=55.8-57.1°C];R_f=0.54 [90/10 diethyl ether/methanol].

$\nu_{(max)}$(Film)cm^{-1}: 3113.0 (Ar, C-H), 1607.6 (Ar, C=C), 1518.1 (N=O), 1436.1 (CH_2); δ_H(400MHz, $CDCl_3$): 8.20 (2H, d, *J*=7.69Hz, Ph-H); 7.57 (1H, s, NCHN Imidazole); 7.24 (2H, d, *J*=7.69Hz, Ph-H); 7.13 (1H, s, NCH Imidazole); 6.89 (1H, s, NCH Imidazole); 5.24 (2H, s, CH_2). δ_C (100MHz, $CDCl_3$): 143.51, 139.79 (C, Ar), 137.65 (**N**CHN), 130.64 (**N**CH), 127.79, 124.35 (Ar, **C**), 119.33 (**N**CH), 49.99 (**C**H_2):GC tR=18.12 min; LRMS (m/z) 203 (M^+, 100%), 136 (M^+-$C_3H_3N_2$, 34%), 120 (M^+-$C_3H_3N_2O$, 4%), 89 (M^+-$C_3H_3N_3O_2$, 41%), 78 (M^+-$C_4H_5N_3O_2$, 61%).

273 2-Methoxybenzyl bromide

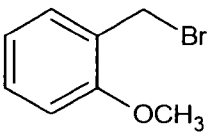

2-Methoxybenzyl Alcohol (5.013g, 36.2mmol) was dissolved in anhydrous diethyl ether (DEE, 150ml) and was left to stir for 5mins. Phosphorus tri-bromide (Pbr_3 10.061g, 37.1mmol) was then added very slowly and the reaction was further left to stir for four days. After stirring, the DEE was removed under vacuum to leave a white coloured solution. This was dissolved in Dichloromethane (DCM, 50ml), neutralised using sodium bicarbonate ($NaHCO_3$, 2 x 40ml) and washed with water (2 x 50ml). The resulting solution was then dried over magnesium sulphate ($MgSO_4$), where it was then filtered under suction and the DEE was removed under vacuum to give **273** (6.27g, yield 86.17%) as a yellow oil; R_f=0.74 [30/70 diethyl ether/petroleum spirit].

$\nu_{(max)}$(Film)cm^{-1}: 3002.7 (Ar, C-H), 1600.5 (Ar, C=C); δ_H (400MHz, $(CD_3)_2CO$): 7.48 (1H, m,Ph-H); 7.42 (1H, m, Ph-H); 7.10 (1H, d, *J*=8.33Hz,Ph-H); 7.02 (1H, m, Ph-H); 4.72 (2H, s, CH_2); 3.98 (3H, s, CH_3).δ_c(100MHz, $(CD_3)_2CO$): 157.73 (Ar, **C**-OCH_3), 131.0, 130.41, 126.23, 120.60, 111.18 (Ar, **C**), 55.19 (**C**H_2), 28.99 (**C**H_3): GC tR=10.09 min; LRMS (m/z) 200 (M^+, 2%), 185 (M^+-CH_3, 1%), 121 (M^+-Br, 75%), 106 (M^+-CH_3Br, 4%), 91 (M^+- C_2H_3Br, 100%), 78 (M^+- C_2H_3Br, 43%).

274 3-Methoxybenzyl bromide

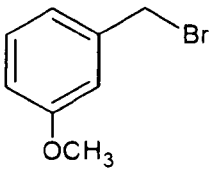

Compound **274** was synthesised in a similar manner to **273** with the exception that 3-methoxybenzyl alcohol (5.03g, 36.4mmol) and PBr_3 (9.81g, 36.2mmol) were used to give **274** (6.34g, yield 86.64%) as a yellow oil; R_f=0.71 [30/70 diethyl ether/petroleum spirit].

$\nu_{(max)}$(Film)cm^{-1}: 3002.5 (Ar, C-H), 1600.5 (Ar, C=C); δ_H (400MHz, $(CD_3)_2CO$): 7.37(1H, t,*J*=8.24Hz,Ph-H); 7.12 (2H, m, Ph-H); 6.98 (1H, m,Ph-H); 4.70 (2H, s, CH_2); 3.90 (3H, s, CH_3).δ_c(100MHz, $(CD_3)_2CO$): 159.98 (Ar, **C**-OCH_3), 139.77, 129.80, 121.39, 114.66, 113.98 (Ar, **C**), 54.76 (**C**H_2), 33.54 (**C**H_3): GC tR=10.43 min; LRMS (m/z) 200 (M^+, 10%), 185 (M^+-CH_3, 1%), 121 (M^+-Br, 100%), 106 (M^+-CH_3Br, 5%), 91 (M^+- C_2H_3Br, 34%), 78 (M^+- C_2H_3Br, 52%).

275 4-Methoxybenzyl bromide

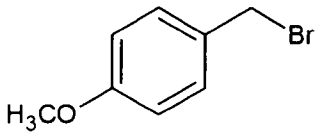

Compound **275** was synthesised in a similar manner to **273** with the exception that 4-methoxybenzyl alcohol (5.01g, 36.3mmol) and PBr_3 (10.02g, 37.0mmol) were used to give **275** (6.22g, yield 85.2%) as a yellow oil; R_f=0.71 [30/70 diethyl ether/petroleum spirit].

$\nu_{(max)}$(Film)cm^{-1}: 3002.6 (Ar, C-H), 1600.5 (Ar, C=C); δ_H (400MHz, $(CD_3)_2CO$): 7.49 (1H, d,*J*=8.79Hz,Ph-H); 7.01 (1H, d,*J*=8.79Hz,Ph-H); 4.73 (2H, s, CH_2); 3.90 (3H, s, CH_3).δ_c(100MHz, $(CD_3)_2CO$): 159.93 (Ar, **C**-OCH_3), 130.69, 130.37, 114.12 (Ar, **C**), 54.81 (**C**H_2), 34.11 (**C**H_3): GC tR=10.09 min; LRMS (m/z) 200 (M^+, 2%), 185 (M^+-CH_3, 1%), 121 (M^+-Br, 100%), 106 (M^+-CH_3Br, 4%), 91 (M^+- C_2H_3Br, 100%), 78 (M^+- C_2H_3Br, 9%).

276 1-(2-methoxybenzyl)-1H-imidazole

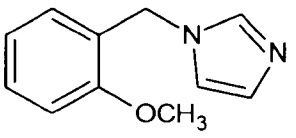

Compound **276** was synthesised in a similar manner to **249** with the exception that imidazole (1.01g, 14.8mmol), anhydrous K_2CO_3 (1.02g, 7.38mmol) 2-methoxybenzyl bromide (1.03g, 5.15mmol) were used. The crude product was recrystallised using a 50:50 solution of water and methylated spirit to give **276** (0.82g, yield 84%) as a yellow oil; R_f=0.43 [90/10 diethyl ether/methanol].

$\nu_{(max)}$(Film)cm^{-1}: 3112.4 (Ar, C-H), 2941.3 (C-H), 1602.5 (Ar, C=C); δ_H (400MHz, $CDCl_3$): 7.49 (1H, s, NC<u>H</u>N Imidazole); 7.27 (1H, m, Ph-<u>H</u>); 7.02 (1H, s, NC<u>H</u> Imidazole); 6.93 (1H, d, *J*=7.32Hz, Ph-<u>H</u>); 6.89 (1H, s, NC<u>H</u> Imidazole); 6.78 (2H, m, Ph-<u>H</u>); 5.12 (2H, s, C<u>H</u>$_2$); 3.80 (3H, s, OC<u>H</u>$_3$). δ_C (100MHz, $CDCl_3$):157.01 (Ar, **C**-OCH_3), 137.75 (N**C**HN), 129.85, 129.24 (Ar, **C**), 129.05 (N**C**H), 124.86, 120.75 (Ar, **C**), 119.52 (N**C**H), 110.55 (Ar, **C**), 55.62 (O**C**H_3)48.40 (**C**H_2): GC tR=14.96 min; LRMS (m/z) 188 (M^+, 52%), 121 (M^+-$C_3H_3N_2$, 100%), 91 (M^+-$C_5H_8N_2$, 90%), 77 (M^+-$C_5H_8N_2O$, 10%).

277 1-(3-methoxybenzyl)-1H-imidazole

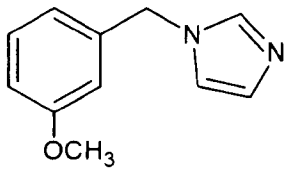

Compound **277** was synthesised in a similar manner to **249** with the exception that imidazole (1.0g, 15.8mmol), anhydrous K_2CO_3 (1.02g, 7.38mmol) 3-methoxybenzyl bromide (1.01g, 5.05mmol) were used. The crude product was recrystallised using a 50:50 solution of water and methylated spirit to give **277** (0.79g, yield 83%) as a yellow oil; R_f=0.41 [90/10 diethyl ether/methanol].

$\nu_{(max)}$(Film)cm^{-1}: 3111.8 (Ar, C-H), 1602.2 (Ar, C=C); δ_H (400MHz, $CDCl_3$): 7.53 (1H, s, NC<u>H</u>N Imidazole); 7.21 (1H, t, *J*=8.24Hz, Ph-<u>H</u>); 7.09 (1H, s, Ph-<u>H</u>); 6.82 (1H, s, NC<u>H</u> Imidazole); 6.79 (1H, m, Ph-<u>H</u>); 6.69 (1H, t, *J*=8.24Hz, Ph-<u>H</u>); 6.61 (1H, s, NC<u>H</u> Imidazole); 5.04 (2H, s, C<u>H</u>$_2$); 3.72 (3H, s, OC<u>H</u>$_3$). δ_C (100MHz, $CDCl_3$):159.06 (Ar, **C**-OCH_3), 137.72 (Ar, **C**),137.44 (N**C**HN), 130.11 (Ar, **C**), 129.63, 119.32 (N**C**H), 114.86,113.75, 113.05 (Ar, **C**), 55.24 (O**C**H_3)49.46 (**C**H_2):GC tR=15.20 min; LRMS (m/z) 188 (M^+, 54%), 173 (M^+-CH_3, 1%), 121 (M^+-$C_3H_3N_2$, 100%), 106 (M^+-$C_4H_6N_2$, 3%), 91 (M^+-$C_5H_8N_2$, 26%), 78 (M^+-$C_5H_8N_2O$, 16%).

278 1-(4-methoxybenzyl)-1H-imidazole

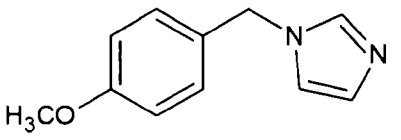

Compound **278** was synthesised in a similar manner to **249** with the exception that imidazole (1.01g, 14.9mmol), anhydrous K_2CO_3 (1.01g, 7.33mmol) 4-methoxybenzyl bromide (1.02g, 5.09mmol) were used. The crude product was recrystallised using a 50:50 solution of water and methylated spirit to give **278** (0.62g, yield 65%) as a yellow oil; R_f=0.39 [90/10 diethyl ether/methanol].

$\nu_{(max)}$(Film)cm^{-1}: 3111.8 (Ar, C-H), 2935.3 (C-H), 1611.5 (Ar, C=C); δ_H(400MHz, $CDCl_3$): 7.44 (1H, s, NC<u>H</u>N Imidazole); 7.18 (2H, d, *J*=8.79Hz, Ph-<u>H</u>); 7.03 (1H, s, NC<u>H</u> Imidazole); 6.78 (2H, d, *J*=8.79Hz, Ph-<u>H</u>); 6.71 (1H, s, NC<u>H</u> Imidazole); 5.12 (2H, s, *C<u>H</u>*$_2$) 3.68 (3H, s, OC<u>H</u>$_3$). δ_C (100MHz, $CDCl_3$):159.23 (Ar, **C**-*OCH*$_3$), *137.34 (**NC**HN)*, 129.79, 129.12 (Ar, **C**), 128.16, 119.14 (**NC**H), 114.77 (Ar, **C**), 55.38 (O**C**H$_3$)49.88 (**C**H$_2$):GC tR=15.59 min; LRMS (m/z) 188 (*M*$^+$, 11%), 173 (*M*$^+$-CH_3, 1%), 121 (*M*$^+$-$C_3H_3N_2$, 100%), 106 (*M*$^+$-$C_4H_6N_2$, 1%), 91 (*M*$^+$-$C_5H_8N_2$, 6%), 78 (*M*$^+$-$C_5H_8N_2O$, 13%).

279 2-Imidazol-1-yl-1-phenyl-ethanone.

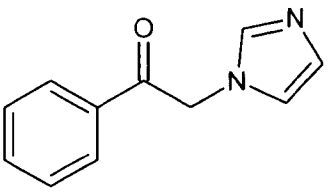

2-Bromoacetophenone (2.0g, 10.04mmol) was added to a mixture of anhydrous potassium carbonate (K_2CO_3) (2.1g, 15.19mmol) and imidazole (2.1g, 30.84mmol) in anhydrous tetrahydrofuran (THF, 175mL) and left to stir for 72h. After stirring, the THF was removed under vacuum to leave red coloured oil. The oil was dissolved in dichloromethane (DCM, 50ml) and washed with water (50mL). The product was then extracted into aqueous hydrochloric acid (1M, 4x50mL) and neutralised using saturated sodium bicarbonate solution ($NaHCO_3$, 300mL). The resulting solution was then extracted into DCM (4x50mL) and dried over anhydrous magnesium sulfate ($MgSO_4$), filtered and the DCM removed under vacuum. The compound was re-crystallised using 50% aqueous ethanol to give **279** as a yellow coloured solid (1.29g, yield 69.35%); [m.p.=119.5-120.4°C]; R_f=0.42 [(90/10) diethyl ether/methanol].

$\nu_{(max)}$(Film)cm^{-1}: 3151.6 (Ar, C-H), 1693.4 (C=O), 1595.8 (Ar, C=C); δ_H (400MHz, $CDCl_3$): 7.95 (2H, m, Ph-H); 7.64 (1H, m, Ph-H); 7.51 (2H, m, Ph-H); 7.49 (1H, s, NC**H**N); 7.12 (1H, s, NCH); 6.92 (1H, s, NCH); 5.38 (2H, s, CH_2). δ_c(100MHz, $CDCl_3$): 191.67 (**C**=O), 138.90 (N**C**HN), 134.49 (NCH), 134.27 (Ar, **C**), 129.79 (N**C**H), 129.22, 128.06, 120.37 (Ar, **C**), 52.54 (**C**H_3): GC tR=17.2 min; LRMS (m/z) 186 (M^+, 19%) 105 (M^+-$C_4H_5N_2$, 100%) 77 (M^+-$C_5H_5N_2O$, 49%).

280 1-(2-Fluoro-phenyl)-2-imidazol-1-yl-ethanone

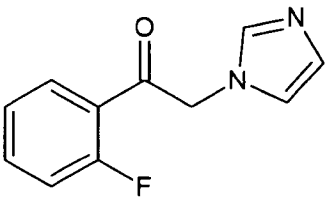

Compound **280** was synthesised in a similar manner to **279** with the exception that imidazole (1.0g, 14.68mmol), anhydrous K_2CO_3 (1.0g, 7.23mmol) and 2-bromo-2-fluoroacetophenone (1.0g, 4.60mmol) were used. The crude product was recrystallised using 50% aqueous ethanol to give **280** as a yellow coloured solid; (0.58g, yield 61%); [m.p.=119.1-119.8°C]; R_f=0.53 [(95/5) diethyl ether/methanol].

$\nu_{(max)}$(Film)cm^{-1}: 3141.9 (Ar, C-H), 1701.1 (C=O), 1609.8 (Ar, C=C); δ_H (400MHz, $CDCl_3$): 7.95 (1H, m, Ph-H); 7.61 (1H, m, Ph-H); 7.47 (1H, s, NC**H**N); 7.28 (1H, m, Ph-H); 7.20 (1H, m, Ph-H); 7.10, s, (NCH); 6.91 (1H, s, NCH); 5.31 (2H, s, CH_2); δ_c(100MHz, $CDCl_3$): 192.15 (**C**=O); 163.37, 160.84 (Ar, **C**-F); 138.89 (N**C**HN); 136.65, 130.92 (Ar, **C**), 128.39 (N**C**H), 125.65, 123.42 (Ar, **C**), 121.44 (N**C**H), 117.67 (Ar, **C**), 56.16 (**C**H_2); GC tR=16.3min; LRMS (m/z) 204 (M^+, 19%), 123 (M^+-$C_4H_5N_2$, 100%) 95 (M^+-$C_5H_5N_2O$, 26%) 75 (M^+-$C_4H_5FN_2$, 13%). HRMS (EI): *m/z* calcd for $C_{11}H_9FN_2O$: 204.200; found: 204.0702.

281 1-(3-Fluoro-phenyl)-2-imidazol-1-yl-ethanone

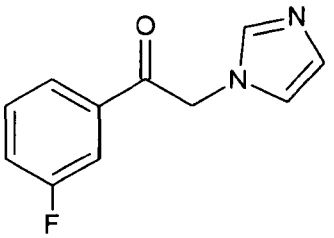

Compound **281** was synthesised in a similar manner to **279** with the exception that imidazole (2.0g, 29.3mmol), anhydrous K_2CO_3 (2.0g, 14.4mmol) and 2-bromo-3-fluoroacetophenone (2.0g, 9.21mmol) were used. The crude product was recrystallised using 50% aqueous ethanol to give **281** as a yellow solid; (1.59g, yield 85%); [m.p.=112.1-113.9°C]; R_f=0.25 [(90/10) diethyl ether/methanol].

$\nu_{(max)}$(Film)cm^{-1}: 3151.3 (Ar, C-H), 1699.3 (C=O), 1591.3 (Ar, C=C); δ_H (400MHz, DMSO): 8.01 (1H, m, Ph-H); 7.95 (1H, m, Ph-H); 7.78 (1H, m, Ph-H); 7.72 (1H, m, Ph-H); 7.70 (1H, s, NCHN); 7.24(1H, s, NCH); 7.04 (1H, s, NCH); 5.86 (2H, s, CH_2); δ_c(100MHz, DMSO): 193.35 (**C**=O); 163.9, 161.5 (Ar, **C**-F); 138.86 (N**C**HN); 137.24, 131.81 (Ar, **C**), 128.51 (N**C**H), 124.80 (Ar, **C**), 121.43 (Ar-**C**), 121.27 (N**C**H), 115.23 (Ar, **C**), 53.34 (**C**H_2); GC tR=16.86min; LRMS (m/z) 204 (M^+, 32%), 123 (M^+-$C_4H_5N_2$, 100%), 95 (M^+-$C_5H_5N_2O$, 44%) 75 (M^+-$C_4H_5N_2F$, 9%): HRMS (EI): *m/z* calcd for $C_{11}H_9FN_2O$: 204.200; found: 204.0691. Elemental analysis: found C 64.60%, H 4.45% and N 13.78% $C_{11}H_9FN_2O$ requires C 64.54%, H 4.43%, N 13.69%.

282 1-(4-Fluoro-phenyl)-2-imidazol-1-yl-ethanone

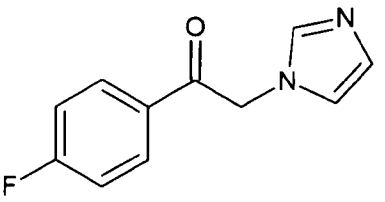

Compound **282** was synthesised in a similar manner to **279** with the exception that imidazole (2.0g, 29.3mmol), anhydrous K_2CO_3 (2.0g, *14.4mmol) and 2-bromo-3-*fluoroacetophenone (2.0g, 9.21mmol) were used. The crude product was recrystallised using 50% aqueous ethanol to give **282** as a light brown solid; (1.63g, yield 87%); [m.p.=149.9-150.6°C]; R_f=0.4 [(90/10) diethyl ether/methanol].

$\nu_{(max)}$(Film)cm^{-1}: 3152.6 (Ar, C-H), 1697.9 (C=O), 1598.1 (Ar, C=C); δ_H (400MHz, $CDCl_3$): 7.98 (2H, dd, J=8.79Hz, Ph-H); 7.48 (1H, s, NCHN); 7.18 (2H, t, J=8.60Hz, Ph-H); 7.11 (1H, s, NCH); 6.91 (1H, s, NCH); 5.35 (2H, s, CH_2); δ_c(100MHz, $CDCl_3$): 190.17 (**C**=O); 167.76, 165.21 (Ar, **C**-F); 138.21 (N**C**HN); 130.88, 130.69 (Ar, **C**), 129.80 (N**C**H), 120.33 (N**C**H), 116.61 (Ar, **C**), 52.42 (**C**H_2); GC tR=16.77min; LRMS (m/z) 204 (M^+, 17%), 123 (M^+-$C_4H_5N_2$, 100%) 95 (M^+-$C_5H_5N_2O$, 39%) 75 (M^+-$C_4H_5N_2F$, 12%): HRMS (EI): *m/z* calcd for $C_{11}H_9FN_2O$: 204.200; found: 204.0702. Elemental analysis: found C 64.53%, H 4.46% and N 13.81% $C_{11}H_9FN_2O$ requires C 64.54%, H 4.43%, N 13.69%.

283 1-(2-Chloro-phenyl)-2-imidazol-1-yl-ethanone

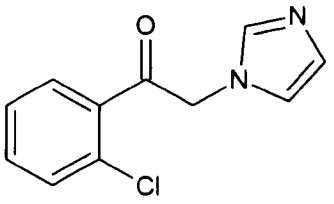

Compound **283** was synthesised in a similar manner to **279** with the exception that imidazole (0.88g, 12.9mmol), anhydrous K_2CO_3 (0.88g, 6.36mmol) and 2-bromo-2-chloroacetophenone (1.0g, 4.28mmol) were used. The crude product was purified by flash chromatography [90:10 diethyl ether/methanol] to give **283** (0.72g, crude yield 90%) as a brown oil; R_f=0.52 [90/10 diethyl ether/methanol].

GC tR=17.72min; LRMS (m/z) 220 (M^+, 15.73%), 139 (M^+-$C_4H_5N_2$, 100%), 111 (M^+-$C_5H_5N_2O$, 30.33%), 75 (M^+-$C_5H_5N_2OCl$, 11.23%).

284 1-(3-Chloro-phenyl)-2-imidazol-1-yl-ethanone

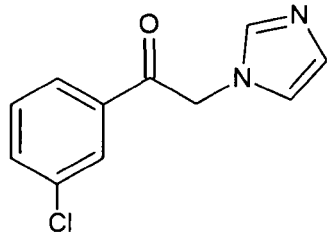

Compound **284** was synthesised in a similar manner to **279** with the exception that imidazole (1.77g, 25.9mmol), anhydrous K_2CO_3 (1.77g, 12.8mmol) and 2-bromo-3-chloroacetophenone (2.0g, 8.56mmol) were used to give **284** as a light yellow solid; (0.82g, yield 43%); [m.p.=108-108.8°C]; R_f=0.39 [(90/10) diethyl ether/methanol].

$\nu_{(max)}$(Film)cm^{-1}: 3153.0 (Ar, C-H), 1697.7 (C=O), 1591.0 (Ar, C=C); δ_H (400MHz, $(CD_3)_2CO$): 8.12 (2H, m, Ph-H); 7.81 (1H, m, Ph-H); 7.70 (1H, t, *J*=7.69, Ph-H), 7.64 (1H, s, NCHN Imidazole); 7.18 (1H, s, NCH Imidazole); 7.04 (1H, s, NCH Imidazole); 5.88 (2H, s, CH_2); δ_c(100MHz, $(CD_3)_2CO$): 192.12 (**C**=O); 138.84 (N**C**HN); 136.79 (Ar, **C**); 134.58 (Ar, **C**-Cl); 133.54, 130.80 (Ar, **C**); 128.55 (N**C**H); 127.83, 126.53 (Ar, **C**); 120.59 (N**C**H); 52.62 (**C**H_2); GC tR=18.91min; LRMS (m/z) 220 (M^+, 21%), 139 (M^+-$C_4H_5N_2$, 100%),111 (M^+-$C_5H_5N_2O$, 41%), 75 (M^+-$C_5H_5N_2OCl$, 17%): HRMS (EI): *m/z* calcd for $C_{11}H_9ClN_2O$: 220.0403; found: 220.0407.

285 1-(4-Chloro-phenyl)-2-imidazol-1-yl-ethanone

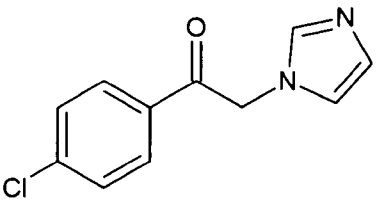

Compound **285** was synthesised in a similar manner to **279** with the exception that imidazole (1.77g, 25.9mmol), anhydrous K_2CO_3 (1.77g, 12.8mmol) and 2-bromo-4-chloroacetophenone (2.0g, 8.56mmol) were used to give **285** as a light yellow solid; (1.24g, yield 65%); [m.p.=161.7-162.5°C]; R_f=0.34 [(90/10) diethyl ether/methanol].

$\nu_{(max)}$(Film)cm^{-1}: 3108.6 (Ar, C-H), 1692.9 (C=O), 1590.3 (Ar, C=C); δ_H (400MHz, $(CD_3)_2CO$): 8.00 (2H, d, J=8.79Hz, Ph-H); 7.53 (2H, d, J=8.79Hz, Ph-H); 7.46 (1H, s, NCHN); 6.99 (1H, s, NCH); 6.85 (1H, s, NCH); 5.66 (2H, s, CH_2); δ_c(100MHz, $(CD_3)_2CO$): 192.06 (**C**=O); 139.48 (Ar, **C**); 138.38 (N**C**HN); 133.64 (Ar, **C-Cl**), 129.82, 129.14 (Ar, **C**); 128.53, 120.59 (N**C**H); 52.49 (**C**H_2); GC tR=18.81min; LRMS (m/z) 220 (M^+, 11%), 139 (M^+-$C_4H_5N_2$, 100%),111 (M^+-$C_5H_5N_2O$, 39%), 75 (M^+-$C_5H_5N_2OCl$, 18%); HRMS (EI): *m/z* calcd for $C_{11}H_9ClN_2O$: 220.0403; found: 220.0386.

286 1-(3, 4-dichloro-phenyl)-2-imidazol-1-yl-propan-1-one

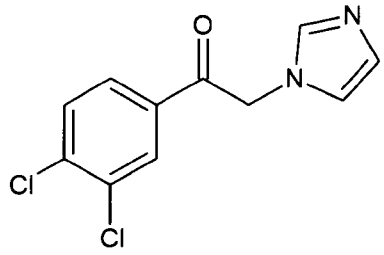

Compound **286** was synthesised in a similar manner to **279** with the exception that Imidazole (1.55g, 22.7mmol), potassium carbonateK_2CO_3 (1.55g, 11.2mmol) and 3, 4-dichloracetophenone (2.0g, 7.46mmol) were used. Removal of DCM under vacuum gave **286** (1.30g, yield 68%) as a yellow solid; [m.p.=123.3-124.1°C]; R_f=0.28 [90/10 diethyl ether/methanol].

$\nu_{(max)}$(Film)cm^{-1}: 3113.4 (Ar, C-H), 1701.6 (C=O), 1584.6 (Ar, C=C); δ_H (400MHz, $CDCl_3$): 8.02 (1H, s, Ph-H); 7.75 (1H, dd, *J*=2.01, 8.24Hz, Ph-H); 7.59 (1H, d, *J*=8.42Hz, Ph-H); 7.47 (1H, s, NCHN Imidazole); 7.11, 6.90 (2H, s, NCH Imidazole); 5.34 (2H, s, CH_2); δ_c(100MHz, $CDCl_3$): 189.83 (**C**=O); 139.29, (Ar-**C**) 138.15 (N**C**HN); 134.08, 133.66 (**C**-Cl); 131.38 (N**C**H); 130.06, 129.91 (Ar, **C**); 126.97 (N**C**H); 120.28 (Ar, **C**); 52.52 (**C**H_2); GC tR=20.44min; LRMS (m/z) 254 (M^+, 16%); 173 (M^+-$C_4H_5N_2$ 100%); 145 (M^+-$C_5H_5N_2O$ 39%); 109 (M^+-$C_5H_5ClN_2O$ 20%); 75 (M^+-$C_5H_5Cl_2N_2O$ 15%). HRMS (EI): *m/z* calcd for $C_{11}H_8Cl_2N_2O$: 255.0997; found: 253.9998 and 256.0037.

287 1-(2-Bromo-phenyl)-2-imidazol-1-yl-ethanone

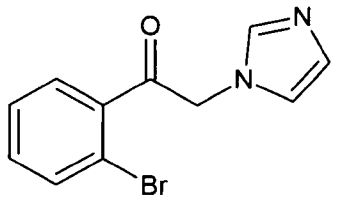

Compound **287** was synthesised in a similar manner to **279** with the exception that imidazole (1.5g, 21.5mmol), anhydrous K_2CO_3 (1.5g, 10.7mmol) and 2,2 dibromoacetophenone (2.0g, 7.19mmol) were used. The crude product was recrystallised using 50% aqueous ethanol to give **287** as a yellow solid; (1.62g, yield 85%); [m.p.=91.9-92.7°C; R_f=0.56 [(90/10) diethyl ether/methanol].

$\nu_{(max)}$(Film)cm^{-1}: 3114.4 (Ar, C-H), 1712.8 (C=O), 1585.5 (Ar, C=C); δ_H (400MHz, $(CD_3)_2CO$): 7.84 (2H, m, Ph-H); 7.67 (1H, s, NCHN Imidazole); 7.63 (1H, m, Ph-H); 7.57 (1H, m, Ph-H); 7.20 (1H, s, NCH Imidazole); 7.03 (1H, s, NCH Imidazole); 5.26 (2H, s, CH_2); δ_c(100MHz, $(CD_3)_2CO$): 196.53 (**C**=O); 138.74 (Ar, **C**); 138.24 (N**C**HN); 133.93, 132.73 (Ar, **C**); 129.11, 128.72 (N**C**H); 127.90, 120.31 (Ar, **C**); 118.65 (Ar, **C**-Br); 54.75 (**C**H_2); GC tR=18.49min; LRMS (m/z) 266 (M^+, 0.88%), 185 (M^+-$C_4H_5N_2$, 100%), 155 (M^+-$C_5H_5N_2O$, 24%), 76 (M^+-$C_5H_5N_2OBr$, 18%). HRMS (EI): *m/z* calcd for $C_{11}H_9BrN_2O$: 263.9897; found: 263.9895$^{(79)}$ and 265.9862$^{(81)}$.

288 1-(3-Bromo-phenyl)-2-imidazol-1-yl-ethanone

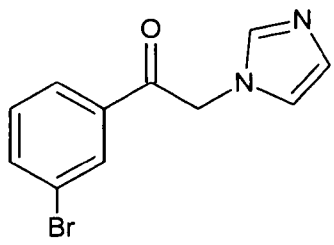

Compound **288** was synthesised in a similar manner to **279** with the exception that imidazole (1.5g, 22.0mmol), anhydrous K_2CO_3 (1.5g, 12.8mmol) and 2,3 dibromoacetophenone (2.0g, 7.19mmol) were used to give **288** (1.25g, yield 65%) as a yellow solid; [m.p.=118.2-119.4°C];R_f=0.56 [90/10 diethyl ether/methanol].

$\nu_{(max)}$(Film)cm^{-1}: 3151.5 (Ar, C-H), 1698.5 (C=O), 1586.7 (Ar, C=C); δ_H (400MHz, DMSO): 7.81 (1H, s, NC<u>H</u>N Imidazole); 7.65 (1H, d, *J*=7.69, Ph-<u>H</u>); 7.55 (1H, m, Ph-<u>H</u>); 7.20 (2H, m, Ph-<u>H</u>); 6.73 (1H, s, NC<u>H</u> Imidazole); 6.55 (NC<u>H</u> Imidazole); 5.37 (2H, s, C<u>H</u>$_2$); δ_c(100MHz, DMSO): 193.33 (**C**=O); 138.84 (N**C**HN); 137.11, 137.02, 131.74, 131.13 (Ar, **C**); 128.50, 127.52 (N**C**H); 122.81 (Ar, **C-Br**); 121.43 (Ar, **C**); 53.26 (**C**H_2); GC tR=15.19min; LRMS (m/z) 264 (M^+, 12%), 183 (M^+-$C_4H_5N_2$, 100%),155 (M^+-$C_5H_5N_2O$, 34%), 76 (M^+-$C_5H_5N_2OBr$, 26%). HRMS (EI): *m/z* calcd for $C_{11}H_9BrN_2O$: 263.9897; found: 263.9898$^{(79)}$ and 265.9928$^{(81)}$.

289 1-(4-Bromo-phenyl)-2-imidazol-1-yl-ethanone

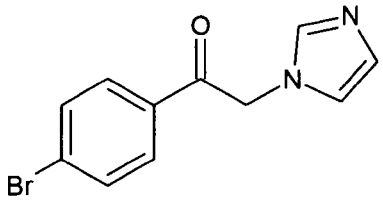

Compound **289** was synthesised in a similar manner to **279** with the exception that imidazole (1.5g, 22.0mmol), anhydrous K_2CO_3 (1.5g, 10.8mmol) and 2,4-dibromoacetophenone (2.0g, 7.19mmol) were used. The crude product was recrystallised using 50% aqueous ethanol to give **289** (1.20g, yield 63%) as a yellow solid; [m.p.=163.9-164.7°C]; R_f=0.27 [90/10 diethyl ether/methanol].

$\nu_{(max)}$(Film)cm^{-1}: 3135.3 (Ar, C-H), 1695.1 (C=O), 1586.8 (Ar, C=C); δ_H (400MHz, $CDCl_3$): 7.89 (2H, d, *J*=8.42Hz, Ph-H); 7.68 (2H, d, *J*=8.42Hz, Ph-H); 7.56 (1H, s, NCHN Imidazole); 7.09 (1H, s, NCH Imidazole); 6.90 (1H, s, NCH Imidazole); 5.71 (2H, s, CH_2); δ_c(100MHz, $CDCl_3$): 193.55 (**C**=O); 138.87 (N**C**HN); 134.08, 132.58, 130.53 (Ar, **C**); 128.58 (Ar, **C**-Br); 128.48, 121.44 (N**C**H); 52.47 (**C**H_2); GC tR=20.07min; LRMS (m/z) 264 (M^+, 18%), 183 (M^+-$C_4H_5N_2$, 100%),155 (M^+-$C_5H_5N_2O$, 28%), 76 (M^+-$C_5H_5BrN_2O$, 21%); HRMS (EI): *m/z* calcd for $C_{11}H_9BrN_2O$: 263.9897; found: 263.9898$^{(79)}$ and 265.9865$^{(81)}$. Elemental analysis: found C 49.80%, H 3.46% and N 10.48% $C_{11}H_9BrN_2O$ requires C 49.84%, H 3.42%, N 10.57%.

290 1-(4-Iodo-phenyl)-2-imidazol-1-yl-ethanone

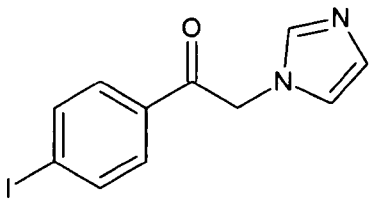

Compound **290** was synthesised in a similar manner to **279** with the exception that Imidazole (0.65g, 9.2mmol), anhydrous K_2CO_3 (0.65g, 4.6mmol) and 4-iodophenacyl bromide (1.0g, 3.06mmol) were used. Removal of DCM under vacuum gave **290** (0.44g, yield 46%) as a yellow solid; [m.p.=247.6-248.7°C];R_f=0.38 [80/20 diethyl ether/methanol].

$\nu_{(max)}$(Film)cm^{-1}: 3134.2 (Ar, C-H), 1696.2 (C=O), 1585.3 (Ar, C=C); δ_H (400MHz, DMSO): 7.98 (2H, d, *J*=8.42Hz, Ph-H); 7.76 (2H, d, *J*=8.42Hz, Ph-H); 7.55 (1H, s, NCHN Imidazole); 7.08, 6.89 (2H, s, NCH Imidazole); 5.68 (2H, s, CH_2); δ_c(100MHz, DMSO): 193.87 (**C**=O); 138.87 (N**C**HN); 138.43, 134.33, 130.17 (Ar, **C**); 128.46, 121.44 (N**C**H); 103.25 (Ar, **C**-I); 51.75 (**C**H_2); GC tR=21.22min; LRMS (m/z) 312 (M^+, 20%); 231 (M^+-$C_4H_5N_2$, 100%); 203 (M^+-$C_5H_5N_2O$, 25%); 76 (M^+-$C_5H_5N_2OI$, 34%). HRMS (EI): *m/z* calcd for $C_{11}H_9IN_2O$: 311.9759; found: 263.976.

291 2-imidazol-1-yl-(2-nitro-phenyl)-ethanone

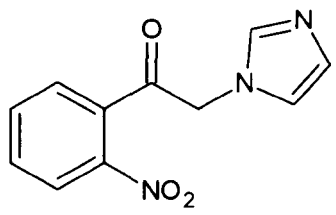

Compound **291** was synthesised in a similar manner to **279** with the exception that imidazole (1.80g, 26.4mmol), anhydrous K_2CO_3 (1.80g, 13.0mmol) and 2-bromo-2-nitroacetophenone (2.0g, 8.19mmol) were used. The crude product was recrystallised using 50% aqueous ethanol to give **291** (0.91g, yield 48%) as a purple solid; [m.p.=145.7-146.3°C]; R_f=0.16 [90/10 diethyl ether/methanol].

$\nu_{(max)}$(Film)cm^{-1}: 3119.8 (Ar, C-H), 1727.1 (C=O), 1570.9 (Ar, C=C); δ_H (400 MHz, $CDCl_3$): 8.18 (1H, d, *J*=8.24Hz, Ph-H); 7.75 (1H, t, *J*=7.51Hz, Ph-H); 7.65 (1H, t, *J*=7.87Hz, Ph-H), 7.45 (1H, s, NCHN Imidazole); 7.34 (1H, d, *J*= 8.24Hz, Ph-H); 7.03, 6.93 (1H, s, NCH Imidazole); 5.07 (2H, s, CH_2); δ_c(100MHz, $CDCl_3$): 196.10 (**C**=O); 145.36 (Ar, **C**-NO_2), 138.15 (N**C**HN), 135.15, 134.93, 131.60 (Ar, **C**) 130.11 (N**C**H), 127.57, 124.85 (Ar, **C**), 120.07 (N**C**H), 52.97 (**C**H_2); GC tR=19.07min; LRMS (m/z) 231 (M^+, 9%), 185 (M^+-NO_2, 3%), 150 (M^+-$C_4H_5N_2$, 9%), 134 (M^+-$C_4H_5N_2O$, 24%), 121 (M^+-$C_5H_5N_2O$, 3%), 104 (M^+-$C_4H_5N_3O_2$, 20%) 81 (M^+-$C_7H_4NO_3$, 100%). HRMS (EI): *m/z* calcd for $C_{10}H_9N_2NO_2$: 231.0643; found: 231.0641.

292 2-imidazol-1-yl-(3-nitro-phenyl)-ethanone

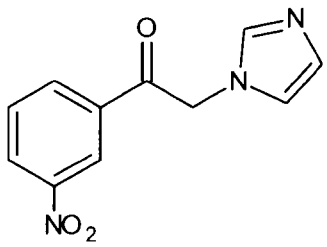

Compound **292** was synthesised in a similar manner to **279** with the exception that imidazole (1.8g, 26.4mmol), anhydrous K_2CO_3 (1.8g, 13.0mmol) and 2-bromo-3-nitroacetophenone (2.0g, 8.19mmol) were used. The crude product was recrystallised using 50% aqueous ethanol to give **292** (1.42g, yield 75.0%) as a purple solid; [m.p.=102.1-103.4°C]; R_f=0.42 [90/10 diethyl ether/methanol].

$\nu_{(max)}$(Film)cm^{-1}: 3112.9 (Ar, C-H), 1710.0 (C=O), 1612.7 (Ar, C=C); δ_H (400MHz, $CDCl_3$): 8.76 (1H, t, *J*=1.83Hz, Ph-H); 8.49 (1H, m, Ph-H); 8.29 (1H, m, Ph-H); 7.75 (1H, t, *J*=8.06Hz , Ph-H); 7.51 (1H, s, NCHN Imidazole); 7.12, 6.94 (1H, s, NCH Imidazole); 5.87 (2H, s, CH_2); δ_c(100MHz, $CDCl_3$): 190.05 (**C**=O); 148.64 (Ar, **C**-NO_2); 138.16 (**NC**HN); 135.38, 133.36 130.69 (Ar, **C**); 130.02 (**NC**H); 128.46, 122.92 (Ar, **C**); 120.29 (**NC**H); 53.17 (**C**H_2); GC tR=21.04min; LRMS (m/z) 231 (M^+, 41%); 150 (M^+-$C_4H_5N_2$, 100%); 134 (M^+-$C_4H_5N_2O$, 6%); 122 (M^+-$C_5H_5N_2O$, 2%); 104 (M^+-$C_5H_5N_2O_2$, 39%) 76 (M^+-$C_5H_5N_3O_3$, 36%). HRMS (EI): *m/z* calcd for $C_{10}H_9N_2NO_2$: 231.0643; found: 231.0633.

293 2-imidazol-1-yl-(4-nitro-phenyl)-ethanone

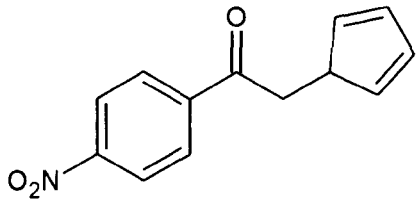

Compound **293** was synthesised in a similar manner to **279** with the exception that imidazole (1.8g, 26.4mmol), anhydrous K_2CO_3 (1.8g, 13.0mmol) and 2-bromo-4-nitroacetophenone (2.0g, 8.19mmol) were used to give **293** (0.89g, yield 47%) as a purple solid; [m.p.=167.8-168.6°C]; R_f=0.42 [90/10 diethyl ether/methanol].

$\nu_{(max)}$(Film)cm^{-1}: 3107.4 (Ar, C-H), 1712.2 (C=O), 1599.7 (Ar, C=C); δ_H (400MHz, $(CD_3)_2CO$): 8.32 (2H, d, *J*=8.97Hz, Ph-H); 8.17 (2H, d, *J*=8.97Hz, Ph-H); 7.56 (1H, s, NCHN Imidazole); 7.11, 6.95 (1H, s, NCH Imidazole); 5.88 (2H, s, CH_2); δ_c(100MHz, $(CD_3)_2CO$): 192.04(**C**=O); 150.88 (Ar, **C**-NO_2); 139.59 (Ar, **C**), 138.38 (N**C**HN), 129.43 (Ar, **C**) 128.64 (N**C**H), 123.98 (Ar, **C**), 120.57 (N**C**H), 52.97 (**C**H_2); GC tR=21.28min; LRMS (m/z) 231 (M^+, 49%), 150 (M^+-$C_4H_5N_2$, 100%), 134 (M^+-$C_4H_5N_2O$, 8%), 104 (M^+-$C_5H_5N_2O_2$ 42%), 81 (M^+-$C_7H_4NO_3$, 50%), 76 (M^+-$C_5H_5N_3O_3$ 30%). Elemental analysis: found C 56.98%, H 3.94% and N 18.05%. $C_{11}H_9N_3O_3$ requires C 57.14%, H 3.92%, N 18.17%. HRMS (EI): *m/z* calcd for $C_{10}H_9N_2NO_2$: 231.0643; found: 231.0648.

294 2-Imidazol-1-yl-1-(2-methoxy-phenyl)-ethanone

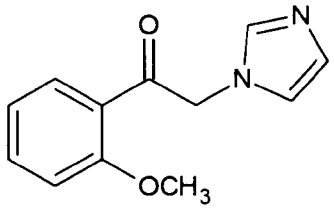

Compound **294** was synthesised in a similar manner to **279** with the exception that imidazole (1.8g, 26.4mmol), anhydrous K_2CO_3 (1.8g, 13.0mmol) and 2-bromo-2-methoxyacetophenone (2.0g, 8.73mmol) were used. The crude product was recrystallised using 50% aqueous ethanol to give **294** (1.42g, yield 75%) as a light yellow solid; [m.p.=69.9-71.3°C];R_f=0.34 [90/10 diethyl ether/methanol].

$\nu_{(max)}$(Film)cm^{-1}: 3131.6 (Ar, C-H), 1680.7 (C=O), 1598.5 (Ar, C=C); δ_H (400MHz, $CDCl_3$): 7.86 (1H, dd, *J*=7.69Hz, Ph-H); 7.54 (1H, m, Ph-H); 7.45 (1H, s, NCHN); 7.08 (1H, s, NCH Imidazole); 7.03 (2H, m, Ph-H); 6.89 (1H, s, NCH Imidazole); 5.30 (2H, s, CH_2), 3.97 (3H, s, CH_3); δ_c(100MHz, $CDCl_3$): 193.23(**C**=O); 159.42 (Ar, **C**-OCH_3); 138.30 (N**C**HN); 135.40, 131.35 (Ar, **C**); 129.37 (N**C**H); 124.58, 121.36 (Ar, **C**); 120.37 (N**C**H); 111.73 (Ar, **C**); 56.98 (**C**H_2); 55.77 (**C**H_3); GC t_R=18.81min; LRMS (m/z) 216 (M^+, 10%), 135 (M^+-$C_4H_5N_2$, 100%), 120 (M^+-$C_5H_8N_2$, 2%), 104 (M^+-$C_5H_8N_2O$, 1%), 92 (M^+-$C_6H_8N_2O$, 13%), 77 (M^+-$C_6H_8N_2O_2$, 25%). HRMS (EI): *m/z* calcd for $C_{12}H_{12}N_2O_2$: 216.0898; found: 216.0879

295 2-Imidazol-1-yl-1-(3-methoxy-phenyl)-ethanone

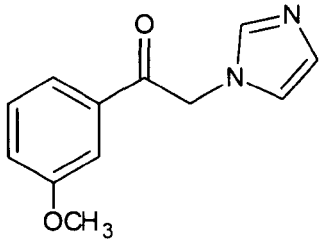

Compound **295** was synthesised in a similar manner to **279** with the exception that imidazole (1.8g, 26.4mmol), anhydrous K_2CO_3 (1.8g, 13.0mmol) and 2-bromo-3-methoxyacetophenone (2.0g, 8.73mmol) were used. The crude product was recrystallised using 50% aqueous ethanol to give **295** (1.58g, yield 84%) as a light yellow solid; [m.p.=113.5-114.2°C]; R_f=0.34 [80/20 diethyl ether/methanol]

$\nu_{(max)}$(Film)cm^{-1}: 3114.2 (Ar, C-H), 1697.9 (C=O), 1598.3 (Ar, C=C); δ_H (400MHz, $CDCl_3$): 7.50 (1H, m, Ph-H); 7.48 (1H, s, NCHN); 7.45 (1H, m, Ph-H); 7.40 (1H, t, *J*=8.06Hz Ph-H); 7.16 (1H, m, Ph-H); 7.11 (1H, s NCH Imidazole); 6.91 (1H, s NCH Imidazole); 5.35 (2H, s, CH_2); 3.83 (3H, s, CH_3); δ_c(100 MHz, $CDCl_3$): 191.57 (**C**=O); 160.23 (Ar, **C**-OCH_3); 138.24 (N**C**HN); 135.55, 130.18, 129.73(Ar, **C**); 120 (N**C**H); 120.38 (Ar, **C**); 112.49 (N**C**H); 55.64 (**C**H_3); 52.63 (**C**H_3); GC t_R=19.15min; LRMS (m/z) 216 (M^+, 21%), 135 (M^+-$C_4H_5N_2$, 100%), 107 (M^+-$C_5H_5N_2O$, 36%), 92 ($C_6H_8N_2O$, 19%), 77 ($C_6H_8N_2O_2$, 27%); HRMS (EI): *m/z* calcd for $C_{12}H_{12}N_2O_2$: 216.0898; found: 216.088; Elemental analysis: found C 66.60%, H 5.58% and N 12.87%. $C_{12}H_{12}N_2O_2$ requires C 66.65%, H 5.59%, N 12.95%.

296 2-Imidazol-1-yl-1-(4-methoxy-phenyl)-ethanone

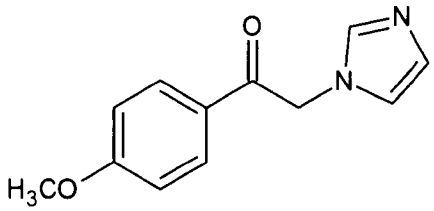

Compound **296** was synthesised in a similar manner to **279** with the exception that imidazole (1.8g, 26.4mmol), anhydrous K_2CO_3 (1.8g, 13.0mmol) and 2-bromo-4-methoxyacetophenone (2.0g, 8.73mmol) were used. The crude product was recrystallised using 50% aqueous ethanol to give **296** (1.37g, yield 72%) as a yellow solid; [m.p.=134.2-135.1°C]; R_f=0.45 [90/10 diethyl ether/methanol].

$\nu_{(max)}$(Film)cm^{-1}: 3133.3 (Ar, C-H), 1687.0 (C=O), 1601.9 (Ar, C=C); δ_H (400MHz, $CDCl_3$): 7.92 (2H, d, *J*=8.79Hz Ph-H); 7.49 (1H, s, NCHN); 7.10 (1H, s, NCH); 6.95 (2H, d, *J*=8.79Hz Ph-H), 6.91 (1H, s, NCH), 5.32 (2H, s, CH_2), 3.86 (3H, s, CH_3); δ_c(100MHz, $CDCl_3$): 190.08 (**C**=O); 164.51 (Ar, **C**-OCH_3); 138.24 (N**C**HN), 130.43 (Ar, **C**) 129.53 (N**C**H), 127.24 (Ar, **C**), 120.41 (N**C**H), 114.38 (Ar, **C**), 55.71 (**C**H_3); 52.23 (**C**H_2); GC tR=20.15min; LRMS (m/z) 216 (M^+, 8%), 135 (M^+- $C_4H_5N_2$, 100%),121 (M^+- $C_5H_8N_2$, 1%),107 (M^+-$C_5H_5N_2O$, 8%), 92 (M^+-$C_6H_8N_2O$, 12%), 77 ($C_6H_8N_2O_2$, 17%); HRMS (EI): *m/z* calcd for $C_{12}H_{12}N_2O_2$: 216.0898; found: 216.0893. Elemental analysis: found C 66.64%, H 5.69% and N 12.75%. $C_{12}H_{12}N_2O_2$ requires C 66.65%, H 5.59%, N 12.95%.

297 2-Imidazol-1-yl-1-p-tolyl-ethanone

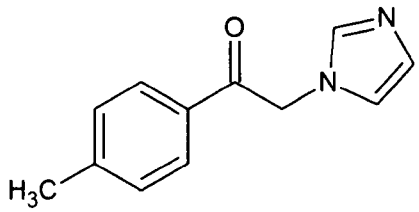

Compound **297** was synthesised in a similar manner to **279** with the exception that imidazole (1.95g, 28.1mmol), anhydrous K_2CO_3 (1.95g, 14.0mmol) and 2-bromo-4-methylacetophenone (2.0g, 9.38mmol) were used. The crude product was re-crystallised using a 50:50 solution of water and methylated spirit to give **297** (1.14g, yield 60.96%) as a yellow solid; [m.p.=139.6-140.4°C]; R_f=0.47 [80/20 diethyl ether/methanol].

$\nu_{(max)}$(Film)cm^{-1}: 3112.6 (Ar, C-H), 1697.4 (C=O), 1604.5 (Ar, C=C); δ_H (400MHz, $CDCl_3$): 7.84 (2H, d, *J*=8.24Hz, Ph-H); 7.49 (1H, s, NCHN Imidazole); 7.29 (2H, d, *J*=8.24Hz, Ph-H); 7.10, 6.92 (1H, s, NCH Imidazole); 5.35 (2H, s, CH_2); δ_c(100MHz, $CDCl_3$): 191.25 (**C**=O); 145.59 (Ar, **C**-CH_3); 138.24 (N**C**HN); 131.78, 129.87 (Ar, **C**); 129.63 (N**C**H); 128.17 (Ar, **C**); 120.39 (N**C**H); 52.36 (**C**H_2); 21.90 (**C**H_3); GC tR=18.15min; LRMS (m/z) 200 (M^+, 12%); 119 (M^+-$C_4H_5N_2$, 100%); 91 (M^+-$C_5H_5N_2O$ 48%). HRMS (EI): *m/z* calcd for $C_{12}H_{12}N_2O$: 200.236; found: 200.0942.

298 3-(2-imidazol-1-yl-acetyl)-benzonitrile

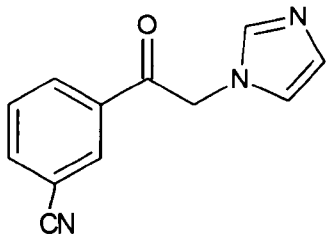

Compound **298** was synthesised in a similar manner to **279** with the exception that imidazole (0.9g, 13.2mmol), anhydrous K_2CO_3 (0.9g, 6.51mmol) and 2-bromo-3-cyanoacetophenone (1.0g, 4.46mmol) were used. Removal of DCM under vacuum gave **298** (0.72g, yield 76.62%) as a solid; [m.p.=161.2-162.4°C]; R_f=0.32 [90/10 diethyl ether/methanol].

$\nu_{(max)}$(Film)cm^{-1}: 3163.3 (Ar, C-H), 2230.9 (C≡N), 1710.7 (C=O), 1596.8 (Ar, C=C); δ_H (400MHz, $(CD_3)_2CO$): 8.52 (1H, m, Ph-H); 8.41 (1H, m, Ph-H); 8.14 (1H, m, Ph-H); 7.88 (1H, m, Ph-H); 7.63 (1H, s, NCHN Imidazole); 7.15 (1H, s, NCH Imidazole); 7.01 (1H, s, NCH Imidazole); 5.90 (2H, s, CH_2); δ_c(100MHz, $(CD_3)_2CO$): 192.73(**C**=O); 139.21 (**NC**HN); 137.61 (Ar, **C**); 136.70 (C≡N); 132.99, 132.61, 131.13 (Ar, **C**); 129.43, 121.40 (**NC**H); 118.52, 113.96 (Ar, **C**); 53.50 (**C**H_2); GC tR=20.13min; LRMS (m/z) 211 (M^+, 35.77%); 130 (M^+-$C_4H_5N_2$, 100%); 102 (M^+-$C_5H_5N_2O$, 44.03%); 75 ($C_6H_5N_3O$, 12.84%). HRMS (EI): *m/z* calcd for $C_{10}H_9N_2CN$: 211.0745; found: 211.0752.

299 4-(2-imidazol-1-yl-acetyl)-benzonitrile

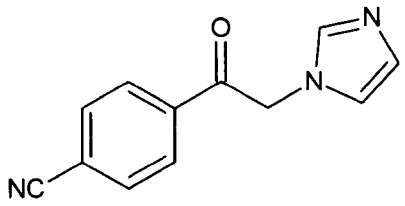

Compound **299** was synthesised in a similar manner to **279** with the exception that imidazole (1.8g, 26.4mmol), anhydrous K_2CO_3 (1.8g, 13.6mmol) and 2-bromo-4-cyanoacetophenone (2.0g, 8.92mmol) were used. Removal of DCM under vacuum gave **299** (1.26g, yield 67%) as a solid; [m.p.=170.3-171.0°C]; R_f=0.32 [90/10 diethyl ether/methanol].

$\nu_{(max)}$(Film)cm^{-1}: 3088.9 (Ar, C-H), 2227.7 (C≡N); 1708.6 (C=O), 1557.9 (Ar, C=C); δ_H(400MHz, DMSO): 8.29 (2H, d, J=8.60Hz, Ph-H); 8.21 (2H, d, J=8.60Hz, Ph-H); 7.70 (1H, s, NCHN); 7.23, 7.05 (2H, s, NCH); 5.90 (2H, s, CH_2); δ_c(100MHz, DMSO): 193.79(**C**=O); 138.84 (N**C**HN); 138.28 (**C**-N); 133.51, 129.18 (Ar, **C**); 128.52, 121.42 (N**C**H); 118.65, 116.30 (Ar, **C**); 53.51 (**C**H_2); GC tR=20.25min; LRMS (m/z) 211 (M^+, 32%), 130 (M^+-$C_4H_5N_2$, 100%), 116 (M^+-$C_4H_5N_3$, 2%), 102 (M^+-$C_5H_5N_2O$, 36%), 89 ($C_5H_5N_3O$, 2%), 75 ($C_6H_5N_3O$, 8%). HRMS (EI): *m/z* calcd for $C_{10}H_9N_2CN$: 211.0745; found: 211.0728.

300 1-Biphenyl-4-yl-2-imidazol-1-yl-ethanone

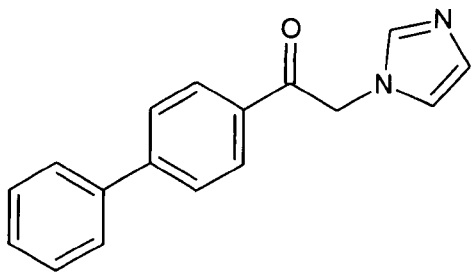

*Compound **300** was synthesised in a similar manner to **279** with the exception that* Imidazole (1.5g, 22.0mmol), anhydrous K_2CO_3 (1.65g, 11.9mmol) and 2-bromo-4-phenylacetophenone (2.0g, 7.27mmol) were used. Removal of DCM under vacuum gave **300** (1.02g, yield 53%) as a yellow solid; [m.p.=201.3-202.4°C];R_f=0 [90/10 diethyl ether/methanol].

$\nu_{(max)}$(Film)cm^{-1}: 3150.0 (Ar, C-H), 1693.1 (C=O), 1602.1 (Ar, C=C); δ_H (400MHz, DMSO): 8.24 (2H, d, *J*=8.24Hz, Ph-H); 8.02 (2H, d, *J*=8.24Hz, Ph-H); 7.91 (2H, d, *J*=8.60Hz, Ph-H); 7.73 (1H, s, NCHN Imidazole); 7.61 (3H, m, Ph-H); 7.26, 7.05 (2H, s, NCH Imidazole); 5.89 (2H, s, CH_2); δ_c(100MHz, DMSO): 193.75 (**C**=O); 145.73, 139.26 (Ar, **C**); 138.92 (N**C**HN); 133.89, 129.35, 129.0 (Ar, **C**); 128.72, 128.37 (N**C**H); 127.38, 121.0 (Ar, **C**); 53.17 (**C**H_2); GC tR=24.78min; LRMS (m/z) 262 (M^+, 11%); 181 (M^+-$C_4H_5N_2$, 100%); 165 (M^+-$C_4H_5N_2O$, 2%); 152 (M^+-$C_5H_5N_2O$ 51%). HRMS (EI): *m/z* calcd for $C_{17}H_{14}N_2O$: 262.3053; found: 262.1092.

301 3-Imidazol-1-yl-1-phenyl-propan-1-one

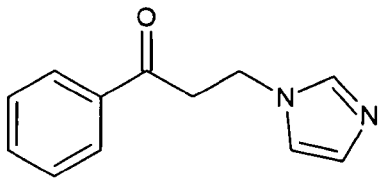

Compound **301** was synthesised in a similar manner to **279** with the exception that Imidazole (1.25g, 18.3mmol), sodium methoxide $Na^{+}CH_3O^{-}$ (1.0g, 18.5mmol) and 3-chloropropiophenone (2.0g, 11.8mmol) were used. Removal of DCM under vacuum gave **301** (1.92g, yield 81%) as a yellow solid; [m.p.=97.7-98.5°C]; R_f=0.22 [90/10 diethyl ether/methanol].

$\nu_{(max)}$(Film)cm^{-1}: 3114.3 (Ar, C-H), 1680.8 (C=O), 1595.7 (Ar, C=C); δ_H (400MHz, $CDCl_3$): 7.89 (2H, m, Ph-H); 7.56 (1H, m, Ph-H); 7.53 (1H, s, NCHN Imidazole); 7.44 (2H, m, Ph-H); 7.00, 6.94 (2H, s, NCH Imidazole); 4.40 (2H, t, *J*=6.59Hz, CH_2); 3.41 (2H, t, *J*=6.59Hz, CH_2); δ_c(100MHz, $CDCl_3$): 196.65 (**C**=O); 137.53 (**NC**HN); 136.20, 133.84, 129.72 (**NC**H); 128.89, 128.05, 119.17 (Ar, **C**); 41.51, 39.97 (**C**H_2); GC tR=18.07min; LRMS (m/z) 200 (M^+, 32%); 132 (M^+-$C_3H_3N_2$, 3%); 105 (M^+-$C_5H_7N_2$, 100%); 89 (M^+-$C_5H_7N_2O$ 1%); 77 (M^+-$C_6H_7N_2O$ 92%). HRMS (EI): *m/z* calcd for $C_{12}H_{12}N_2O$: 200.236; found: 200.0939.

302 1-(4-fluoro-phenyl)-3-imidazol-1-yl-propan-1-one.

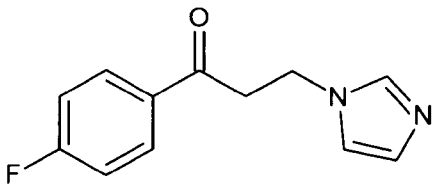

Compound **302** was synthesised in a similar manner to **279** with the exception that Imidazole (0.94g, 13.8mmol), sodium methoxide $Na^+CH_3O^-$ (0.74g, 13.6mmol) and 3-chloro-4-fluoropropiophenone (2.0g, 10.7mmol) were used. Removal of DCM under vacuum gave **302** (1.55g, yield 66%) as a yellow solid; [m.p.=54.6-55.7°C]; R_f=0.32 [90/10 diethyl ether/methanol].

$\nu_{(max)}$(Film)cm^{-1}: 3113.2 (Ar, C-H), 1683.0 (C=O), 1597.8 (Ar, C=C); δ_H (400MHz, $CDCl_3$): 7.91 (2H, d, *J*=8.79Hz, Ph-H); 7.54 (1H, s, NCHN Imidazole); 7.10 (2H, t, *J*=8.60Hz, Ph-H); 7.00, 6.93 (2H, s, NCH Imidazole); 4.40 (2H, t, *J*=6.59Hz, CH_2); 3.38 (2H, t, *J*=6.59Hz, CH_2); δ_c(100MHz, $CDCl_3$): 195.04 (**C**=O); 167.40, 164.86 (**C**-F) 137.53 (**NC**HN); 132.68, 130.80 (Ar, **C**); 129.75 , 119.15 (**NC**H); 116.18 (Ar, **C**); 41.44, 39.90 (**C**H_2); GC tR=17.88min; LRMS (m/z) 218 (M^+, 20%); 151 (M^+-$C_3H_3N_2$ 2%); 123 (M^+-$C_5H_7N_2$ 65%); 95 (M^+-$C_6H_7N_2O$ 100%); 75 (M^+-$C_6H_7N_2OF$ 15%). HRMS (EI): *m/z* calcd for $C_{12}H_{11}FN_2O$: 218.2265; found: 218.0847.

303 1-(4-chloro-phenyl)-3-imidazol-1-yl-propan-1-one

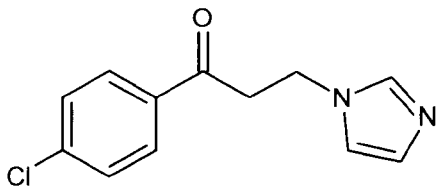

Compound **303** was synthesised in a similar manner to **279** with the exception that Imidazole (0.8g, 11.7mmol), sodium methoxide Na^+CH3^- (0.6g, 11.1mmol) and 3-chloro-4-chloropropiophenone (2.0g, 9.84mmol) were used. Removal of DCM under vacuum gave **303** (2.11g, yield 91%) as a yellow solid; R_f=0 [90/10 diethyl ether/methanol].

$\nu_{(max)}$(Film)cm^{-1}: 3113.4 (Ar, C-H), 1683.5 (C=O), 1589.3 (Ar, C=C); δ_H (400MHz, $(CD_3)_2CO$): 8.07 (2H, d, *J*=8.71Hz Ph-H); 7.63 (1H, s, NCHN Imidazole); 7.59 (2H, d, *J*=8.07Hz Ph-H); 7.17(1H, s, NCH Imidazole); 6.91 (1H, s, NCH Imidazole); 4.49 (2H, t, *J*=6.70Hz, CH_2); 3.67 (2H, t, *J*=6.70Hz, CH_2); δ_c(100MHz, $(CD_3)_2CO$): 197.03 (**C**=O); 139.89 (**C**-Cl) 138.35 (N**C**HN); 136.20, 130.66, 129.75 (Ar, **C**); 129.68, 119.94 (N**C**H); 42.11, 40.55 (**C**H_2);GC tR=17.89min; LRMS (m/z) 218 (M^+, 20.0%); 123 (M^+-$C_5H_7N_2$ 65.21%); 95 (M^+-$C_6H_7N_2$,O 100%); 75 (M^+-$C_6H_7N_2OF$ 15.21%). HRMS (EI): *m/z* calcd for $C_{12}H_{11}N_2OCl$: 234.0559; found: 234.0549.

304 1-(4-bromo-phenyl)-3-imidazol-1-yl-propan-1-one

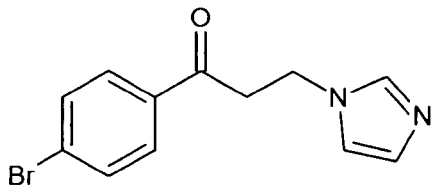

Compound **304** was synthesised in a similar manner to **279** with the exception that Imidazole (0.25g, 3.67mmol), sodium methoxide $Na^{+}CH3^{-}$ (0.2g, 3.70mmol) and 3-chloro-4-bromopropiophenone (0.7g, 2.82mmol) were used. Removal of DCM under vacuum gave **304** (0.32g, yield 41%) as a yellow solid; R_f=0 [90/10 diethyl ether/methanol].

$\nu_{(max)}$(Film)cm^{-1}: 3110.4 (Ar, C-H), 1682.6 (C=O), 1585.0 (Ar, C=C); δ_H (400MHz, $(CD_3)_2CO$): 7.93 (2H, d, *J*=8.42Hz Ph-H); 7.76 (2H, d, *J*=8.42Hz Ph-H); 7.62 (1H, s, NCHN Imidazole); 7.17(1H, s, NCH Imidazole); 6.91 (1H, s, NCH Imidazole); 4.48 (2H, t, *J*=6.70Hz, CH_2); 3.67 (2H, t, *J*=6.70Hz, CH_2); δ_c(100MHz, $(CD_3)_2CO$): 197.24 (**C**=O); 138.34 (N**C**HN); 136.56 (**C**-Br) 132.79, 130.75 (Ar, **C**); 129.69 (N**C**H); 128.63 (Ar, **C**); 119.92 (N**C**H); 42.09, 40.53 ($\mathbf{C}H_2$); GC tR=17.89min; LRMS (m/z) 218 (M^+, 20.0%); 123 (M^+-$C_5H_7N_2$ 65.21%); 95 (M^+-$C_6H_7N_2$,O 100%); 75 (M^+-$C_6H_7N_2OF$ 15.21%). HRMS (EI): *m/z* calcd for $C_{12}H_{11}BrN_2O$: 279.1321; found: 278.0037$^{(79)}$ and 280.0102$^{(81)}$.

7.0 References

(1) Suzuki R, Allen NE, Key TJ, Appleby PN. A prospective analysis of the association between dietary fibre intake and prostate cancer risk in EPIC. *Int J Cancer* 2009;**124**:245-249.

(2) Jemal A, Siegal R, Ward E, Hao Y, Xu J, Murray T, Thun MJ. Cancer statistics, 2006. *CA Cancer J Clin* 2006;**56**:106-130.

(3) Ferlay J, Autier P, Boniol M, Heanue M, Colombet M, Boyle P. Estimates of the cancer incidence and mortality in Europe in 2006. *Annals of Oncology* 2007;**18**:581-592.

(4) Parkin DM, Whelan SL, Ferlay J, Storm H. Cancer incidence in five continents, vol I-VIII. Lyon, France: International Agency for Research on Cancer, 2005. *IARC Cancer Base No.7.*

(5) Beiki O, Ekbom A, Allebeck P, Moradi T. Risk of prostate cancer among Swedish-born and foreign-born men in Sweden, 1961-2004. *Int J Cancer* 2009;**124**:1941-1953.

(6) Grönberg Henrik. Prostate Cancer Epidemiology. The Lancet 2003;361:859-864.

(7) Giovannucci E, Liu Y, Platz EA, Stampfer MJ, Willett WC. *Int J Cancer* 2007;**121**(**7**):1571-1578.

(8) Boffetta P and Nyberg F. Contribution of environmental factors to cancer risk. *British Medical Bulletin* 2003;**68**:71-94.

(9) Herceg Z. Epigenetics and cancer: towards an evaluation of the impact of environmental and dietary factors. *Mutagenesis* 2007;**22**(**2**):91-103.

(10) Platz EA, Giovannucci E. The epidemiology of sex steroid hormones and their Signalling and metabolic pathways in the etiology of prostate cancer. *J Steroid Biochem & Mol Biol* 2004;**92**:237-253.

(11) Chen Y, Zajac JD, MacLean HE. Androgen regulation of satellite cell function. *J*

Endocrinology 2005;**186**:21-31.

(12) Simon H. Prostate cancer in depth. *Harvard Medical School* 2006.

(13) Claus FG, Hricak H, Hattery RR. Pre-treatment evaluation of prostate cancer: Role of MR imaging and ^{1}H MR spectroscopy[1]. *Radiographics* 2004;**24**:S167-180.

(14) Choi YJ, Kim JK, Kim N, Kim KW, Choi EK and Cho KS.Functional MR imaging of Prostate Cancer. *Radiographics* 2007;**27**:63-77.

(15) DeMarzo AM, Platz EA, Sutcliffe S, Xu J, Gronberg H, Drake CG, Nakai Y, Isaacs WB and Nelson WG. Inflammation in prostate carcinogenesis. *Natural Reviews Cancer* 2007;**7**:256-269.

(16) Gann PH, Hennekans CH, Stampfer MJ. A prospective evaluation of plasma prostate specific antigen for detection of prostatic cancer. *JAMA* 1995;**273(4)**;289-294.

(17) Grossmann ME, Huang H, Tindall DJ. Androgen receptor signalling in androgen-refractory prostate cancer. *J Nat. Cancer Institute* 2001;**93(2)**:1687-1697.

(18) Ankley GT and Johnson RD. Small fish models for identifying and assessing the effects of endocrine-disrupting chemicals. *ILAR Journal* 2004;**45(4)**:469-483.

(19) Broqua P, Riviere PJ-M, Conn PM, Rivier JE, Aubert ML and Junien J-L. Pharmacological profile of a new, potent and long-acting gonadotropin-releasing hormone antagonist:Dararelix. *JPET* 2002;**301**:95-102.

(20) Miller WL. Androgen biosynthesis from cholesterol to DHEA. *Mol & Cellular Endocrinology* 2002;**198**:7-14.

(21) Auchus RJ and Miller WL. Molecular modelling of human P450c17 (17α-hydroxylase/17, 20-lyase): insights into reaction mechanisms and effects of mutations. *Mol. Endocr.* 1999;**13(7)**:1169-1182.

(22) Akhtar MK, Kelly SL and Kaderbhai MA. Cytochrome b5 modulation of 17α-hydroxylase and 17-20 lyase (CYP17) activities in steroidogenesis. *J Endocr.* 2005;**187**:267-274.

(23) Bruchovsky N, Wilson JD. The conversion of testosterone to 5α-Androstan-17α-ol-3-one by rat prostate in vivo and in vitro. *J Biol Chem* 1968; **243**(**8**):2012-2021.

(24) Feldman BJ & Feldman D. The development of androgen-independent prostate cancer. *Nature reviews* 2001;**1**:34-45.

(25) Taplin ME and HO SM. The endocrinology of prostate cancer. *J Clin. Endocrinology and Metabolism* 2001;**86**(**8**):3467-3477.

(26) Tindall DJ & Debes JD. The role of androgens and the androgen receptor in prostate cancer. *Cancer letters* 2002;**187**:1-7.

(27) Gao W, Bohl CE & Dalton JT. Chemistry and structural biology of androgen receptor. *Chem.Rev.* 2005;**105**:3352-3370.

(28) Dehm SM & Tindall DJ. Molecular regulation of androgen action in prostate cancer. *J Cell Biochem* 2006;**99**:333-334.

(29) Carter HB, Pearson JD, Metter J, Brant LJ, Chan DW, Andres R, Fozard JL. Longitudinal evaluation of prostate-specific antigen levels in men with and without prostate disease. *JAMA* 1992;**267**(**16**):2215-2220.

(30) Balk SP, Ko YJ, Bubley GJ. Biology of PBalk SP, Ko YJ, Bubley GJ.Biology of Prostate-specific Antigen. *J Clin.Oncol.* 2003;**21**(**2**):383-391

(31) Matzkin H, Eber P, Todd B, Van Der Zwagg R, Soloway MS. Prognostic significance of changes in prostate-specific markers after endocrine treatment of stage D2 prostatic cancer. *CANCER* 1992;**70**(**9**):2302-2309.

(32) So A, Gleave M, Hurtado-Col A and Nelson C. Mechanisms of the development of androgen independence in prostate cancer. *World J Urol* 2005;**23**:1-9.

(33) Stanbrough M, Bubley GJ, Ross K, Golub TR, Rubin MA, Penning TM, Febbo PG and Bulk SP. Increased expression of genes converting adrenal androgens to testosterone in androgen-independent prostate cancer. *Cancer Res.* 2006;**66**:2815-2825.

(34) Mostaghel EA and Nelson PS. Intracrine androgen metabolism in prostate cancer progression: mechanisms of castration resistance and therapeutic implications. *Best.Pract.Res.Clin.Endocrinol.Metab.* 2008;**22**:243-258.

(35) Montgomery RB, Mostaghel EA, Vessella R, Hess DL, Kalhorn TF, Higano CS, True LD, Nelson PS. Maintenance of intratumoral androgens in metastatic prostate cancer: A mechanism for castration-resistant tumor growth. *Cancer Res.* 2008;**68**(**11**):4447-4454.

(36) Yap TA, Carden CP, Attard G and De bono JS. Targeting CYP17: established and novel approaches in prostate cancer. *Curr. Opin, Pharmacol.* 2008;**8**:449-457.

(37) Hakki T and Bernhardt R. Associate editor: Kaminsky LS. CYP17- and CYP11B-dependent steroid hydroxylases as drug development targets. *Pharmacol. Therapeutics* 2006;**111**:27-52.

(38) Werck-Reichhart D and Feyereisen R. *Genome Biology* 2000;**1**(**6**):3003.1-3003.9.

(39) Meunier B, de Visser SP and Shaik S. Mechanism of oxidation reactions catalyzed by Cytochrome P450 enzymes. *Chem.Rev.*2004;**104**:3947-3980.

(40) Denisov IG, Makris TM, Sligar SG and Schlichting I. Structure and chemistry of cytochrome P450. *Chem.Rev.*2005;**105**(**6**):2253-2277.

(41) Sligar SG and Suslick KS and Benson DE. Reduced oxy intermediate observed in D251N cytochrome $P450_{cam}$. *Biochemistry* 1997;**36**:5104-5107.

(42) Ortiz de Montellano PR and De Voss JJ. Oxidizing species in the mechanism of cytochrome P450. *Nat. Prod. Rep.* 2002;**19**:477-493.

(43) Ichiwara Y and Yamano T. Reconversion of detergent- and sulfhydryl reagent-produced P-420 to P-450 by polyols and glutathione. *Biochim.Biophys.Acta.* 1967;**131**:490-497.

(44) Pandey AV and Miller WL. Regulation of 17, 20 lyase activity by cytochrome b_5

and by serine phosphorylation of P450 c17. *J Biol. Chem.* 2005;**280**(**14**):13265-13271.

(45) Nakajin S and Hall PF. Microsomal cytochrome P-450 from neonatal pig testis. *J Biol. Chem.* 1981;**256**(**8**):3871-3876.

(46) Angelastro MR, Marquart AL, Weintraub PM, Gates CA, Laughlin ME, Blohm TR and Peet NP. Time-dependent inactivation of steroid C17(20) lyase by 17β-cyclopropyl ether-substituted steroids. *Bioorg & Medicinal Chem. Letters* 1996;**6**(**1**):97-100.

(47) Nakajin S, Shinoda M, Haniu M, Shively JE and Hall PF. C_{21} Steroid side chain cleavage enzyme from porcine adrenal microsomes. *J Biol. Chem.* 1984;**259**(**6**):3971-3976.

(48) Hartmann RW, Haider S, Ehmer PB, Hartmann CB and Barassin S. Effects of novel 17α-hyroxylase/C17, 20 lyase (P450 17, CYP 17) inhibitors on androgen biosynthesis in vitro and in vivo. *J Steroid Biochem & Mol. Biol.* 2003;**84**:555-562.

(49) Ortiz de Montellano PR and Stearns RA. Timing of a radical recombination step in cytochrome P-450 catalysis with ring-stained probes. *J Am.Chem.Soc.* 1987;**109**:3415-3420.

(50) Ahmed S and Owen CP. Mechanism of 17α-hydroxylase/17,20-lyase – an initial geometric perspective for lyase of the C(17)-C(20) bond of C_{21} steroids. *Bioorg.& Med. Chem. Letts.* 1998;**8**:1023-1028.

(51) Laughton CA, Neidle S, Zvelebil MJJM and Sternberg MJE. A molecular model for the enzyme cytochrome $P450_{17\alpha}$, a major target for the chemotherapy of prostate cancer. *Biochem & Biophysical Research Communications* 1990;**171**(**3**):1160-1167.

(52) Poulos TL, Finzel BC and Howard AJ. High-resolution crystal structure of cytochrome P450cam. *J.Mol.Biol.*1987;**195**:687-700.

(53) Burke DF, Laughton CA and Neidle S. Homology modelling of the enzyme P450 17α-hydroxylase/17,20-lyase: a target for prostate cancer therapy from the crystal structure of P450BM-3. *Anti-Cancer Drug Design* 1997;**12**:113-123.

(54) Lee-Robichaud P, Akhtar ME and Akhtar M. Control of androgen biosynthesis in the human through the interaction of Arg^{347} and Arg^{358} of CYP17 with cytochrome b_5. *J Biochem* 1998;**332**:293-296.

(55) Ahmed S, James K, Owen CP and Patel CK. Synthesis and biochemical evaluation of novel and potent inhibitors of the enzyme oestrone sulphatase (ES). *J Steroid Biochem & Mol. Biol.* 2002;**80**(**4**):419-427.

(56) Akhtar M, Neville Wright J and Lee-Robichaud P. A review of mechanistic studies on aromatase (CYP 19) and 17α-hydroxylase-17,20-lyase (CYP17). *J.Ster.Biochem & Mol.Biol.* 2011;**125**:2-12.

(57) Ahmed S. Complete derivation of the active site of the cytochrome P-450 enzyme 17α-hydroxylase/17, 20-lyase (P450 17α) using the novel substrate-haem complex approach. *J.Pharmacy & Pharmacology*1998;**50**(**S9**):253.

(58) Brodie AMH and Njar VCO. Inhibitors of 17α-hydroxylase/17,20-lyase (CYP17): Potential agents for the treatment of prostate cancer. *Current Pharmaceutical Design* 1999;**5**:163-180.

(59) Haider S and Hartmann RW. C16 and C17 substituted derivatives of Pregnenolone and Progesterone as inhibitors of 17α-Hydroxylase-C17, 20-lyase: Synthesis and Biological Evaluation. *Arch.Pharm.PharmMed.Chem.*2002;**335**:526-534.

(60) Angelastro MR, Laughlin ME, Schatzman GL, Bey P and Blohm TR. 17β-(Cyclopropylamino)-androst-5-en-3β-ol, a selective mechanism-based inhibitor of cytochrome $P450_{17\alpha}$ (steroid 17α-hydroxylase/$C_{17\text{-}20}$ lyase). *Biochem & Biophys. Res. Comm.* 1989;**162**(**3**):1571-1577.

(61) Burkhart JP, Weintraub PM, Gates CA, Resvick RJ, Vas RJ, Friedrich D, Angelastro MR, Bey P and Peet NP. Novel steroidal vinyl fluorides as inhibitors of steroid $C_{17(20)}$ lyase. *Bioorg & Med Chem.* 2002;**10**:929-934.

(62) Weintraub PM, Holland AK, Gates CA, Moore WR, Resvick RJ, Bey P and Peet NP. Synthesis of 21, 21-difluoro-3β-hydroxy-20-methylpregna-5, 20-diene and 5, 16, 20-triene as potential inhibitors of steroid $C_{17(20)}$ lyase. *Bioorg & Med.Chem* 2003;**11**:427-431.

(63) Njar VCO, Klus GT, Johnson HH and Brodie AMH. Synthesis of novel 21-trifluoropregnane steroids: inhibitors of 17α-hydroxylase/17, 20-lyase (17α-lyase). *Steroids* 1997;**62**:468-473.

(64) Schenkman JB, Remmer H and Estabrook RW. Spectral studies of drug interaction with hepatic microsomal cytochrome. *Mol. Pharmacol.* 1967; **3**(**2**):113-123.

(65) Li J-S, Li Y, Son C and Brodie AMH.Synthesis and evaluation of pregnane derivatives as inhibitors of human testicular 17α-hydroxylase/C_{17-20}-lyase. *J.Med.Chem.* 1996;**39**:4335-4339.

(66) Matsunaga N, Kaku T, Itoh F, Tanaka T, Hara T, Miki H, Iwasaki M, Aono T, Yamaoka M, Kusaka M and Tasaka A. C_{17-20}-Lyase inhibitors I. Structure-based de novo design and SAR study of C_{17-20}-lyase inhibitors. *Bioorg & Med.Chem.* 2004;**12**: 2251-2273.

(67) Ling Y, Li J, Kato K, Liu Y, Wang X, Klus GT, Marat K, Nnane IP and Brodie AMH. Synthesis and in vitro activity of some epimeric 20α-hydroxy, 20-oxime and aziridine pregnene derivatives as inhibitors of human 17α-hydroxylase/C_{17-20}-lyase and 5α-reductase. *Bioorg & Med.Chem.* 1998;**6**:1683-1693.

(68) Auchus RJ, Kumar AS, Boswell CA, Gupta MK, Bruce K, Rath NP and Covey DF. The enantiomers of progesterone (*ent*-progesterone) is a competitive inhibitor of human cytochromes P450c17and P450c21. *Archives of Biochem &Biophys.* 2003;**409**:134-144.

(69) Dawson JH, Andersson LA and Sono M. Spectroscopic investigations of ferric cytochrome P-450-CAM ligand complexes. *J Biol.Chem.* 1982;**257**:3606-3617.

(70) Hall PF. Cytochromes P-450 and the regulation of steroid biosynthesis. *Steroids*1986;**48**(**3-4**):131-96.

(71) Potter GA, Barrie SE, Jarman M and Rowlands GA. Novel steroidal inhibitors of human cytochrome $P450_{17\alpha}$ (17α-hydroxylase-C_{17-20}-lyase): Potential agents for the treatment of prostate cancer. *J. Med.Chem.* 1995;**38**:2463-2471.

(72) Potter GA, Jarman M, Neidle S, Laughton CA, Snook CF and Burke DF. Active-site conformation of 17-(3-pyridyl)androsta-5, 16-dien-3β-ol, a potent inhibitor of the P450 enzyme C17α-hydroxylase/C17-20 lyase. *Bioorg & Med.Chem letters* 1995;**5**:1125-1130.

(73) Neidle S, Burke DF, Laughton CA, Snook CF, Potter GA and Jarman M. Active-site conformation of 17-(3-pyridyl)androsta-5, 16-dien-3β-ol, a potent inhibitor of the P450 enzyme C17α-hydroxylase/C17-20 lyase. *Bioorg & Med.Chem.Letts* 1995;**5**(**11**):1125-1130.

(74) Barrie SE, Potter GA, Jarman M, Goddard PM, Haynes BP and Dowsett M. Pharmacology of novel steroidal inhibitors of cytochrome P45017α-hydroxylase/C17-20 lyase. *J Steroid Biochem & Mol. Biology* 1994;**50**:267-273.

(75) Attard G, Reid AHM, Yap TA, Raynaud F, Dowsett M, Settatree S, Barrett M, Parker C, Martins V, Folkerd E, Clark J, Cooper CS, Kaye SB, Dearnaley D and de bono JS. Phase I clinical trial of a selective inhibitor of CYP17, abiraterone acetate, confirms that castration-resistant prostate cancer commonly remains hormone driven. *J Clin.Oncol.* 2008;**26**:4563-4571.

(76) Burkhart JP, Gates CA, Laughlin ME, Resvick RJ and Peet NP. Inhibition of steroid $C_{17(20)}$ Lyase with C-17-heteroaryl steroids. *Bioorg & Med.Chem.* 1996:**4**(**9**);1411-1420.

(77) Zhu NA, Ling L, Lei X, Handratta V and Brodie AMH. Novel $P450_{17\alpha}$ inhibitors: 17-(2'-oxazolyl)-and 17-(2'-thiazolyl)-androstene derivatives. *Steroids*2003;**68**:603-611.

(78) Ling Y-Z, Li J-S, Liu Y, Kato K, Klus GT and Brodie AMH. 17-imidazolyl, pyrazolyl and Isoxazolyl androstene derivatives.Novel steroidal inhibitors of human cytochrome C_{17-20}-lyase ($P450_{17\alpha}$). *J. Med.Chem.* 1997;**40**:3297-3304.

(79) Njar VCO, Kato K, Nnane IP, Grigoryev DN, Long BJ and Brodie AMH. Novel 17-azolyl steroids, potent inhibitors of human cytochrome 17α-hydroxylase-C_{17-20}-lyase ($P450_{17\alpha}$): Potential agents for the treatment of prostate cancer. *J. Med.Chem.* 1998;**41**:902-912.

(80) Handratta VD, Vasaitis TS, Njar VCO, Gediya LK, Kataria R, Chopra P, Newman D, Farquhar R, Guo Z, Qiu Y, Brodie AMH. Novel C-17-heteroaryl steroidal CYP17 inhibitors/antiandrogens: Synthesis, in vitro biological activity, pharmacokinetics, and antitumor activity in the LAPC4 human prostate cancer xenograft model. J. Med. Chem. 2005;48:2972-2984.

(81) Hartmann RW, Hector M, Haider S, Ehmer PB, Reichert W and Jose J. Synthesis and evaluation of novel steroidal oxime inhibitors of P450 17 (17α-Hydroxylase/C17-20-Lyase) and 5α-reductase types 1 and 2. *J. Med.Chem.* 2000;**43**:4266-4277.

(82) Haider S, Ehmer PB and Hartman RW. Novel steroidal pyrimidyl inhibitors of $P450_{17}$(17α-hydroxylase/C17-20-lyase). *Arch.Pharm.Pharm.Med.Chem.* 2001;**334**:373-374.

(83) Defelice R, Johnson DG and Galgiani JN. Gynaecomastia with Ketoconazole. *Antimicrobial Agents and Chemotherapy* 1981:1073-1074.

(84) Loose DS, Kan PB, Hirst MA, Marcus RA and Feldman D. Ketoconazole blocks adrenal steroidogenesis by inhibiting cytochrome P450-dependent enzyme. *J. Clin. Investigation*1983;**71**(**5**):1495-1499.

(85) Trachtenberg J and Pont A. Ketoconazole therapy for advanced prostate cancer. *The Lancet* 1984;**324**:433-435.

(86) Kunio N, Isamu M, Masatoshi I, Hideo K, Ryoyu T, Katsuko S and Masayuki K. Effect of ketoconazole (an imidazole antimycotics agent) and other inhibitors of steroidogenesis on cytochrome P450-catalyzed reactions. 1986;**24**(**1**):321-323.

(87) Figg WD, Woo S, Zhu W, Chen X, Ajiboye AS, Steinberg SM, Price DK, Wright JJ, Parnes HL, Arlen PM, Gulley JL and Dahut WL. A phase I clinical study of high dose Ketoconazole plus weekly Docetaxel for metastatic castration resistant prostate cancer. *J. Urology* 2010;**183**(**6**):2219-2226.

(88) Ahmed S. Molecular modelling of inhibitors of 17α-hydroxylase - a novel approach. *Bioorg & Medicinal Chemistry Letts*1995;**5**(**23**):2795-2800.

(89) Sergejew T and Hartmann RW. Pyridyl substituted benzocycloalkenes: New inhibitors of 17α-hydroxylase/17,20-lyase (P450 17α). *J. Enz.Inhib & Med.Chem.* 1994;**8**(**2**):113-122.

(90) Rowlands MG, Barrie SE, Chan F, Houghton J, Jarman M, McCague R and Potter GA. Esters of 3-pyridylacetic acid that combine potent inhibition of 17α-hydroxylase/C_{17-20}-lyase (Cytochrome P45017α) with resistance to esterase hydrolysis. *J. Med.Chem* 1995;**38**:4191- 4197.

(91) Ahmed S, Smith JH, Nicholls PJ, Whomsley R and Caruik P. Synthesis and biological evaluation of novel pyrrolidine-2,5-dione inhibitors as potential antitumour agents. *Drug.Des & Dis.*1995;**12**(**4**):275-287.

(92) Ideyama Y, Kudoh M, Tanimoto K, Susaki Y, Nanya T, Nakahara T, Ishikawa H, Yoden T, Okada M, Fujikura T, Akaza H and Shikama H. Novel nonsteroidal inhibitor of cytochrome $P450_{17\alpha}$ (17α-hydroxylase/C17-20 lyase), YM116, decreased prostatic weights by reducing serum concentrations of testosterone and adrenal androgens in rats. *The Prostate* 1998;**37**:10-18.

(93) Ideyama Y, Kudoh M, Tanimoto K, Susaki Y, Nanya T, Nakahara T, Ishikawa H, Fujikura T, Akaza H and Shikama H. YM116, 2-(1*H*-imidazol-4-ylmethyl)-9*H*-carbazole,

decreases adrenal androgen synthesis by inhibiting C17-20 lyase activity in NCI-H295 human adrenocortical carcinoma cells. *Jpn. J. Pharmacol.* 1999;**79**:213-220.

(94) Wachall BG, Hector M, Zhuang Y and Hartmann RW. Imidazole substituted biphenyls: A new class of highly potent and in vivo active inhibitors of P450 17 as potential therapeutics for treatment of prostate cancer. *Bioorg & Med.Chem.* 1999;**7**:1913-1924.

(95) Zhuang Y, Wachall BG and Hartmann RW. Novel imidazolyl and triazolyl substituted biphenyl compounds: Synthesis and evaluation as nonsteroidal inhibitors of human 17α-hysroxylase-C17, 20-lyase (P450 17). *Bioorg & Med.Chem.* 2000;**8**:1245-1252.

(96) Leroux F, Hutschenreuter TU, Charriere C, Scopelliti R and Hartmann RW. *N*-(4-Biphenylmethyl)imidazoles as potential therapeutics for the treatment of prostate cancer: Metabolic robustness due to fluorine substitution. *Helvetica Chimica Acta* 2003;**86**:2671-2686.

(97) Hartmann RW, Palusczak A, Lacan F, Riccib G and Ruzziconi R. CYP17 and CYP19 inhibitors: Evaluation of fluorine effects on the inhibiting activity of regioselectivity fluorinated 1-(naphthalene-2-ylmethyl)imidazoles. *J Enz.Inhib.Med. Chem* 2004;**19**(**2**):145-155.

(98) Matsunaga N, Kaku T, Ojida A, Tanaka T, Hara T, Yamaoka M, Kusaka M and Tasaka A. C_{17-20}-Lyase inhibitors II. Design, synthesis and structure-activity relationships of (2-naphthylmethyl)-1*H*-imidazoles as novel C_{17-20}-lyase inhibitors. *Bioorg & Med.Chem.* 2004;**12**: 4313-4336.

(99) Jagusch C, Negri M, Hille UE, Hu Q, Bartels M, Jahn-Hoffmann K, Mendieta M, Rodenwaldt B, Muller-Vieira U, Schmidt D, Lauterbach T, Recanatini M, Cavalli A and Hartmann RW. Synthesis, biological evaluation and molecular modelling studies of methyleneimidazole substituted biaryls as inhibitors of human 17α-hydroxylase-17,20-

lyase (CYP17). Part 1: Heterocyclic modifications of the core structure. *Bioorg.Med.Chem.*2008;**16**(**4**):1992-2010.

(100) Lewis DFV and Lee-Robichaud P. Molecular modelling of steroidogenic cytochromes P450 from families CYP11, CUP17, CYP19 and CYP21 based on the CYP102 crystal structure. *J Steroid Biochem & Mol.Biol.* 1998;**66**(**4**);217-233.

(101) Ahmed S and Davis PJ.Molecular modelling of inhibitors of aromatase – a novel approach. *Bioorg.Med.Chem.Lett* 1995;**5**(**15**):1673-1678.

(102) Ahmed S and Davis PJ.The mechanism of aromatase – a molecular modelling perspective. *Bioorg.Med.Chem.Lett* 1995;**5**(**23**):2789-2794.

(103) Ahmed S and Owen C. A Novel Molecular-modelling study of some inhibitors of 17,20-lyase.*The Substrate-Haem Complex Approach*. 1996;**2**(**5**):247-249.

(104) Ahmed S. Molecular modelling of inhibitors of 17α-Hydroxylase – a novel approach. *Bioorg.Med.Chem*1995;**5**(**23**):2795-2800.

(105) Cannon WN, Powell CE, Jones RG. Studies of Imidazoles. VII. Substituted 1-Phenethylimidazoles and related compounds. *J. Org.Chem* 1957;**22**(**11**):1323-1326.

(106) Muzart J, Thorey C and Henin F. Enantioselective hydrogenation of α,β-unsaturated ketones over palladium on charcoal in the presence of (-)-ephedrine. *Tedrahedron: Asymmetry.* 1996;**7**(**4**):975-976.

(107) Seki et al, 2001

(108) Ahmed S, Shah K, Jandu B and Abdullah A. Synthesis, Biochemical Evaluation and Rationalisation of the Inhibitory Activity of a Range of Derivatives of 2-imidazol-1-yl-1-phenyl-ethanone as Potential Novel Inhibitors of 17α-hydroxylase/17,20-lyase (P-$450_{17\alpha}$). *Lett.Drug Des & Dis.*2011;**8**:516-522.

(109) Grimmett MR. Advances in Imidazole Chemistry. *Adv.Heterocycl.Chem* 1970;**12**:103-183.

(110) Buelow M T, Immaraporn B and Gellman A J. The transition state for surface-

catalysed dehalogenation: C-Cl cleavage on Pd. *J Catalysis.* 2001;**203**:41-50.

(111) Abdullah A. Inhibitors of cytochrome P450 emzymes CYP17 and 3β-HSD3: their role in the treatment of hormone dependent prostate and breast cancer. 2012.

(112) Scott HM, MacLeod DJ, Sharpe RM, Welsh M, Fisken M, Hutchison GR, Drake AJ and Van Den Driesche S. Androgen action in the masculinisation programming window and development of male reproductive organs. *Int. J Andrology.* 2010;**33**(**2**):279-287.

(113) Payne AH and Hales DB. Overview of steroidogenic enzymes in the pathway from cholesterol to active steroid hormones. *Endocrine Review.* 2004;**25**(**6**):947-970.

(114) Lowry OH, Rosebrough NJ, Farr AL and Randall RJ. Protein measurement with the Folin phenol reagent. *J Biol. Chem.* 1951;**193**(**1**):265-275.

(115) Gibson GG and Skett P. Introduction to Drug Metabolism. *Science.* 2004;**3RD Edn**.

(116) Mosmann T. Rapid colorimetric assay for cellular growth and survival:application to proliferation and cytotoxicity assays. *J Immunological Methods.* 1983;**65**(**1-2**):55-63.

(117) Tunney MM, Ramage G, Field TR, Moriarty TF, Storey DG. Rapid colorimetric assay for antimicrobial susceptibility testing of *pseudomonas aeruginosa. Antimicrob. Agents. Chemother.* 2004;**48**:1879-1881.

(118) Rahman M, Kuhn L, Rahman M, Olsson-Liljequist B, Mollby R. Evaluation of a scanner-assisted colorimetric MIC method for susceptibility testing of gram-negative fermentative bacteria. *Appl. Environ. Microbiol.* 2004;**70**:2398-2403.